Chemical-biology based approaches to discovering and characterizing antimicrobial peptides

Op chemische biologie gebaseerde technieken voor het ontdekken en karakteriseren van antimicrobiële peptiden
(met een samenvatting in het Nederlands)

Proefschrift

ter verkrijging van de graad van doctor aan de Universiteit Utrecht op gezag van de rector magnificus, prof.dr. G.J. van der Zwaan, ingevolge het besluit van het college voor promoties in het openbaar te verdedigen op maandag 4 april 2016 des middags te 2.30 uur

door

Peter 't Hart

geboren op 29 september 1986
te Krimpen aan den IJssel

Promotor: Prof. Dr. R.J. Pieters

Copromotor: Dr. N.I. Martin

Printed by: Proefschriftmaken.nl || Uitgeverij BOXPress
Cover design by: Peter ‘t Hart & Niek Guis

The printing of this thesis was financially supported by:

Utrecht Institute of Pharmaceutical Sciences (UIPS)

Screening Devices b.v. Amersfoort

Shimadzu Benelux b.v. ‘s-Hertogenbosch

Table of contents

List of abbreviations

aDMA	asymmetric $N^{\eta 1}$,$N^{\eta 1}$-dimethyl-arginine
AdoHcy	S-adenosyl homocysteine
AdoMet	S-adenosyl methionine
AMP	antimicrobial peptide
BOP	benzotriazole-1-yl-oxy-tris-(dimethylamino)-phosphonium hexafluorophosphate
Cbz	carboxybenzyl
CDI	carbonyldiimidazole
CF	carboxyfluorescein
COSY	correlation spectroscopy
DBU	1,8-diazabicycloundec-7-ene
DIPEA	diisopropylethylamine
DMB	dimethoxybenzyl
DOPC	1,2-dioleoyl-sn-glycero-3-phosphocholine
EDCI	1-ethyl-3-(3-dimethylaminopropyl)carbodiimide
EDT	ethanedithiol
EDTA	ethylenediaminetetraacetic acid
ESI-TOF MS	electrospray ionization - time of flight mass spectrometry
GlcNAc	*N*-acetyl-d-glucosamine
HBTU	2-(1H-benzotriazol-1-yl)-1,1,3,3-tetramethyluronium hexafluorophosphate
HFIP	hexafluoroisopropanol
HGT	horizontal gene transfer
HOBt	hydroxybenzotriazole
HPLC	high-performance liquid chromatography
HRMS	high-resolution mass spectrometry
HSQC	heteronuclear single quantum coherence spectroscopy
ITC	isothermal titration calorimetry
LPS	lipopolysaccharide
LRMS	low-resolution mass spectrometry
LUV	large unilamellar vescicle
MIC	minimum inhibitory concentration
MMA	N^{η}-monomethyl-arginine
MRSA	methicillin-resistant *Staphylococcus aureus*
MurNAc	*N*-acetyl-d-muramic acid

NHS	*N*-hydroxysuccinimide
NMR	nuclear magnetic resonance
NOESY	nuclear Overhauser effect spectroscopy
PBP	penicillin-binding protein
PBS	phosphate buffered saline
PEG	polyethylene glycol
PG	peptidoglycan
PRMT	protein arginine *N*-methyltransferase
sDMA	symmetric $N^{\eta 1}$,$N^{\eta 2}$-dimethyl-arginine
SPPS	solid-phase peptide synthesis
TBAF	tetrabutylammonium fluoride
TBMB	1,3,5-tris(bromomethyl)benzene
TCEP	tris(2-carboxyethyl)phosphine
Teoc	trimethylsilylethoxycarbonyl
TFA	trifluoroacetic acid
TIPS	triisopropylsilane
TLC	thin-layer chromatography
TOCSY	total correlation spectroscopy
UDP	uridine diphosphate
VRE	vancomycin-resistant enterococci
WTA	wall teichoic acid

Chapter 1

General introduction

1

1.1 Need for new antibiotics

With the advent of the "post-antibiotic" era, there is a dire need for novel antimicrobial drugs. Antibiotics have revolutionized modern medicine since their introduction in the early 20th century. However, the still ongoing increase in resistant bacterial strains will be a threat that we have to deal with soon. In general, the problems caused by resistant bacteria can be divided into three categories. First, the duration of infection will be extended and mortality will be increased, second, the costs of treatment will rise, and third, without active antibiotics several (surgical) procedures become impossible to perform.[1] It is estimated that, with no improvement on the current situation, 300 million premature deaths will have been caused by resistant pathogens by 2050.[2]

Beyond the large human burden there is also the economic burden that comes along with the associated costs of healthcare. In 2008 it was estimated that the costs attributable to antimicrobial resistance in the USA was approximately $30 billion.[3] It is further estimated that by 2050 the total global GDP-loss due to dealing with antimicrobial resistance will be $100 trillion dollars.[4] Although regulation for appropriate and conservative use of existing antibiotics is important and can at least slow down the onset of antibiotic resistance, it is inevitable that new antibiotic compounds will be required in the future.[5]

1.2 Antibiotic discovery

The use of antibiotics started with the discovery of arsphenamine (salvasan), which was introduced in 1910 against syphilis.[6] More famous are the sulphonamides, a class of compounds that originated in the dye-industry and were optimized for their activity against microorganisms.[6,7] However, it wasn't until the 1940's that the "golden age" of antibiotic discovery started and many new classes of antibiotics were introduced. These new classes included the penicillins, cephalosporins, macrolides and the glycopeptide vancomycin (Figure 1).[5,8] The golden age ended in the 1960's and it wasn't until the year 2000 before the first new class of antibiotics (the oxazolidinones) was introduced to the market.[5,9] The time between 1960 and 2000 is referred to as the "innovation gap" and in this time no new classes of drugs were introduced. The introduction of new antibiotics relied purely on modification of existing scaffolds.[9,10]

1.3 Clinically used antibiotics

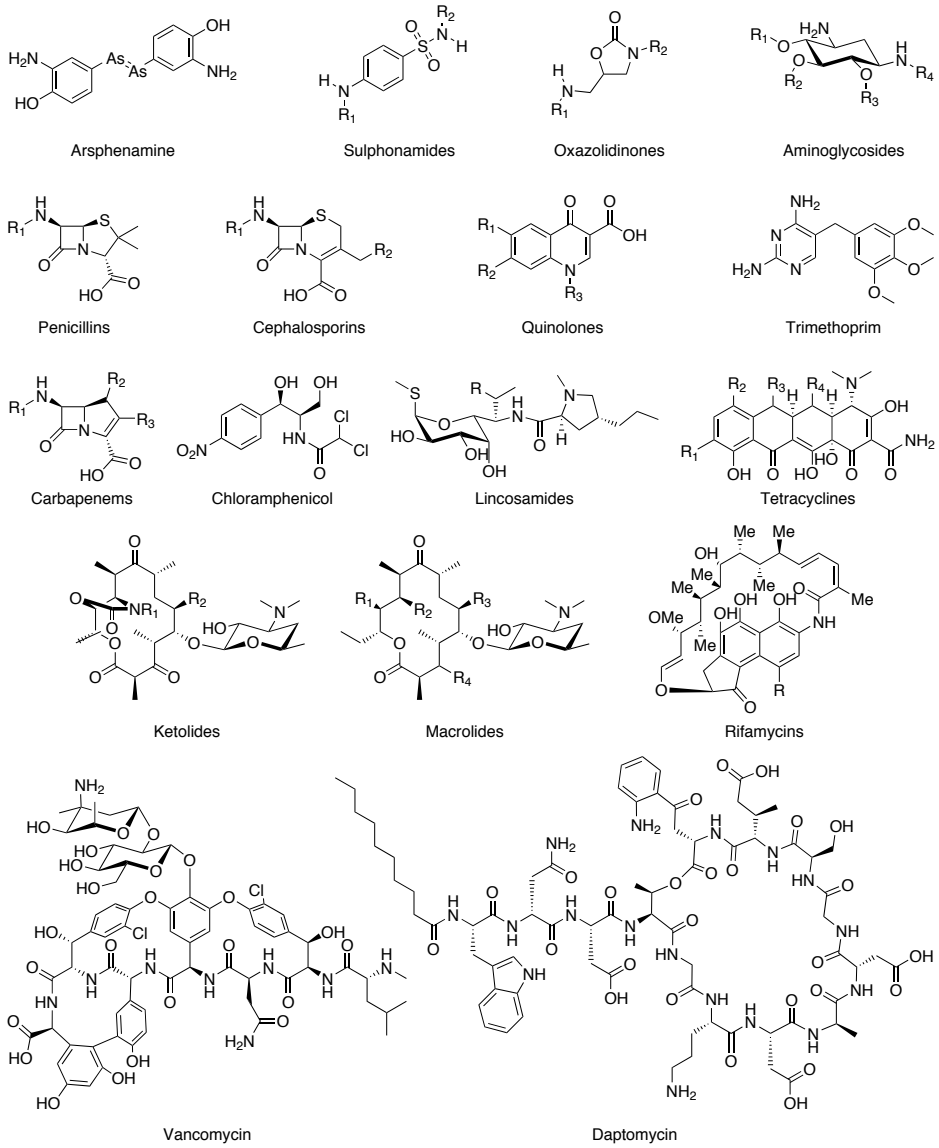

Figure 1: Chemical structures of several clinically used antibiotic families.

All major classes of clinically used antibiotics can be categorized by their modes of action. Inhibition of the bacterial cell wall synthesis pathway is a commonly found strategy and includes the well-known penicillins and cephalosporins (See Figure 1). Many variants of these molecules have been

prepared to improve the spectrum of their activity and overcome resistance. These molecules work through inactivation of the transpeptidase activity of the penicillin binding proteins (PBPs) that crosslink peptidoglycan which makes up the bacterial cell wall.[11] Carbapenems are also part of the ß-lactam family and have an overall broader spectrum of activity as well as a slightly higher stability against ß-lactamases.[12] Besides the ß-lactam family, there is also the family of glycopeptides as typified by vancomycin which interfere with cell wall synthesis. As they are more relevant to the research discussed in this thesis they will be discussed further detail in section 1.6.3.

The aminoglycosides are the biggest class of antibiotics that interfere with bacterial protein synthesis. They bind to the 30S subunit of the bacterial ribosome and interfere with the proper delivery or translocation of tRNAs.[13,14] Other classes of antibiotics that target protein synthesis pathways are: tetracyclines, chloramphenicols, macrolides, ketolides, lincosamides, oxazolidinones, streptogramins.[14,15] The availability of X-ray crystal structures of different ribosomal subunits complexed with several of these antibiotics led to the development of many different varieties within these classes.[16]

Inhibition of RNA synthesis is done by the rifamycins. They have a strong affinity for the prokaryotic RNA polymerase and thereby inhibit the translation of DNA to RNA.[17] Quinolones are inhibitors of gyrase and topoisomerase IV. These enzymes play critical roles in processes that maintain the proper structure of DNA, for example by removing knots in the bacterial chromosome. Interfering with these processes, as is done by the quinolones, leads to an increase in DNA-strand breaks which eventually causes cell death.[18] Alternatively, the sulphonamides and trimethoprim act through inhibition of the folic acid metabolism. They inhibit the synthesis of tetrahydrofolic acid and other essential molecules that come from the folic acid pathway.[19,20] One of the latest added new classes of antibiotics are the lipopeptides. They only have one member at the moment (daptomycin) but that could be extended in the future. They act by disruption of the bacterial cell membrane although the exact way this effect is achieved is not fully understood.[21] Daptomycin and the hypothesis about its mode of action will be further discussed in chapter 5.

1.4 Resistance

Although the modification of existing antibiotic scaffolds has yielded many variants that overcome resistance, it is not likely that such medicinal chemistry

efforts can succeed indefinitely.[5] Furthermore, the lifetime of such a new antibiotic derivative is typically short, since the selective pressure created by using it will yield bacteria with newly acquired resistance.[5,22] In some cases, the onset of resistance has been found within as little as a year of the drug reaching the market.[23] The problem is further increased by the exchange of genetic material between bacteria known as horizontal gene transfer (HGT). Three different mechanism are known to cause transfer of genetic material and these are shown in Figure 2.[24–26]

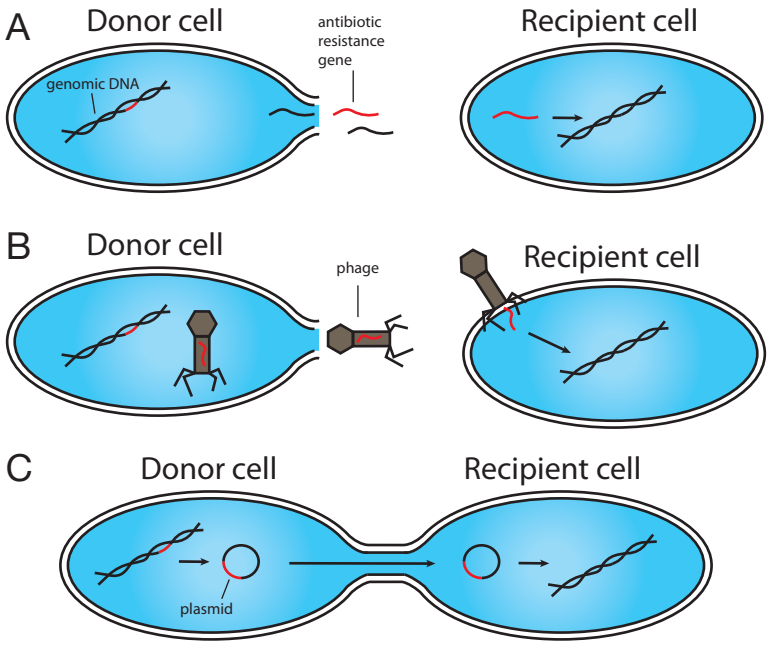

Figure 2: Mechanisms of horizontal gene transfer. A) Transformation. Occurs after lysis of the donor cell causing release of genetic material which can be taken up and integrated by the recipient cell. B) Transduction. Antibiotic resistance genes can be transferred by phages (bacterioviruses) that take up genetic information from the donor cell and transferring it by infecting the recipient cell next. C) Conjugation. If there is direct contact between two bacterial cells, genetic information can be transferred by exchanging plasmids (circular pieces of DNA).[26]

1.4.1 Mechanisms of antibiotic resistance

There are several different mechanisms by which resistance can occur. A well-known mechanism, especially for ß-lactam antibiotics, is chemical modification of the antibiotic itself. The ß-lactamases, which hydrolyze ß-lactam compounds to an inactive form, are now plasmid mediated and can therefore rapidly spread to other organisms.[27] More than 530 different ß-lactamases have been described

and this number is still increasing.[28] Besides enzymes that destroy the antibiotic, there are also enzymes that add different groups to the molecule and thereby render it inactive. Amongst others there are kinases, adenylyltransferases and acetyltransferases.[29,30]

Mutation of the antibiotic target site is also an effective way to generate resistance. The penicillin binding proteins (PBPs) undergo mutation to avoid the inhibition of ß-lactam compounds while still being able to process the bacterial cell wall synthesis. Mutation of the target site is also commonly found for inhibitors of protein synthesis.[31] Likewise, vancomycin resistance is also caused by mutation of its target, in this case lipid II, a resistance mechanism that will be further discussed in section 1.6.5.

Direct modification of the drug or target are only a few methods of resistance. Other mechanisms include decreased permeability of the membrane to the drug (shielding), efflux of the antibiotic from the cell, overproduction of the target, and bypassing the inhibited pathway.[10,25,32,33]

1.4.2 Resistome

As bacteria evolved to produce metabolites that would harm different species while competing for the same environment, they also evolved self-protection genes along with it.[34,35] These genes are often comparable to the genes found on transferable plasmids that give clinical strains their resistance.[36] Considering this, it is reasonable to expect that antibiotics isolated from natural sources have resistance pathways already evolved against them and this is referred to as the resistome. The ß-lactamases were discovered even before the first ß-lactam antibiotic reached the market.[37] Considering the sequence homology of ß-lactamases with the PBPs, it is thought that they have evolved from these proteins through the selective pressure caused by ß-lactam producing organisms.[27] Even more striking is a report by D'Costa et al. showing that a 30,000 year old DNA sample from permafrost soil contained genes that encode resistance against ß-lactams, tetracyclines and glycopeptides. Using X-ray crystallography they fully elucidated the protein encoded by a gene with high similarity to the vancomycin resistance VanA gene and showed it to be highly similar.[38] Combined with HGT it is clear to see how bacteria acquire their resistance and it may therefore be advantageous to look into sources other than natural products for novel antibiotics.

1.5 Lipid II, structure, synthesis and properties

Lipid II is the monomeric precursor to the polymeric bacterial cell wall and has received much attention since its discovery (Figure 3).[39,40] The polymeric structure consists of repeating units of crosslinked disaccharides and peptides. The crosslinking creates a rigid network that is called peptidoglycan (PG) which envelops the cytoplasmic membrane and protects the bacterium from osmotic challenges and mechanical stress.[41,42]

1.5.1 Structure of lipid II

The lipid II molecule is build up from two carbohydrates, a pentapeptide, a pyrophosphate linkage and undecaprenol (Figure 3). The core carbohydrate is *N*-acetyl-muramic acid (MurNAc), to which all the other components are connected. The second carbohydrate is *N*-acetyl-glucosamine and it is connected through a ß-1,4 glycosidic bond to the muramic acid core. The pyrophosphate that links MurNAc to undecaprenol is connected to the anomeric position of MurNAc in the α-configuration. The pentapeptide is connected to the lactic acid moiety on the MurNAc and consists of L-Alanine, D-iso-Glutamic acid, L-Lysine, D-Alanine and D-Alanine. This composition is a generalization of the most commonly found lipid II structure in Gram-positive bacteria and many variations within the peptide stem are observed.[41] The most commonly encountered variation is found in most Gram-negative bacteria where the L-lysine is replaced by meso-diaminopimelic acid.[43,44] Other diamino acids (e.g. L-ornithine or diaminobutyric acid) are also found in this position.[45,46]

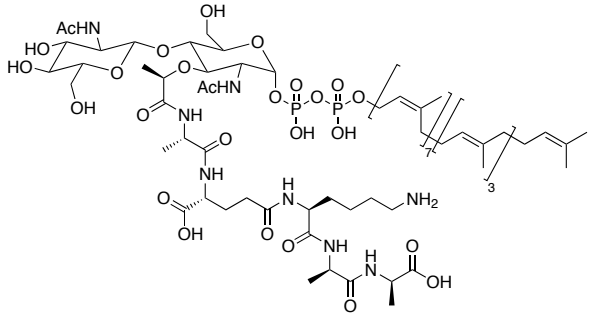

Figure 3: Chemical structure of lipid II.

1.5.2 Biosynthesis of lipid II

Synthesis of the lipid II molecule starts in the cytoplasm from UDP-*N*-acetyl-

glucosamine (UDP-GlcNAc) which is converted by the enzymes MurA and MurB to UDP-*N*-acetyl-muramic acid (UDP-MurNAc). Three amino acid ligases (MurC-MurE) each install one of the first three amino acids of the pentapeptide chain, l-Ala, D-Glu and l-Lys respectively. The pentapeptide is then finalized by MurF which installs the dipeptide D-Ala-D-Ala on the C-terminus. Next, the UDP-MurNAc-pentapeptide is anchored onto undecaprenol-phosphate (C_{55}-P), which is embedded in the cytoplasmic membrane (Figure 4). The reaction is catalysed by the membrane protein MraY and forms uridyl-phosphate as a side-product.[47] At this point, the intermediate formed is called lipid I and this is the final precursor to lipid II. The last step in the synthesis is attachment of *N*-acetyl-glucosamine through a ß-1,4 linkage to the MurNAc core. Another membrane protein, MurG, catalyzes this reaction by using UDP-GlcNAc and lipid I as substrates.[42,48] Once the synthesis is complete, lipid II has to be flipped across the membrane and can be incorporated into the ever growing peptidoglycan layer. The exact method of membrane flipping is still one of the aspects of the cell wall synthesis that requires more investigation. Although MurJ has been proposed as the flippase, it still remains subject of discussion.[49]

1.5.3 Biosynthesis of peptidoglycan

At the periplasmic side of the bacterial membrane the PBPs are responsible for extension of the PG layer by newly synthesized lipid II. The PBPs have a dual catalytic activity. First, they act as glycosyl transferases, forming the glycan strands consisting of the repeating GlcNAc-MurNAc disaccharide from lipid II (Figure 4). In doing so undecaprenol pyrophosphate (C_{55}-PP) is liberated and then recycled for new lipid II synthesis. Second, the PBPs act as transpeptidases, crosslinking the pentapeptide chains to give the peptidoglycan layer its rigidity. Since the cell wall is an ever changing and growing structure it is necessary that it is well regulated and properly constructed. The PBP proteins are divided in classes that catalyse peptidoglycan synthesis during different stages of cell growth (cell elongation, cell division).[42] Several other proteins form a complex with the PBPs and control proper direction of peptidoglycan synthesis and thereby regulate cell morphology. Especially MreB and MreD seem to play an important role in recruiting and positioning the cell wall synthesis machinery, including most of the Mur enzymes that synthesize lipid II and PG.[50] The peptidoglycan layer that is formed is on average 20 layers thick in Gram-positive bacteria. For Gram-negative bacteria an average of only 1.5 layers is observed.[51,52]

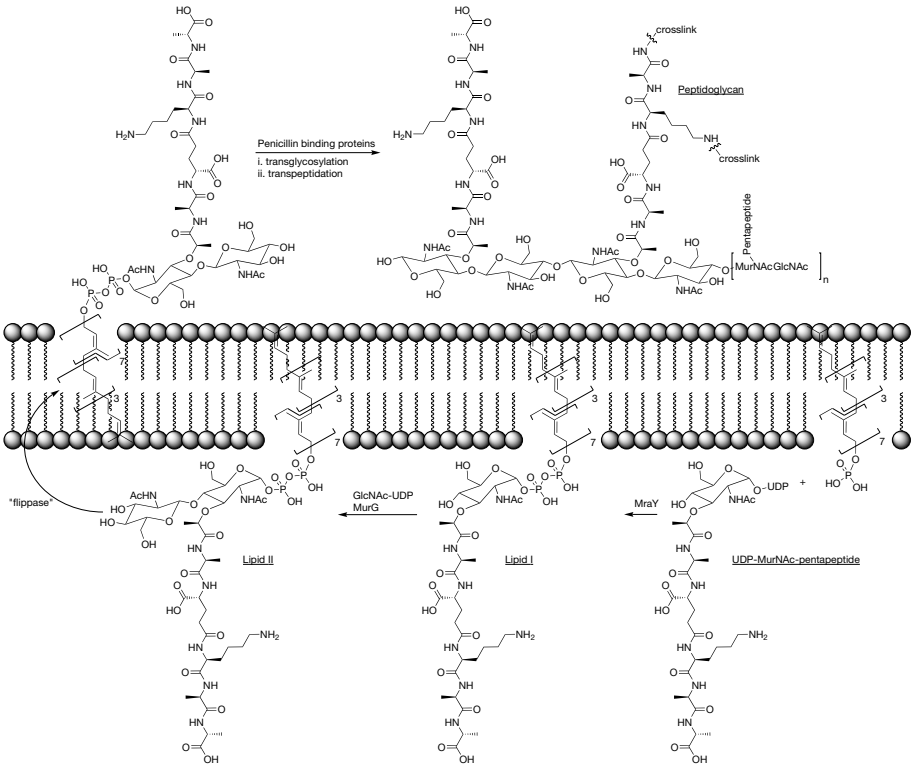

Figure 4: Last steps in lipid II synthesis and the incorporation into peptidoglycan.

1.5.4 Properties of lipid II

Although lipid II is essential for bacterial growth and survival it is present in very low quantities at any given time. For Gram-negative bacteria, with a thin peptidoglycan layer, an estimation of 1000-2000 lipid II molecules per cell was made.[53] Comparatively, Gram-positive bacteria have been estimated to have a higher number of lipid II molecules (estimates range from 34000 to 200000) correlating with the thicker peptidoglycan layer.[54,55] The low numbers indicate that the turnover rate has to be high and this has been estimated at a rate of 1-3 passages through the membrane per prenyl chain per second.[56] The high turnover rate combined with the low number of molecules makes lipid II the bottleneck in cell wall synthesis and an ideal target for antibiotic development.[51]

1.6 Lipid II binding antibiotics

Nature has produced many (often peptidic) antibiotic compounds that use lipid II as a target for their mode of action. Although they all exploit the same

target, their modes of action can be very different. Lipid II targeting antibiotics are intriguing evolutionary products which are inspirational to modern antibacterial research.

1.6.1 Lantibiotics

The lantibiotics are a subset of the so called lantipeptide family and possess antibiotic activity. The name was proposed in 1988 and refers to the lanthionine amino acids that are found in the sequence of these peptides (Figure 5).[57] The most common lanthionines found in these peptides are meso-lanthionine (Lan) and (2S,3S,6R)-3-methyllanthionine (MeLan).[51,58,59] These thioether bridges arise from the enzymatic dehydration of serine and threonine residues to form either dehydroalanine (Dha) or dehydrobutyrine (Dhb) respectively. In a subsequent stereospecific Michael addition reaction with the thiol group of a cysteine residue in the peptide the lanthionine bridge is formed.[60] With more than 60 members identified to date, the lantibiotics represent a large and growing family of biologically active peptides.[61]

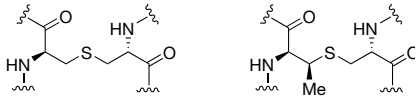

Figure 5: Structure of meso-lanthionine (Lan) and (2S,3S,6R)-3-methyllanthionine (MeLan).

1.6.2 Nisin

The most thoroughly studied lantibiotic is nisin. Nisin is produced by *Lactococcus lactis* strains and is commercially used in the conservation of food products. The inhibitory properties of the producing strain were discovered in 1928 and the responsible peptide was isolated in 1947.[62,63] However, nisin started to receive much more attention when its structure was determined in 1971.[64] Nisin is a 34 amino acid peptide containing 5 lanthionine rings (Figure 6) and several dehydrated amino acids. It has very potent activity against a wide range of Gram-positive bacteria. The biosynthesis of nisin involves several enzymes that regulate its posttranslational modification and excretion (Figure 6). First, nisin is ribosomally synthesized connected to a 23 amino acid leader peptide. All serine and threonine residues, except Ser29, are phosphorylated and then dehydrated by the NisB enzyme. Cyclization between several of the dehydrated residues and cysteines downstream is catalysed by NisC.[59,65,66]

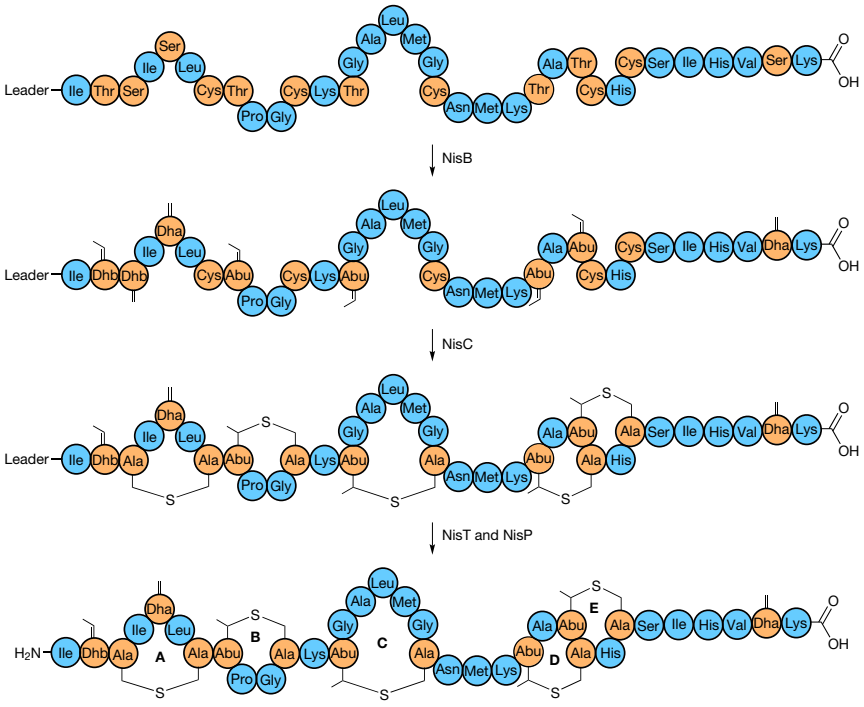

Figure 6: Biosynthesis of nisin.

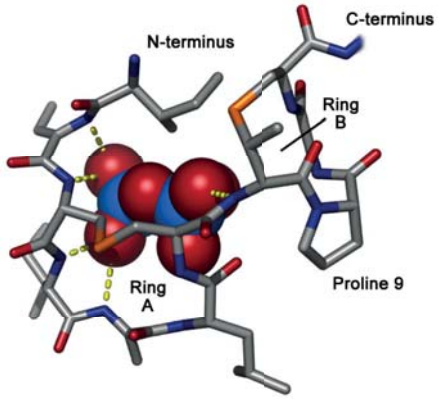

Figure 7: NMR solution structure of the A and B ring of nisin interacting with the pyrophosphate moiety of lipid II. Nisin is represented as sticks and the pyrophosphate as balls. For clarity only the pyrophosphate of lipid II is shown and other parts are omitted in this figure.

Finally, the transporter enzyme NisT, transfers the peptide out of the cell with concomitant cleavage of the leader peptide by NisP to yield active nisin.[67,68]

Nisin has a very distinct dual mode of action involving binding to lipid II followed by membrane insertion and formation of a pore complex. The pore causes essential components to leak out of the cell and results in rapid cell death.[69] Rings A and B are involved in binding to the pyrophosphate part of lipid II as established by the NMR structure of this complex reported in 2004 (Figure 7).[70] The other part of the peptide (rings C-E) is involved in the formation of a stable pore with lipid II. The proposed stoichiometry for the nisin-lipid II interaction is 2:1 and in a fully assembled pore complex there are proposed to be 8 nisin and 4 lipid II molecules.[71]

1.6.3 Glycopeptides

Discovered in 1950, vancomycin was the first clinically used lipid II binding antibiotic (Figure 8). It is the most studied member of the glycopeptide family, which are non-ribosomally synthesized peptides produced by *Amycolaptosis* and *Streptomyces* strains.[72] It's mode of action involves binding to the D-Ala-D-Ala fragment of lipid II and thereby inhibiting the ability of transpeptidases to form crosslinks in peptidoglycan.[73,74] It is now commonly accepted that this is the target of all known glycopeptide antibiotics. Another glycopeptide is teicoplanin, which contains an additional ring and a different glycosylation pattern compared to vancomycin. Furthermore, one of the carbohydrates is modified with a lipid which helps it to retain activity against some vancomycin resistant strains.[74] As this class of antibiotics remains important in the fight against drug-resistant Gram-positive pathogens, several other glycopeptide antibiotics have reached the clinic. These include oritavancin, telavancin, and the recently approved dalbavancin.[75,76] All of these are semisynthetic analogues of either vancomycin (telavancin and oritivancin) or teicoplanin (dalbavancin).[76,77]

1.6.4 Other lipid II binding antibiotics

Although the lantibiotics and glycopeptides are the most thoroughly investigated classes of lipid II binding antibiotics there are several others. Ramoplanin is a 17 amino acid cyclic peptide produced by non-ribosomal peptide synthesis and includes several D-amino acids (Figure 9). The sequence is modified by a short lipid tail and two mannoses.[78] Studies using NMR and water soluble lipid II analogues showed that the pyrophosphate was required for recognition.[79] As its total synthesis is available it has been studied extensively

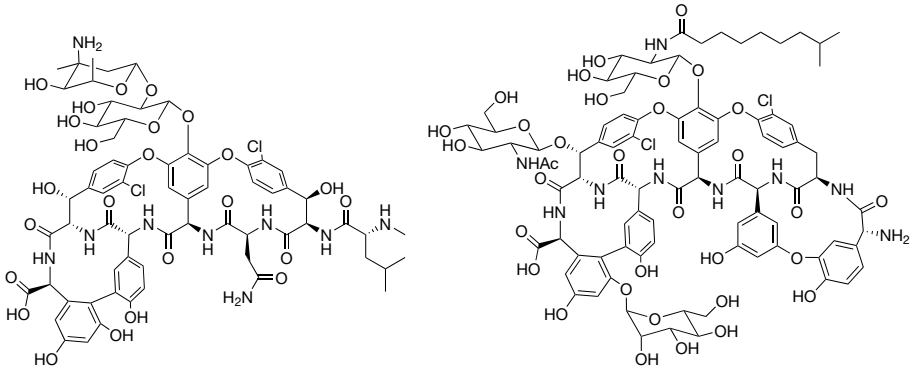

Figure 8: Structures of vancomycin and teicoplanin.

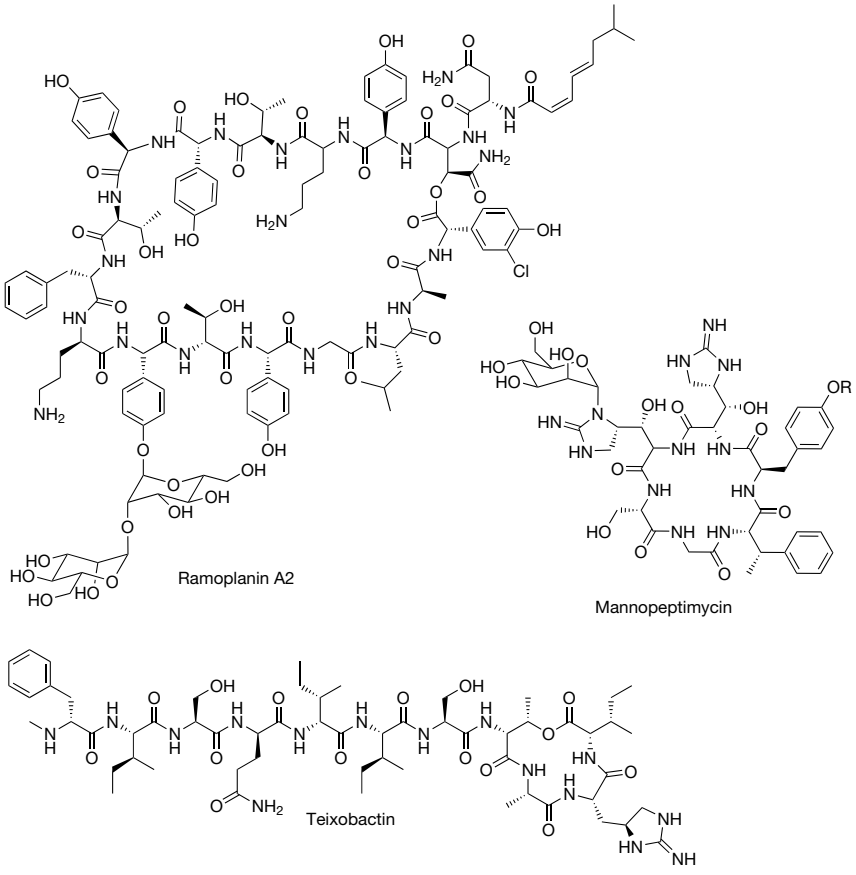

Figure 9: Structures of ramoplanin, the common core of the mannopeptimycins, and teixobactin.

by mutation of amino acids as well as modification of the lipid.[80,81] It was granted fast-track status by the FDA and is used as an orally administered treatment for *C. difficile* infections.

Mannopeptimycins are small 6 amino acid cyclic peptides modified with several mannose units that often contain a small hydrophilic modification.[82] In vitro studies showed that there was no spontaneous resistance which makes the mannopeptimycins attractive as possible therapeutic agents. Several modifications have been made to optimize their activity against a wide variety of organisms including vancomycin resistant strains.[83]

A recently discovered lipid II binding antibiotic reported by Ling et al. is teixobactin.[84] It was discovered using the so-called "iChip" technology that allows soil-bacteria, that are otherwise non-culturable under laboratory conditions, to grow to full colonies.[85] The iChip allows culturing of approximately 50% of all soil dwelling bacteria, while estimates for standard lab culturing conditions are only around 1%. By screening the isolates from the iChip for antimicrobial activity against *S. aureus*, a new species, *Eleftheria terrae*, was found to have good activity. After purification of the active substance a wide variety of assays were applied to determine teixobactin's structure, activity and mode of action. Most notably was its activity against *C. difficile* and *B. anthracis* with MICs of 5 and 20 ng/ml respectively. After serial passage of *S. aureus* with sub-MIC doses of teixobactin for 27 days no resistance was noted. It was also found that lipid II, lipid I and C_{55}-PP are all bound by teixobactin as well as the wall teichoic acid precursor lipid III. To further study the therapeutic potential of teixobactin, it was used in a mouse septicaemia model and showed 100% survival at a 0.5 mg/kg dose.

1.6.5 Resistance to lipid II binding antibiotics

Although resistance against lipid II binding compounds does occur, it is much less pronounced and slower of onset when compared to other antibiotics. Only two mechanisms of resistance are typically observed, shielding by reducing access to lipid II, or mutation of the lipid II peptide stem.[51] Other resistance mechanisms like efflux from the cell or bypassing of cell wall synthesis are either not relevant or possible. For antibiotics like nisin, very little resistance is observed and even if it is detected it is often reversed when nisin pressure is removed.[86] It was found that nisin resistance does not occur by altering lipid II levels as these were similar for both resistant and susceptible strains. The reduced susceptibility to nisin seems to be caused by alteration of wall teichoic acids

(WTA) present in the bacterial cell wall. The addition of D-alanine to WTA reduces the overall negative charge of the cell wall thereby reducing the accessibility of lipid II for the positively charged nisin.[87,88] Ramoplanin resistance is not yet clinically observed but can be forced in a laboratory setting and seems to be related to a thickened cell wall. However, when the drug is removed from the resistant bacterial cultures, the resistance is completely reversed.[89]

A very different mechanism is at work in vancomycin resistance. As discussed in paragraph 1.4.2 vancomycin resistance has coevolved with vancomycin itself and has led to the VanA gene that encodes for vancomycin resistance. Besides the VanA gene there are several other genes encoding for vancomycin resistance.[90,91] These genes encode for enzymes that replace the D-Ala found at the C-terminus of the lipid II peptide for D-lactate or D-serine. By modifying the recognition site of vancomycin, its affinity for lipid II is drastically lowered and resistance occurs. Besides those enzymes there are also others that can remove the C-terminal D-Ala entirely.[90] Since vancomycin is an antibiotic of "last-resort" resistance to it can be a big threat as there are a very limited number of alternative treatment options. In this regard infections with vancomycin-resistant enterococci (VRE) are a major clinical problem with *E. faecium* infections being resistant in 80-95% of the cases.[92] It is important to note that it took more then 30 years after introduction of vancomycin to the clinic before resistance was observed. Compared to other antibiotics this is much longer which makes lipid II still a very attractive target for drug development.[5]

1.7 Phage display

Phage display was introduced in 1985 and has since then been developed into a common technique for the identification of novel peptides and antibodies that bind to a given target.[93] Phages are simple viruses that specifically infect and replicate in bacterial cells. The technique is based on the genetic incorporation of random DNA fragments into the phage plasmid DNA. The products of these DNA-fragments are then expressed as peptides, proteins or antibodies connected to one of the phage envelope proteins.[94] Using this method large libraries of potential binders can be rapidly screened against a target of interest. Phage display has proven to be a very powerful technique, especially for the development of new therapeutic antibodies. In 2014 there were 6 approved therapeutic antibodies on the market that found their origin in phage display.[95] The work described in this thesis relied heavily on peptide phage display.

Traditionally peptides have not been considered to be drug-like molecules as they typically have poor pharmacokinetic properties, are rapidly degraded, and have poor absorption through the intestine.[96,97] However, this view is rapidly changing as more and more peptide or peptide-based drugs reach the market. Therapeutic peptides are now available for many different indications ranging from angina to multiple myeloma.[97,98] Most of the pharmacokinetic problems that peptides encounter are due to proteolytic instability in the human blood. It is the advances made in modification strategies that have helped to overcome this instability, allowing many new peptidic drugs to be developed.[99,100] At present one peptide (Ecallantide) that originated from phage display has been approved for clinical use in hereditary angioedema and several others are in clinical trials for chronic kidney disease, cystic fibrosis and oncology.[97,101]

1.7.1 Filamentous phage biology

Although different systems are available, the most commonly used phage for phage display is the filamentous M13 phage (Figure 10).[94] An M13 phage particle consist of a single stranded piece of circular DNA which is coated with several proteins. They infect by binding to the extracellular filament known as the F pilus that can be expressed by certain Gram-negative bacteria (e.g. *E. coli*).[102] The DNA is about 6000-8000 basepairs and encodes for 11 proteins (pI-pXI), of which 5 are coat proteins, 3 are DNA replication proteins and the other 3 are involved in the assembly of the phage particle.[97,102,103] The protein coat is almost entirely made from pVIII with 2700 copies covering the entire DNA strand lengthwise. Coat proteins pIII and pVI each have 5 copies on one end of the phage, while pVII and pIX also have 5 copies at the other end of the phage. Filamentous phage are typically non-lytic and leave their host cell intact during production.

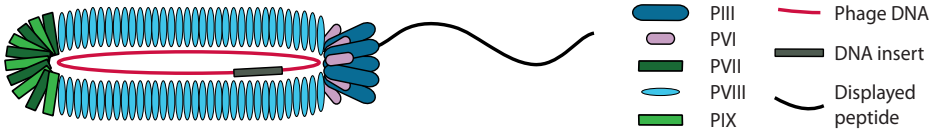

Figure 10: Schematic representation of the M13 filamentous phage.

The first step in the phage lifecycle is infection of the bacterial host through binding to the F pilus by pIII. The pilus retracts and the phage DNA is introduced into the bacterial cell. Proteins from the bacterial host itself as well as pII and pX from the phage are involved in the amplification of the phage plasmid. In the next step of assembly, the newly formed plasmid is coated by several copies

of pV after which it locates to the cell membrane. In the membrane the export machinery, assembled from pI, pIV, pXI and thioredoxin, then will extrude the phage out of the cell. During the extrusion process, pV is removed from the plasmid followed by addition of the coat proteins to yield the mature phage.[102,104]

1.7.2 Peptide phage display library construction

To perform a peptide phage display screening experiment, a phage library has to be prepared. Several commercial libraries are available and include both linear (Ph.D.™-7 and Ph.D.™-12 from New England Biolabs and T7Select® from Merck) and disulfide cyclized peptides (Ph.D.™-C7C). It is also possible to generate libraries by molecular cloning techniques, which allows the user to incorporate specific sequences. To generate a large diversity of peptides it is common to use chemically synthesized DNA inserts to encode for the peptides. These inserts are made by using NNK codons, where N is an equimolar mixture of all four bases and K and equimolar mixture of only G and T. Using NNK codons is specifically done as it allows all 20 amino acids to be encoded while decreasing the possibility for a stop codon. If an NNN codon would be used, all three stop codons (TAA, TGA and TAG) could be incorporated but with NNK only one (TAG) can be generated.[97,102] After the synthetic DNA strands have been incorporated into the phage vector by ligation techniques, the plasmids can be transformed into E. coli where the phage are produced. The number of possible peptides produced is determined by the length of the peptide and can be described by 20^n, where n is the number of amino acids in the peptide. Although practically this number is never achieved because of limitations in transformation efficiency and diversity is typically between 10^8-10^{10} peptides.[105]

1.7.3 Selection protocols

Once a phage library has been constructed it can be screened against a target of interest, a process commonly referred to as “biopanning”. In a typical phage display experiment the target is immobilized onto a surface (e.g. tubes, 96-wells plates, or magnetic beads) as shown in Figure 11 (step 1). Immobilization can be done by passive adsorption or through any number of immobilization techniques including the biotin/streptavidin interaction. For small molecule targets it is also possible to use a chemically modified surface to attach the target covalently. It is important to note however, that the immobilization step has to be chosen so that the binding possibilities to the target are not disturbed.[106] The phage are

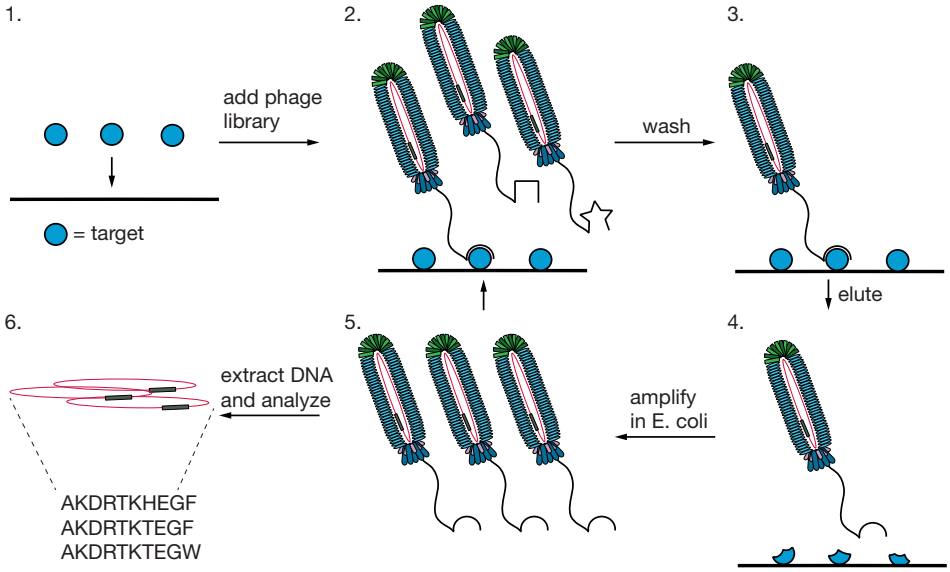

Figure 11: All steps in a phage display experiment.

then incubated with the immobilized target (Figure 11, step 2), followed by a washing step to remove non-binding phage (step 3). To select for high-affinity binders, the stringency of the washing step can be increased each round.[94,106] Increasing the stringency can be done by either including more washes, higher detergent concentrations, or by changing the pH of the washing buffer.[105] After washing the binding phage are eluted (step 4) and again several methods can be chosen to do so, with one of the more common techniques being treating the bound phage with a low pH buffer (pH 2.2). Most peptide/protein interactions will be disturbed by such a low pH but the highly stable phage will survive. Other non-specific methods include elution with high pH, denaturation, the addition of excess target, excess biotin, ultrasound, or proteolytic degradation of the target. If a binder to a specific site of a protein target is desired (e.g. an enzyme inhibitor), elution can be performed with an excess of a known binder or an endogenous ligand.[94,102,107] After the binding phage have been eluted, they are incubated with *E.coli* to infect and amplify (step 5). Each eluted phage will replicate several times and the new phage pool can be taken through another round of biopanning (starting from step 2). When several rounds have been completed, phage clones are isolated and their DNA analyzed (step 6). If the selection is successful, a consensus peptide sequence is identified after analyzing the DNA. Chemical synthesis of the consensus peptide sequence in turn then allows further analysis and optimization of the peptide binder identified.

1.7.4 Selection bias and high-throughput DNA analysis in phage display

Although the extraction of DNA from a single phage clone is not difficult, it is very laborious to characterize many clones so as to obtain the level of information wanted. Multiple selection rounds are typically required to get enough enrichment of a single peptide sequence, especially when using small molecular targets or when only low affinity binders can be identified. In such cases it is not advantageous to perform many biopanning rounds, as selection can also be driven by factors other than target binding. A higher infectivity or faster propagation rate of a particular phage clone or other non-specific interactions can cause off target enrichment.[108] These non-specific interactions can include phage that bind to material used during screening, for example plastics, streptavidin, or bovine serum albumin.[109] Such peptides are known as target-unrelated peptides (TUPs) and databases of these TUPs have been generated to help researches identify false positives.[110] A good solution to avoid the need for multiple rounds of selection is the use of high-throughput sequencing techniques (also referred to as next-generation sequencing or deep sequencing). DNA analysis techniques have developed significantly over the last decade and platforms like Illumina or IonTorrent can supply millions of reads from a single sample.[111] Previous work has shown that using high-throughput sequencing techniques can separate binding clones from background phage already after a single round of selection.[112] Using these techniques it is not required to isolate single phage clones, as the entire eluted phage pool is subjected to sequencing analysis instead. Several algorithms have been developed to analyse the data obtained from such an analyses to give the user information about sequence abundance and homology.[111,113]

1.7.5 Bicyclic phage display

Many variations on the original peptide phage display protocol have been described and the one used in the research described in this thesis is bicyclic peptide phage display. Bicyclic peptide phage display was developed by Heinis and coworkers in 2009 and used to identify bicyclic peptides with low nanomolar affinities to the human plasma protein kallikrein.[114] The bicyclic phage display method uses a phage peptide library that always has three cysteine residues at fixed positions. Prior to screening, the phage library is treated with 1,3,5-tris(bromomethyl)benzene which rapidly and selectively reacts with the cysteines to generate a bicyclic peptide on the phage (see Figure 12).

[114,115] The use of cysteine-free phages makes sure the reagent doesn't react anywhere else on the phage surface. Bicyclization of peptides using this so-called "CLIPS" reaction was first described by Timmerman et al. in 2005 and they showed that these cyclized peptides had improved binding properties over their linear counterparts.[116] Since these peptides are less flexible, the loss of entropy upon binding to a target is decreased when compared to linear versions. Furthermore, the bicyclic peptides have a significantly increased proteolytic stability. Degradation of monocyclic and linear analogues of an urokinase-type plasminogen activator (uPA) inhibitor in plasma was found to be much faster than the bicyclic version of this peptide.[117]

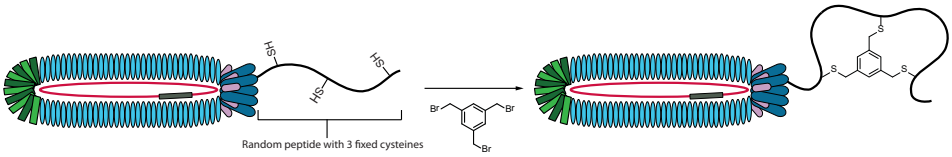

Figure 12: Bicyclization using the CLIPS-reaction on a phage particle.

Initially the phage libraries were designed so that each loop in the bicyclic peptide contained 6 amino acids and the cyclization reagent used was 1,3,5-tris(bromomethyl)benzene. To date several other options have been explored and libraries containing 3-6 amino acids per loop and combinations of different loops sizes are available.[118] The cyclization reagent can be changed to generate different linkages and produce a more diverse chemical space. Besides the original bromide reagent multiple reagents have been developed, all with threefold rotational symmetry to generate a single isomer in the bicyclization reaction. These reagents are based on bromoacetamide or acrylamide on either a benzene or triazinane core.[119] Another more recently developed approach is to use a photoswitchable cyclization reagent, allowing the binding bicyclic peptide ligand to be switched on and off using UV-light.[120]

1.7.6 Mirror image phage display

Another strategy to improve the stability of peptides is by making them from D-amino acids. Since proteins and peptides in nature are almost exclusively made of L-amino acids, D-amino acid peptides are generally not recognized by proteases and left intact. To identify D-amino acid peptides by phage display, a method was developed by Schumacher et al. in 1996.[121] The method was dubbed "mirror-image" phage display and requires the target to be presented in the exact opposite enantiomeric form. With the target presented as the

enantiomer a normal L-peptide phage library is then used to screen for binding peptides. Through the rules of symmetry, it is given that the D-enantiomer of any binding peptide identified will have the same affinity for the normal, non-enantiomeric form of the target. Most commonly this is done with protein targets that can be prepared in D-form through a combination of peptide synthesis and ligation methods.[122] Several targets have been applied to mirror-image phage with succes including the HIV-1 gp41 protein.[123,124]

1.8 Outline

In this thesis we describe research done on both natural and novel antimicrobial peptides. Considering the advantages of lipid II as a target of antibiotics we investigated its use as a target in peptide phage display screens to identify novel binders. This required the synthesis of various analogues of lipid II as described in chapter 2. Although the synthesis is largely based on literature, several steps were optimized and several new modifications were introduced.

The synthetic lipid II analogues were used for phage display selection as described in chapter 3. Although phage display is a commonly used technique, there are very few descriptions of its use with small molecular targets in the literature. Optimization of the selection protocol was therefore required as well as analysis of the output by high-throughput DNA sequencing. We further describe the synthesis, antimicrobial analysis, and optimization of the peptides that came from the screening experiments in chapter 3.

In chapter 4 the use of synthetic analogues of lipid II for examining nisin's mode of action is described. By employing isothermal titration calorimetry (ITC) we investigated the binding affinity of nisin for several truncated lipid II analogues. These analogues were incorporated into large unilamellar vesicles (LUVs) of DOPC and titrated into nisin. The binding affinity and thermodynamic parameters obtained provided new insights into the structure activity relationship of nisin and lipid II. Besides vesicle-based titrations we also performed a titration with a synthetic water soluble lipid II analogue to demonstrate the importance of a lipid environment.

Chapter 5 describes the synthesis and evaluation of several analogues of the clinically used antibiotic daptomycin. To investigate the role of a chiral target in daptomycin's mode of action we synthesized analogues of daptomycin in its unnatural enantiomeric form. Our results indicated that a chiral target seems to be present for daptomycin.

In chapter 6 we describe the design and synthesis of three series of peptides as inhibitors of the protein arginine methyltransferases (PRMTs). The first series was based on a known PRMT substrate peptide known as "R1". The single arginine in this peptide was modified with differently fluorinated ethyl groups and tested as substrates and inhibitors of PRMT1, -4 and -6. They showed low micromolar IC_{50} values against PRMT 1 and 6. The second set was designed as partial bisubstrate inhibitors based on the same R1 peptide sequence and the PRMT cofactor S-adenosyl-L-methionine (AdoMet). Two peptides were prepared of which one (R1-Lys) was an inhibitor of all tested PRMTs (1, 4 and 6) and the other peptide (R1-Orn) was selective for PRMT6. The third set of peptides was based on the cell penetrating HIV-Tat peptide. Although multiple arginine residues are present in this sequence it had previously been show that one residue was selectively recognized by PRMT6. With several modifications of this residue we attempted to find potent PRMT6 selective inhibitors. Although PRMT6 was inhibited with low micromolar IC_{50} values, the designed peptides also inhibited PRMT1.

References

[1] R. Laxminarayan, A. Duse, C. Wattal, A. K. M. Zaidi, H. F. L. Wertheim, N. Sumpradit, E. Vlieghe, G. L. Hara, I. M. Gould, H. Goossens, et al., *Lancet Infect. Dis.* **2013**, *13*, 1057–1098.

[2] C. A. Arias, B. E. Murray, *N. Engl. J. Med.* **2015**, *372*, 1168–1170.

[3] L. L. Maragakis, E. N. Perencevich, S. E. Cosgrove, *Expert Rev. Anti. Infect. Ther.* **2008**, *6*, 751–763.

[1] R. Laxminarayan, A. Duse, C. Wattal, A. K. M. Zaidi, H. F. L. Wertheim, N. Sumpradit, E. Vlieghe, G. L. Hara, I. M. Gould, H. Goossens, et al., *Lancet Infect. Dis.* **2013**, *13*, 1057–1098.

[2] C. A. Arias, B. E. Murray, *N. Engl. J. Med.* **2015**, *372*, 1168–1170.

[3] L. L. Maragakis, E. N. Perencevich, S. E. Cosgrove, *Expert Rev. Anti. Infect. Ther.* **2008**, *6*, 751–763.

[4] Review on Antimicrobial Resistance, *UK Gov.* **2014**.

[5] C. T. Walsh, T. A. Wencewicz, *J. Antibiot.* **2013**, 1–16.

[6] L. Zaffiri, J. Gardner, L. H. Toledo-Pereyra, *J. Investig. Surg.* **2012**, *25*, 67–77.

[7] H. Otten, *J. Antimicrob. Chemother.* **1986**, *17*, 689–696.

[8] D. M. Livermore, *J. Antimicrob. Chemother.* **2011**, *66*, 1941–1944.

[9] M. A. Fischbach, C. T. Walsh, *Science* **2009**, *325*, 1089–1093.
[10] A. R. Coates, G. Halls, Y. Hu, *Br. J. Pharmacol.* **2011**, *163*, 184–194.
[11] J.-M. Frère, M. G. Page, *Curr. Opin. Pharmacol.* **2014**, *18*, 112–119.
[12] K. M. Papp-Wallace, A. Endimiani, M. A. Taracila, R. A. Bonomo, *Antimicrob. Agents Chemother.* **2011**, *55*, 4943–4960.
[13] M. L. Avent, B. A. Rogers, A. C. Cheng, D. L. Paterson, *Intern. Med. J.* **2011**, *41*, 441–449.
[14] D. N. Wilson, *Nat. Rev. Microbiol.* **2014**, *12*, 35–48.
[15] G. G. Zhanel, M. Dueck, D. J. Hoban, L. M. Vercaigne, J. M. Embil, A. S. Gin, J. A. Karlowsky, *Drugs* **2001**, *61*, 443–498.
[16] J. A. Sutcliffe, *Curr. Opin. Microbiol.* **2005**, *8*, 534–542.
[17] H. G. Floss, T.-W. Yu, *Chem. Rev.* **2005**, *105*, 621–632.
[18] K. J. Aldred, R. J. Kerns, N. Osheroff, *Biochemistry* **2014**, *53*, 1565–1574.
[19] E. L. Stokstad, T. H. Jukes, *J. Nutr.* **1987**, *117*, 1335–1341.
[20] H. Brötz-Oesterhelt, N. A. Brunner, *Curr. Opin. Pharmacol.* **2008**, *8*, 564–573.
[21] L. Robbel, M. A. Marahiel, *J. Biol. Chem.* **2010**, *285*, 27501–27508.
[22] S. R. Palumbi, *Science* **2001**, *293*, 1786–1790.
[23] D. R. Gentry, L. McCloskey, M. N. Gwynn, S. F. Rittenhouse, N. Scangarella, R. Shawar, D. J. Holmes, *Antimicrob. Agents Chemother.* **2008**, *52*, 4507–4509.
[24] P. Courvalin, *J. Intern. Med.* **2008**, *264*, 4–16.
[25] L. L. Silver, *Clin. Microbiol. Rev.* **2011**, *24*, 71–109.
[26] E. Y. Furuya, F. D. Lowy, *Nat. Rev. Microbiol.* **2006**, *4*, 36–45.
[27] P. A. Bradford, *Clin. Microbiol. Rev.* **2001**, *14*, 933–951.
[28] M. Babic, A. M. Hujer, R. A. Bonomo, *Drug Resist. Updat.* **2006**, *9*, 142–156.
[29] G. D. Wright, *Chem. Commun.* **2011**, *47*, 4055–4061.
[30] G. De Pascale, G. D. Wright, *ChemBioChem* **2010**, *11*, 1325–1334.
[31] P. F. McDermott, R. D. Walker, D. G. White, *Int. J. Toxicol.* **2003**, *22*, 135–143.
[32] M. A. Webber, L. J. V Piddock, *J. Antimicrob. Chemother.* **2003**, *51*, 9–11.
[33] L. V. J. Blair, J. M. A., Webber, M. A., Baylay, A. J., Ogbolu, D. O, Piddock, *Nat. Rev. Microbiol.* **2011**, *42*, 42–51.
[34] E. Cundliffe, N. Bate, A. Butler, S. Fish, A. Gandecha, L. Merson-

Davies, *Anton. Leeuw. Int. J. G.* **2001**, *79*, 229–234.
[35] G. D. Wright, *Nat. Rev. Microbiol.* **2007**, *5*, 175–186.
[36] V. M. D'Costa, K. M. McGrann, D. W. Hughes, G. D. Wright, *Science* **2006**, *311*, 374–377.
[37] E. P. Abraham, E. Chain, *Nature* **1940**, *146*, 837.
[38] V. M. D'Costa, C. E. King, L. Kalan, M. Morar, W. W. L. Sung, C. Schwarz, D. Froese, G. Zazula, F. Calmels, R. Debruyne, et al., *Nature* **2011**, *477*, 457–461.
[39] A. N. Chatterjee, J. T. Park, *Proc. Natl. Acad. Sci. U. S. A.* **1964**, *51*, 9–16.
[40] J. S. Anderson, M. Matsuhashi, M. A. Haskin, J. L. Strominger, *Proc. Natl. Acad. Sci. U. S. A.* **1965**, *53*, 881–889.
[41] W. Vollmer, D. Blanot, M. A. de Pedro, *FEMS Microbiol. Rev.* **2008**, *32*, 149–167.
[42] A. Typas, M. Banzhaf, C. A. Gross, W. Vollmer, *Nat. Rev. Microbiol.* **2011**, *10*, 123–136.
[43] D. Patin, A. Boniface, A. Kovač, M. Hervé, S. Dementin, H. Barreteau, D. Mengin-Lecreulx, D. Blanot, *Biochimie* **2010**, *92*, 1793–1800.
[44] J. van Heijenoort, *Microbiol. Mol. Biol. Rev.* **2007**, *71*, 620–635.
[45] D. Munch, I. Engels, A. Muller, K. Reder-Christ, H. Falkenstein-Paul, G. Bierbaum, F. Grein, G. Bendas, H.-G. Sahl, T. Schneider, *Antimicrob. Agents Chemother.* **2014**, *49*, DOI 10.1128/AAC.02663-14.
[46] D. Münch, I. Engels, A. Müller, K. Reder-Christ, H. Falkenstein-Paul, G. Bierbaum, F. Grein, G. Bendas, H.-G. Sahl, T. Schneider, *Antimicrob. Agents Chemother.* **2015**, *59*, 772–781.
[47] A. Bouhss, M. Crouvoisier, D. Blanot, D. Mengin-Lecreulx, *J. Biol. Chem.* **2004**, *279*, 29974–2 9980.
[48] L.-Y. Huang, S.-H. Huang, Y.-C. Chang, W.-C. Cheng, T.-J. R. Cheng, C.-H. Wong, *Angew. Chem. Int. Ed.* **2014**, *402*, 8060–8065.
[49] L.-T. Sham, E. K. Butler, M. D. Lebar, D. Kahne, T. G. Bernhardt, N. Ruiz, *Science* **2014**, *345*, 220–222.
[50] C. L. White, A. Kitich, J. W. Gober, *Mol. Microbiol.* **2010**, *76*, 616–633.
[51] E. Breukink, B. de Kruijff, *Nat. Rev. Drug Discov.* **2006**, *5*, 321–332.
[52] H. Labischinski, E. W. Goodell, A. Goodell, M. L. Hochberg, *J. Bacteriol.* **1991**, *173*, 751–756.
[53] M. Gomez, M. Derrien, J. Ayala, J. van Heijenoort, **1992**, *174*, 3549–3557.

[54] E. Fuchs-Cleveland, C. Gilvarg, *Proc. Natl. Acad. Sci. U. S. A.* **1976**, *73*, 4200–4204.
[55] H. Brötz, G. Bierbaum, K. Leopold, P. E. Reynolds, H.-G. Sahl, *Antimicrob. Agents Chemother.* **1998**, *42*, 154–160.
[56] M. A. McCloskey, F. A. Troy, *Biochemistry* **1980**, *19*, 2061–2066.
[57] N. Schnell, K. D. Entian, U. Schneider, F. Götz, H. Zähner, R. Kellner, G. Jung, *Nature* **1988**, *333*, 276–278.
[58] C. Chatterjee, M. Paul, L. Xie, W. A. van der Donk, *Chem. Rev.* **2005**, *105*, 633–683.
[59] N. I. Martin, E. Breukink, *Future Microbiol.* **2007**, *2*, 513–525.
[60] J. M. Willey, W. A. van der Donk, *Annu. Rev. Microbiol.* **2007**, *61*, 477–501.
[61] G. Bierbaum, H.-G. Sahl, *Curr. Pharm. Biotechnol.* **2009**, *10*, 2–18.
[62] L. A. Rogers, *J. Bacteriol.* **1928**, 321–325.
[63] A. T. R. Mattick, A. Hirsch, *Lancet* **1947**, *2*, 5–8.
[64] E. Gross, J. L. Morell, *J. Am. Chem. Soc.* **1971**, *93*, 4634–4635.
[65] B. Li, J. P. J. Yu, J. S. Brunzelle, G. N. Moll, W. A. van der Donk, S. K. Nair, *Science* **2006**, *311*, 1464–1467.
[66] O. Koponen, M. Tolonen, M. Qiao, G. Wahlström, J. Helin, P. E. J. Saris, *Microbiology* **2002**, *148*, 3561–3568.
[67] J. R. Van der Meer, J. Polman, M. M. Beerthuyzen, R. J. Siezen, O. P. Kuipers, W. M. De Vos, *J. Bacteriol.* **1993**, *175*, 2578–2588.
[68] M. Qiao, P. E. J. Saris, *FEMS Microbiol. Lett.* **1996**, *144*, 89–93.
[69] E. Ruhr, H.-G. Sahl, *Antimicrob. Agents Chemother.* **1985**, *27*, 841–845.
[70] S.-T. D. Hsu, E. Breukink, E. Tischenko, M. A. G. Lutters, B. de Kruijff, R. Kaptein, A. M. J. J. Bonvin, N. A. J. van Nuland, *Nat. Struct. Mol. Biol.* **2004**, *11*, 963–967.
[71] H. E. Hasper, B. de Kruijff, E. Breukink, *Biochemistry* **2004**, *43*, 11567–11575.
[72] B. K. Hubbard, C. T. Walsh, *Angew. Chem. Int. Ed.* **2003**, *42*, 730–765.
[73] D. H. Williams, M. P. Williamson, D. W. Butcher, S. J. Hammond, *J. Am. Chem. Soc.* **1983**, *105*, 1332–1339.
[74] D. Kahne, C. Leimkuhler, W. Lu, C. Walsh, *Chem. Rev.* **2005**, *105*, 425–448.
[75] G. D. Wright, *Chem. Biol.* **2012**, *19*, 3–10.
[76] K. D. Leuthner, A. Yuen, Y. Mao, **2015**, 149–159.
[77] R. C. James, J. G. Pierce, A. Okano, J. Xie, D. L. Boger, *ACS Chem.*

Biol. **2012**.

[78] B. Cavalleri, H. Pagani, G. Volpe, E. Selva, F. Parenti, *J. Antibiot.* **1983**, *37*, 309–317.

[79] P. Cudic, J. K. Kranz, D. C. Behenna, R. G. Kruger, H. Tadesse, A. J. Wand, Y. I. Veklich, J. W. Weisel, D. G. McCafferty, *Proc. Natl. Acad. Sci. U. S. A.* **2002**, *99*, 7384–7389.

[80] S. Walker, L. Chen, Y. Hu, Y. Rew, D. Shin, D. L. Boger, *Chem. Rev.* **2005**, *105*, 449–475.

[81] W. Jiang, J. Wanner, R. J. Lee, P. Y. Bounaud, D. L. Boger, *J. Am. Chem. Soc.* **2003**, *125*, 1877–1887.

[82] H. He, R. T. Williamson, B. Shen, E. I. Graziani, H. Y. Yang, S. M. Sakya, P. J. Petersen, G. T. Carter, *J. Am. Chem. Soc.* **2002**, *124*, 9729–9736.

[83] A. Ruzin, G. Singh, A. Severin, Y. Yang, R. G. Dushin, A. G. Sutherland, A. Minnick, M. Greenstein, M. K. May, D. M. Shlaes, et al., *Antimicrob. Agents Chemother.* **2004**, *48*, 728–738.

[84] L. L. Ling, T. Schneider, A. J. Peoples, A. L. Spoering, I. Engels, B. P. Conlon, A. Mueller, D. E. Hughes, S. Epstein, M. Jones, et al., *Nature* **2015**, *517*, 455–459.

[85] D. Nichols, N. Cahoon, E. M. Trakhtenberg, L. Pham, A. Mehta, A. Belanger, T. Kanigan, K. Lewis, S. S. Epstein, *Appl. Environ. Microbiol.* **2010**, *76*, 2445–2450.

[86] N. E. Kramer, E. J. Smid, J. Kok, B. De Kruijff, O. P. Kuipers, E. Breukink, *FEMS Microbiol. Lett.* **2004**, *239*, 157–161.

[87] F. C. Neuhaus, J. Baddiley, *Microbiol. Mol. Biol. Rev.* **2003**, *67*, 686–723.

[88] E. A. Davies, M. B. Falahee, M. R. Adams, *J. Appl. Bacteriol.* **1996**, *81*, 139–146.

[89] J. W. Schmidt, A. Greenough, M. Burns, A. E. Luteran, D. G. McCafferty, *FEMS Microbiol. Lett.* **2010**, *310*, 104–111.

[90] D. Meziane-Cherif, P. J. Stogios, E. Evdokimova, A. Savchenko, P. Courvalin, *Proc. Natl. Acad. Sci. U. S. A.* **2014**, *111*, 5872–5877.

[91] V. L. Healy, D. I. Roper, J. R. Knox, C. T. Walsh, *Chem. Biol.* **2000**, *7*, 109–119.

[92] K. Hayakawa, E. T. Martin, U. M. Gudur, D. Marchaim, D. Dalle, K. Alshabani, K. S. Muppavarapu, F. Jaydev, P. Bathina, P. R. Sundaragiri, et al., *Antimicrob. Agents Chemother.* **2014**, *58*, 3968–3975.

[93] G. P. Smith, *Science* **1985**, *228*, 1315–1317.

[94] J. Pande, M. M. Szewczyk, A. K. Grover, *Biotechnol. Adv.* **2010**, *28*, 849–858.
[95] A. E. Nixon, D. J. Sexton, R. C. Ladner, *mAbs* **2014**, *6*, 73–85.
[96] M. Morishita, N. A. Peppas, *Drug Discov. Today* **2006**, *11*, 905–910.
[97] M. Hamzeh-Mivehroud, A. A. Alizadeh, M. B. Morris, W. Bret Church, S. Dastmalchi, *Drug Discov. Today* **2013**, *18*, 1144–1157.
[98] P. Vlieghe, V. Lisowski, J. Martinez, M. Khrestchatisky, *Drug Discov. Today* **2010**, *15*, 40–56.
[99] P. Thapa, M. J. Espiritu, C. Cabalteja, J. P. Bingham, *Int. J. Pept. Res. Ther.* **2014**, 545–551.
[100] J. S. Davies, *J. Pept. Sci.* **2003**, *9*, 471–501.
[101] A. Lehmann, *Expert Opin. Biol. Ther.* **2008**, *8*, 1187–1199.
[102] J. W. Kehoe, B. K. Kay, *Chem. Rev.* **2005**, *105*, 4056–4072.
[103] M. Paschke, *Appl. Microbiol. Biotechnol.* **2006**, *70*, 2–11.
[104] D. K. Marciano, M. Russel, S. M. Simon, *Science* **1999**, *284*, 1516–1519.
[105] T. Bratkovič, *Cell. Mol. Life Sci.* **2009**, *67*, 749–767.
[106] B. Van Dorst, J. Mehta, E. Rouah-Martin, R. Blust, J. Robbens, *Methods* **2012**, *58*, 56–61.
[107] M. Lunder, T. Bratkovic, S. Kreft, B. Strukelj, *J. Lipid Res.* **2005**, *46*, 1512–1516.
[108] W. D. Thomas, M. Golomb, G. P. Smith, *Anal. Biochem.* **2010**, *407*, 237–240.
[109] M. Vodnik, U. Zager, B. Strukelj, M. Lunder, *Molecules* **2011**, *16*, 790–817.
[110] J. Huang, B. Ru, S. Li, H. Lin, F.-B. Guo, *J. Biomed. Biotechnol.* **2010**, *2010*, 1–7.
[111] I. Rentero Rebollo, M. Sabisz, V. Baeriswyl, C. Heinis, *Nucleic Acids Res.* **2014**, *42*, e169.
[112] P. A. C. 't Hoen, S. M. G. Jirka, B. R. Ten Broeke, E. A. Schultes, B. Aguilera, K. H. Pang, H. Heemskerk, A. Aartsma-Rus, G. J. van Ommen, J. T. den Dunnen, *Anal. Biochem.* **2012**, *421*, 622–31.
[113] W. L. Matochko, K. Chu, B. Jin, S. W. Lee, G. M. Whitesides, R. Derda, *Methods* **2012**, *58*, 47–55.
[114] C. Heinis, T. Rutherford, S. Freund, G. Winter, *Nat. Chem. Biol.* **2009**, *5*, 502–507.
[115] I. Rentero Rebollo, C. Heinis, *Methods* **2013**, *60*, 46–54.
[116] P. Timmerman, J. Beld, W. C. Puijk, R. H. Meloen, *ChemBioChem*

2005, *6*, 821–824.
[117] A. Angelini, J. Morales-Sanfrutos, P. Diderich, S. Chen, C. Heinis, *J. Med. Chem.* **2012**, *55*, 10187–10197.
[118] I. R. Rebollo, A. Angelini, C. Heinis, *MedChemComm* **2012**, 145–150.
[119] S. Chen, J. Morales-Sanfrutos, A. Angelini, B. Cutting, C. Heinis, *ChemBioChem* **2012**, *13*, 1032–1038.
[120] S. Bellotto, S. Chen, I. Rentero Rebollo, H. A. Wegner, C. Heinis, *J. Am. Chem. Soc.* **2014**, *136*, 5880–5883.
[121] T. Schumacher, L. Mayr, D. Minor Jr., M. Milhollen, M. Burgess, P. Kim, *Science* **1996**, *271*, 1854–1857.
[122] L. Zhao, W. Lu, *Curr. Opin. Chem. Biol.* **2014**, *22*, 56–61.
[123] N. Sun, S. A. Funke, D. Willbold, *J. Biotechnol.* **2012**, *161*, 121–125.
[124] D. M. Eckert, V. N. Malashkevich, L. H. Hong, P. A. Carr, P. S. Kim, *Cell* **1999**, *99*, 103–115.

Chapter 2

Synthesis of lipid II analogues

To screen for lipid II binding peptides we designed and synthesized several lipid II analogues containing a spacer and biotin-label. To generate D-amino acid peptides from our library screen we also synthesized a fully enantiomeric analogue of lipid II. To obtain this molecule a route to N-acetyl-L-glucosamine was developed. To direct the binding of potential hits to the pentapeptide of lipid II we also synthesized the pentapeptide attached to a PEF-spacer and a biotin label (and its enantiomeric equivalent). For lipid II binding studies using nisin we designed and synthesized several truncated lipid II analogues, where either the peptide part or the lipid part was truncated.

2.1 Total synthesis of UDP-MurNAc-pentapeptide, lipid I and lipid II

The research described in chapter 3 and 4 revolves around the bacterial biomolecule lipid II. As described in the introduction, lipid II is an important component of the bacterial cell wall synthesis machinery and a validated antimicrobial target. In the lab lipid II can either be produced enzymatically or chemically. Although some modifications to lipid II have been produced enzymatically, the possibilities are limited by the substrate recognition of the required enzymes. Modifications produced through biological means include variations of the lipid, both in length and saturation pattern.[1] Total synthesis approaches have led to modifications like fluorination, biotinylation and the synthesis of peptidoglycan fragments to study the mechanisms of peptidoglycan synthesis and the mode of action of antibiotics.[2–4] Chemical synthesis of lipid II is a laborious endeavour but allows for a wide range of possible modifications.

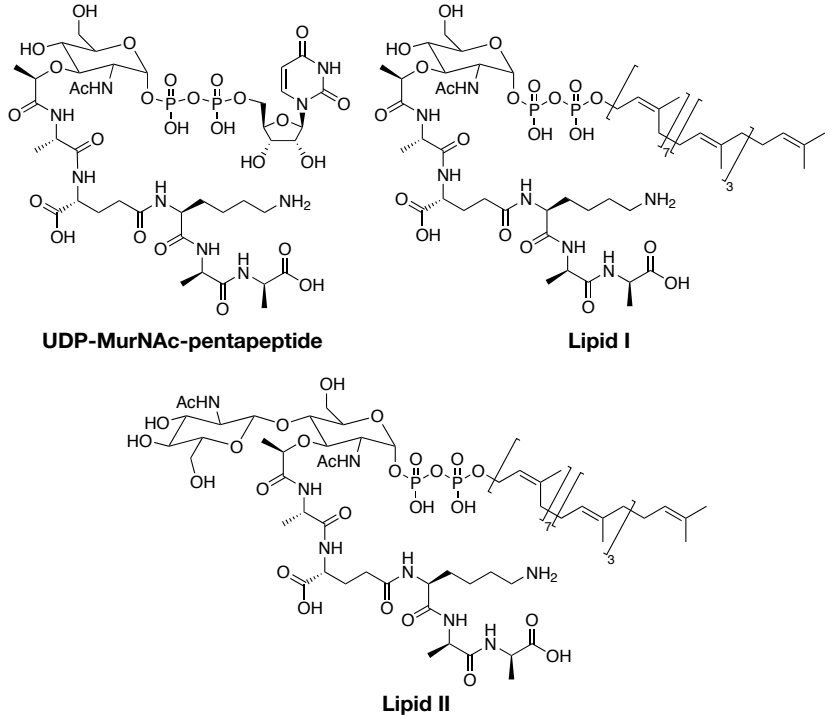

Figure 1: Chemical structure of UDP-MurNAc-pentapeptide, lipid I and lipid II.

The first reports describing the total synthesis of lipid II and its precursors were made by the group of Blaszczak at Eli Lilly. They initially described the

total synthesis of UDP-MurNAc-pentapeptide (Figure 1) starting from a suitably protected MurNAc core.[5] The pentapeptide was synthesized separately and coupled to the MurNAc lactic acid. Forming the pyrophosphate with an activated uridine monophosphate, followed by a global deprotection yielded the final product. The protection group scheme was chosen so that all groups could be removed by basic hydrolysis. Basic conditions are compatible with the glycosyl-pyrophosphate bond which is known to be acid sensitive. A similar synthesis was described by the group of Walker to make an analogue with citronellol on the pyrophosphate instead of the uridyl-group to make substrates for MurG. They used silyl-based protecting groups on the pentapeptide that could be removed by treatment with TBAF.[3]

In a later paper the Blaszczak group describes the total synthesis of lipid I, the direct precursor of lipid II as described in chapter 1 and shown in Figure 1.[6] The major difference in this paper was the reaction with undecaprenyl phosphate instead of uridyl-phosphate. The hurdle of forming the pyrophosphate was overcome by activating the phosphate of the MurNAc unit and reacting it with the phosphate lipid. Following the method initially described by Walker et. al[3] they used 1*H*-tetrazole as a catalyst for phosphorylation of the anomeric centre of MurNAc. This yielded the preferred α-anomer with better selectivity than the previously used 1,2,4-triazole.

With these synthetic routes as a basis, two total synthesis approaches towards full lipid II were reported around the same time by two different groups. Both are highly similar but differ in the protecting group strategy on the pentapeptide.[7,8] The method described by the group of Wang[7] uses TBAF sensitive protecting groups and the approach by Blaszczak uses the previously used hydroxide sensitive protecting groups.[8] The higher yielding strategy used by Blaszczak makes it possible to remove all protecting groups in one reaction step while the Wang strategy requires a two-stage deprotection, first with TBAF followed by NaOMe.

2.2 Design of lipid II analogues for phage display

2.2.1 Design of immobilizable lipid II targets

Several different lipid II analogues were required for the projects described in chapter 3 and 4. For the project described in chapter 3 an immobilizable lipid II

analogue was designed that would be used as a target in peptide library screening by (mirror image) phage display to identify novel lipid II binding peptides. To use lipid II in such a screen several requirements have to be considered:

- The target has to be immobilized, preferably using a biotin/streptavidin system.
- Immobilization should not interfere with target accessibility.
- As phage display experiments are performed in aqueous buffers the target has to be water soluble.
- To be able to perform mirror-image phage display the lipid II target also has to be synthetically accessible in the enantiomeric form.

A biotinylated lipid II analogue was described previously by the Walker group, who attached the biotin to the lysine side-chain amine. We deemed this strategy not useful for a peptide library screen as the lysine side chain could be important in recognition of a binding peptide. Another biotinylated lipid II analogue was described Huang et al. where the last three amino acids of the pentapeptide were substituted by a PEG-spacer and a biotin tag.[9] Also this strategy seems not useful as a large part of the molecule is omitted, including the D-ala-D-ala motif that is recognized by glycopeptide antibiotics.[10]

In the initial design of our target we envisioned replacing the GlcNAc connected to the C4-position of the MurNAc by a PEG-spacer and a biotin tag. The lipid for this molecule would be changed to the shorter nerol to make it water-soluble. However, we found the target was synthetically challenging and changed the design to the one shown in Figure 2 (target 1). In this new design the spacer-biotin modification would replace the undecaprenol lipid (target 1 in Figure 2). In the biological context of lipid II, the undecaprenol lipid is embedded in the membrane of a bacterium and therefore not accessible for binding by a peptide. It seems therefore reasonable to truncate the lipid and use it as a site for biotinylation (Figure 2). Furthermore, we chose to use a simple saturated alkane chain instead of a PEG-spacer to mimic the hydrophobic nature of the undecaprenol. The saturated alkyl-chain also results in a more stable connection, as the allylic pyrophosphate found in authentic lipid II is rather unstable.[3] Furthermore, as the lipid chain is now much shorter it still kept the target water soluble. It is important to note that we kept the original pyrophosphate intact as this is the recognition site for several antibiotics including nisin.[11]

For the purpose of mirror-image phage display (discussed in detail in chapter 3) the target was also required in the enantiomeric form (target 2 in Figure 2). Making this compound makes use of the same chemistry but requires enantiomeric starting materials (except for the biotin label). For synthetic ease

A

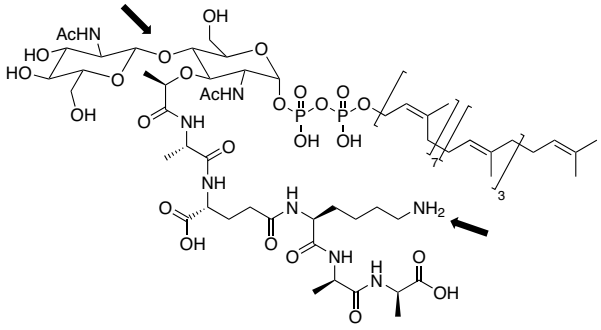

Lipid II

B

omission of GlcNAc
for easier synthesis

Lipid replaced by spacer and biotin

extended spacer for good target access

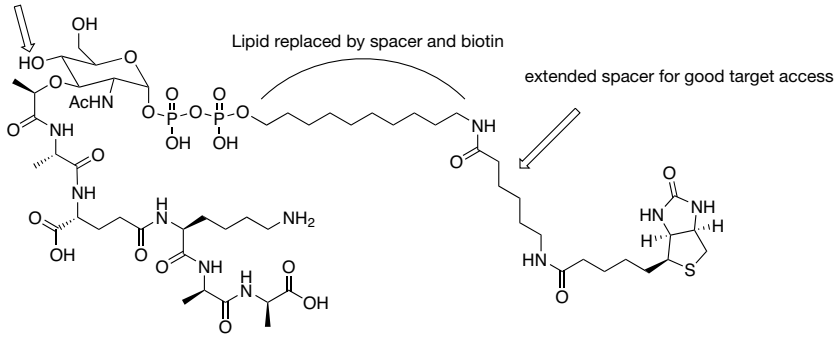

Target 1

C

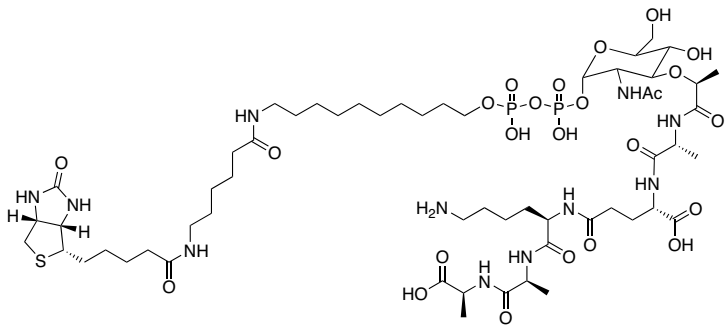

Target 2

Figure 2: Design of immobilizable lipid II analogues for use in phage display. **A**) Lipid II, arrows indicate other sites of biotinylation that were evaluated. **B**) Target 1 and the modifications made compared to lipid II. **C**) Target 2, the enantiomeric analogue of Target 1.

of both targets, targets, the GlcNAc of lipid II was omitted to provide a target molecule more accurately described as lipid I. It has been shown that many lipid II binding antibiotics are found to bind lipid I equally well as lipid II.[12–16] In most cases the binding is directed to either the pyrophosphate unit or the D-ala-D-ala motif and seems not to be influenced by the GlcNAc.

2.2.2 Design of immobilizable pentapeptide targets

Two additional targets were designed for the phage display experiments. These were based solely on the pentapeptide part of lipid II (Figure 3). The C-terminal D-ala-D-ala motif is the recognition site for the glycopeptide antibiotics and it was therefore reasoned that these target might also yield peptides with similar binding properties. If successful, the targets could also be synthesized as the pentapeptides found in vancomycin resistant bacteria containing D-Lac instead of the C-terminal D-Ala. Such targets could be used to identify novel peptides that bind specifically to the lipid II found in vancomycin resistant strains. Instead of a saturated alkyl chain as spacer we chose to use a PEG spacer instead. In these analogues it replaces the polar carbohydrate instead of the lipid part of lipid II.

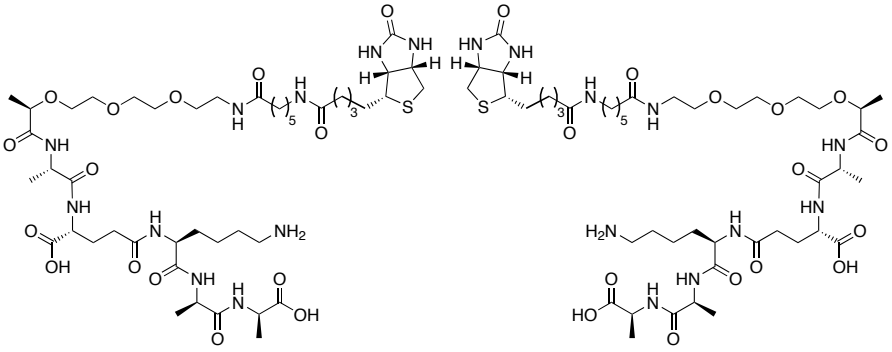

Target 3 **Target 4**

Figure 3: Design of immobilizable (enantiomeric) pentapeptide analogues (target 3 and 4) for use in phage display.

2.2.3 Retrosynthetic analysis of lipid II analogues

Scheme 1 illustrates the representative retrosynthetic analysis applied to target 1. The target molecule can be broken down into four fragments, the carbohydrate, the pentapeptide, the spacer (or lipid), and the biotin tag. In previously published synthetic routes the biotin tag was introduced to a completely deprotected

product, however in our strategy there are two amines so we chose to install the biotin prior to global deprotection. A suitably protected amine spacer, orthogonal to the other base-labile protecting groups, was therefore required. We chose to use the Cbz-group since it is easily installed and the conditions for removal (hydrogenation using Pd/C) were compatible with the protecting groups present. The pyrophosphate linkage was installed in a similar fashion as described for the reported total syntheses of lipid I and II.[6–8] However, we chose to activate the phosphate on the spacer instead of the carbohydrate. The spacer was a far less valuable molecule in our route and using this method it was possible to add multiple equivalents of activated spacer to drive the reaction to completion. From this point the rest of the synthesis is according to literature and will be discussed in the next sections.

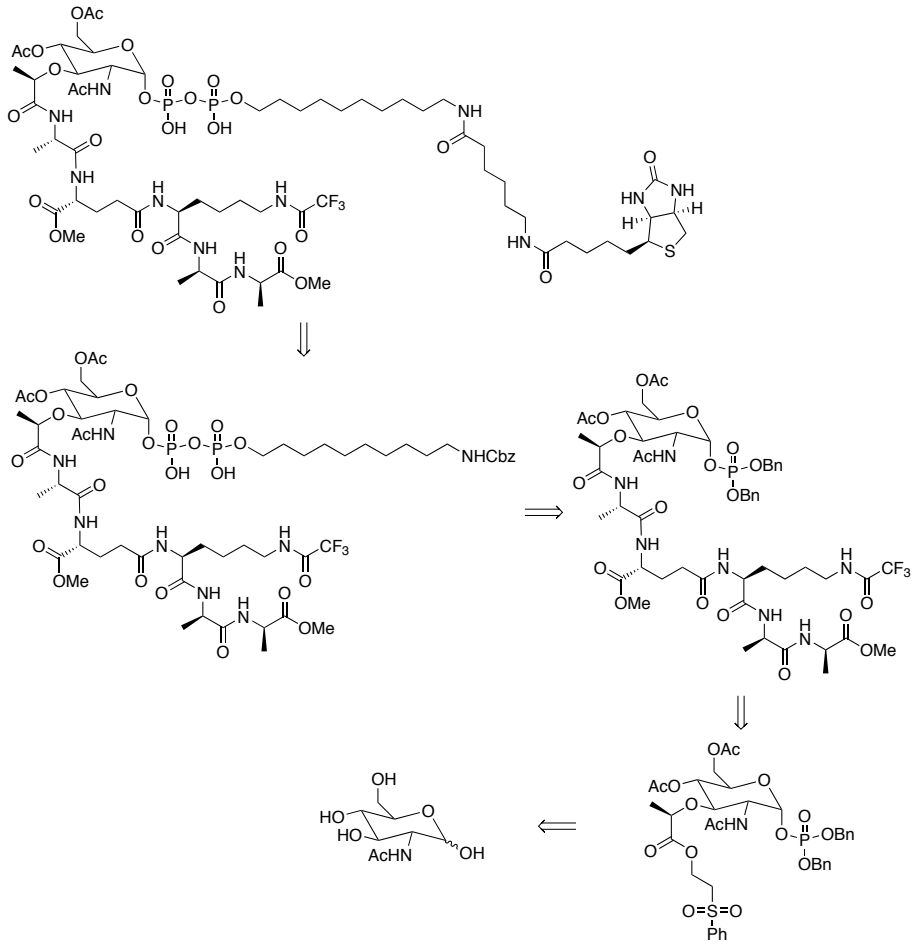

Scheme 1: Retrosynthetic analysis of target 1.

2.3 Synthesis of Target 1 and 2

2.3.1 Synthesis of the MurNAc core

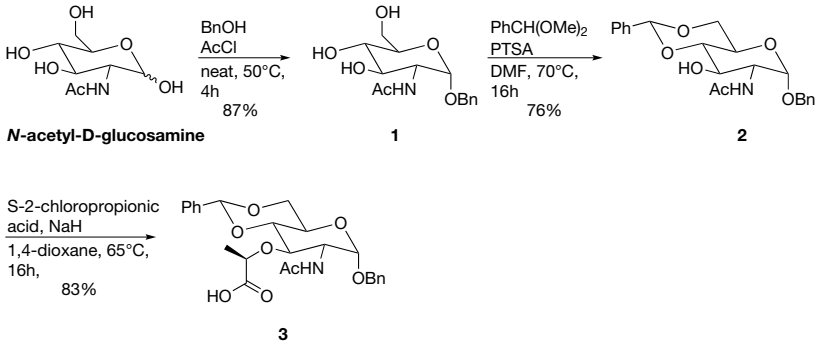

Scheme 2: Synthesis of the protected MurNAc intermediate **3**.

For all synthetic routes described in the literature the starting point is the commercially available *N*-acetyl-D-glucosamine (GlcNAc). To convert it to the required MurNAc the hydroxyl groups have to be protected so the C3-position is available for selective modification. First, the anomeric position is protected with a benzyl-group by reacting it with benzyl alcohol in the presence of acetyl chloride which gave the desired product in good yield. The C4 and C6 positions are protected simultaneously by installing a benzylidene group. Reacting compound **1** with benzaldehyde dimethyl acetal using p-toluene sulfonic acid as the catalyst yielded the required compound. With only the C3 position available it was now possible to convert GlcNAc to MurNAc. Although several strategies were available we found that an older method first described in 1964 worked best.[17] After treating compound **2** with a large excess of NaH at 95°C the reaction was cooled down to 65°C before S-2-chloropropionic acid was added to form compound **3**. By using this method a good yield of 83% was obtained while other methods were typically limited to yields of approximately 35% in our hands.

An orthogonal protecting group was next required for the carboxylic acid in compound **3** so that the anomeric position could be subsequently modified. Several protecting groups had been described for this position and the first we tried was based on the total synthesis of lipid II as described by the group of Wang (left row in Scheme 3).[7] Compound **3** was reacted with H-L-Ala-OTMSE to simultaneously install the first amino acid of the pentapeptide and protect the carboxylic acid. Without intermediate purification the benzylidene was removed and the C4 and C6 positions were acetylated. At this stage the compound could

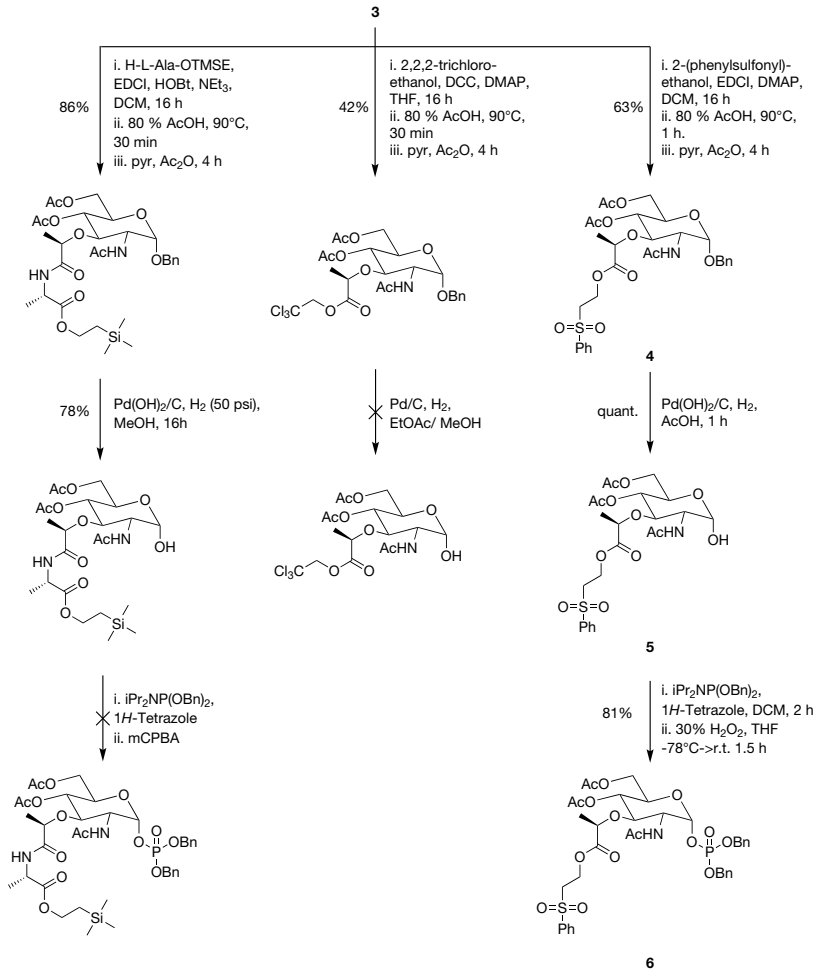

Scheme 3: Different protecting group strategies for the carboxylic acid of MurNAc.

be purified and was isolated in good yield. The following hydrogenolysis step was performed as described in the original literature (Pd/C in MeOH)[7] however, in our hands, this reaction did not proceed even under higher H_2 pressure (50 PSI). When the reaction conditions were changed to $Pd(OH)_2/C$ as catalyst and AcOH as solvent good conversion was observed. Unfortunately, the subsequent phosphorylation of the anomeric centre did not succeed despite numerous attempts and the route was therefore abandoned. In the next strategy investigated, the protecting group at the carboxylic acid in **3** was changed to the trichloroethyl-group as described by the Walker group (middle row in Scheme 3).[3,18] They next reported that a quick hydrogenation of 30 minutes could

remove the benzyl group while leaving the trichloroethyl group intact. However, we found that under these conditions several products were obtained which were a combination of partial or complete reduction of the trichloroethyl group in combination with partial reduction of the benzyl-group. We were unable to find conditions that selectively removed the benzyl group and therefore decided to use the phenylsulfonylethyl group that was described in the total synthesis of lipid I by the Blaszczak group (right row in Scheme 3).[6] The phenylsulfonylgroup was easily installed using its alcohol and EDCI as a coupling reagent to yield compound **4**. Initial attempt at removing the benzyl group using the same conditions as described by Blaszczak gave very low yields. Extended times and high catalyst loadings were required to observe conversion, but when the catalyst was changed to $Pd(OH)_2/C$ the conversion was complete after 1 h. Using these conditions compound **5** was isolated in quantitative yield, a significant improvement over the 53% that was reported when using Pd/C.[6] Phosphorylation of the anomeric centre was accomplished by reacting it with dibenzyl diisopropylphosphoramidite with 1*H*-tetrazole as the catalyst. The group of Walker first used this catalyst instead of triazole, which is also commonly used to activate phosphoramidite reagents.[3] They demonstrated that by using 1*H*-tetrazole a better α-selectivity was obtained which was further confirmed by the group of Blasczcak.[6] It is speculated that this is due to the lower pKa of tetrazole (4.9 vs 10.0 for triazole) which enhances the equilibrium of activated phosphoramidite reagent. The hydroxyl-group is now captured much faster so that it has no time for anomerization. The intermediate phosphite thus obtained was directly oxidized with hydrogen peroxide and yielded the required α-product (compound **6**) in good yields of up to 81% after purification.

2.3.2 Synthesis of the pentapeptide

The next part of the convergent synthesis was assembly of the pentapeptide with suitable protecting groups (Scheme 4). Two of the required amino acids had to be synthesized from commercially available starting materials. First, Boc-L-Lys($COCF_3$)-OH (**7**) was synthesized in one step from Boc-L-Lys-OH using ethyl trifluoroacetate (Scheme 4A). Second, Boc-D-Glu-OMe (**9**) was synthesized from Boc-D-Glu(OBn)-OH (Scheme 4B) by preparing the methyl-ester using methyl iodide followed by removal of the benzyl group under standard hydrogenation conditions. With all required amino acids in hand the pentapeptide could now be assembled. The synthesis started from the C-terminus and an iterative Boc-deprotection/coupling route was used based on the route previously described

by the group of Blasczcak (Scheme 4C).[6] In this regards D-alanine was first transformed into its methyl ester and coupled to Boc-D-Ala-OH using standard BOP conditions to yield compound **10**. After TFA removal, the previously prepared Boc-L-Lys($COCF_3$)-OH (**7**) was coupled to give compound **11**, again using standard BOP conditions. The same steps were used for the coupling of Boc-D-Glu-OMe (**9**) to give compound **12**. For the coupling of the last amino acid the stronger EDCI/HOBt coupling conditions were used and the pentapeptide (**13**) was obtained in good yield.[6]

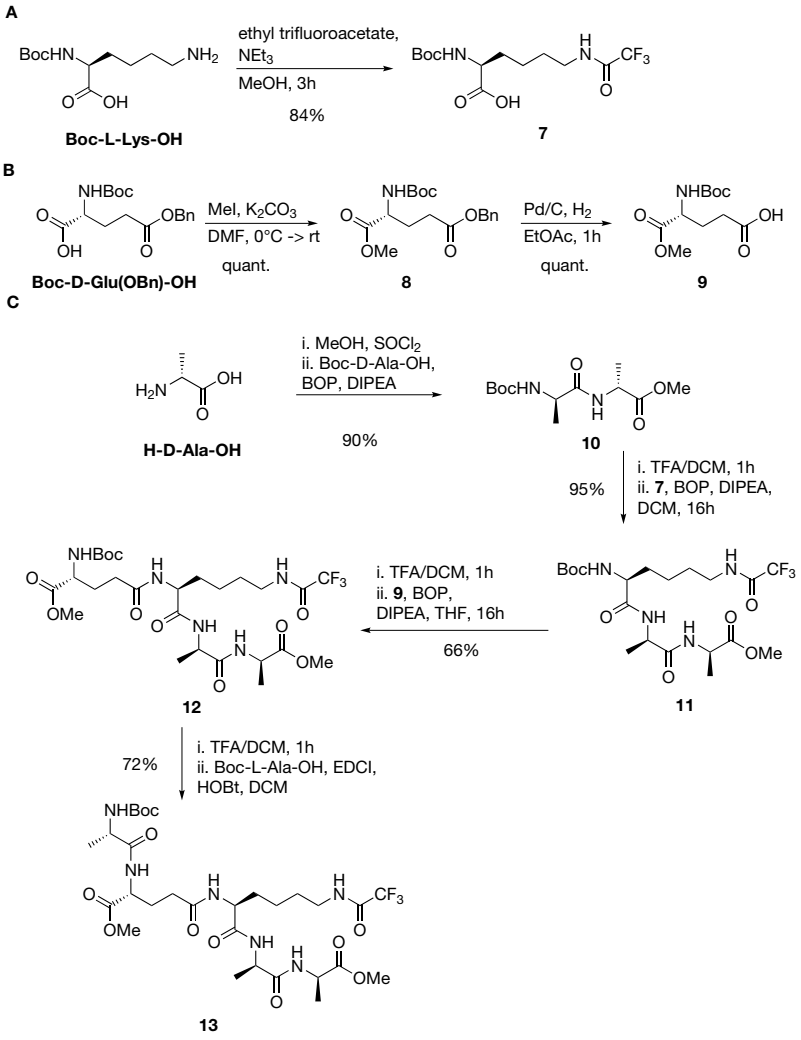

Scheme 4: Synthesis of pentapeptide **13**.

2.3.3 Synthesis of a phosphorylated alkane spacer

As discussed in section 2.2.3, the immobilized lipid II analogue synthesis also required a spacer of 10 carbon atoms functionalized with a phosphate group on one end and an orthogonally protected amine on the other. Initially a trimethylsilylethoxycarbonyl (Teoc) protecting group was used to protect the amine, based on the synthetic routes to lipid II analogues described by the group of Walker.[19] However, removal of the Teoc-group later in the synthesis proved to be problematic. We chose to use Cbz instead since the use of hydrogenolysis was compatible with the carbohydrate-pentapeptide precursor. The spacer was easily synthesized starting from 10-amino-1-decanol (Scheme 5). The Cbz-group was installed by a quick reaction with Cbz-Cl in aqueous THF to form compound **14**. The increased hydrophobicity of the product thus formed led to its precipitation from solution and allowed for quantitative isolation after filtration. In the next reaction step the increase in polarity by the phosphate group caused a similar precipitation from organic solvent allowing another convenient isolation of compound **15**.

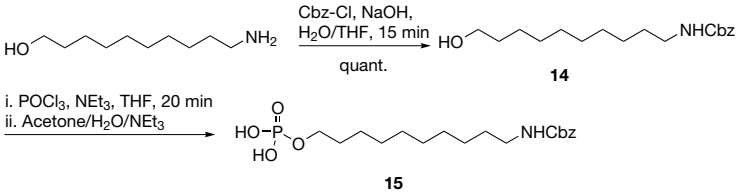

Scheme 5: Synthesis of the phosphorylated spacer.

2.3.4 Assembly of the biotinylated lipid II analogue

With all the separate building blocks in hand the stage was set for the assembly of the target molecule. The first step was to connect the MurNAc core (**6**) and the pentapeptide (**13**) as shown in Scheme 6. The carboxylic acid functionality of **6** was easily deprotected using DBU and compound **13** was treated with TFA to remove the Boc-group. BOP coupling of the deprotected intermediates provided the required compound **18** in acceptable yield. To form the pyrophosphate, the benzyl groups on the anomeric phosphate in intermediate **18** were first removed under standard hydrogenation conditions (Scheme 7). Next the phosphate group on the spacer molecule was activated using carbonyldiimidazole (CDI) and added to the deprotected phosphate derived from **18**. Although most synthetic routes activate the carbohydrate phosphate, we chose to activate the

spacer instead. By using this method additional equivalents of spacer could be activated and added to the reaction until all of the more valuable compound **18** had been consumed. The product (**19**) was purified by preparative HPLC and was isolated in a good yield of 70%.

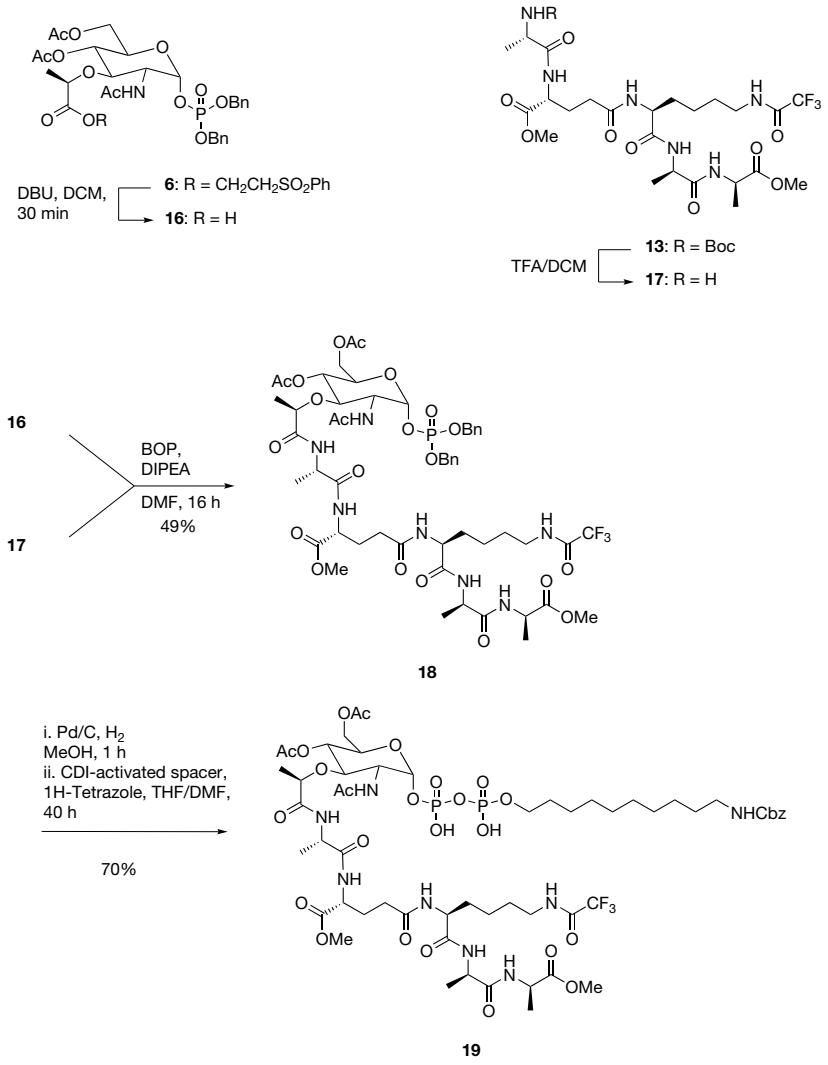

Scheme 6: Assembly of the MurNAc and pentapeptide components and subsequent pyrophosphorylation.

Removal of the Cbz-group from compound **19** was accomplished using standard hydrogenation conditions and the free amine was treated with NHS-activated biotin (Scheme 7). Initially, we chose to purify the compound at this

point to remove the excess biotin NHS reagent which could potentially react with the lysine side chain amine under the basic deprotection conditions of the final step. However, we found it was more convenient to add glycine to consume the excess biotin reagent, followed by treatment with NaOH and a single HPLC purification step to give the final product **20** in good yield.

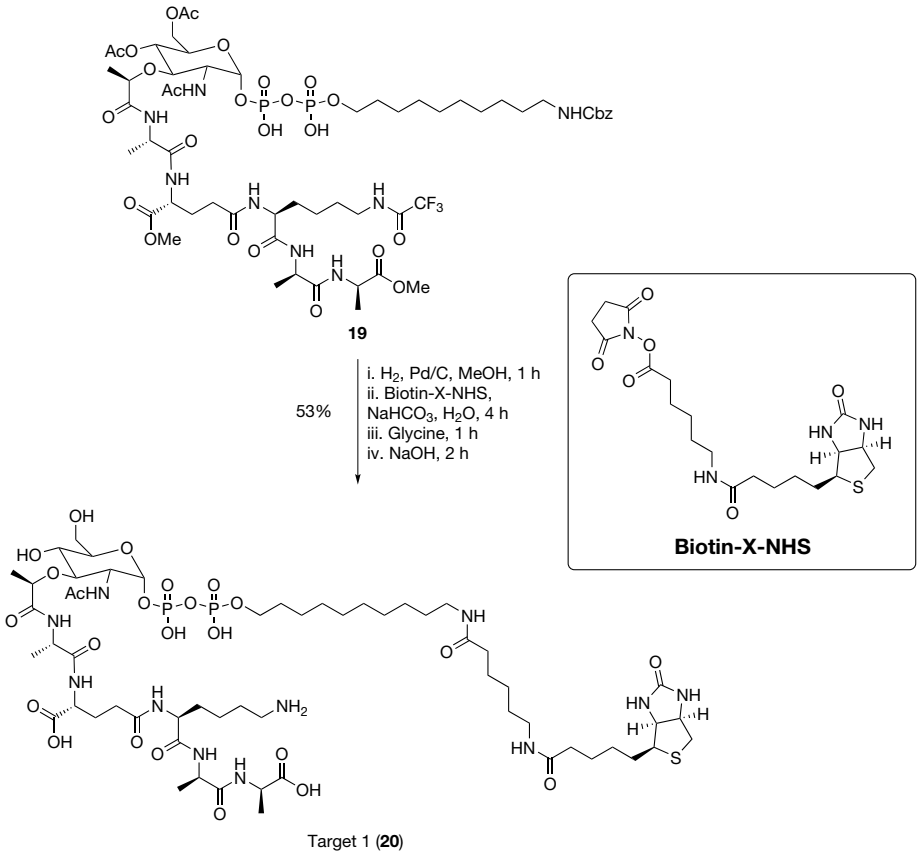

Scheme 7: Final steps of the synthesis of target 1.

2.3.5 Synthesis of *N*-acetyl-L-glucosamine

To synthesize the enantiomeric Target 2 all necessary starting materials were required in their enantiomeric form. All of the enantiomeric compounds were commercially available with the exception of *N*-acetyl-L-glucosamine. A synthetic route to *N*-acetyl-L-glucosamine was described in 1955, and uses a variation of the Killiani-Fischer synthesis starting from L-arabinose (Scheme 8).[20] As the method required the use of highly toxic liquid hydrogen cyanide, we modified

the procedure to be able to use it more safely. L-Arabinose was first treated with benzylamine under reflux conditions to form the corresponding imine followed by stereospecific addition of a nitrile group. The hydrogen cyanide required for this reaction was generated in situ by adding solid potassium cyanide to the reaction mixture followed by dropwise addition of acetic acid. The product crystallizes from the reaction solvent and can be isolated easily by filtration. In the next step compound **21** is reduced using palladium oxide and hydrogen gas in dilute hydrochloric acid. The hydrogenation serves to remove the benzylgroup from the amine and also reduces the nitrile to the imine. The imine is spontaneously hydrolysed to the aldehyde to form L-glucosamine (**22**). Acetylation of the amine produced the required *N*-acetyl-L-glucosamine (**23**) in good yield.

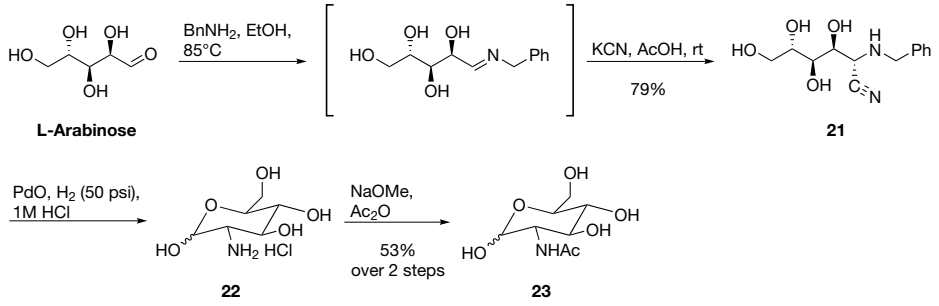

Scheme 8: Synthesis of *N*-acetyl-L-Glucosamine from L-arabinose.

2.3.6 Assembly of enantiomeric intermediates and target 2

With *N*-acetyl-L-glucosamine (**23**) in hand, the same synthetic route as described in section 2.3.1 was used to obtain the protected carbohydrate intermediate (**24**). The enantiomeric pentapeptide (**25**) was synthesized as shown in scheme 4 from the corresponding enantiomeric amino acids. Compound **24** and **25** were coupled using the same reagents as for compound **18**, followed by connection of the spacer (**15**) via formation of the pyrophosphate to yield compound **26**. The final product was assembled as described in section 2.3.4 to yield Target 2 (**27**). Intermediates **19** and **26** and final compounds **20** and **27** were analyzed by HPLC for their purity and the traces are shown in figures 4 and 5.

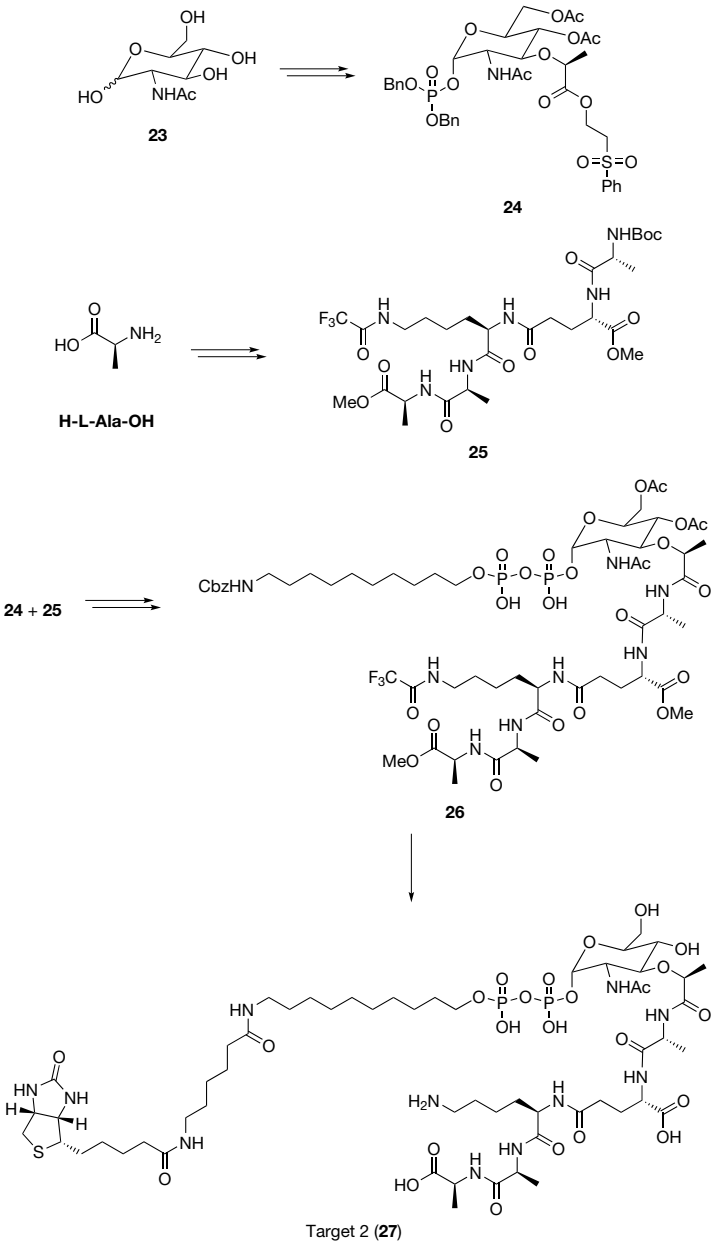

Scheme 9: Synthesis of the enantiomeric Target 2 (**27**).

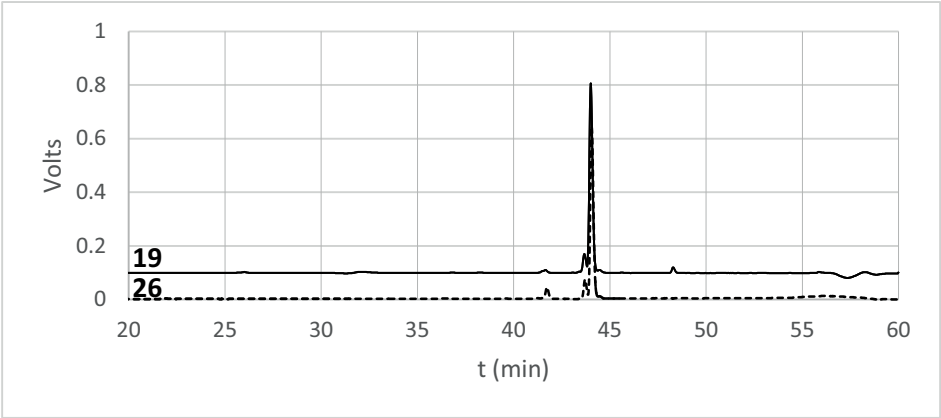

Figure 4: HPLC analysis of enantiomeric compounds **19** and **26**.

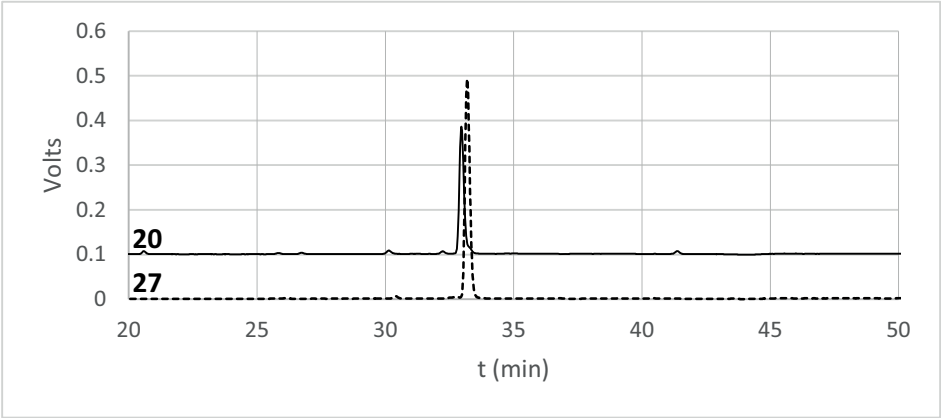

Figure 5: HPLC analysis of compounds **20** and **27**. As compounds **20** and **27** are not true enantiomers they showed a slight variation in the retention time.

2.4 Synthesis of Target 3 and 4

2.4.1 Synthesis of the biotinylated pentapeptide Target 3

For the synthesis of the biotinylated pentapeptide targets 3 and 4 a different spacer was chosen. Specifically, a lactic acid modified PEG-spacer was used to connect the pentapeptide and the biotin label. The synthesis started from triethylene glycol chloride (Scheme 10) which was converted to the azide (**28**) by treating it with sodium azide under reflux conditions.[21] Next, the alcohol was converted to the lactic acid ether **29** similar to the C3 position of MurNAc. By using standard BOP coupling conditions the spacer was then coupled to pentapeptide

13 (see scheme 4) to form compound **30**. The azide was then reduced to the amine, followed by reaction with biotin-X-NHS, removal of the excess biotin with glycine treatment and a global deprotection to yield compound **31** (Target 3).

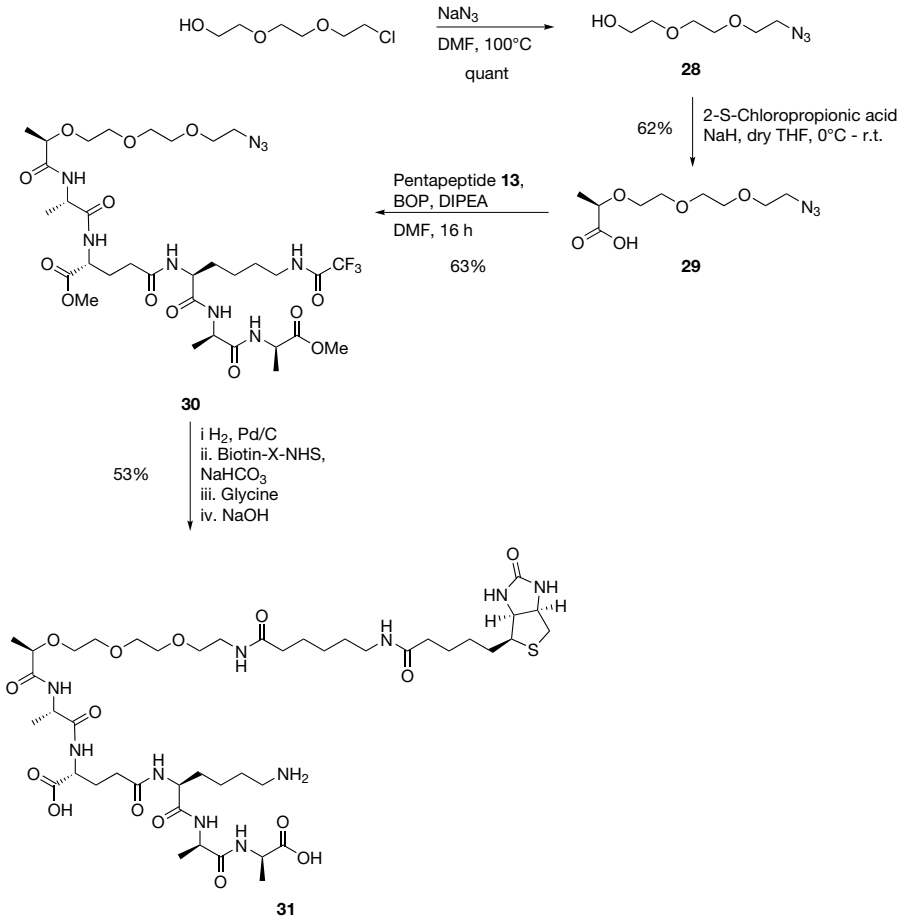

Scheme 10: Synthesis of the biotinylated pentapeptide **31** (target 3).

2.4.2 Synthesis of Target 4

To prepare the enantiomeric pentapeptide target 4 (Scheme 11), the spacer had to be prepared with the opposite stereochemistry as well. By using 2-R-chloropropionic acid it was prepared using the same method as for compound **29** (scheme 10). Further reaction with the enantiomeric pentapeptide **25** (see scheme 9), followed by biotinylation and deprotection yielded enantiomeric target 4 (**33**).

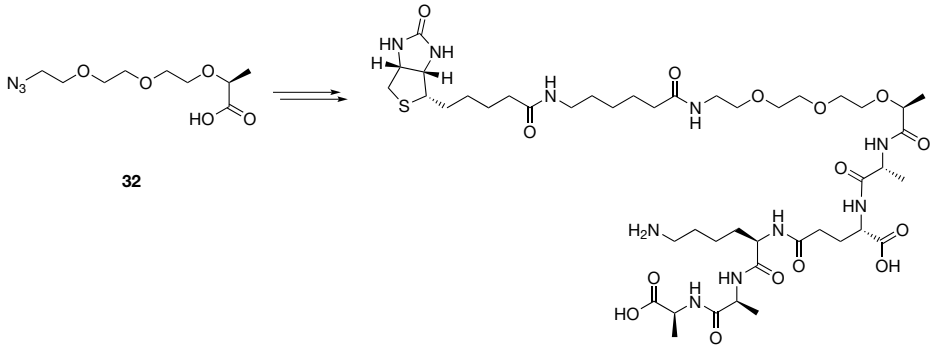

32

Target 4 (**33**)

Scheme 11: Synthesis of enantiomeric target 4 (**33**).

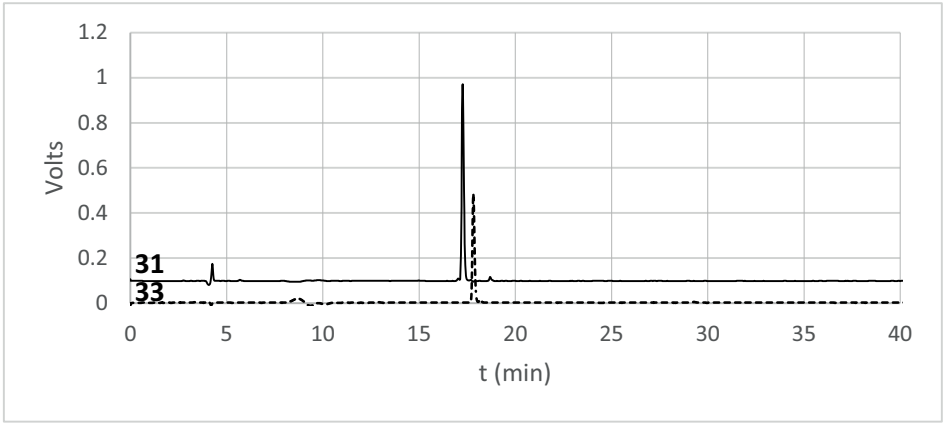

Figure 6: HPLC analysis of compounds **31** and **33**. As compounds **31** and **33** are not true enantiomers they showed a slight variation in the retention time.

2.5 Design and synthesis of truncated lipid II analogues for studying nisin-lipid II interaction

Chapter 4 describes approaches for studying the interaction between nisin and lipid II using isothermal titration calorimetry (ITC). To examine the role of the lipid II structure we designed truncated species that would allow us to determine the role that individual components of lipid II play in nisin binding (see figure 7). Here we describe the design and synthesis of the truncated analogues.

2.5.1 Design of truncated lipid II analogues

To be able to perform ITC measurements the lipid II analogues either had to be water soluble (farnesyl compounds) or had to be incorporated into DOPC

vesicles (undecaprenyl compounds). Lipid I was synthetically accessible by the same route as described in the section 2.2. Also, by amidating the MurNAc core we created a peptide-less lipid I analogue (C_{55}MurNAc) that would be used to identify the importance of the pentapeptide in the nisin–lipid II interaction. Furthermore, undecaprenol pyrophosphate (C_{55}PP) and undecaprenol phosphate (C_{55}P) were synthesized as these are naturally occurring lipids in the lipid II synthesis cycle. A lipid I variant was also prepared containing farnesyl as the lipid to make it water soluble as this would allow us to study the interaction with nisin outside of a lipid membrane environment.

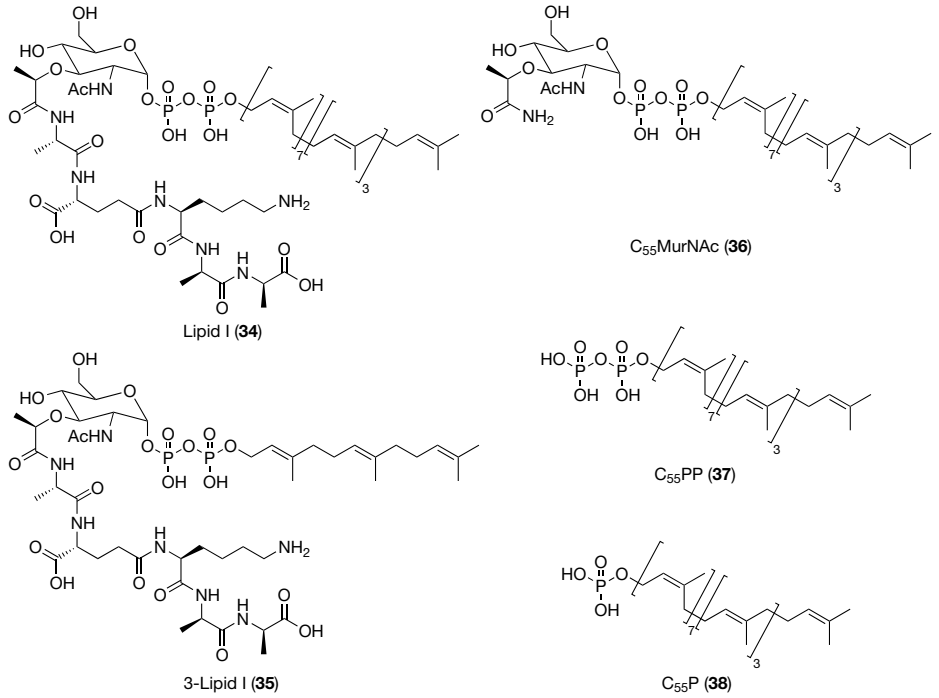

Figure 7: Design of simplified lipid II analogues for ITC studies.

2.5.2 Phosphorylation of lipid alcohols

To be able to synthesize the designed compounds illustrated in figure 7 (except C_{55}PP) we had to phosphorylate the corresponding lipids (farnesyl and undecaprenol). A method described by Lira et al. was used to prepare both farnesol-phosphate and undecaprenol-phosphate by reacting the respective alcohols with trichloroacetonitrile and tetrabutylammonium dihydrogenphosphate (see scheme 12).[22]

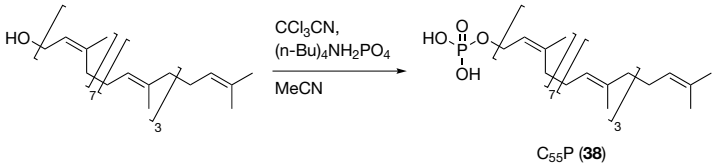

Scheme 12: Synthesis of undecaprenol phosphate (**38**).

2.5.3 Pyrophosphorylation of undecaprenol

Although the use of C_{55}PP has been reported in the literature, no concise synthesis had been described. C_{55}PP was observed as a small side product formed in the reaction to prepare C_{55}P (**38**). We therefore attempted to force this reaction by adding multiple equivalents of the reagents relative to the alcohol. Even after extended reaction times this approach still gave very low yields and a mixture of mono-, di- and triphosphates was obtained which were hard to separate. To avoid this problem we changed the synthetic route by first converting the alcohol to the bromide by using Appel-reaction conditions followed by treatment of the bromide with the tris(tetrabutylammonium) salt of pyrophosphate (Scheme 13).[23] The main advantage of this approach is that there is no formation of mono- or triphosphates which simplifies the purification and it gave the desired product in an acceptable yield after purification. Due to the instability of the product as a dry solid, it was extracted into a mixture of chloroform and methanol (1:1) and the yield was determined by determining the amount of inorganic phosphate after destruction of the sample following the method as described by Rouser et al.[24] For long term storage it is advisable to add a small quantity of base (1% NH_4OH) to the organic solution. However, as we expected this would interfere with the planned ITC measurements we used the product immediately.

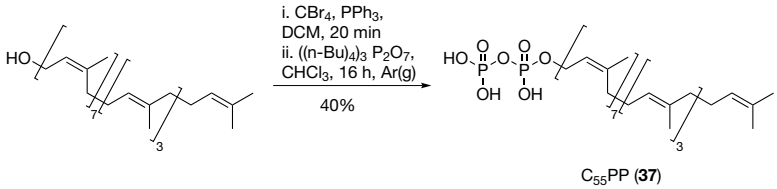

Scheme 13: Synthesis of C_{55}PP (**37**).

2.5.4 Synthesis of Undecaprenyl-MurNAc-amide building block

The lipid I analogue without the pentapeptide was prepared by first amidating

the carboxylic acid of the MurNAc intermediate (**6**) by treatment with NH_4Cl and BOP as shown in Scheme 14. It could then be used in the pyrophosphate forming reaction with undecaprenol phosphate (compound **38**) to form C_{55}MurNAc (**36**).

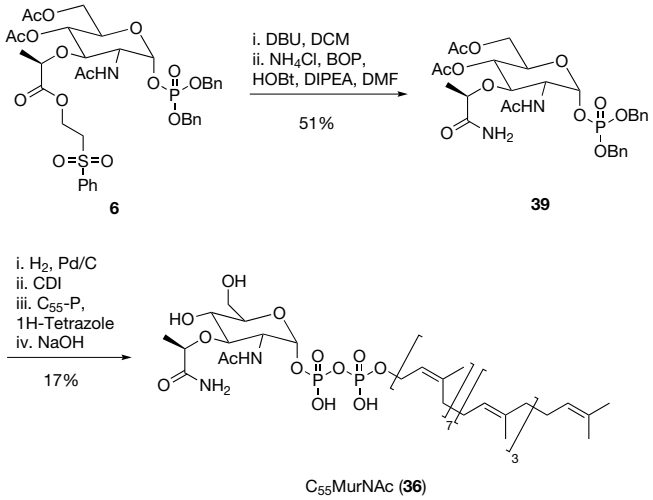

Scheme 14: Synthesis of C_{55}MurNAc (**36**).

2.5.5 Synthesis of lipid I and farnesyl-lipid I

To prepare a fully synthetic analogue of lipid I, the MurNAc-pentapeptide (compound **18**) described in section 2.3.4 (Scheme 6) was reacted with either C_{55}P (**38**) or farnesyl-phosphate. Both compounds were prepared using the method as described by Blasczcak as shown in scheme 15.[6]

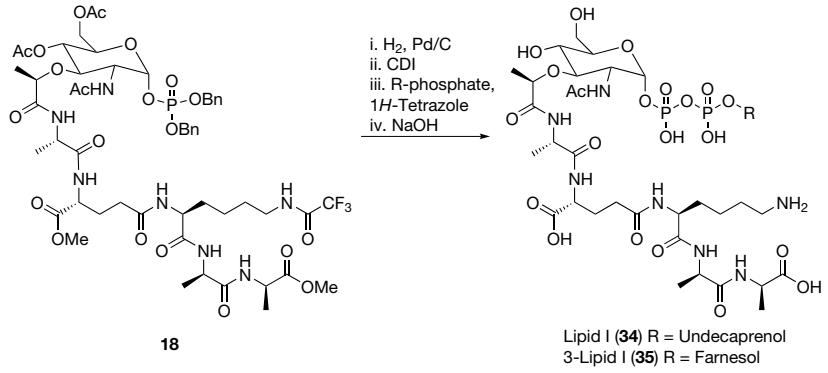

Scheme 15. Synthesis of lipid I and farnesyl-lipid I.

2.6 Conclusion

The synthetic routes described in this chapter yielded several lipid II analogues that were essential for the investigations described in chapters 2 and 3. The synthesis of the carbohydrate-pentapeptide intermediate (compound **18**) was based on the robust route described by the group of Blaszczak. This valuable intermediate was modified with several lipids to yield a variety of useful compounds including the orthogonally protected compound **19**. Such a compound could potentially be modified with all kinds of useful handles including fluorescent tags or immobilization handles. With such modification the molecules could be useful for the study of lipid II itself and lipid II binding peptides and proteins.

2.7 Experimental

2.7.1 Synthesis of all described compounds

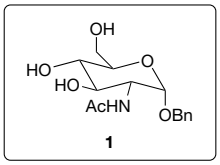

1

N-((2S,3R,4R,5S,6R)-2-(benzyloxy)-4,5-dihydroxy-6-(hydroxymethyl)tetrahydro-2H-pyran-3-yl)acetamide (1). As described by Yamaguchi et al.[25] N-Acetyl-D-glucosamine (15.50 g, 70.1 mmol) was suspended in benzylalcohol (55 ml, 528.9 mmol) and acetylchloride (4.98 ml, 70.1 mmol) was added dropwise. The mixture was stirred for 2 h at r.t. and 4 h at 50°C. After cooling to r.t. the mixture as poured into cold Et_2O (600 ml) and stirred vigorously overnight at 0°C. The product was isolated by filtration as an off-white powder. Yield: 18.94 g (60.8 mmol; 87%) R_f: 0.41 (MeOH/DCM, 1:4) ^1H NMR (300 MHz, dmso) δ 7.80 (d, *J* = 8.0 Hz, 1H), 7.31 (m, 5H), 4.99 (d, *J* = 5.5 Hz, 1H), 4.76 – 4.61 (m, 3H), 4.52 (t, *J* = 5.0 Hz, 1H), 4.40 (d, *J* = 12.5 Hz, 1H), 3.65 (m, 2H), 3.58 – 3.36 (m, 3H), 3.14 (dd, *J* = 14.4, 8.9 Hz, 1H), 1.81 (s, 3H). Analytical data corresponds with literature values.[25]

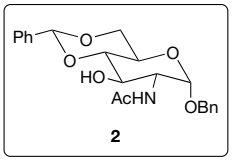

2

N-((2R,4aR,6S,7R,8R,8aS)-6-(benzyloxy)-8-hydroxy-2-phenylhexahydropyrano[3,2-d][1,3]dioxin-7-yl) acetamide (2)

As described by Yamaguchi et al.[25] Compound **1** (5 g, 16.06 mmol), $PhCH(OMe)_2$ (4.82 ml, 32.12 mmol) and p-toluenesulfonic acid (150 mg, 0.87 mmo) were dissolved in dry DMF (40 ml) and stirred at 70°C for 16 h. The mixture was cooled to 0°C and NEt_3 (0.8 ml) was added. After stirring for 30 min at r.t. the solvents were evaporated and the residue was suspended in MeOH (100 ml). The suspension was stirred vigorously

for 5 min and the product was obtained by filtration. Yield: 4.89 g (12.2 mmol; 76%) R_f: 0.27 (EtOAc) ^{1}H NMR (300 MHz, dmso) δ 8.00 (d, *J* = 8.1 Hz, 1H), 7.50 – 7.25 (m, 10H), 5.62 (s, 1H), 5.18 (d, *J* = 5.6 Hz, 1H), 4.79 (d, *J* = 3.4 Hz, 1H), 4.60 (dd, *J* = 63.9, 12.6 Hz, 2H), 4.14 (d, *J* = 5.4 Hz, 1H), 3.90 - 3.79 (m, 1H), 3.79 - 3.64 (m, 3H), 3.51 (t, *J* = 8.8 Hz, 1H), 1.85 (s, 3H). Analytical data corresponds with literature values.[25]

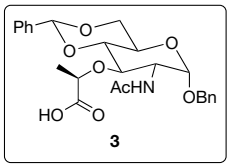

3

(R)-2-(((2R,4aR,6S,7R,8R,8aS)-7-acetamido-6-(benzyloxy)-2-phenylhexahydropyrano[3,2-d][1,3]dioxin-8-yl)oxy)propanoic acid (3)

As described by Osawa et al.[17] Compound **2** (6.4 g, 16.0 mmol) and NaH (60% dispersion in mineral oil, 3 g, 75 mmol) were suspended in dry dioxane (400 ml) and heated to 95°C for 1h. The mixture was cooled to 65°C before S-2-chloropropionic acid (3.8 ml, 41.5 mmol) was added. After 1h more NaH (12.7 g, 317.5 mmol) was added and the mixture was stirred at 65°C for 16 h. The reaction mixture was cooled and H_2O (200 ml) was added carefully. The organic solvent was removed by evaporation and the remaining aqueous solution was extracted with $CHCl_3$ (200ml). The aqueous solution was cooled on ice, $CHCl_3$ (200 ml) was added and the pH was slowly adjusted to 2 with 1M HCl while vigorously stirring. The layers were separated and the aqueous layer was quickly extracted with $CHCl_3$ (2 x 200 ml). The organic layers were combined and washed with H_2O (200 ml), dried over Na_2SO_4, filtered and evaporated to dryness. The resulting solids were suspended in MeOH (160 ml), heated to 60°C and filtered hot. The product was recrystallized from MeOH. Yield: 6.09 g (13.4 mmol; 83%) Rf: 0.40 (5% MeOH in DCM + 1% AcOH) ^{1}H NMR (300 MHz, dmso) δ 7.99 (d, *J* = 5.0 Hz, 1H), 7.46 – 7.25 (m, 10H), 5.70 (s, 1H), 5.04 (d, *J* = 3.2 Hz, 1H), 4.59 (dd, *J* = 62.0, 12.4 Hz, 2H), 4.28 (q, *J* = 6.9 Hz, 1H), 4.15 (d, *J* = 8.0 Hz, 1H), 3.85 – 3.64 (m, 5H), 1.83 (s, 3H), 1.27 (d, *J* = 6.9 Hz, 3H). Analytical data corresponds with literature values.[26]

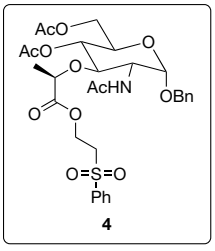

4

2-(Phenylsulfonyl)ethyl (R)-2-(((2S,3R,4R,5S,6R)-3-acetamido-5-acetoxy-6-(acetoxymethyl)-2-(benzyloxy) tetrahydro-2H-pyran-4-yl)oxy)propanoate (4)

Synthesis adapted from Hitchcock et al.[5] Several steps were combined to give the following protocol: Compound 3 (5.89 g, 12.5 mmol), DMAP (76.4 mg, 0.625 mmol) and 2-(phenylsulfonyl)ethanol (2.99 ml, 25 mmol) were dissolved in DCM (75 ml). The solution was cooled on ice before EDCI (4.79 g, 25 mmol)

was added. After stirring for 1 h the ice-bath was removed and the mixture was stirred for another 16 h. DCM was added to a total volume of 250 ml and the mixture was extracted with 1M $KHSO_4$ (3 x 250 ml) and H_2O (1 x 250 ml). The organic layer was dried over Na_2SO_4, filtered and evaporated to dryness. The crude solid was dissolved in AcOH/H_2O (4:1, 250 ml) and stirred at 90°C for 1h. Solvents were removed under vacuum and the solid material was coevaporated with toluene five times. The residue was dissolved in pyridine (180 ml), cooled to 0°C and acetic anhydride (28.5 ml) was added dropwise. The reaction was stirred for 16 h at r.t. and then evaporated under vacuum. Coevaporation from toluene was done five times to remove traces of pyridine before the product was applied to a silica column eluting with EtOAc/Hex (4:1). Yield 5.02 (7.90 mmol; 63%) R_f: 0.29 (EtOAc/Hex, 4:1) ^{1}H NMR (300 MHz, $CDCl_3$) δ 7.91 (d, *J* = 7.7 Hz, 2H), 7.72 – 7.50 (m, 3H), 7.39 (d, *J* = 5.6 Hz, 1H), 7.34 (m, 5H), 5.37 (d, *J* = 3.1 Hz, 1H), 5.07 (t, *J* = 9.6 Hz, 1H), 4.75 – 4.32 (m, 5H), 4.26 – 4.03 (m, 2H), 4.02 – 3.72 (m, 5H), 3.47 (t, *J* = 5.9 Hz, 2H), 2.09 (s, 6H), 2.00 (s, 3H), 1.23 (d, *J* = 7.0 Hz, 3H). Analytical data corresponds with literature values.[5]

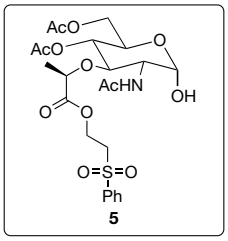

5

2-(Phenylsulfonyl)ethyl (R)-2-(((3R,4R,5S,6R)-3-acetamido-5-acetoxy-6-(acetoxymethyl)-2-hydroxytetrahydro-2H-pyran-4-yl)oxy)propanoate (5)

Compound 4 (2.71 g, 4.26 mmol) was dissolved in 75 ml AcOH and $Pd(OH)_2$/C was added as a suspension in 10 ml AcOH. The mixture was stirred for 1 h under a hydrogen atmosphere before it was filtered over celite. The filtrate was evaporated to dryness and the product was obtained as a white foam. Yield: quant. R_f: 0.12 (EtOAc) ^{1}H NMR (300 MHz, $CDCl_3$) δ 7.95 (d, *J* = 7.2 Hz, 1H), 7.77 – 7.56 (m, 4H), 5.68 (s, 1H), 5.07 (t, *J* = 9.0 Hz, 1H), 4.56 (t, *J* = 5.9 Hz, 2H), 4.26 – 4.00 (m, 5H), 3.89 – 3.68 (m, 2H), 3.48 (t, *J* = 5.1 Hz, 2H), 2.11 (s, 3H), 2.08 (s, 3H), 2.03 (s, 3H), 1.26 (d, *J* = 7.0 Hz, 3H). Analytical data corresponds with literature values.[5]

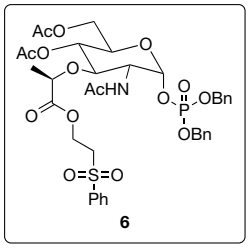

6

2-(Phenylsulfonyl)ethyl (R)-2-(((2R,3R,4R,5S,6R)-3-acetamido-5-acetoxy-6-(acetoxymethyl)-2-((bis(benzyloxy)phosphoryl)oxy)tetrahydro-2H-pyran-4-yl)oxy)propanoate (6)

Synthesis according to VanNieuwenhze et al.[6] R_f: 0.52 (EtOAc) $[\alpha]_D$ = +60.3 (c 0.4, MeOH) ^{1}H NMR (300 MHz, $CDCl_3$) δ 7.93 (d, 2H), 7.68 (t, 1H), 7.59 (t, 2H), 7.33 (s, 10H),

6.10 (dd, *J* = 5.8, 2.9 Hz, 3H), 5.10 (t, *J* = 9.6 Hz, 1H), 5.04 (m, 4H), 4.56 (t, *J* = 5.9 Hz, 2H), 4.16-4.03 (m, 2H), 4.03-3.86 (m, 3H), 3.78 – 3.68 (m, 1H), 3.47 (dd, *J* = 10.8, 5.6 Hz, 2H), 2.10 (s, 3H), 1.98 (s, 3H), 1.86 (s, 3H), 1.64 (s, 1H), 1.25 (d, *J* = 7.0 Hz, 3H). Analytical data corresponds with literature values.[6]

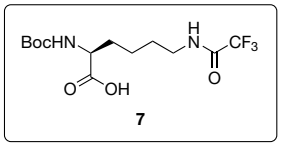

7

N2-(Tert-butoxycarbonyl)-N6-(2,2,2-trifluoroacetyl)-L-lysine (7)

Synthesis according to Eid et al.[27] Boc-L-Lys-OH (4.93 g, 20 mmol) was dissolved in MeOH (50 ml) and ethyl 2,2,2-trifluoroacetate (2.86 ml, 24 mmol) was added followed by NEt_3 (2.93 ml, 21 mmol) and the mixture was stirred for 3 h. After removing the solvents under vacuum the product was dissolved in DCM (100 ml) and washed with 0.1M HCl (100 ml) and water (100 ml). The organic layer was dried over Na_2SO_4, filtered and evaporated to dryness. The product was further dried under high vacuum and used without further purification. Yield: 5.78 g (16.9 mmol; 84%) ^{1}H NMR (300 MHz, $CDCl_3$) δ 7.82 (bs, 1H), 7.05 (bs, 1H), 5.27 (d, *J* = 7.7 Hz, 1H), 4.31 – 4.16 (m, 1H), 3.36 (q, *J* = 6.6 Hz, 2H), 1.96 – 1.80 (m, 1H), 1.66 (m, 3H), 1.44 (s, 11H), 1.27 (t, *J* = 7.3 Hz, 2H). Analytical data corresponds with literature values.[27]

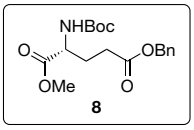

8

5-Benzyl 1-methyl (tert-butoxycarbonyl)-D-glutamate (8)

Boc-D-Glu(OBn)-OH (5 g, 14.82 mmol) was dissolved in DMF (100 ml) and cooled to 0°C. K_2CO_3 (2.46 g, 17.78 mmol) was added followed by MeI (2.77 ml, 44.46 mmol) and the mixture was allowed to warm to r.t. and stirred for 16 h. Solvents were removed under vacuum and the product was dissolved in EtOAc (100 ml) and washed with H_2O (100 ml). The aqueous layer was extracted with EtOAc (2 x 100 ml). The combined organic layers were dried over Na_2SO_4, filtered and concentrated under vacuum. Purification of the product was done by applying it to a silica column eluting with EtOAc/Hex (1:2). Yield: quant. R_f: 0.62 (EtOAc/Hex, 1:1) ^{1}H NMR (300 MHz, $CDCl_3$) δ 7.39 – 7.30 (m, 5H), 5.12 (s, 2H), 4.34 (m, 1H), 3.73 (s, 3H), 2.56 – 2.36 (m, 2H), 2.20 (m, 1H), 1.96 (m, 1H), 1.43 (s, 9H). Analytical data corresponds with literature values.[28]

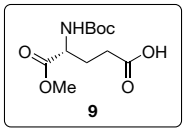

9

(R)-4-((tert-butoxycarbonyl)amino)-5-methoxy-5-oxopentanoic acid (9)

Compound **8** (5.21 g, 14.82 mmol) was dissolved in EtOAc (40 ml) and Pd/C (1 g) was added as a suspension in EtOAc (10

ml). The solution was stirred under a hydrogen atmosphere for 1h. The solution was filtered through celite and the filtrate was evaporated to dryness and used without further purification.

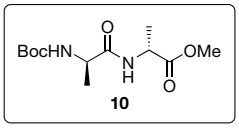

10

Methyl (tert-butoxycarbonyl)-D-alanyl-D-alaninate (10)
MeOH (20 ml) was cooled using a salt/ice bath and $SOCl_2$ (1.74 ml, 24 mmol) was added dropwise. H-D-Ala-OH (1.78 g, 20 mmol) was added in one portion and the the mixture was allowed to warm to r.t. and then refluxed for 2h. After evaporation to dryness the crude solids were dissolved in 500 ml DCM and Boc-D-Ala-OH (4.16 g, 22 mmol), BOP (9.70 g, 22 mmol) and DIPEA (10.45 ml, 60 mmol) were added. The mixture was stirred for 2.5 h before the solvents were removed under vacuum. The crude product was dissolved in EtOAc (500 ml) and extracted with 1 M $KHSO_4$ (2 x 500 ml), sat $NaHCO_3$ (2 x 500 ml) and brine (1 x 500 ml). The organic layer was dried over Na_2SO_4, filtered and concentrated under vacuum before it was applied to a silica column eluting with EtOAc/Hex (1:1). The product was isolated as a white solid. Yield: 4.85 g (17.7 mmol; 88%) Rf: 0.32 (EtOAc/Hex, 1:1) ^{1}H NMR (300 MHz, $CDCl_3$) δ 6.64 (d, *J* = 6.3 Hz, 1H), 5.01 (bs, 1H), 4.56 (p, *J* = 7.2 Hz, 1H), 4.16 (dt, *J* = 13.1, 6.5 Hz, 1H), 3.74 (s, 3H), 1.44 (s, 9H), 1.39 (d, *J* = 7.2 Hz, 3H), 1.35 (d, *J* = 7.1 Hz, 3H). Analytical data corresponds with literature values.[29]

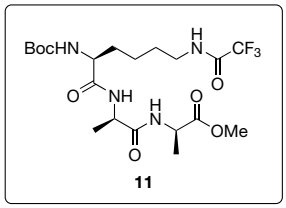

11

Methyl N2-(tert-butoxycarbonyl)-N6-(2,2,2-trifluoroacetyl)-L-lysyl-D-alanyl-D-alaninate (11)
Compound **10** (4.22 g, 15.4 mmol) was stirred in TFA/DCM (1:1, 100 ml) for 1h. After evaporation to dryness the obtained solid was dissolved in chloroform and evaporated again and this was repeated 4 times more. The residue was dissolved in DCM (250 ml) and compound **7** (5.78 g, 16.9 mmol) was added, followed by BOP (7.47 g, 16.9 mmol) and DIPEA (8.04 ml, 46.2 mmol). The mixture was stirred for 16 h and then evaporated to dryness. The crude material was dissolved in EtOAc (400 ml) and washed with 1M $KHSO_4$ (2 x 400 ml), sat $NaHCO_3$ (2 x 400 ml) and brine (1 x 400 ml). The organic layer was dried over Na_2SO_4, filtered and evaporated to dryness. Yield: 8.34 g (16.7 mmol, 99%) Rf: 0.24 (EtOAc/Hex, 4:1) ^{1}H NMR (300 MHz, $CHCl_3$) δ 7.00 (m, 2H), 6.90 (d, *J* = 7.3 Hz, 1H), 5.29 (d, *J* = 7.5 Hz, 1H), 4.57 – 4.43 (m, 2H), 4.09 (m, 1H), 3.73 (s, 3H), 3.35 (q, *J* = 6.5 Hz, 2H), 1.91 – 1.75 (m, 1H), 1.73 – 1.55 (m, 3H), 1.48 – 1.32

(m, 16H). Analytical data corresponds with literature values.[27]

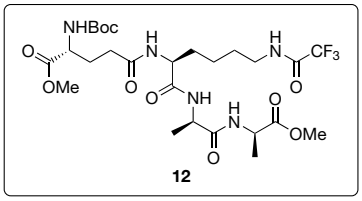

12

Methyl N2-(tert-butoxycarbonyl)-N5-((S)-1-(((R)-1-(((R)-1-methoxy-1-oxopropan-2-yl) amino)-1-oxopropan-2-yl)amino)-1-oxo-6-(2,2,2-trifluoroacetamido)hexan-2-yl)-D-glutaminate (12)

Compound **11** (1.89 g, 3.79 mmol) was stirred in TFA/DCM (1:1, 10 ml) for 1h. The reaction was evaporated to dryness and dissolved in a minimal amount of TFA. The solution was added dropwise to DCM/Et_2O (1:1, 100 ml) and the peptide was collected by centrifugation. The obtained peptide pellet was dissolved in dry DMF (25 ml) and compound **9** (1.09 g, 4.17 mmol), BOP (1.84 g, 4.17 mmol) and DIPEA (1.98 ml, 11.37 mmol) were added. The reaction was stirred for 16 h before it was evaporated to dryness. The residue was dissolved in EtOAc (250 ml) and washed with 5% $KHSO_4$ (1 x 250 ml), 5% $NaHCO_3$ (1 x 250 ml) and brine (1 x 250 ml). The organic layer is dried over Na_2SO_4, filtered and evaporated to dryness. The crude peptide was absorbed onto silica and applied to a silica column eluting with EtOAc -> 2% MeOH in EtOAc. Yield: 1.70 g (2.65 mmol; 66%) R_f: 0.43 (5% MeOH in EtOAc) ^{1}H NMR (300 MHz, CD_3OD) δ 4.44 – 4.29 (m, 2H), 4.19 (t, *J* = 7.1 Hz, 1H), 4.14 – 4.05 (m, 1H), 3.71 (s, 3H), 3.68 (s, 3H), 2.34 (t, *J* = 7.4 Hz, 2H), 2.17 – 1.99 (m, 1H), 1.98 – 1.83 (m, 1H), 1.82 – 1.65 (m, 2H), 1.59 (m, 2H), 1.43 (s, 9H), 1.41 (d, *J* = 7.3 Hz, 2H) , 1.36 (d, *J* = 7.2 Hz, 2H). Analytical data corresponds with literature values.[27]

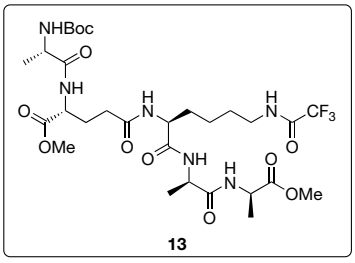

13

Methyl N2-((tert-butoxycarbonyl)-L-alanyl)-N5-((S)-1-(((R)-1-(((R)-1-methoxy-1-oxopropan-2-yl)amino)-1-oxopropan-2-yl) amino)-1-oxo-6-(2,2,2-trifluoroacetamido) hexan-2-yl)-D-glutaminate (13)

Compound **12** (1.28 g, 2.00 mmol) was stirred in TFA/DCM (1:1, 10 ml) for 1h. The reaction was evaporated to dryness and dissolved in a minimal amount of TFA. The solution was added dropwise to MTBE/Hex (1:1, 80 ml) and the peptide was collected by centrifugation (3500 rpm for 5 min). Boc-L-Ala-OH (454 mg, 2.40 mmol) was dissolved in DCM (15 ml) and cooled to 0°C before EDCI (460 mg, 2.4 mmol), HOBt (367 mg, 2.40 mmol), DIPEA (0.8 ml, 4.80 mmol) and the peptide (as a solution in 10 ml DMF) were added. The reaction mixture was allowed to warm to r.t. and stirred for 16 h. The solvents were removed

under vacuum and the residue was dissolved in 250 ml EtOAc. To completely dissolve everything a small amount of iPrOH was added. The solution was washed with 5% $NaHCO_3$ (1 x 250 ml) and H_2O (1 x 250 ml). After drying over Na_2SO_4 the solution was filtered and evaporated to dryness. The product was further purified on a silica column eluting with 5% MeOH in DCM. Yield: 1.03 g (1.44 mmol; 72%), Rf: 0.5 (10% MeOH in DCM), $[\alpha]_D$ = +20.2 (c 0.2, MeOH) ^{1}H NMR (400 MHz, CD_3OD) δ 4.37 (p, *J* = 7.2 Hz, 2H), 4.20 – 4.11 (m, 1H), 4.06 (m, 1H), 3.69 (s, 3H), 3.67 (s, 3H), 3.27 (m, 2H, overlaps with CD_3OD signal) , 2.28 (t, *J* = 13.6 Hz, 2H), 1.97 – 1.85 (m, 1H), 1.84 – 1.74 (m, 1H), 1.74 – 1.62 (m, 2H), 1.62-1.52 (m, 2H), 1.43 (s, 9H), 1.40 (d, *J* = 7.3 Hz, 3H), 1.36 (d, *J* = 7.2 Hz, 3H), 1.31 (d, *J* = 7.2 Hz, 3H). Analytical data corresponds with literature values.[27]

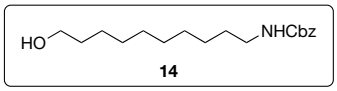

14

Benzyl (10-hydroxydecyl)carbamate (14)

Synthesis adapted from a method described by Delcros et al.[30] NaOH (127.2 mg, 3.18 mmol) was dissolved in H_2O (10 ml) and 10-amino-1-decanol (500 mg, 2.89 mmol) was added. THF (10 ml) was added to completely dissolve everything before benzylchloroformate was added dropwise. After 15 min the formed precipitate was filtered off and washed with water. The product was dried under high vacuum. Yield: 876 mg (2.85 mmol; 99%). R_f: 0.5 (EtOAc/Hex 1:1) ^{1}H NMR (300 MHz, $CDCl_3$) δ 7.39 – 7.28 (m, 5H), 5.09 (s, 2H), 4.71 (bs, 1H), 3.63 (q, *J* = 6.0 Hz, 2H), 3.18 (q, *J* = 6.0 Hz, 2H), 1.53 (m, 4H), 1.28 (s, 12H). ^{13}C NMR (101 MHz, $cdcl_3$) δ 156.5, 136.8, 128.6 (x2), 128.2, 128.2, 77.5, 77.2, 76.8, 66.7, 63.1, 41.2, 32.9, 30.1, 29.6, 29.5, 29.5, 29.3, 26.8, 25.8. HRMS ESI-TOF m/z calcd for $C_{18}H_{29}NO_3$ ($[M+H]^+$): 308.2226, Found 308.2252

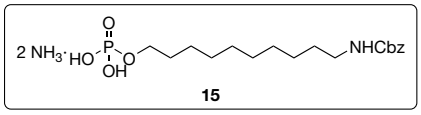

15

Benzyl (10-(phosphonooxy)decyl) carbamate (15)

$POCl_3$ (466 µl, 5 mmol) was dissolved in THF (10ml) and NEt_3 was added and stirred for 5 min before compound **14** (307.4 mg, 1 mmol) was added as a solution in 5 ml THF. After 20 stirring for 20 min the reaction mixture is poured into acetone/H_2O/NEt_3 (88:10:2, 50 ml) and stirred for 1h. Organic solvents were removed under reduced pressure and an aqueous suspension was obtained. The solid material was filtered, washed with H_2O and dissolved in 25% NH_4OH (50 ml). The aqueous solution was extracted with DCM (50 ml) before it was evaporated to dryness to obtain the product as a white powder. Yield: 300.6 mg (0.71 mmol;

71%) ^{1}H NMR (300 MHz, dmso) δ 7.39 – 7.11 (m, 5H), 6.55 (s, 3H), 5.08 (s, 2H), 3.97 (q, *J* = 6.0 Hz, 2H), 3.15 (q, *J* = 6.1 Hz, 2H), 1.69-1.55 (m, 2H), 1.54 – 1.41 (m, 2H), 1.26 (s, 12H). ^{13}C NMR (101 MHz, dmso) δ 156.1, 137.3, 128.3, 127.7, 127.7, 65.0, 64.5, 64.4, 45.3, 30.2, 30.1, 29.4, 29.0, 28.8, 26.3, 25.3, 8.4. HRMS ESI-TOF m/z calcd for $C_{18}H_{30}NO_6P$ ([M-H]$^-$): 386.1733, Found 386.1784

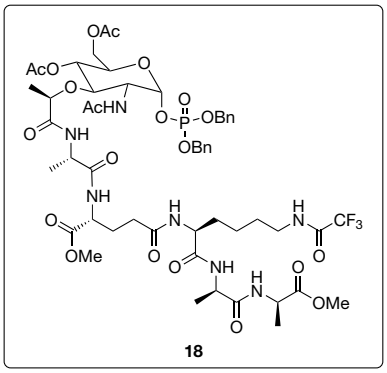

18

Protected MurNAc-pentapeptide-phosphate 18

Synthesis based on the procedure described by VanNieuwenhze et al.[6] Compound **6** (300 mg, 0.372 mmol) was dissolved in dry DCM (10 ml) and DBU (55.6 µl; 0.372 mmol) was added. After 15 min, TLC analysis indicated that the starting material was still present. More DBU (20 µl, 0.134 mmol) was added and TLC analysis after 10 min showed the reaction was complete. The mixture was diluted with DCM (10 ml) and extracted with 1M HCl (20 ml). The organic layer was diluted again with DCM (30 ml) and extracted with sat. $NaHCO_3$ (50 ml). The aqueous layer was acidified with 1M HCl to pH 2.0 and extracted with 10% iPrOH in chloroform (2 x 50 ml). The combined organic layers were dried over Na_2SO_4, filtered and evaporated to dryness. The residue was dissolved in dry DMF (5 ml) and EDCI (93 mg, 0.484 mmol) and N-hydroxysuccinimide (51 mg, 0.446 mmol) were added. The mixture was stirred for 2.5 h after which it was partitioned between EtOAc (50 ml) and H_2O (50 ml). The organic layer was dried over Na_2SO_4, filtered and evaporated to dryness. Compound **13** (241 mg, 0.338 mmol) was dissolved in TFA/DCM (10 ml) and stirred for 1 h. The solution was added dropwise to MTBE/Hex (1:1, 40 ml) and centrifuged at 5000 rpm for 5 min. The NHS-activated carbohydrate and the deprotected peptide were dissolved in 10 ml DMF and DIPEA (120 µl, 0.688 mmol) was added. The mixture was stirred for 16 h before it was concentrated under vacuum and partitioned between 10% IPA in $CHCl_3$ (25 ml) and water (25 ml). The organic layer was washed with brine (25 ml), dried over Na_2SO_4, filtered and concentrated under vacuum. The product was then applied to a silica column eluting with 5% EtOH in DCM -> 10% EtOH in DCM. Yield: 203 mg (0.165 mmol, 49%). R_f: 0.46 (10% EtOH in DCM) ^{1}H NMR (300 MHz, $CDCl_3$) δ 7.53 (d, *J* = 7.7 Hz, 1H), 7.48 – 7.29 (m, 10H), 7.17 (m, 2H), 7.11 (d, *J* = 7.5 Hz, 1H), 6.94 (d, *J* = 8.7 Hz, 1H), 6.55 (d, *J* = 8.9 Hz, 1H), 5.62 (dd, *J* = 5.8, 3.2 Hz,

1H), 5.15-5.00 (m, 4H), 4.58-4.44 (m, 3H), 4.42 – 4.31 (m, 2H), 4.26 – 4.09 (m, 2H), 4.02 (q, *J* = 6.4 Hz, 1H), 3.98 – 3.88 (m, 2H), 3.73 (s, 3H), 3.70 (s, 3H), 3.54 (t, *J* = 9.7 Hz, 1H), 3.42 – 3.24 (m, 2H), 2.49- 2.33(m, 1H), 2.30 – 2.18 (m, 1H), 2.08 (s, 3H), 2.01 (s, 3H), 1.79 (s, 3H), 1.45 (d, *J* = 7.2 Hz, 3H), 1.41 (m, 4H), 1.38 (d, *J* = 7.1 Hz, 3H), 1.30 (d, *J* = 6.7 Hz, 3H). Analytical data corresponds with literature values.[6]

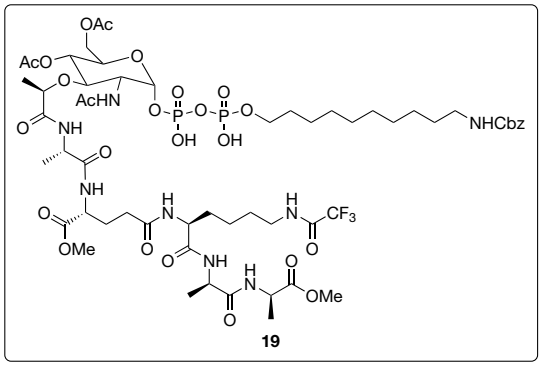

19

Pyrophosphate intermediate 19
Compound **18** (25 mg, 20.3 µmol) was dissolved in 5 ml MeOH and Pd/C (50 mg) was added. The mixture was stirred under H_2 atmosphere and after 45 min TLC (10% MeOH in DCM) indicated that the starting material was consumed. The catalyst was removed by filtration over celite and the solvents were evaporated. The deprotected compound was evaporated from toluene 5 times. Compound **15** (15.7 mg, 40.6 µmol) was dried by coevaporation from toluene (5x) and suspended in 5 ml dry THF and CDI (32.9 mg, 203 µmol) was added. The reaction was stirred for 2h under Ar (g). To quench the excess CDI, dry MeOH (1.5 ml) was added and the mixture was stirred for another 15 min. After evaporation of solvents the activated spacer was coevaporated from toluene 5 times. Deprotected compound **18** was added and the mixture was coevaporated from toluene 5 times. The dry solids are dissolved in 0.5 ml dry DMF and 1 ml dry THF, followed by addition of 1*H*-Tetrazole (3 mg, 42.8 µmol). The mixture was stirred for 16 h when HPLC analysis indicated compound 18 was still present. More compound 15 (23.6 mg, 61 µmol) was activated with CDI (49.4 mg, 304.8 µmol) and added to the reaction as a solution in 0.75 ml dry THF. After another 24 h all starting material was consumed and the product was purified by preparative HPLC (Dr.Maisch ReproSil-Pur 120 C18-AQ, 10 µm, 250 x 22 mm) using a gradient of 50-100% buffer B over 65 min at a flow rate of 8.4 ml/min. Buffer A: 50 mM NH_4HCO_3, Buffer B: MeOH. Fraction containing pure product were pooled and lyophilized. Yield: 20.7 mg (14.2 µmol; 70 %). $[\alpha]_D$ = +35.9 ± 1.0 (c 0.28, MeOH/H_2O 1:1) HRMS ESI-TOF m/z calcd for $C_{57}H_{89}F_3N_8O_{26}P_2$ ($[M-H]^-$): 1419.5237, Found 1419.5258. NMR analysis is discussed in section 2.7.2.1

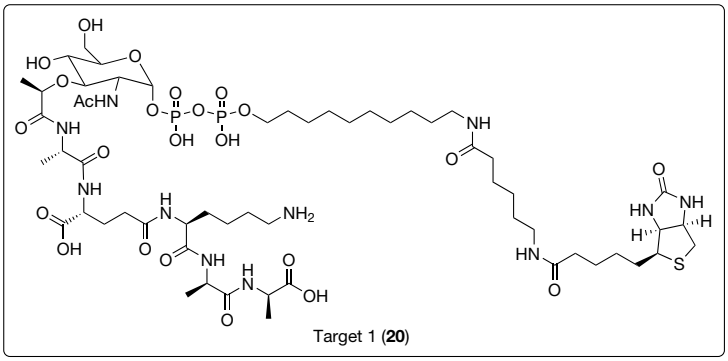

Target 1 (**20**)

Target 1 (20)

Compound **19** (26.5 mg, 18.6 µmol) was dissolved in MeOH (2.5 ml) and Pd/C was added as a suspension in MeOH (2.5 ml). The mixture was stirred under a hydrogen atmosphere for 2 h. The catalyst was removed by filtration over celite and the filtrate was evaporated to dryness. The deprotected product was dissolved in H_2O/dioxane (1:1, 2 ml) and $NaHCO_3$ (3.13 mg, 37.2 µmol) was added followed by biotin-X-NHS (10.8 mg, 22.4 µmol). The mixture was stirred until all starting material had been consumed (as analyzed by HPLC). Glycine (1.4 mg, 18.6 µmol) was added to quench the excess biotin-X-NHS and the mixture was stirred for 1h. After addition of 1M NaOH (186 µl) the mixture was stirred for another 2 h before the dioxane was removed by evaporation under vacuum. The product was immediately purified by preparative HPLC (Dr.Maisch ReproSil-Pur 120 C18-AQ, 10 µm, 250 x 22 mm) using a gradient of 30-100% buffer B over 105 min at a flow rate of 8.4 ml/min. Buffer A: 50 mM NH_4HCO_3, Buffer B: MeOH. Fraction containing product were pooled and lyophilized. Yield: 14.7 mg (9.9 µmol, 53%). HRMS ESI-TOF m/z calcd for $C_{57}H_{101}N_{11}O_{24}P_2S$ ([M-H]$^-$): 1416.6139, Found 1416.6169. NMR analysis is discussed in section 2.7.2.2.

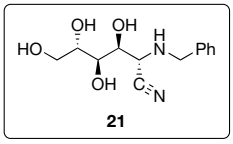

21

(2R,3S,4R,5S)-2-(benzylamino)-3,4,5,6-tetrahydroxyhexanenitrile (21)

Method adapted from Kuhn et al.[20] L-Arabinose (10 g, 66.6 mmol) was suspended in dry EtOH (40 ml) and benzylamine (10 ml, 91.6 mmol) was added. The mixture was heated to 85°C until everything dissolved. After cooling to 30°C KCN (4.76 g, 73.1 mmol) was added and the flask was sealed with a septum. AcOH (5.78 ml, 10.1 mmol) was added while vigorously stirring the suspension until it becomes homogenous. The solution was stirred at r.t. for 30 min before a precipitate starts to form. The mixture is cooled on ice for 1h and the solids are collected by filtration and washed with cold EtOH. Yield: 13.92 g (52.3 mmol, 79%) R_f: 0.76 (MeOH/n-

BuOH/H2O/conc. Ammonia 80:20:10:3) ^{1}H NMR (400 MHz, dmso) δ 7.41 – 7.21 (m, 5H), 4.97 (d, *J* = 6.0 Hz, 1H), 4.69 (d, *J* = 5.9 Hz, 1H), 4.55 (d, *J* = 4.2 Hz, 1H), 4.36 (t, *J* = 5.4 Hz, 1H), 4.02 – 3.87 (m, 2H), 3.79 – 3.66 (m, 2H), 3.64 – 3.54 (m, 1H), 3.48 (d, *J* = 2.6 Hz, 2H), 3.41 (dd, *J* = 10.3, 4.9 Hz, 1H), 2.94 (q, *J* = 6.2 Hz, 1H). ^{13}C NMR (101 MHz, dmso) δ 139.2, 128.3, 128.1, 127.0, 119.5, 71.0, 70.8, 69.4, 63.3, 52.7, 50.8. HRMS ESI-TOF m/z calcd for $C_{13}H_{18}N_2O_4$ ([M+Na]$^+$): 289.1164, Found 289.1208

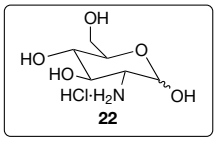

22

L-glucosamine hydrochloride (22)

Method adapted from Kuhn et al.[20] Compound **21** (13.92 g, 52.3 mmol) was dissolved in 1M HCl (125 ml) and Pd(II)O hydrate (70-80% Pd) was added. The mixture was hydrogenated at 50 PSI for 24 h when TLC indicated full consumption of the starting material. The catalyst was removed by filtration over celite and the aqueous solution was evaporated to dryness. A yellowish powder was obtained and digested in EtOH at 60°C. After cooling to 0°C the product was obtained by filtration as an off-white powder. The product was used without further purification. Yield: 7.42 g (34.4 mmol; 66%) R_f: 0.37 (MeOH/n-BuOH/H_2O/conc. Ammonia 80:20:10:3)

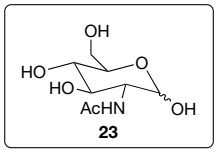

23

***N*-acetyl-L-glucosamine (23)**

Method described by Berger et al.[31] Freshly cut sodium (0.95 g, 41.3 mmol) was dissolved in dry MeOH (75 ml) and added to a suspension of compound **22** (7.42 g, 34.4 mmol). The mixture was stirred for 30 min before Ac_2O (8.1 ml, 86 mmol) was added and left to stir overnight. The mixture was cooled to -20°C and allowed to precipitate for 24 h. The precipitate was collected by filtration and washed with Et_2O and dried under vacuum. Yield: 6.13 g, (27.7 mmol, 53% from **21**) R_f: 0.6 (MeOH/n-BuOH/H2O/conc. Ammonia 80:20:10:3). ^{1}H NMR (400 MHz, dmso) δ 7.70 (d, *J* = 7.1 Hz, 1H), 6.40 (d, *J* = 4.4 Hz, 1H), 4.99 (d, *J* = 5.0 Hz, 1H), 4.92 (dd, *J* = 4.2, 2.4 Hz, 1H), 4.76 (d, *J* = 3.7 Hz, 1H), 4.45 (t, *J* = 5.8 Hz, 1H), 3.64 – 3.42 (m, 5H), 3.19 – 3.03 (m, 2H), 1.82 (s, 3H). ^{13}C NMR (101 MHz, dmso) δ 169.4, 90.6, 72.1, 71.2, 70.5, 61.2, 54.3, 22.7. NMR corresponds with *N*-acetyl-D-glucosamine. HRMS ESI-TOF m/z calcd for $C_8H_{15}NO_6$ ([M+H]$^+$): 222.0978, Found 222.1000

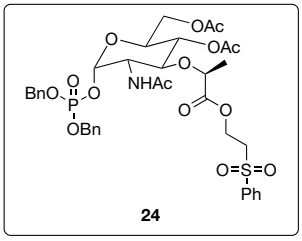

24

2-(phenylsulfonyl)ethyl (S)-2-(((2S,3S,4S,5R,6S)-3-acetamido-5-acetoxy-6-(acetoxymethyl)-2-((bis(benzyloxy)phosphoryl)-oxy)tetrahydro-2H-pyran-4-yl)oxy)propanoate (24)

See synthesis of **6**. Analytical data matched the data from compound **6**. $[\alpha]_D$ = -62.6 (c 0.4, MeOH)

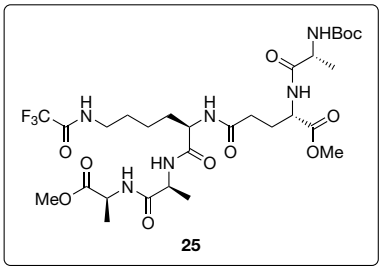

25

Methyl N2-((tert-butoxycarbonyl)-D-alanyl)-N5-((R)-1-(((S)-1-(((S)-1-methoxy-1-oxopropan-2-yl)amino)-1-oxopropan-2-yl) amino)-1-oxo-6-(2,2,2-trifluoro-acetamido) hexan-2-yl)-L-glutaminate (25)

See synthesis of **13**. Analytical data matched the data from compound **13**. $[\alpha]_D$ = -20.8 (c 0.2, MeOH)

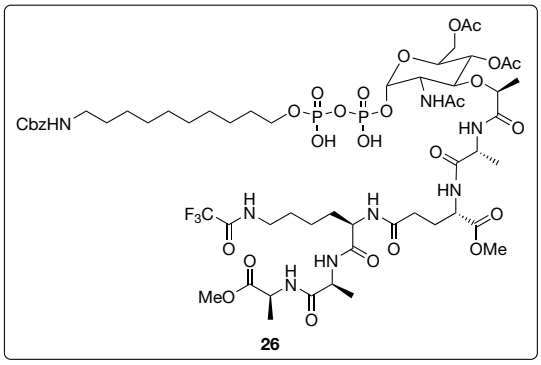

26

Pyrophosphate intermediate 26

See synthesis of compound **19**. $[\alpha]_D$ = +33.9 ± 1.6 (c 0.29, MeOH/H_2O 1:1) HRMS ESI-TOF m/z calcd for $C_{57}H_{89}F_3N_8O_{26}P_2$ ($[M-2H]^{2-}$): 709.2580, Found: 709.2575. NMR analysis is discussed in section 2.7.2.1.

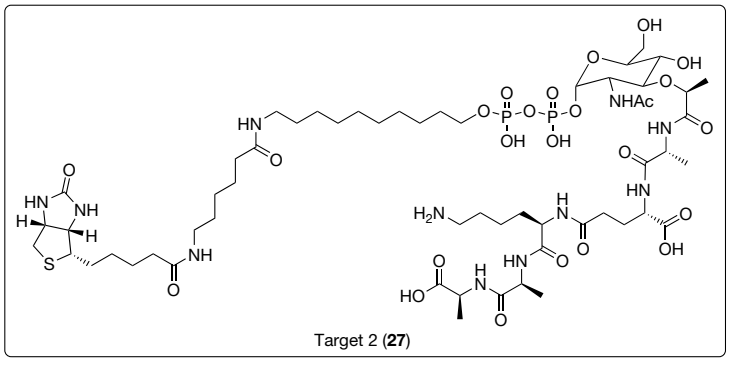

Target 2 (**27**)

Target 2 (27)

See the synthesis of target 1 (**20**). HRMS ESI-TOF m/z calcd for $C_{57}H_{101}N_{11}O_{24}P_2S$ ($[M-H]^-$): 1416.6139, Found 1416.6187. NMR analysis is discussed in section 2.7.2.2.

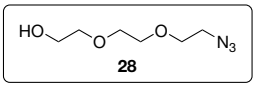

28

Synthesis of 2-(2-(2-azidoethoxy)ethoxy)ethan-1-ol (28)

2-(2-(2-chloroethoxy)ethoxy)ethanol (10 g, 59.3 mmol) was dissolved in DMF (100 ml) and NaN_3 (5.78 g, 89.0 mmol) was added. The mixture was stirred at a 100°C for 16 h. After cooling to r.t. the mixture was filtered over celite and evaporated to dryness. The resulting oil was dissolved in DCM (100 ml) and washed with H_2O (50 ml). The aqueous phase was extracted with DCM (50 ml) and the combined organic phases were dried over Na_2SO_4, filtered and evaporated to dryness. Yield: quant. R_f: 0.40 (EtOAc). ^{1}H NMR (300 MHz, $CDCl_3$) δ 3.81 – 3.66 (m, 8H), 3.62 (t, *J* = 4.5 Hz, 2H), 3.41 (t, *J* = 4.8 Hz, 2H), 2.24 (t, *J* = 6.1 Hz, 1H). Analytical data corresponds with literature values.[32]

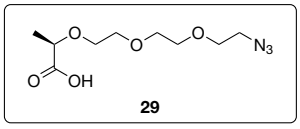

29

Synthesis of (R)-2-(2-(2-(2-azidoethoxy)ethoxy) ethoxy)propanoic acid (29)

Compound **28** (500 mg, 2.85 mmol) and S-2-chloropropionic acid (384 µl, 4.43 mmol) were dissolved in dry THF (15 ml). The mixture was cooled on ice and NaH (60% dispersion in mineral oil, 706 mg, 17.70 mmol) was added in portions. After stirring for 30 min the ice bath was removed and the mixture was stirred for another 2h. TLC analysis indicated the starting material was still present and therefore more S-2-chloropropionic acid (154 µl, 1.77 mmol) was added. After 1h TLC analysis showed the starting material was still present and another addition of S-2-chloropropionic acid (77 µl, 0.89 mmol) was made. TLC analysis after 1 h showed all the starting material had been consumed. The mixture was cooled on ice and H_2O (55 ml) was added slowly. The mixture was extracted with EtOAc (3 x 50 ml) and the aqueous solution was acidified on ice with 2M HCl to pH 2. The aqueous layer was then extracted with EtOAc (4 x 50 ml) and the combined organic layers were dried over Na_2SO_4, filtered and evaporated to dryness. Further purification was done on a silica column eluting with EtOAc + 1% AcOH. Yield: 434 mg (1.75 mmol, 62%) Rf: 0.22 (EtOAc + 1% AcOH). ^{1}H NMR (300 MHz, $CDCl_3$) δ 7.35 (bs, 1H), 4.06 (q, *J* = 6.9 Hz, 1H), 3.87 – 3.59 (m, 10H), 3.41 (t, *J* = 4.8Hz, 2H), 1.46 (d, *J* = 6.9 Hz, 3H). ^{13}C NMR (101 MHz, $CDCl_3$) δ 175.7, 75.5, 70.6, 70.4, 70.2, 70.0, 69.7, 50.6, 18.3. HRMS ESI-TOF m/z calcd for $C_9H_{17}N_3O_5$ ([M+Na]$^+$): 270.1066, Found 270.1111.

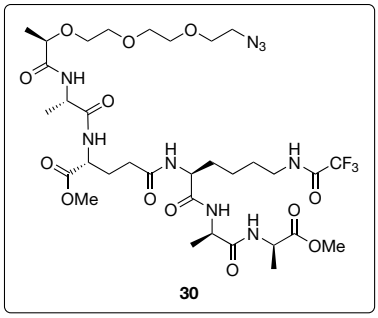

30

Azidospacer modified pentapeptide (30)

Compound **13** (171 mg, 0.240 mmol) was dissolved in TFA/DCM (1:1, 10 ml) and stirred for 1h. The solution was added dropwise to MTBE/Hex (1:1, 80 ml) and centrifuged at 5000 rpm for 5 min. The pellets were dissolved in DMF (10 ml) followed by the addition of compound **29** (74 mg, 0.300 mmol), BOP (133 mg, 0.300 mmol) and DIPEA (125 µl, 0.720 mmol). The reaction mixture was stirred for 16 h and then evaporated to dryness. The residue was dissolved in EtOAc (25 ml) and washed with 1M $KHSO_4$ (25 ml), 5% $NaHCO_3$ (25 ml) and brine (25 ml). The organic layer was dried over Na_2SO_4, filtered and evaporated to dryness. The crude product was further purified on a silica column eluting with 5% MeOH in DCM -> 7% MeOH in DCM. Yield: 127 mg (0.151 mmol; 63%). R_f: 0.47 (10% MeOH in DCM) ^{1}H NMR (400 MHz, dmso) δ 9.37 (t, *J* = 5.1 Hz, 1H), 8.37 (t, *J* = 9.4 Hz, 1H), 8.18 (t, *J* = 6.8 Hz, 2H), 8.00 (t, *J* = 10.9 Hz, 1H), 7.67 (d, *J* = 7.9 Hz, 1H), 4.42 – 4.32 (m, 1H), 4.32 – 4.27 (m, 1H), 4.27 – 4.13 (m, 3H), 3.85 (q, *J* = 6.6 Hz, 1H), 3.62 (s, 3H), 3.60 (s, 3H), 3.59 – 3.47 (m, 8H), 3.38 (t, *J* = 4.7 Hz, 2H), 3.15 (q, *J* = 6.5 Hz, 2H), 2.25 – 2.12 (m, 2H), 1.98 – 1.71 (m, 3H), 1.65 – 1.53 (m, 2H), 1.53 – 1.39 (m, 3H), 1.29 (d, *J* = 7.2 Hz, 3H), 1.24 (d, *J* = 7.0 Hz, 3H), 1.23 – 1.16 (m, 6H). HRMS ESI-TOF m/z calcd for $C_{33}H_{54}F_3N_9O_{13}$ ([M+H]$^+$): 842.3871, Found 842.3840.

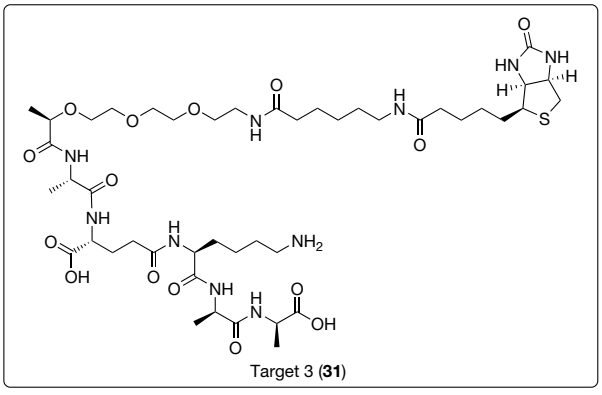

Target 3 (**31**)

Target 3 (31)

Compound **30** (50 mg, 59.4 µmol) was dissolved in MeOH (10 ml) and Pd/C (25 mg) was added as a suspension in MeOH (2.5 ml). The mixture was stirred under a hydrogen atmosphere for 1 h. The catalyst was removed by filtration over celite and the filtrate was evaporated to dryness. The deprotected product was dissolved in H_2O/dioxane (1:1, 6 ml) and $NaHCO_3$ (10 mg, 118.8 µmol) was added followed by biotin-X-NHS (34.4 mg, 71.3 µmol). The mixture was stirred until all starting

material had been consumed (as analyzed by HPLC). Glycine (4.5 mg, 59.4 µmol) was added to quench the excess biotin-X-NHS and the mixture was stirred for 2 h. After addition of 1M NaOH (354 µl) the mixture was stirred for another 2 h before the dioxane was removed by evaporation under vacuum. The product was immediately purified by preparative HPLC (Dr.Maisch ReproSil-Pur 120 C18-AQ, 10 µm, 250 x 22 mm) using a gradient of 30-100% buffer B over 105 min at a flow rate of 8.4 ml/min. Buffer A: 50 mM NH_4HCO_3, Buffer B: MeOH. Fraction containing product were pooled and lyophilized. Yield: 14.7 mg (9.9 µmol, 53%) HRMS ESI-TOF m/z calcd for $C_{45}H_{78}N_{10}O_{15}S$ ($[M+H]^+$): 1031.5447, Found 1031.5474. NMR analysis is discussed in section 2.7.2.3.

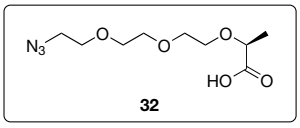

32

(S)-2-(2-(2-(2-azidoethoxy)ethoxy)ethoxy) propanoic acid (32)

Synthesis as for compound **29** but with R-2-chloropropionic acid. HRMS ESI-TOF m/z calcd for $C_9H_{17}N_3O_5$ ($[M+Na]^+$): 270.1066, Found 270.1068

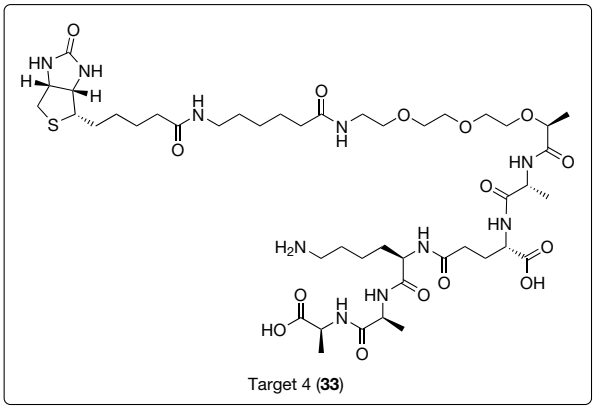

Target 4 (**33**)

Target 4 (33)

See the synthesis of target 3 (**31**). HRMS ESI-TOF m/z calcd for $C_{45}H_{78}N_{10}O_{15}S$ ($[M+H]^+$): 1031.5447, Found 1031.5476. NMR analysis is discussed in section 2.7.2.3

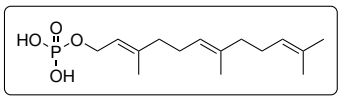

Trans,trans-farnesyl phosphate

Synthesis as described by Lira et al. starting from trans,trans-farnesol (260 µl, 1.04 mmol).[22] Yield: 88.7 mg (0.278 mmol, 29%)

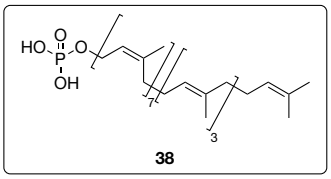

38

Undecaprenol phosphate (38)

Synthesis adapted from Lira et al with the following changes: Undecaprenol (160 mg, 209 µmol) was dissolved in $CHCl_3$ (0.2 ml) and trichloroacetonitrile (50.3 µl, 502 µmol) was added followed by a slow

addition of tetrabutylammonium dihydrogenphosphate (141.9 mg, 418 µmol) as a solution in $CHCl_3$ (1 ml). From here the protocol was followed as described.[22] Yield: 61.6 mg (73 µmol, 35%) R_f: 0.46 ($CHCl_3$/MeOH/H_2O/NH_4OH, 88:48:10:1)

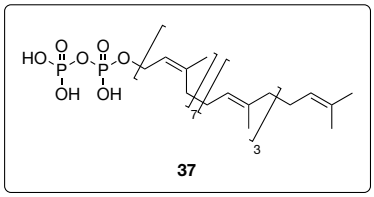

37

Undecaprenyl-pyrophosphate (C_{55}PP) (37)
Undecaprenol (11.3 mg, 14.8 µmol) was dissolved in dry DCM (2 ml) and CBr_4 (14.7 mg, 44.4 µmol) was added, followed by PPh_3 (9.7 mg, 37 µmol). After 20 min TLC indicated full consumption of the starting material. The reaction mixture was evaporated to dryness and applied to a short silica column eluting with 5% EtOAc in hexanes + 1% NEt_3. Fractions containing product were pooled evaporated and immediately dissolved in dry chloroform (0.5 ml), tris(tetra-n-butylammonium) hydrogen pyrophosphate (53.7 mg, 59.5 µmol) was added and the mixture was stirred for 16 h under an argon atmosphere. The reaction mixture was diluted with (iPrOH/25% NH_4OH/H_2O 7:2:1) until a homogenous solution was obtained. The solution was applied to a silica column eluting with iPrOH/25% NH_4OH/H_2O (7:2:1). Fractions containing product were pooled and concentrated to approx. 0.5 ml. After dilution with 25 mM NH_4HCO_3 (10 ml) Dowex 50wx8 (NH_4^+-form) was added and the mixture was shaken for 1h. The Dowex was removed by filtration and the aqueous solution concentrated to 5 ml. Chloroform (5 ml) was added and after thorough shaking a suspension was obtained. Addition of small amounts of MeOH allowed the mixture to separate. The aqueous solution was treated this way once more and the organic layers were combined. After drying over Na_2SO_4 the product was kept in the organic solution (MeOH/$CHCl_3$) as rapid degradation of the dried compound was observed. The yield was determined by measuring the total amount of free phosphate by the method of Rouser et al.[24] (5.64 mg, 5.89 µmol, 39.8%) R_f: 0.37 ($CHCl_3$/MeOH/H_2O/NH_4OH, 88:48:10:1) HRMS ESI-TOF m/z calcd for $C_{26}H_{46}N_2O_{13}P_2$ ($[M-H]^-$): 925.6245, Found 925.6227. Material should be stored –20 °C at 10 mg/ mL in 10 mM ammonium bicarbonate or at –80 °C at 1 mg/mL in chloroform/methanol/1% NH4OH (65/35/4), respectively.

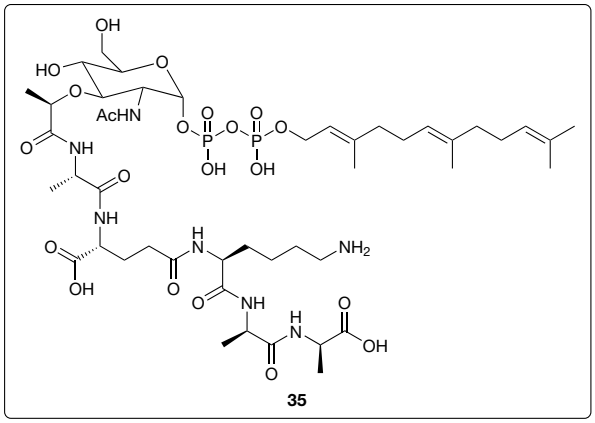

Farnesyl-Lipid I (35)

Synthesis done as described by Blasczcak et al. using compound **18** and farnesylphosphate.[6] Compound **35** was purified using a Maisch ReproSil-Pur 120 C18-AQ column (250 x 22 mm, 10 µm) eluting with a gradient of 0% to 100 % buffer B over 90 min with a flow of 12 ml/min. Product eluted at 37.7 min. Buffer A: 10 mM NH_4HCO_3, Buffer B: MeCN. Yield: 15.4 mg (13.7 µmol, 33.8%) HRMS ESI-TOF m/z calcd for $C_{46}H_{79}N_7O_{21}P_2$ ([M-H]$^-$): 1126.4732, Found: 1126.4785. NMR data corresponds with previously published.[19]

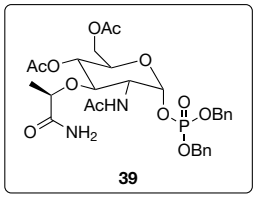

(2R,3S,4R,5R,6R)-5-acetamido-2-(acetoxymethyl)-4-(((R)-1-amino-1-oxopropan-2-yl)oxy)-6-((bis(benzyloxy)phosphoryl)oxy)tetrahydro-2H-pyran-3-yl acetate (39)

Compound **6** (303.1 mg, 0.38 mmol) was dissolved in DCM (10 ml) and DBU (112 µl, 0.75 mmol) was added dropwise. The mixture was stirred for 2 h before it was diluted with DCM (10 ml) and extracted with 1M HCl (20 ml). The organic layer was dried over Na_2SO_4, filtered and evaporated to dryness. The compound was further purified by column chromatography (5% MeOH in DCM -> 5% MeOH in DCM + 1% AcOH). After dissolving the free carboxylic acid in DMF (4 ml), BOP (417.2 mg, 0.94 mmol), NH_4Cl (207.5 mg, 3.88 mmol) and DIPEA (660 µl, 3.80 mmol) were added and the mixture was stirred for 24 h. After removal of the solvents under vacuum, the residue was dissolved in EtOAc (20 ml) and extracted with 1M $KHSO_4$ (10 ml), sat $NaHCO_3$ (10 ml), and brine (10 ml). The organic layer was dried over Na_2SO_4, filtered and evaporated to dryness. The compound was further purified by column chromatography ($CHCl_3$/Acetone 2:1 -> 1:2). Fractions containing product were pooled and the product was obtained as an off white solid. Yield: 121.2 mg (0.190 mmol, 51%). HRMS ESI-TOF m/z calcd for $C_{29}H_{37}N_2O_{12}P$ ([M+Na]$^+$): 659.1976, found: 659.1975. ^{1}H NMR (400 MHz, $CDCl_3$) δ 7.41 – 7.30 (m, 10H), 6.39 (s, 1H), 6.00 (d, *J* = 9.5 Hz, 1H), 5.56 (dd, *J* =

5.8, 3.2 Hz, 1H), 5.32 (s, 1H), 5.14 – 4.99 (m, 5H), 4.40 – 4.32 (m, 1H), 4.10 (dd, *J* = 13.0, 4.6 Hz, 1H), 3.91 (t, *J* = 2.4 Hz, 1H), 3.90 – 3.82 (m, 2H), 3.43 (t, 1H), 2.07 (s, 3H), 1.99 (s, 3H), 1.76 (s, 3H), 1.30 (d, *J* = 6.8 Hz, 3H). ^{13}C NMR (101 MHz, $CDCl_3$) δ 174.7, 171.0, 170.7, 169.2, 129.3 (2x), 129.0 (2x), 128.3 (2x), 97.2, 79.1, 78.0, 70.4, 70.3, 70.2, 68.8, 61.6, 52.9 (2x), 23.2, 21.0, 20.9, 18.82.

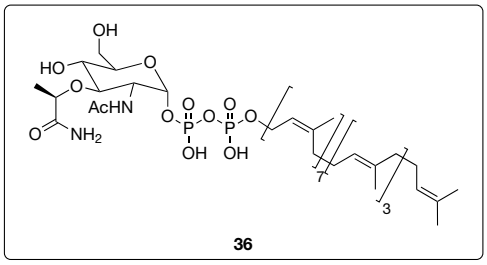

36

Undecaprenol-MurNAc-amide (36)

Synthesis done as described by Blasczcak et al. but starting from compound **39** (22.5 mg, 35.4 µmol).[6] Compound **36** was purified using a Dr. Maisch Reprospher 100 C8-Aqua column (250 x 20 mm, 10 µm) eluting with a gradient of 25% to 100% buffer B over 1 h with a flow of 12 ml/min. Product eluted at 43.0 min. Buffer A: 10 mM NH_4HCO_3, Buffer B: MeCN. Yield: 7.1 mg (5.91 µmol, 17%). R_f: 0.48 ($CHCl_3$/MeOH/H_2O/NH_4OH, 88:48:10:1) HRMS ESI-TOF m/z calcd for $C_{66}H_{110}N_2O_{13}P_2$ ([M-H]$^-$): 1199.7410, Found 1199.7447. ^{1}H NMR (500 MHz, CD_3OD/$CDCl_3$ (1:1)) δ 5.50 (d, 1H), 5.41 (t, 1H), 5.14 (s, 11H), 4.48 (s, 2H), 4.18 (q, 1H) 4.13 (d, 1H) 3.99 (t, *J* = 10.8 Hz, 2H), 3.72 – 3.54 (m, 3H), 3.32 (t, 1H), 2.14-1.92 (m, 43H), 1.74 (s, 3H), 1.69 (s, 21H), 1.62 (s, 3H), 1.60 (s, 9 H), 1.44 (d, *J* = 6.6 Hz, 3H). ^{13}C NMR (125 MHz, CD_3OD/$CDCl_3$ (1:1)) δ 147.2, 146.7, 143.9, 117.1, 103.0, 100.5, 95.9, 92.9, 85.5, 84.5, 75.4, 62.1, 54.5, 48.7, 46.3, 45.4, 45.3, 44.4, 41.0, 37.9

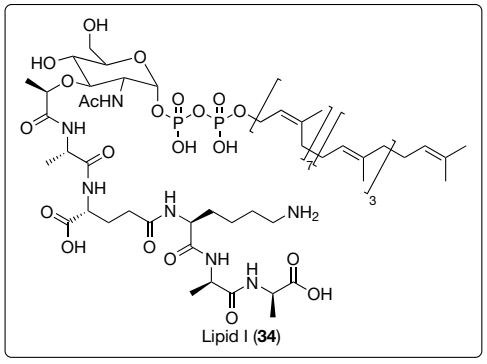

Lipid I (**34**)

Lipid I (34)

Synthesis done as described by Blasczcak et al. starting from compound **18** (43.6 mg, 35.4 µmol).[6] Compound **34** was purified using a Maisch C8-AQ column (250 x 22 mm, 10 µm) eluting with a gradient of 25% to 100 % buffer B over 90 min with a flow of 12 ml/min. Buffer A: 10 mM NH_4HCO_3, Buffer B: MeCN. Yield: 17.8 mg (10.6 µmol, 30%) R_f: 0.13 ($CHCl_3$/MeOH/H_2O/NH_4OH, 88:48:10:1). Analytical data corresponds with previously published.[19]

2.7.2 NMR-analysis of compounds 26, 27 and 33

To analyse the chemical structure of the novel compounds **26**, **27** and **33** several 2D-NMR techniques were employed. These included COSY, TOCSY, HSQC and NOESY measurements to observe the full composition and connectivity of our compounds.

2.7.2.1 NMR analysis of compound 26

The results of the NMR analysis are shown in table 1. TOCSY, NOESY and HSQC (figure 9 and 10) were measured in H_2O/D_2O (9:1) and COSY in D_2O. Identical spectra were recorded for compound **19**.

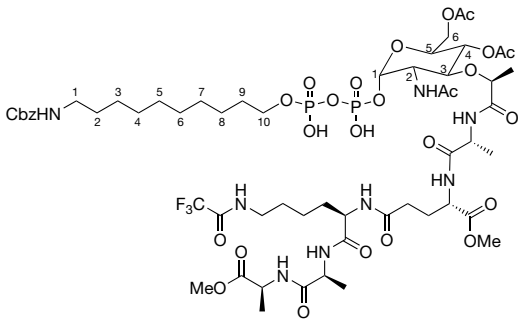

Figure 8: Structure of compound **26** and numbering used for the assignment of NMR peaks.

Table 1: Chemical shift assignments for compound 26. See figure 8 for numbering scheme.

Assignment	Peaks ^{1}H (δ in ppm)	Peaks ^{13}C (δ in ppm)
Carbohydrate:		
C1	5.44	95.3
C2	4.24	54.5
C3	4.01	78.5
C4	5.01	Overlaps with solvent
C5	4.33	69.8
C6	4.45, 4.13	62.8
Lactic acid	4.10 (CH), 1.25 (CH_3)	79.2 (CH), 19.5 (CH_3)
NH-C2	8.65	
Acetyl-NH	1.95	23.1
Acetyl-C4	2.12	21.4
Acetyl-C6	2.07	21.2
Pentapeptide:		
D-Ala1	8.39 (NH), 4.34 (αCH), 3.68 (OCH_3), 1.38 (βCH_3)	49.7 (αCH), 53.9 (OCH_3), 16.9 (βCH_3)
D-Ala2	8.56 (NH), 4.24 (αCH), 1.34 (βCH_3)	50.6 (αCH), 17.4 (βCH_3)
L-Lys3	9.40 (εNH_2), 8.33 (αNH), 4.13 (αCH), 3.27 (εCH_2), 1.70 (βCH_2), 1.55 (δCH_2), 1.37 (γCH_2-1), 1.31 (γCH_2-2),	55.3 (αCH), 40.4 (εCH_2), 31.2 (βCH_2), 28.3 (δCH_2), 23.2 (γCH_2-1 + γCH_2-2)

Assignment	Peaks ^{1}H (δ in ppm)	Peaks ^{13}C (δ in ppm)
D-Glu4	8.54 (NH), 4.29 (αCH), 3.68 (OCH_3), 2.29 (γCH_2), 2.15 (βCH_2-1), 1.91 (βCH_2-2)	52.9 (αCH), 53.9 (OCH_3), 32.0 (γCH_2), 27.1 (βCH_2-1 + βCH_2-2)
L-Ala5	7.92 (NH), 4.16 (αCH), 1.39 (βCH_3)	50.9 (αCH), 17.5 (βCH_3)
Spacer:		
C10-chain	6.94 (NH), 3.91 (C10), 3.07 (C1), 1.61 (C9), 1.43 (C2), 1.33 (C8), 1.28 – 1.24 (C3-7),	67.8 (C10), 41.5 (C1), 30.8 (C9), 29.7 (C2), 26.0 (C8), 29.5 + 26.8 (C3-7)
Cbz-group	7.38, 7.36, 7.34 (aromatic), 5.05 (CH_2)	129.6, 128.5, 129.1 (aromatic), CH_2 overlaps with solvent

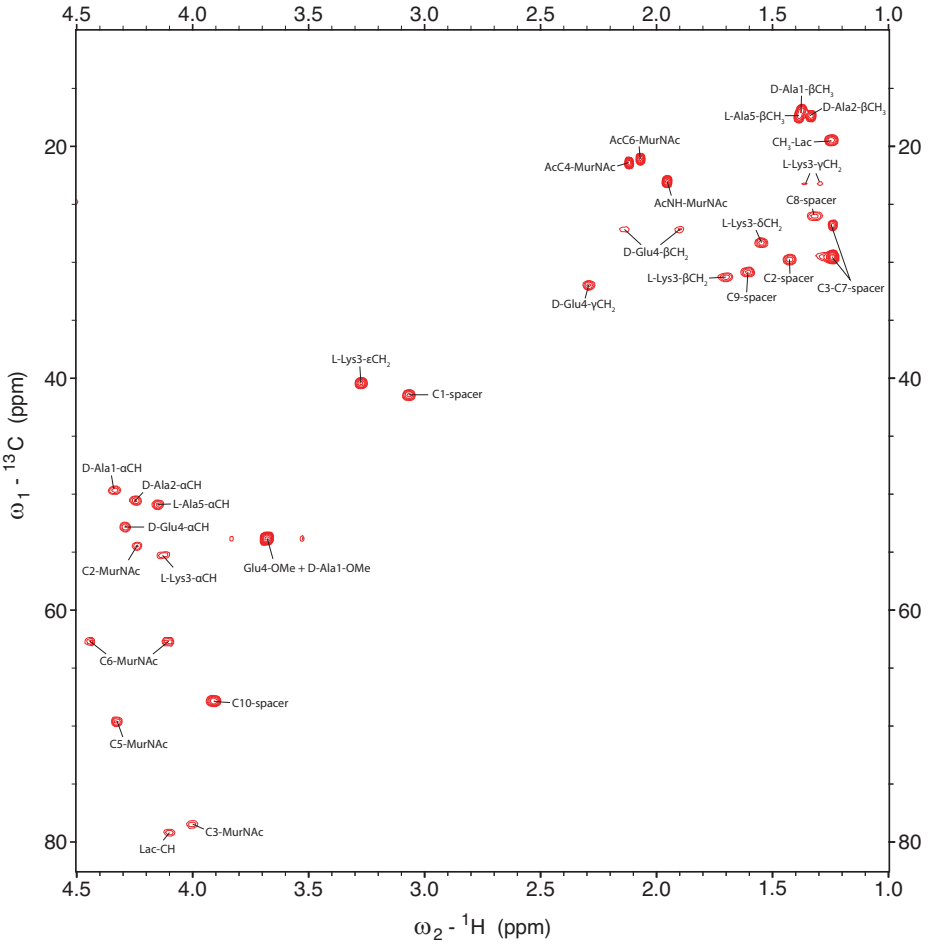

Figure 9: Cutout of HSQC spectrum of compound **26**. Outside of this view are the signal for the anomeric centre of MurNAc (C1) and the aromatic signals of the Cbz-group.

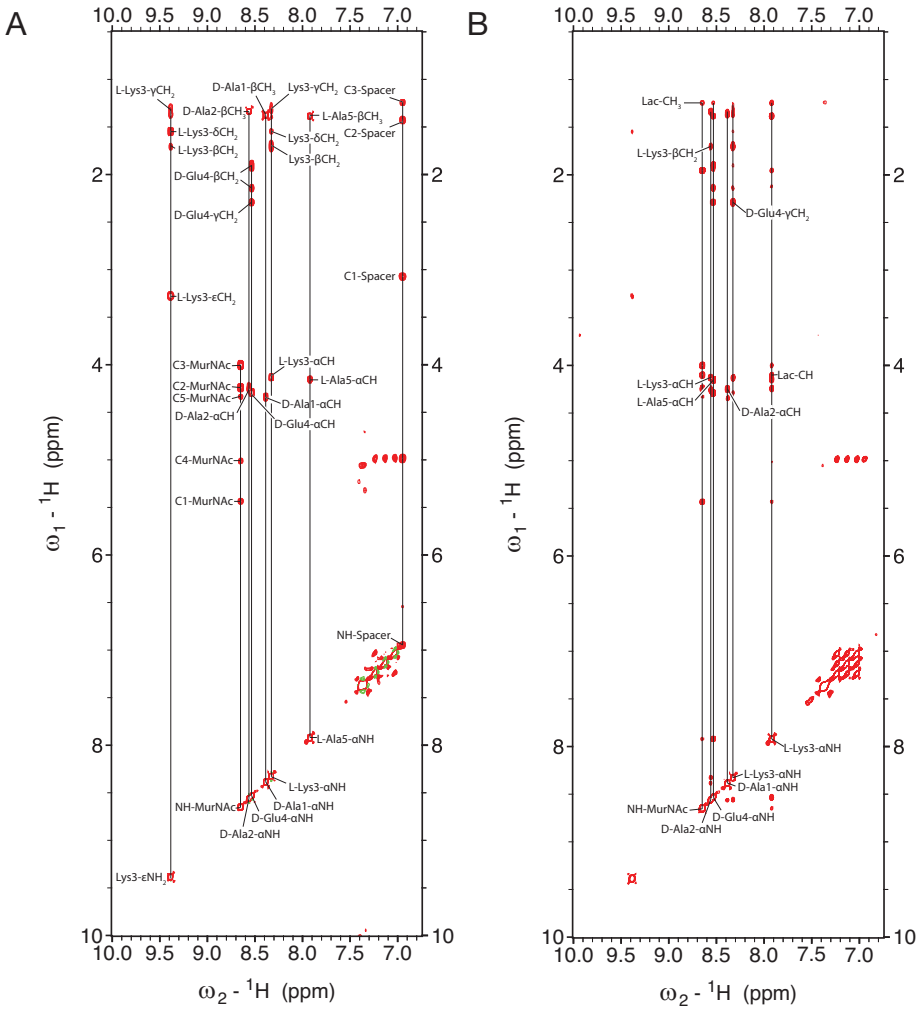

Figure 10: A) Detail of the TOCSY spectrum of compound **26** showing the assigned spinsystems. B) Detail of the NOESY spectrum of compound **26** indicating the correct connectivity of all amide bonds.

2.7.2.2 NMR assignments of compound 27

The results of the NMR analysis are shown in table 2. TOCSY, NOESY and HSQC (figure 12 and 13) were measured in H_2O/D_2O (9:1) and COSY in D_2O. Identical spectra were recorded for compound **20**.

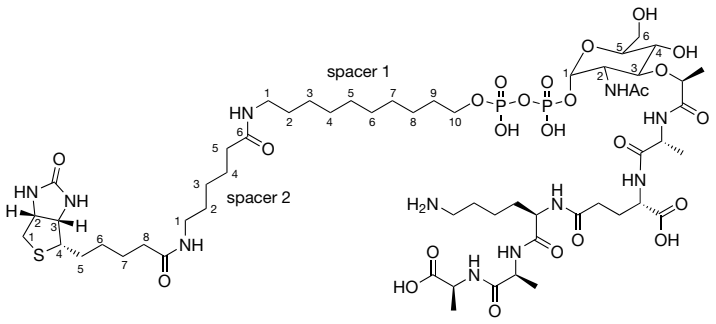

Figure 11: Structure of compound **27** and numbering used for the assignment of NMR peaks.

Table 2: Chemical shift assignments for compound **27**. See figure 11 for numbering scheme.

Assignment	Peaks ^{1}H (δ in ppm)	Peaks ^{13}C (δ in ppm)
Carbohydrate:		
C1	5.40	95.6
C2	4.09	54.5
C3	3.76	80.8
C4	3.61	68.9
C5	3.91	73.9
C6	3.83	61.2
Lactic acid	4.18 (CH), 1.37 (CH_3)	80.0 (CH), 19.6 (CH_3)
Acetyl-NH	1.97	23.1
NH-C2	8.58	
Pentapeptide:		
D-Ala1	8.24 (NH), 4.19 (αCH), 1.35 (βCH_3)	51.1 (αCH), 19.6 (βCH_3)
D-Ala2	8.48 (NH), 4.28 (αCH), 1.34 (βCH_3)	50.7 (αCH), 17.5 (βCH_3)
L-Lys3	7.59 (εNH_2), 8.36 (αNH), 4.15 (αCH), 2.96 (εCH_2), 1.76 (βCH_2), 1.65 (CH_2), 1.41 (γCH_2)	55.4 (αCH), 40.3 (εCH_2), 31.3 (βCH_2), 27.4 (δCH_2), 23.1 (γCH_2)
D-Glu4	8.14 (NH), 4.17 (αCH), 2.29 (γCH_2), 2.16 (βCH_2-1), 1.88 (βCH_2-2)	54.4 (αCH), 32.5 (γCH_2), 28.4 (βCH_2-1 + βCH_2-2)
L-Ala5	8.03 (NH), 4.21 (αCH), 1.42 (βCH_3)	51.1 (αCH), 17.8 (βCH_3)
Spacers + biotin:		
C10-spacer	8.08 (NH), 3.90 (C10), 3.13 (C1), 1.59 (C9), 1.57 (C2), 1.47 (C8), 1.28 - 1.20(C3-7),	67.9 (C10), 40.3 (C1), 30.9 (C9), 26.2 (C2), 29.1 (C8), 30.6 – 26.2 (C3-7)
C6-spacer	8.14 (NH), 3.13 (C1), 2.21 (C5), 1.57 (C4), 1.46 (C2), 1.28 (C3)	40.3 (C1), 36.6 (C5), 26.2 (C4), 29.1 (C2), 26.2 (C3)
Biotin	6.59 (NHx2) 4.57 (C2), 4.39 (C3), 3.29 (C4), 2.96 + 2.75 (C1), 2.21 (C8), 1.68 (C5), 1.55 (C7), 1.36 (C6)	61.3 (C2), 63.2 (C3), 56.5 (C4), 40.7 (C1), 36.6 (C8), 28.7 (C5), 28.7 (C7), 28.9 (C6)

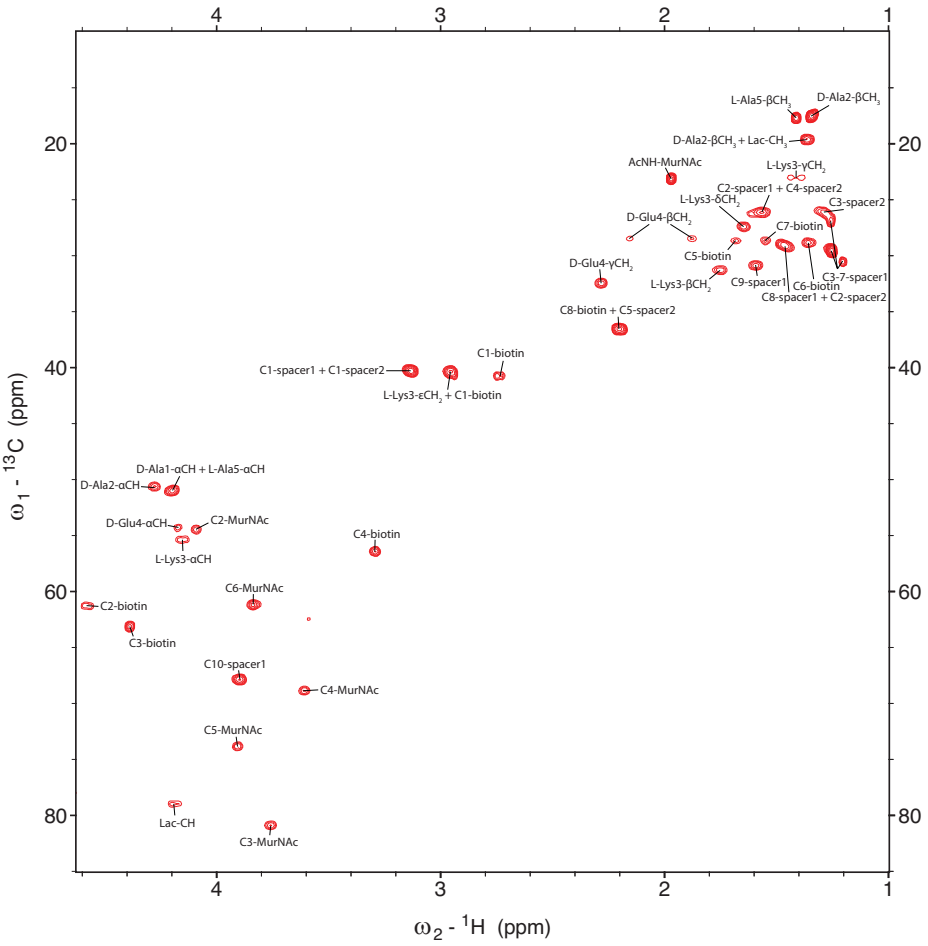

Figure 12: Cutout of HSQC spectrum of compound **27**. Outside of this view is the signal for the anomeric centre of MurNAc (C1).

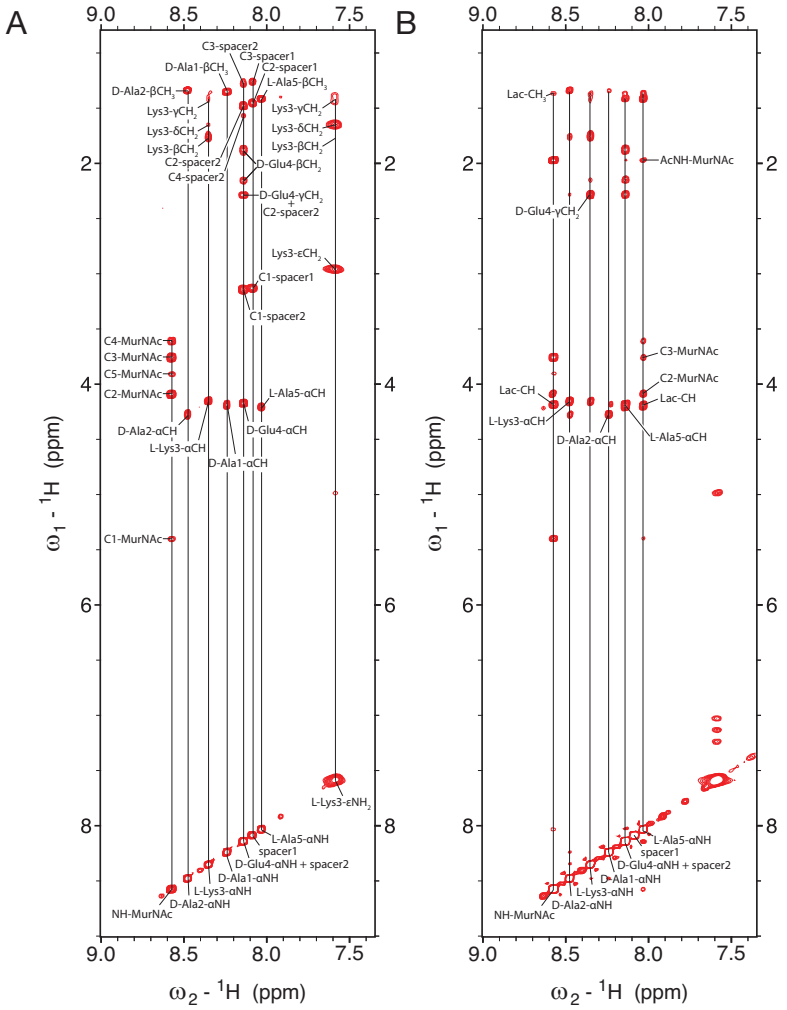

Figure 13: A) Detail of the TOCSY spectrum of compound **27** showing the assigned spinsystems. B) Detail of the NOESY spectrum of compound **27** indicating the correct connectivity of all amide bonds

2.7.2.3 NMR analysis of compound 33

The results of the NMR analysis are shown in table 3. TOCSY, NOESY and HSQC (figure 15 and 16) were measured in H_2O/D_2O (9:1) and COSY in D_2O. Identical spectra were recorded for compound **31**.

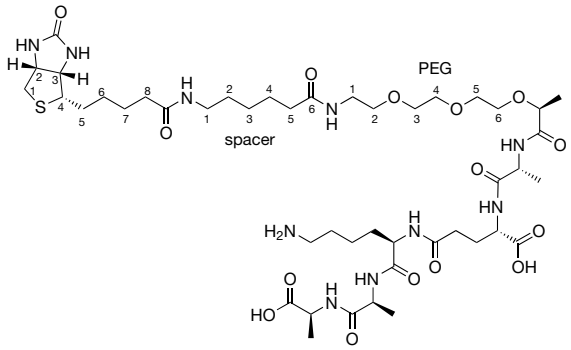

Figure 14: Structure of compound **33** and numbering used for the assignment of NMR peaks.

Table 3: Chemical shift assignments for compound **33**. See figure 14 for numbering scheme.

Assignment	Peaks ^{1}H (δ in ppm)	Peaks ^{13}C (δ in ppm)
Pentapeptide:		
D-Ala1	8.05 (NH), 4.05 (αCH), 1.29 (βCH_3)	52.1 (αCH), 18.3 (βCH_3)
D-Ala2	8.41 (NH), 4.29 (αCH), 1.32 (βCH_3)	50.6 (αCH), 17.6 (βCH_3)
L-Lys3	8.37 (εNH_2), 8.37 (αNH), 4.17 (αCH), 2.95 (εCH_2), 1.76 (βCH_2), 1.64 (δCH_2), 1.40 (γCH_2)	55.3 (αCH), 40.3 (εCH_2), 31.5 (βCH_2), 27.4 (δCH_2), 23.0 (γCH_2)
D-Glu4	7.98 (NH), 4.13 (αCH), 2.27 (γCH_2), 2.11 (βCH_2-1), 1.86 (βCH_2-2)	55.2 (αCH), 32.6 (γCH_2), 29.0 (βCH_2-1 + βCH_2-2)
L-Ala5	8.50 (NH), 4.33 (αCH), 1.39 (βCH_3)	50.8 (αCH), 18.0 (βCH_3)
Spacers + biotin:		
PEG-spacer	3.67-3.65 (C3-C6), 3.57 (C2), 3.34 (C1)	70.6-69.5 (C3-C6), 69.8 (C2), 39.9 (C1)
C6-spacer	8.14 (NH), 3.13 (C1), 2.21 (C5), 1.56 (C4), 1.27 (C3), 1.47 (C2)	40.2 (C1), 36.5 (C5), 26.1 (C4), 26.5 (C3), 29.0 (C2)
Biotin	6.58 (NH1), 6.49 (NH2), 4.57 (C2), 4.38 (C3), 3.29 (C4), 2.93 (C1-1), 2.73 (C1-2), 2.21 (C8), 1.67 (C5), 1.54 (C7), 1.35 (C6)	61.3 (C2), 63.1 (C3), 56.4 (C4), 40.7 (C1), 36.5 (C8), 28.7 (C5), 28.6 (C7), 28.8 (C6)

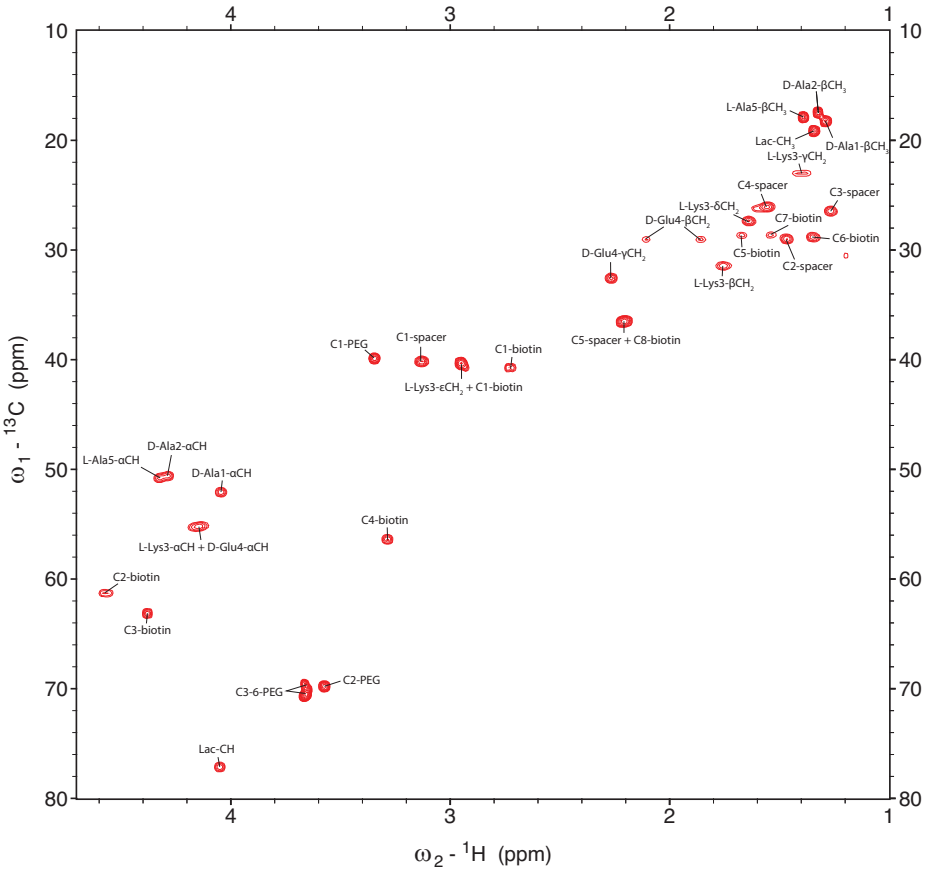

Figure 15: Cutout of HSQC spectrum of compound **33**. There were no signals observed outside of the viewed area.

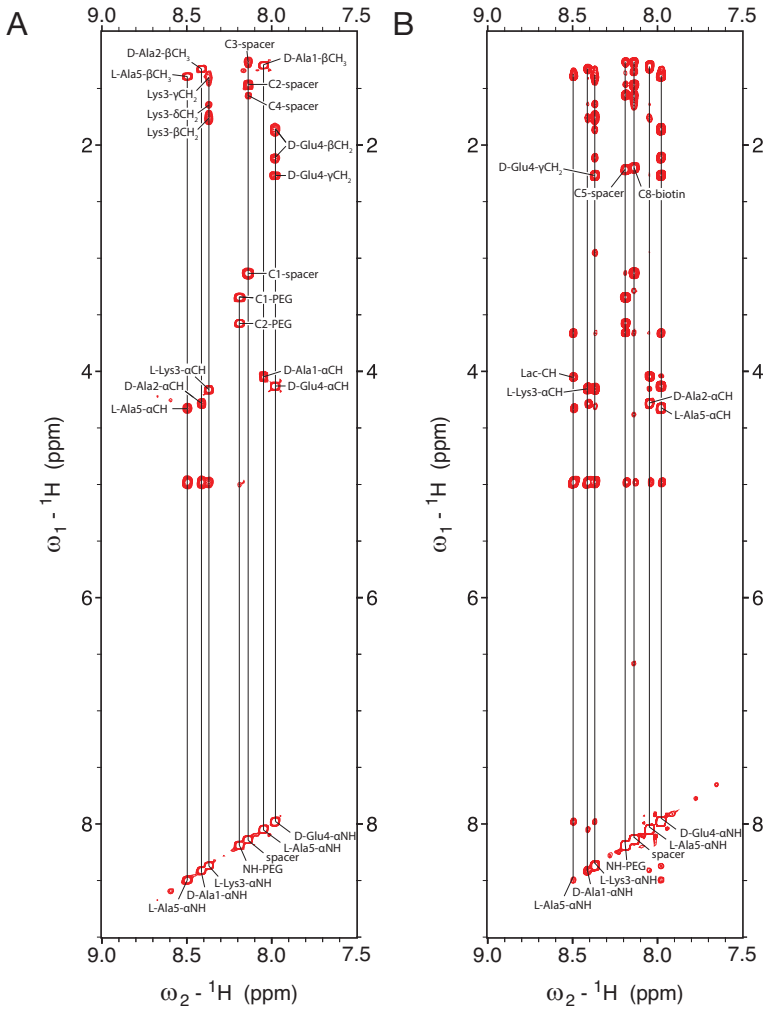

Figure 16: A) Detail of the TOCSY spectrum of compound **33** showing the assigned spinsystems. B) Detail of the NOESY spectrum of compound **33** indicating the correct connectivity of all amide bonds.

References

[1] E. Breukink, H. E. van Heusden, P. J. Vollmerhaus, E. Swiezewska, L. Brunner, S. Walker, A. J. R. Heck, B. de Kruijff, *J. Biol. Chem.* **2003**, *278*, 19898–19903.

[2] T. Ueda, F. Feng, R. Sadamoto, K. Niikura, K. Monde, S. Nishimura, *Org. Lett.* **2004**, *6*, S1–9.

[3] H. Men, P. Park, M. Ge, S. Walker, *J. Am. Chem. Soc.* **1998**, *120*, 2484–2485.

[4] Y. Zhang, E. J. Fechter, T. A. Wang, D. Barrett, S. Walker, D. E. Kahne, *J. Am. Chem. Soc.* **2007**, *129*, 1–21.

[5] S. A. Hitchcock, C. N. Eid, J. A. Aikins, M. Zia-Ebrahimi, L. C. Blaszczak, *J. Am. Chem. Soc.* **1998**, *120*, 1916–1917.

[6] M. S. VanNieuwenhze, S. C. Mauldin, M. Zia-Ebrahimi, J. A. Aikins, L. C. Blaszczak, *J. Am. Chem. Soc.* **2001**, *123*, 6983–6988.

[7] B. Schwartz, J. A. Markwalder, Y. Wang, *J. Am. Chem. Soc.* **2001**, *123*, 11638–11643.

[8] M. S. VanNieuwenhze, S. C. Mauldin, M. Zia-Ebrahimi, B. E. Winger, W. J. Hornback, S. L. Saha, J. A. Aikins, L. C. Blaszczak, *J. Am. Chem. Soc.* **2002**, *124*, 3656–3660.

[9] C.-Y. Huang, H.-W. Shih, L.-Y. Lin, Y.-W. Tien, T.-J. R. Cheng, W.-C. Cheng, C.-H. Wong, C. Ma, *Proc. Natl. Acad. Sci.* **2012**, *109*, 6496–6501.

[10] D. Kahne, C. Leimkuhler, W. Lu, C. Walsh, *Chem. Rev.* **2005**, *105*, 425–448.

[11] S.-T. D. Hsu, E. Breukink, E. Tischenko, M. A. G. Lutters, B. de Kruijff, R. Kaptein, A. M. J. J. Bonvin, N. A. J. van Nuland, *Nat. Struct. Mol. Biol.* **2004**, *11*, 963–967.

[12] S. Walker, L. Chen, Y. Hu, Y. Rew, D. Shin, D. L. Boger, *Chem. Rev.* **2005**, *105*, 449–475.

[13] T. Schneider, T. Kruse, R. Wimmer, I. Wiedemann, V. Sass, U. Pag, A. Jansen, A. K. Nielsen, P. H. Mygind, D. S. Raventos, et al., *Science* **2010**, *328*, 1168–1172.

[14] H. Brötz, M. Josten, I. Wiedemann, U. Schneider, F. Götz, G. Bierbaum, H.-G. Sahl, *Mol. Microbiol.* **1998**, *30*, 317–327.

[15] M. R. Islam, M. Nishie, J. Nagao, T. Zendo, S. Keller, J. Nakayama, D. Kohda, H.-G. Sahl, K. Sonomoto, *J. Am. Chem. Soc.* **2012**, *134*, 3687–

3690.
[16] L. L. Ling, T. Schneider, A. J. Peoples, A. L. Spoering, I. Engels, B. P. Conlon, A. Mueller, D. E. Hughes, S. Epstein, M. Jones, et al., *Nature* **2015**, *517*, 455–459.
[17] T. Osawa, R. Jeanloz, *J. Org. Chem.* **1965**, *30*, 448–450.
[18] S. Ha, E. Chang, M.-C. Lo, H. Men, P. Park, M. Ge, S. Walker, *J. Am. Chem. Soc.* **1999**, *121*, 8415–8426.
[19] X. Ye, M. Lo, L. Brunner, D. Walker, D. Kahne, S. Walker, *J. Am. Chem. Soc.* **2001**, *123*, 3155–3156.
[20] R. Kuhn, W. Kirschenlohr, *Angew. Chemie* **1955**, *67*, 786.
[21] C. Behrens, J. Lau, J. Kodra, M. Kofod-Hansen, T. Hoeg-Jensen, P. Madsen, S. Havelund, *Insulin Derivatives Conjugated with Structurally Well Defined Branched Polymers*, **2009**.
[22] L. M. Lira, D. Vasilev, R. A. Pilli, L. A. Wessjohann, *Tetrahedron Lett.* **2013**, *54*, 1690–1692.
[23] A. P. C. Chen, Y. H. Chen, H. P. Liu, Y. C. Li, C. T. Chen, P. H. Liang, *J. Am. Chem. Soc.* **2002**, *124*, 15217–15224.
[24] G. Rouser, S. Fleischer, A. Yamamoto, *Lipids* **1970**, *5*, 494–496.
[25] T. Yamaguchi, D. Hesek, M. Lee, A. G. Oliver, S. Mobashery, *J. Org. Chem.* **2010**, *75*, 3515–3517.
[26] H.-J. Kohlblau, J. Tschakert, R. A. Al-Qawasmeh, T. A. Nizami, A. Malik, W. Voelter, *Zeitschrift fur Naturforsch.* **1998**, *53b*, 753–764.
[27] C. N. Eid, M. J. Nesler, M. Zia-ebrahimi, C. E. Wu, R. Yao, K. Cox, J. Richardson, *J. Label. Compd. Radiopharm.* **1998**, *41*, 705–716.
[28] T. Hu, J. S. Panek, *J Am Chem Soc* **2002**, *124*, 11368–11378.
[29] E. C. Roos, P. Bernabé, H. Hiemstra, W. N. Speckamp, *J. Org. Chem.* **1995**, *60*, 1733–1740.
[30] J. G. Delcros, S. Tomasi, S. Carrington, B. Martin, J. Renault, I. S. Blagbrough, P. Uriac, *J. Med. Chem.* **2002**, *45*, 5098–5111.
[31] I. Berger, A. A. Nazarov, C. G. Hartinger, M. Groessl, S.-M. Valiahdi, M. A. Jakupec, B. K. Keppler, *ChemMedChem* **2007**, *2*, 505–514.
[32] A. R. Schneekloth, M. Pucheault, H. S. Tae, C. M. Crews, *Bioorganic Med. Chem. Lett.* **2008**, *18*, 5904–5908.

Chapter 3

Identification of novel lipid II binding bicyclic peptides using phage display and synthetic lipid II analogues

3.1 Phage display as a source of novel antimicrobials

3.1.1 The resistome and sources of antibiotics

With the threat posed by the "post-antibiotic era", antibiotics research must be innovative to find new antimicrobial substances that do not generate resistance rapidly. Almost all of the clinically used antibiotics come from natural sources. Although these sources (e.g. soil microbes) are rich in antimicrobially active compounds, they have also coevolved with organisms that protect themselves against these compounds.[1] This theory is referred to as the "resistome" and is described in more detail in section 1.4.2. These resistance mechanisms can be transferred between different strains of bacteria through horizontal gene transfer and can eventually end up in pathogenic strains.[2] To avoid this problem we envisioned that the use of non-natural sources (phage display) should allow the identification of new antibiotics with reduced susceptibility to resistance.

New antimicrobial discovery has relied strongly on the specialized metabolites produced by soil-bacteria (e.g. actinomycetes) as a source of novel compounds. However, evolution has led to the production of similar compounds by different strains and the same scaffolds keep being identified.[3–5] Depletion of the so called "low hanging fruit" when it comes to naturally occurring antibiotics and the general disinterest of big pharma over the past two decades has led to a near empty antibacterials pipeline. [6] For reasons such as these novel, non-natural sources of antibiotics that explore new chemical space can be used to avoid the rediscovery of already existing antibiotics.

In this chapter we describe the use of peptide phage display libraries to identify novel antimicrobial peptides. Such a source does not have any resistance genes evolved against it (there is no "resistome") and when combined with a target that has not been applied before to such a library screen, one does not expect to rediscover existing antibiotics.

3.1.2 Phage display

Peptide phage display is a commonly applied technique to identify peptides binding to a target of interest. The peptide libraries generated are typically of high diversity containing approximately 10^9-10^{10} different sequences.[7,8] These can easily be screened in a single experiment, allowing many different conditions to be tested rapidly (e.g. different libraries, changes in binding conditions, changes in washing conditions, different elution methods, etc.). Phage display is

explained in detail in section 1.7.

3.1.2.1 Peptides as inhibitors of bacterial enzymes identified by phage display

Since the discovery of phage display in 1985, several groups have attempted to identify novel antibiotic peptides by applying this high-throughput technique to potential antibacterial targets.[9] The group of Levesque has reported several attempts at identifying peptides that inhibit bacterial proteins. These include several of the Mur enzymes involved in lipid II synthesis and the cell-division proteins FtsA and FtsZ.[10–16] They described peptidic inhibitors with IC_{50} values in the low-millimolar to low-micromolar range in enzyme assays. However, no inhibition of bacterial growth was reported for these peptides. All of the chosen protein targets are intracellular and the developed peptides are not likely to pass through the bacterial membrane. Besides protein targets, phage display has been used to identify peptides that bind to bacterial ribosomal subunits. These are validated targets for several clinically used antibiotics (e.g. aminoglycosides, tetracyclines etc.) and novel inhibitors could prove to be useful. Although binding peptides were identified (low micromolar – high nanomolar affinity), no antimicrobial activity data was reported as they also suffer from permeability problems.[17–19] While not likely to be drug candidates, such peptides could prove useful for the development of displacement high throughput assays or as leads for modification by peptidomimetic approaches to improve their drug-like properties.

3.1.2.2 Phage display using whole cells as target

To date, a few papers have reported the use of phage display screening against whole cell targets. These allowed identification of antimicrobial peptides with activity against *E. coli*, *P. aeruginosa* and *C. jejuni*.[20,21] Most notably is the peptide with activity against *E.coli* with an MIC of 8 µg/ml. The peptide is strongly positively charged (+7) and appears to be α-helical in an aqueous environment. Rapid depolarization of the bacterial membrane was observed resulting in fast killing of bacterial cells. A tetrameric version of one of the identified peptides is currently being developed as a drug candidate by the company SetLance and expected to enter clinical trials soon.[22]

3.1.2.3 Phage display against lipopolysaccharides

The glycolipids known as lipopolysaccharides (LPS) are found in the outer-membrane of Gram-negative bacteria. Neutralization of LPS by binding peptides

can be of major benefit for treating systemic Gram-negative infections. Since 2001 several groups have reported the use of LPS or fragments thereof (Lipid A) in peptide phage display experiments.[23–28] The experiment typically resulted in rather hydrophobic peptides that contain a few basic residues. The peptides could be used to detect the specific strain corresponding with the strain of the LPS used. Binding affinities as determined by SPR could be in the low nanomolar range and some peptides were shown to be able to neutralize LPS at least partially.[28]

3.1.3 Lipid II as a validated antibacterial target

Lipid II (figure 1) is a highly conserved molecule produced by almost all bacteria as a precursor to the peptidoglycan chains that make up the bacterial cell wall. For the approach here described we chose lipid II as the target for development of novel antibiotics. Nature itself has proven that the inhibition of bacterial cell wall synthesis is an effective way of eliciting a bacteriocidal effect. Although this can be achieved through inhibition of the enzymes involved (e.g. β-lactam compounds) it can also be done by sequestering lipid II (vancomycin, nisin, ramoplanin, etc.). One of the main advantages of targeting lipid II is that it is presented on the outside of the bacterial membrane (for Gram-positive bacteria) and is therefore easily acessable for peptide antibiotics.[29,30]

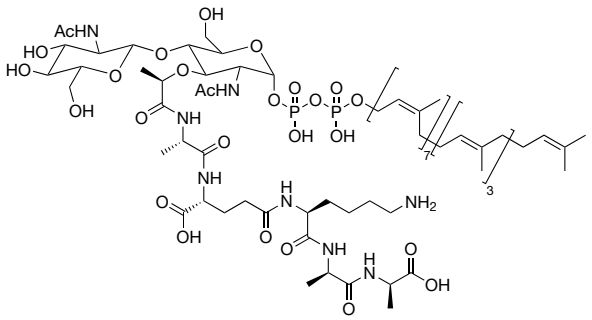

Lipid II

Figure 1: Chemical structure of lipid II.

Targeting lipid II also covers several advantages with respect to resistance. When considering the molecular mechanisms of resistance, they can be either specific to a certain class of antibiotics (e.g. beta-lactamases), or they can be non-specific changes that protect the bacterium (e.g. increased efflux of foreign molecules).[1,2,31] Fully synthetic antibiotics are less likely to suffer from molecule specific resistance pathways but they are susceptible to the non-specific

resistance mechanisms. The fluoroquinolones for example, which are fully synthetic, still suffer from mechanisms like reduced permeability of the bacterial membrane, overexpression of efflux systems, or mutations in the target site.[32] Resistance through reduced membrane permeability or increased efflux will not be a problem for lipid II binding antibiotics as they do not have to cross the membrane. Mutation of lipid II is possible, but seems to be limited to the pentapeptide part of lipid II. Vancomycin resistance (discussed in section 1.6.5) is caused by mutation of the D-Ala-D-Ala motif but took approximately 30 years to appear from the time vancomycin was first introduced into the clinic. Other known lipid II binders (i.e. nisin and related lantibiotics) do not seem to suffer from target-mutation related resistance making it an attractive target.

3.2 Experimental design

3.2.1 Bicyclic phage display

For the purpose of our screening experiments we chose to use a bicyclic phage display method where each peptide in the library has three fixed cysteine residues. The phage-bound peptides are treated with a tribromide (1,3,5-tris(bromomethyl) benzene) reagent that selectively reacts with the cysteine thiols to form bicyclic peptides (the so-called "CLIPS" reaction, shown in figure 2).[7,33] The constraint imposed by cyclization of the peptides reduces their flexibility and can increase binding affinity for their target(s) relative to their linear counter parts. A reduction in flexibility reduces the entropic penalty to be paid upon binding to a target resulting in a higher affinity.[34] Increased affinity is an important consideration in the choice of phage libraries used but we also hypothesized that the bicyclic peptides could be seen as mimics of naturally occurring lipid II binders. Nisin has a bicyclic peptide structure as its lipid II binding domain (ring A and B, figure 7 chapter 1) as do many other related lantibiotics.[35] Vancomycin has a tricyclic structure and almost every other known lipid II binder is a cyclic peptide.[30] In the group of Heinis, several different library types have been developed. These include libraries with different loop sizes (3-6 amino acids per loop) that can be chosen as different options to identify lipid II binders.[36] Although smaller loops might be even less flexible and advantageous in selection against a small molecular target like lipid II, in the experiments we describe below the best results were obtained with Heinis' original library of bicyclic peptides comprised of loops of 6 amino acids possibly because it has the highest diversity of peptide sequences (4×10^9).[8]

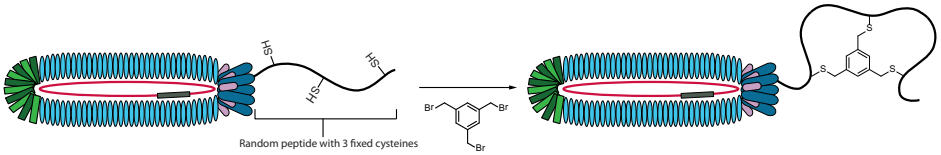

Figure 2: CLIPS bicyclization reaction on phage surface.

Another advantage arises from using bicyclic phage display versus linear peptide phage display; if a phage particle carries a lipid II binding peptide it could potentially bind to the lipid II in the host *E. coli* cell. As soon as the phage starts replicating in the host cell, numerous copies of this peptide are produced. The high concentration of these peptides could potentially kill the host cell preventing the amplification of this important phage clone and eliminating it from the library. In bicyclic phage display however, the displayed peptides are screened against the target in the bicyclic form. During the subsequent amplification stage in the host cell the peptides are not yet cyclized and are in the presumably non-active linear form. The Heinis group has shown that the linear versions of such peptides typically do not bind to the target or with strongly reduced affinity.[7,37]

3.2.2 Enantiomeric lipid II analogues for mirror-image phage display

Besides using bicyclic phage display we also designed our approach to make use of the so-called mirror-image phage display technique. The concept of mirror image phage display is described in detail in section 1.7.6 and illustrated in Figure 3. In short, mirror image phage display uses an enantiomeric target with the standard phage library of L-amino acid peptides. Any identified binding peptides will then be synthesised from D-amino acids and, by symmetry, are expected to bind the natural target.[38,39] By using this method we effectively double the chemical space explored while using the same library as for the normal target. In addition, peptides made from D-amino acids are often more resistant to proteolysis[40,41] and in some cases less immunogenic.[42,43] Furthermore, the use of mirror-image phage display should reduce the risk of premature killing of the *E. coli* host cells due to lipid II binding of the linear precursor peptides on the phage particles.

3.2.3 Design of the lipid II analogues

Multiple total synthesis routes towards lipid II and analogues thereof were previously described including modifications for immobilization (biotinylation).[44–47] By using these methods we were able to design and synthesize four different

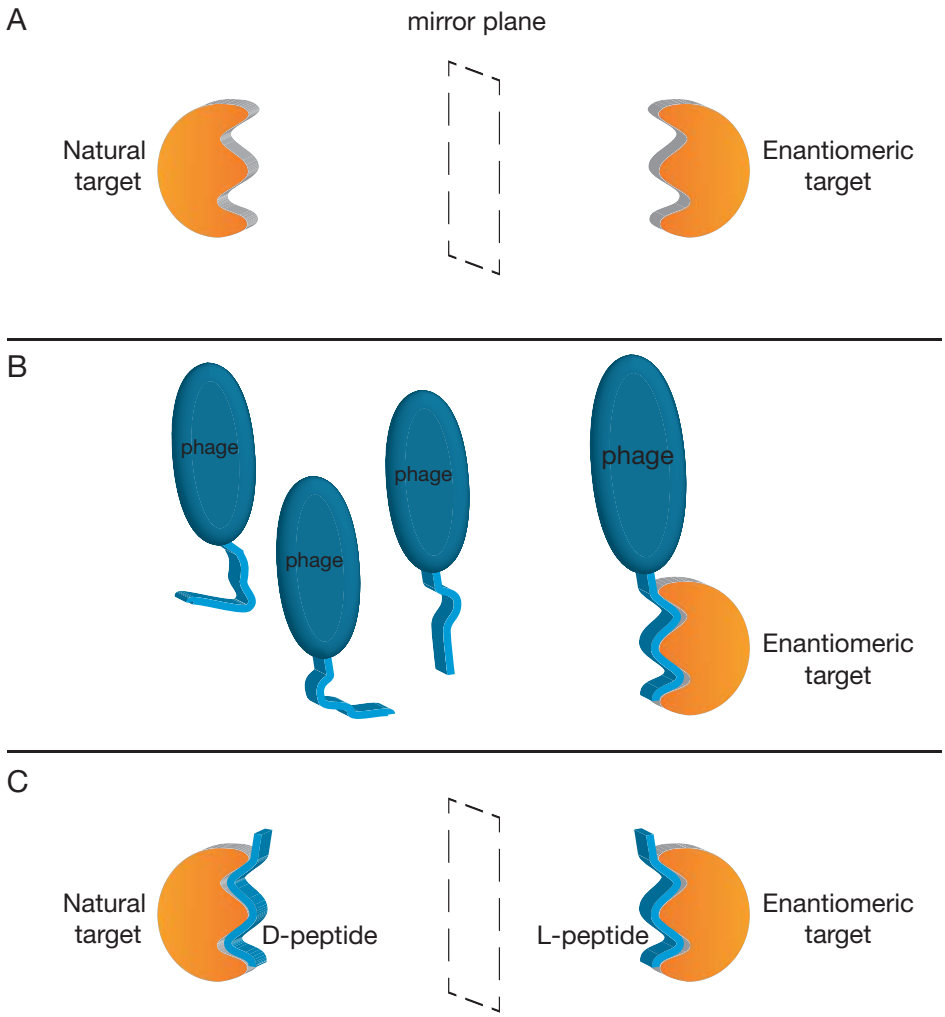

Figure 3: Schematic representation of a mirror image phage display experiment. **A**) The target is prepared in its enantiomeric form. **B**) The enantiomeric target is exposed to a phage library carrying L-peptides. **C**) The L-peptide sequence identified from the phage display experiment is synthesised in its D-form and binds to the natural target. lipid II based targets which are shown in Figure 4 and 5 and the synthesis of which is described in chapter 2.

Target **1** is the closest analogue of lipid II and has several modifications made to it. Most striking is the replacement of the original undecaprenyl lipid with a much shorter saturated alkyl-chain terminating in a biotin tag (as shown in figure 4). The original 55 carbon lipid makes the lipid II molecule insoluble under the aqueous conditions required for phage display. Furthermore, the lipid is embedded in the bacterial membrane and not easily available for binding by peptidic molecules. Also, for synthetic ease, target **1** was designed to lack the *N*-acetyl-

L-glucosamine moiety found in lipid II making it more accurately described as an analogue of lipid I. Removal of this carbohydrate was not expected to negatively affect our screening as it is known not to be required for the high affinity binding of many naturally occurring lipid II binding antibiotics. In general, peptides that are able to bind to lipid I almost always are able to bind lipid II equally well.[48,49] Target **2** is similar to target **1** except that all stereocenters are inverted (with the exception of the biotin-tag) making it a target for mirror-image phage display as described above.

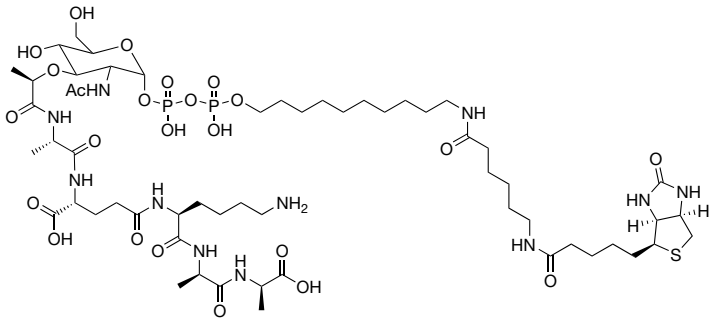

Target 1 (Lipid I)

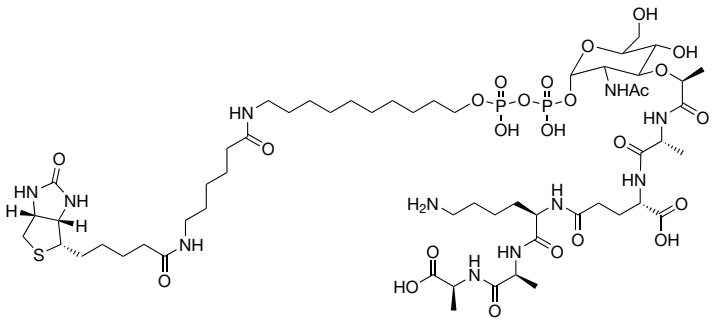

Target 2 (Lipid I-ent)

Figure 4: Structure of targets **1** and **2** to be used in phage display.

Target **3** was designed to detect peptides that bind directly to the pentapeptide part of lipid II (see figure 5). In this way we attempted to mimic the mode of action of vancomycin. Although this part of lipid II can mutate to avoid vancomycin binding, it would theoretically also be possible to synthesize the mutant target peptides and identify novel peptides with activity against vancomycin resistant strains. Target **4** in turn is comprised of the enantiomeric pentapeptide with the biotin label retaining its native stereochemistry.

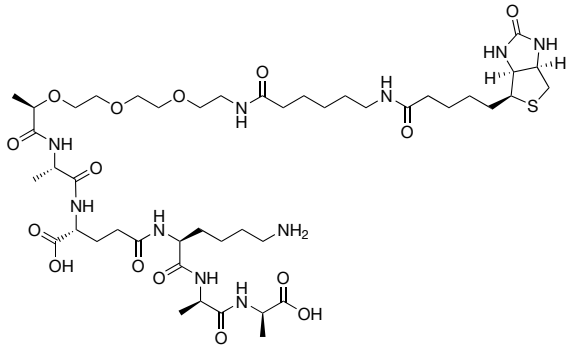

Target 3 (pentapeptide)

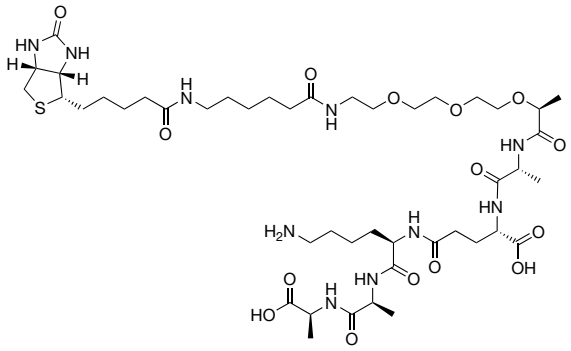

Target 4 (pentapeptide-ent)

Figure 5: Chemical structure of target **3** and **4**.

3.3 Phage display experiments

3.3.1 Phage display against small molecular targets

With our synthetic lipid II-based targets in hand we set out to explore the correct conditions for the phage display screening experiments. In most cases the target used in a phage display experiment is a protein or even an intact cell. Our targets however are much smaller in size and there have been much fewer reports of peptide phage display against small molecules. Among the non-protein targets that have been used previously by others are lipopolysaccharides, trimannosides, or even small molecules like paracetamol.[27,28,50,51] Several other targets have been reported as well, but what is easily observed is that there is no general strategy for immobilizing the target, performing the incubation, or the method of washing during the phage display experiment.[52,53] In contrast,

the elution conditions seems to be the same for most reported experiments (Glycine-HCl buffer, pH 2.2).[53]

3.3.2 Phage display experiment 1

Since there is no general consensus method for small molecule phage display we performed our first experiment using the conditions as developed by the group of Heinis for screening bicyclic peptide phage libraries against protein targets.[8] Three different libraries were combined to perform the initial experiments. These libraries contained peptides with two loops of three amino acids each (3x3), peptides with two loops of four amino acids each (4x4), and a library with two loops of variable size between 3 and 5 amino acids (VL1).[36] Libraries with small peptide loops were initially chosen to mimic natural lipid II binders as these tend to have relatively small loops as well.

3.3.2.1 Phage production

We obtained the libraries from the Heinis lab and started with phage production as described.[8] Cultures of the phage infected *E. coli* TG1 cells were prepared after inoculation at a relatively high OD_{600} of 0.1. The high inoculation is required to ensure that the entire library is covered. After overnight incubation the cells are removed by centrifugation and the phage are isolated from the supernatant by precipitation with PEG-6000. To ensure that the subsequent cyclization step of the cysteine containing phage displayed peptide proceeds optimally, the phage are next treated with the reducing agent TCEP. After removal of excess TCEP the linear peptides are transformed into the corresponding bicyclic species by addition of the cyclization reagent 1,3,5-tris(bromomethyl)benzene (TBMB). After the cyclization step the phage are once more purified by precipitation with PEG-6000. In between each step a small sample is taken to determine the phage titer and ensure the viability of the phage.

3.3.2.2 Biopanning according to the original protocol

The steps taken in the biopanning of the phage against our targets were preformed according to the method originally developed in the group of Heinis and are illustrated in Figure 6. The biotinylated target compound **1**-**4** were immobilized on magnetic streptavidin beads. Next, the phage were exposed to the beads for thirty minutes at room temperature after which they were washed four times with buffer containing 0.1% Tween-20. Elution was performed using a solution of vancomycin for targets **1** and **3** (vancomycin elution is not relevant for enantiomeric target **2** and **4**) followed by elution with glycine-HCl (pH 2.2). In

the second round of biopanning, neutravidin beads were used instead to avoid the enrichment of streptavidin binding peptides as neutravidin is structurally different.

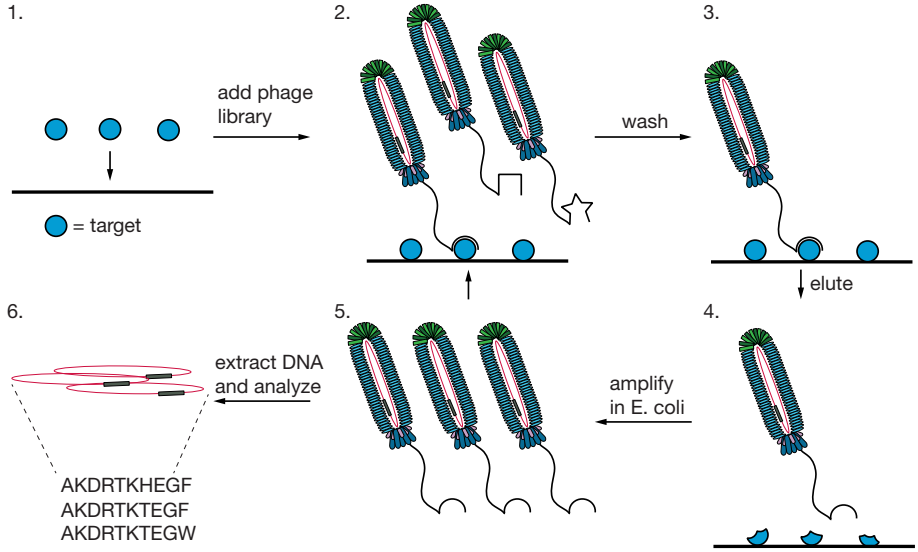

Figure 6: The standard phage display biopanning protocol as used for experiment 1. Step 1: immobilization of the target. Step 2: Incubation of the phage library with the immobilized target. Step 3: Washing of the surface to remove non-bound and weak-binding phage. Step 4: Elution of binding phage. Step 5: Amplification of eluted phage in *E. coli*. DNA can be analysed after this step.

3.3.2.3 Results from the initial experiments

After the third round of affinity selection individual phage clones were isolated and their DNA was analysed by standard sequencing of isolated clones. As shown in table 1 for all of the targets a similar peptide was isolated. The peptide sequence is larger than the used libraries (two loops of six amino acids each (6x6)). As phage are notoriously difficult to remove from laboratory equipment (e.g. centrifuge bottles), this unexpected hit sequence was probably obtained inadvertently during phage production. The sequence of the peptide contains the HPQ-motif which is a known streptavidin binding sequence.[8] Although, neutravidin beads were used in the second round of selection, enough streptavidin selective phage likely survived so as to overwhelm the library. It is a clear indicator that the method used is not suitable for small molecule targets as the much larger streptavidin protein dominates peptide selection.

Table 1: DNA analysis results for phage display experiment 1 after three rounds of biopanning.

Target **1** (Lipid I)		Target **2** (Lipid I-ent)	
Sequence	Abundance	Sequence	Abundance
ACHPQFEGCRQSVLTCG	9/10	ACHPQFEGCRQSVLTCG	9/10
QCWAQSCWWYWCP	1/10	ACLVQCGFTQCG	1/10

Target **3** (pentapeptide)		Target **4** (pentapeptide-ent)	
Sequence	Abundance	Sequence	Abundance
ACHPQFEGCRQSVLTCG	8/9	ACHPQFEGCRQSVLTCG	7/10
ACVQQGPCHTDCG	1/9	ACQDICPYIDCG	1/10
		ACGEPCQLLVRCG	1/10
		SCRYRLCLDDYCI	1/10

3.3.3 Phage display experiment 2

To prevent selection of streptavidin binding peptides we chose to change the order of events during biopanning. Instead of immobilizing the target before exposing it to the phage library we incubated the targets with the library in solution followed by a quick capture with streptavidin beads (Figure 7). In other words, we allowed the phage to interact properly with just the target before adding streptavidin to the experiment. Short exposure to the streptavidin coated

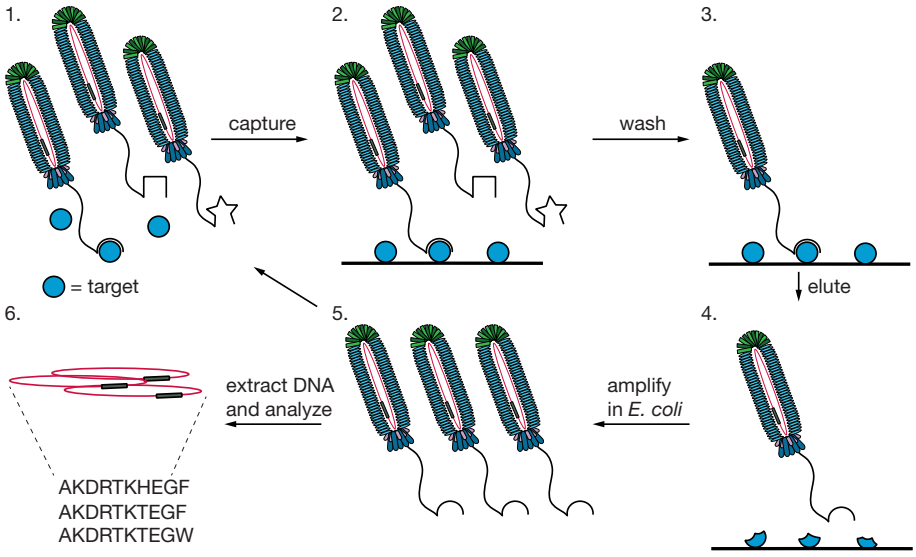

Figure 7: Optimized protocol for phage display with minimized risk of identifying streptavidin binding peptides. Step 1: Incubate phage library with target in solution. Step 2: Add a streptavidin coated surface to capture the target and any binding phage (in our experiments we chose to use magnetic beads). Step 3: Wash away all non-binding phage. Step 4: Elute binding phage. Step 5: Amplification of eluted phage in *E. coli* and possible DNA analysis.

beads should minimize the amount of off-target binders. The washing steps were kept the same and the phage were eluted under acidic conditions rather than using vancomycin solution. Again, phage DNA was analysed after three rounds of selection (table 2).

The results in table 2 show that similar peptide sequences are isolated from different targets. Although there could be some promiscuity between the different targets it is more logical to expect these peptides to be off target binders as well. Again the most abundant peptide is one from the 6x6 library that was not used in this experiment. It is important to note that none of them have the HPQ-motif and streptavidin binding therefore seems to have been eliminated. However, Target 4 seems to have yielded a unique peptide sequence.

Table 2: DNA analysis results for phage display experiment 2.

Target **1** (Lipid I)		Target **2** (Lipid I-ent)	
Sequence	Abundance	Sequence	Abundance
ACVSWYCQHYCG	4/9	ACRYPLWYCLHYQVSCG	5/10
ACRYPLWYCLHYQVSCG	3/9	ACVSWYCQHYCG	4/10
GCGDWGCYWSQSF	1/9	ACPPNWYCRYYCG	1/10
ACLSCNCSTRQA	1/9		

Target **3** (pentapeptide)		Target **4** (pentapeptide-ent)	
Sequence	Abundance	Sequence	Abundance
ACRYPLWYCLHYQVSCG	9/10	SCRYRLCLDDYCI	7/10
ACVSWYCQHYCGG	1/10	ACVSWYCQHYCG	1/10
		VCSWWWCGFQLCP	1/10
		VCYIYWCPWWECQ	1/10

3.3.4 Phage display experiment 3

For the third experiment we kept the conditions the same as for experiment 2 but used different libraries instead. The libraries used were the 6x6 library and two others containing loops of variable sizes (3 to 6 amino acids per loop). We chose to use other libraries to see if any peptides would be enriched more strongly than the off target peptides. The phage were analysed after round 3 and the results are shown in Table 3. Again similar sequences are observed for all peptides indicating the off target binding is also an issue with these libraries. The only target that shows an enriched sequence that is unique is again target **4**. All peptides that appeared more than once after analysis of experiments 2 and 3 were synthesized and tested for activity against *Micrococcus luteus*. None of these peptides showed activity even at concentrations as high as 512 µg/ml.

Table 3: DNA analysis results for phage display experiment 3.

Target **1** (Lipid I)		Target **2** (Lipid I-ent)	
Sequence	Abundance	Sequence	Abundance
ACYVYSSACWAQDYCG	5/10	ACYVYSSACWAQDYCG	5/10
ACYMLSQCWQHTCG	2/10	ACYMLSQCWQHTCG	1/10
ACGSMLMQCSQGSRCCG	1/10	ACGVKWGGCLYGNQLCG	1/10
ACLVYSVECWQSLPCG	1/10	ACLAQRLSCPDTIANCG	1/10
ACKYILLCCLMLFCG	1/10	ACFLLVQCREMVALCG	1/10
		ACKRMKCHCQWLRTPCG	1/10

Target **3** (pentapeptide)		Target **4** (pentapeptide-ent)	
Sequence	Abundance	Sequence	Abundance
ACYMLSQCWQHTCG	4/9	ACWQPLWWCTYYKESCG	3/10
ACYVYSSACWAQDYCG	3/9	ACYMLSQCWQHTCG	2/10
ACMRPLRQCHTLVDHCG	1/9	ACYVYSSACWAQDYCG	1/10
ACPNSQNLCFSRVRSCG	1/9	ACENYTPGCQLDTLACG	1/10
		ACPLWAGGCSAQLPCCG	1/10
		ACFDQLCWFYGICG	1/10
		ACRLQLSICKWFCVQCG	1/10

3.3.5 Phage display experiment 4

Given that the first three biopanning experiments failed to provide clear results we set out to optimize the conditions once again. For the next experiment we chose to use just a single library so as not to complicate the results. The 6x6 library has the highest diversity of peptides (4×10^9) and was therefore chosen for this experiment. To further increase the chance of a good interaction between the phage peptides and the targets we also opted to increase the incubation time to 16 hours. Besides that we hypothesized that the peptide parts of the targets might have a high degree of flexibility and therefore all the binding, washing and elution steps were performed at 4°C. Considering that the screening is performed against a small molecule target with relatively few interaction possibilities it is also reasonable to expect that binding peptides may not necessarily have a high affinity for the target. To avoid losing weaker interacting peptides we therefore decided to wash the bound phage only four times per round. Also, our collaborators in the Heinis group recently developed a method to apply high-throughput DNA analysis methods using the IonTorrent platform to phage output DNA.[8] Especially in the case of peptides with weak-to-moderate affinity for the target, it is advantageous to reduce the number of selection rounds to avoid the

enrichment of off-target binding peptides. This issue is discussed in more detail in section 1.7.4. We therefore decided to analyse the output phage after just the second round using high-throughput DNA analysis, the results of which are shown in table 4.

Table 4: DNA analysis results for phage display experiment 4 as a determined by IonTorrent analysis.

Target **1** (Lipid I)		Target **2** (Lipid I-ent)	
Sequence	Abundance	Sequence	Abundance
ACDWPDWQCYGWSSHCG	4.2 %	ACLLQSLLCPYSTHRCG	97.7 %
ACKHQAQECVAIREGCG	3.1 %		
ACWAMPMWCDSWSQNCG	1.8 %		
ACRPQKFNCISANIRCG	1.5 %		
ACKAMIGACVAMQFACG	1.2 %		
ACYPVDWYCLFQTVDCG	1.1 %		
ACRYVSGDCYYAQAHCG	1.0 %		

Target **3** (pentapeptide)		Target **4** (pentapeptide-ent)	
Sequence	Abundance	Sequence	Abundance
ACREASVVCGSTQLSCG	4.5 %	ACLRRVWACERVGQPCG	2.8 %
ACLPHEWQCQLASRPCG	2.3 %	ACKRSHGPCIQLAFSCG	2.4 %
ACDPHWQGCPFGTSICG	1.5 %	ACLSRDGQCWVGFNLCG	1.6 %
ACGSGPKWCQDKNLACG	1.2 %	ACPRHWSECLLPLPQCG	1.1 %
ACQPLLTNCDGRESKCG	1.0 %		
ACAGSPQLCSMFQAACG	1.0 %		

The high-throughput DNA analysis gave a much deeper insight into the distribution of phage clones in each phage pool than in our previous experiments. The results were filtered by removing any peptide that had either less or more than the expected three cysteines. For these peptides it is unknown what their exact configuration is after exposure to the cyclization reagent. The abundance was determined by dividing the number each peptide was observed by the total amount of reads in the analysis. Contrary to the previous experiments, the sequences found for each target are unique. These results could indicate that non-specific binding was avoided during this experiment and the identified peptides are actual lipid II binders. The striking results observed for Target **2** indicated a very strong enrichment of a single peptide sequence with the potential of being a strong binder. For all other three targets the enrichment was not nearly as strong. Given the success of this phage display experiment in identifying unique sequences we next set out to evaluate the peptides obtained by synthesizing and testing them.

3.4 Synthesis and evaluation of lipid II binding peptide candidates

3.4.1 Synthesis of the bicyclic peptides

Any peptide that was enriched more than 1% of the entire phage pool in the fourth phage display screen was synthesized and evaluated. The synthesis of the peptides was accomplished by solid phase peptide synthesis (SPPS) using standard Fmoc/tBu-peptide chemistry as shown in scheme 1. During the phage display experiments the peptides are attached to the phage PIII protein via their C-terminus. To avoid introducing an extra negative charge the Rink-amide resin was used to produce the peptides as C-terminal amides. The N-terminus is not modified as this is also free in the phage displayed peptides. After solid phase synthesis the peptides are cleaved from the resin under reducing conditions, followed directly by cyclization using TBMB in a mild basic buffer (20 mM NH_4HCO_3). All peptides were then purified to homogeneity by preparative HPLC and lyophilized. It is to be noted that the peptides identified by screening against the enantiomeric targets 2 and 4 were prepared from the corresponding D-amino acids.

3.4.2 Evaluation of the antibacterial activity of the candidate peptides

To select promising lead peptides from the phage display results we chose to use an antibacterial activity assay to determine their potency. Although some peptides might bind to a lipid II-based target in solution it is not guaranteed that they are also able to bind lipid II in its biological context of the bacterial membrane. An assay where we could directly read out the antibacterial potency was therefore preferred. In this stage of the project we were interested to identify lead peptides that could be further optimized for their antibacterial effect. We chose the indicator strain *Micrococcus luteus* as it is known to be very sensitive to lipid II binding antibiotics (nisin MIC: 0.07 μg/ml).[54] A broth microdilution assay was used where a dilution series of the peptide is made in bacterial growth medium in a 96-wells plate. A known inoculum (5 x 10^5 CFU/ml) of *M. luteus* is added to each dilution and the plates are incubated overnight at the preferred growth temperature of the organism (30°C). After incubation the microtiter plates

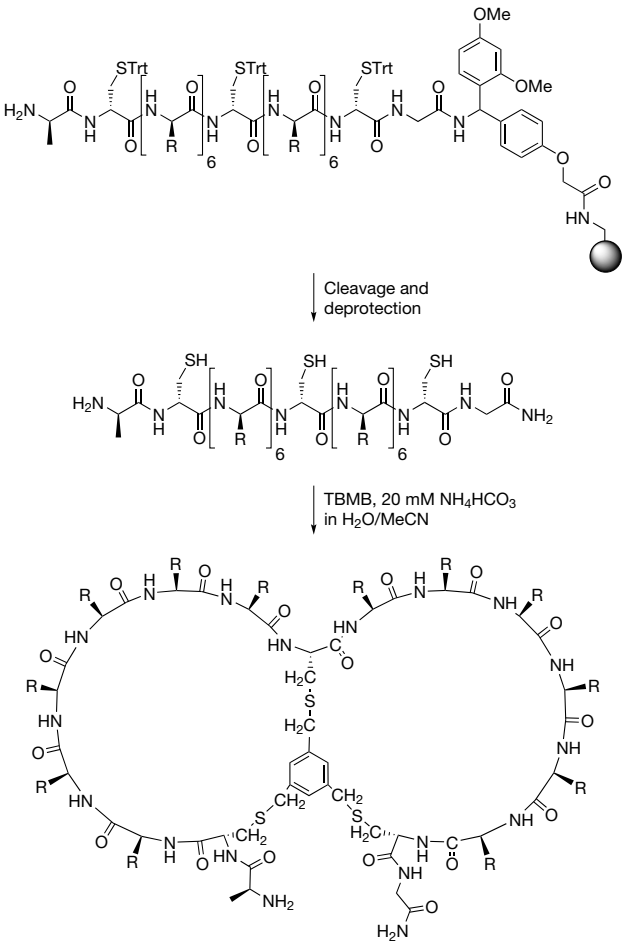

Scheme 1: Synthesis of bicyclic peptides.

are inspected visually to determine the turbidity of each well. In wells where the concentration of the peptide was high enough to interrupt bacterial growth clear medium is observed while the other wells will be turbid from bacterial growth. The lowest concentration where no growth is observed is referred to as the minimum inhibitory concentration (MIC) and is a measure for the potency of an antibiotic. All synthesised peptides were tested in this way and the results are summarized in table 5.

Table 5: Results of the MIC assay using *M.luteus* as an indicator strain.

Peptide	Sequence	Isolated from Target	MIC (μg/ml)
T1-1	ACDWPDWQCYGWSSHCG	**1** (Lipid I)	n.a.
T1-2	ACKHQAQECVAIREGCG	**1**	n.a.
T1-3	ACWAMPMWCDSWSQNCG	**1**	n.a.
T1-4	ACRPQKFNCISANIRCG	**1**	64
T1-5	ACKAMIGACVAMQFACG	**1**	n.t.
T1-6	ACYPVDWYCLFQTVDCG	**1**	128
T1-7	ACRYVSGDCYYAQAHCG	**1**	n.a.
T2-1	ACLLQSLLCPYSTHRCG	**2** (Lipid I-ent)	128
T3-1	ACREASVVCGSTQLSCG	**3** (pentapeptide)	n.a.
T3-2	ACLPHEWQCQLASRPCG	**3**	n.a.
T3-3	ACDPHWQGCPFGTSICG	**3**	n.a.
T3-4	ACGSGPKWCQDKNLACG	**3**	n.a.
T3-5	ACQPLLTNCDGRESKCG	**3**	n.a.
T3-6	ACAGSPQLCSMFQAACG	**3**	n.a.
T4-1	ACLRRVWACERVGQPCG	**4** (pentapeptide-ent)	64
T4-2	ACKRSHGPCIQLAFSCG	**4**	200
T4-3	ACLSRDGQCWVGFNLCG	**4**	n.a.
T4-4	ACPRHWSECLLPLPQCG	**4**	512
Nisin			0.06

n.a. = not active, n.t. = not tested (peptide could not be synthesized). Highest concentration of all tested peptides was at least 512 μg /ml.

3.4.3 Modification of identified peptides with lipids

As several of the peptides that were synthesized showed antimicrobial activity, we made a further selection of those that were deemed interesting for further development. Although some peptides from target **4** showed activity we decided to first focus on the peptides from target **1** and **2** as these targets are most closely related to lipid II. The modest antimicrobial activity seen with these peptides (MIC 64-128 μg/mL) is interesting but nowhere near that of antibiotics that are used in a clinical setting. One explanation for the low activity could be that the binding affinity of the peptides for lipid II is not very strong and as a result the lipid II processing enzymes can displace them easily. We next reasoned that a relatively simple modification that might enhance the affinity for lipid II and thus strengthen its sequestration of lipid II would be lipidation of the

lead peptides. Lipidation could anchor the peptides in the bacterial membrane while interacting with lipid II and strengthen the interaction or even disturb the membrane in a lipid II targeted manner. There are several examples of potent lipid II binding peptides that are modified with lipids (ramoplanin, teicoplanin). Peptides that interact with lipid II-related targets (e.g. $C_{55}P$ and $C_{55}P$) such as friulimicin and bacitracin carry lipids as well. Furthermore, our group recently reported that the modification of the nisin A/B ring fragment with several lipids significantly increases the antimicrobial activity of this lipid II binding motif.[55]

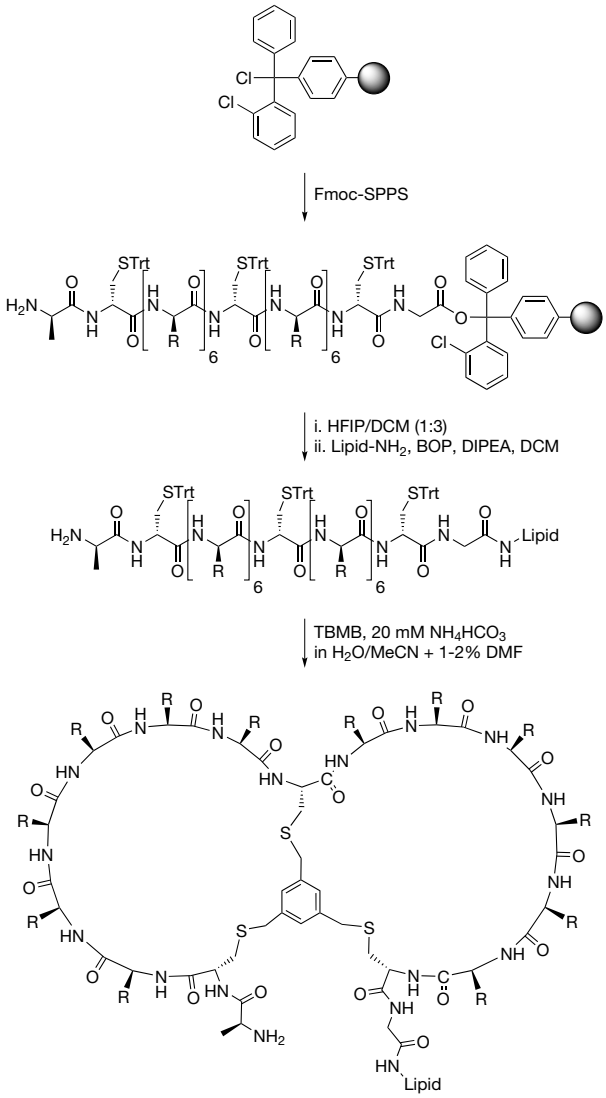

Scheme 2: Synthesis of C-terminally lipidated peptides.

To begin we chose to add a simple 10 carbon saturated lipid to either the N- or C-terminus of the pepides designated T1-4, T1-6 and T2-1 (see table 5 for sequences). For N-terminal lipidation we used decanoic acid (capric acid) which was added by a standard BOP coupling step during Fmoc SPPS. For C-terminal lipidation the peptides were first synthesized on chlorotrityl chloride resin, followed by mild cleavage using hexafluoroisopropanol (HFIP) (see scheme 2). This yielded protected peptides with a free C-terminus that could be converted to the corresponding lipid bearing amide by coupling with decylamine in solution using BOP as an activating agent. Finally the peptide was deprotected and cyclized to yield the desired product.

The lipidated peptides were initially tested in the same antimicrobial activity assay as before using *M. luteus* as indicator strain. The results as shown in Table 6 show a strong improvement in the antibacterial activity of the peptides compared to their original structures when C-terminally lipidated. Interestingly, for T1-4 and T2-1 the N-terminal modification completely abolished antimicrobial activity. Encouraged by these results we chose to test the peptides against a panel of bacterial strains including clinically relevant drug-resistant species (also shown in table 6). Although all the peptides were found to be inactive against methicillin resistant *S. aureus* (MRSA), T2-1-C10 displayed a particularly promising activity against a vancomycin resistant *E. faecium* strain (VRE E155). Although T1-6-C10 was the most active against *M. luteus* with an MIC value of 2 μg/mL, it showed no activity against the other strains tested.

Table 6: MIC (µg/mL) assay results for all lipidated peptides and their parent peptides against a broader range of strains.

Peptide	*M. luteus*	*B. subtilis*	*S. cohnii*	*E. coli* 8397	*E. faecium* E980	VRE E155	*S. aureus* 29213	MRSA USA300
T1-4	64	n.a.	-	-	-	-	-	-
C10-T1-4	n.a.	n.a.	n.a.	n.a.	-	n.a.	n.a.	n.a.
T1-4-C10	8	8-16	16	n.a.	-	n.a.	n.a.	n.a.
T1-6	128	n.a.	-	-	-	-	-	-
C10-T1-6	4	n.a.	n.a.	n.a.	-	n.a.	n.a.	n.a.
T1-6-C10	2	n.a.	n.a.	n.a.	-	n.a.	n.a.	n.a.
T2-1	128	1024	-	-	-	-	-	-
C10-T2-1	n.a.	n.a.	n.a.	n.a.	n.a.	n.a.	n.a.	n.a.
T2-1-C10	4	8	16-32	n.a.	32	8	n.a.	n.a.

n.a. = no activity

3.4.4 Haemolysis evaluation

Antimicrobial peptides are commonly tested for their haemolytic properties, especially if they are believed to act on membranes. The haemolytic activities of the most promising C10 lipidated peptides (T1-4-C10, T1-6-10, and T2-1-C10) were therefore tested by incubating the compounds with red blood cells obtained from sheep. The peptides were incubated with the blood cells at a concentration of range of 64 µg/ml to 0.5 µg/ml at 37°C for 1 h. After centrifugation the absorption of the supernatant is analysed at 414 nm as a measure for free haemoglobin. As shown in figure 8, the positively charged peptides T1-4-C10 and T2-1-C10 did exhibit some haemolytic acitivity albeit at concentrations higher than the MICs measured. In contrast are the results for the negatively charged T1-6-C10 which shows no haemolysis at all.

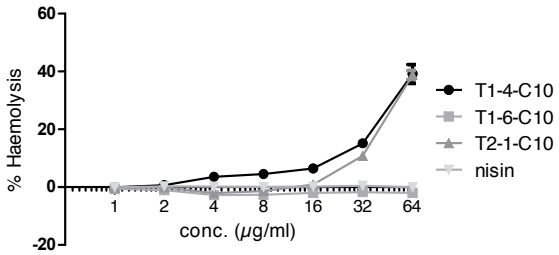

Figure 8: Haemolysis of the C-terminally lipidated peptides.

3.4.5 Antagonization of active peptides by lipid II

To analyse whether the active peptides were capable of binding to lipid II, we tested them in an established lipid II antagonization assay. To do so the active peptides are administered at 4x their MIC and lipid II was added in a range of molar equivalents relative to the final peptide concentrations. The highest concentration of lipid II used was four fold the concentration of the peptide. The peptide – lipid II mixtures were then incubated with *M. luteus* to see if there was any growth. In cases where growth is observed it can be interpreted that the activity of the peptide is inhibited due to lipid II binding/antagonization. Table 7 shows that T2-1-C10 was inhibited even by addition of only 1 eq of lipid II suggesting a strong interaction. For T1-4-C10 more equivalents of lipid II were required (2x excess) to observe antagonization and even more for T1-6-C10. If the results of this assay are taken to be an indication of the affinity for lipid II it can be concluded that T2-1 is the strongest binder, followed by T1-4 and then T1-6. Interestingly, this order of suggested affinity correlates with the enrichment in the phage display screening.

Table 7: Antagonization of peptide activity with lipid II.

Relative Lipid II conc.	T1-4-C10	T1-6-C10	T2-1-C10	Nisin	Ampicillin
4 x	+	+	+	+	-
2 x	+	-	+	+	-
1 x	-	-	+	+	-
0.5 x	-	-	-	-	-
0 x	-	-	-	-	-

+ indicates antagonization of the antimicrobial activity of the peptide, - inidicates no antagonization.

3.5 Analysis of T2-1

3.5.1 Choice of T2-1 as lead structure

At this point we set out to further optimize the most promising peptide sequence in an attempt to obtain a compound with preferred antibiotic properties. Although T1-6-C10 showed no haemolysis, it also showed no activity against strains other than *M. luteus*. The T1-6-C10 peptide was also only slightly antagonized by lipid II possibly indicating a weaker interaction. In addition, T1-4-C10 is highly positively charged and exhibits a relativey high rate of haemolysis. The most promising candidate for further optimization was therefore T2-1-C10 which showed activity against the clinically relevant strain VRE with a lower haemolytic behaviour. For clarity the entire chemical structure of T2-1 is shown in figure 9.

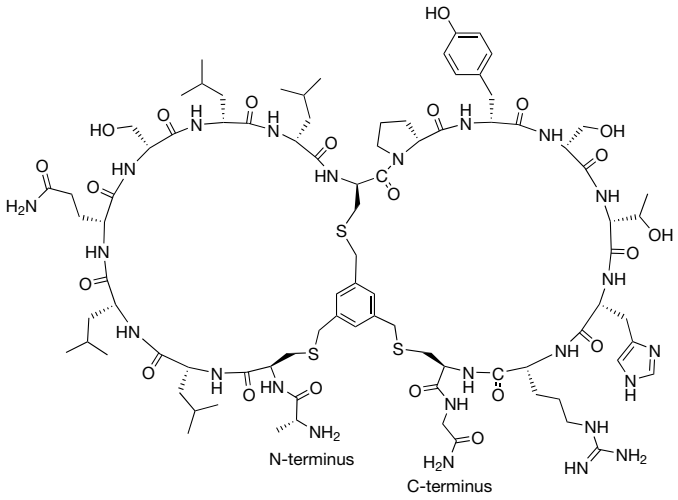

Figure 9: Chemical structure of T2-1.

3.5.2 Alanine scan of T2-1

As the C10 lipidated T2-1 peptide showed the most promising MIC values, especially against VRE E155, and displayed relatively low haemolysis we chose this as our lead compound for further optimization. Optimization in this case denoting improving both the antimicrobial activity while reducing the haemolytic properties. To obtain information about the importance of each separate amino acid in a peptide sequence a so-called “alanine scan” can be performed.[56,57] In such an experiment the peptide is produced each time with one amino acid replaced by an alanine. When tested in an activity based assay valuable structure-activity information can be revealed. Such an experiment was therefore performed for T2-1 where each of the non-cysteine amino acids in the loops were mutated. The peptides were synthesized and tested in non-lipidated form again using *M. luteus* as an indicator strain. The results of the alanine scan (table 8) indicate that there are several residues important for the activity of the peptide. Especially residues 3-5 are critical as their respective alanine mutants lost activity completely. A strong increase of the MIC was observed for residues 7, 11, 12 and 13 as well. Two residues (6 and 14) however, seem to show a slight decrease in MIC (i.e. enhanced activity) upon mutation, suggesting such variants might be interesting for future optimization studies.

Table 8: Results of the alanine scan of T2-1.

Peptide	Sequence	MIC (μg/ml)
T2-1	ACLLQSLLCPYSTHRCG	128[a]
T2-1_L3A	ACALQSLLCPYSTHRCG	>512
T2-1_L4A	ACLAQSLLCPYSTHRCG	>512
T2-1_Q5A	ACLLASLLCPYSTHRCG	>512
T2-1_S6A	ACLLQALLCPYSTHRCG	64-128
T2-1_L7A	ACLLQSALCPYSTHRCG	512
T2-1_L8A	ACLLQSLACPYSTHRCG	128-256
T2-1_P10A	ACLLQSLLCAYSTHRCG	128
T2-1_Y11A	ACLLQSLLCPASTHRCG	512
T2-1_S12A	ACLLQSLLCPYATHRCG	512
T2-1_T13A	ACLLQSLLCPYSAHRCG	512
T2-1_H14A	ACLLQSLLCPYSTARCG	64-128
T2-1_R15A	ACLLQSLLCPYSTHACG	128-256

[a] A method using 1% DMSO to dissolve the peptides was used. Although this did not give the most potent activity it did dissolve all the peptides equally well.

3

3.5.3 Lipid scan of T2-1

As we could improve the activity of T2-1 significantly by attaching a 10 carbon lipid to the C-terminus we also wanted to investigate the effect of the length of the lipid. The length of the lipid can be an important factor in the activity of an antimicrobial compound. Our group previously showed that by modifiying the nisin A/B-ring fragment with varying lipids, different MIC values between different strains are observed.[55] To get insight into the optimal length of the lipid we prepared five variants of T2-1 with lipid lengths varying from 6 to 14 carbon atoms. The compounds were tested both against *M. luteus* and VRE E155 and by evaluating their haemolytic properties (table 9).

Table 9: Effect of the lipid length on MIC and haemolysis.

	MIC (μg/ml)		Haemolysis
Peptide	*M. luteus*	VRE E155	32 μg/ml (after 1 h)
T2-1-C6	32	16-32	n.t.
T2-1-C8	16	8-16	n.t.
T2-1-C10	8	8	6 %
T2-1-C12	4-8	8	9 %
T2-1-C14	4->64	4->64	12.3 %

The results obtained for the T2-1 lipid variants indicate that the introduction of longer lipids generally lead to a better antimicrobial effect. Activity assays with T2-1-C14 in some cases indicated improved MIC values however they proved irreproducible. We suspect that over the course of the activity assay the more hydrophobic C14 analogue might precipitate from the culture medium in which the peptides have to be dissolved or possiblly interacts and binds

with the plastic assay plates. Several conditions to avoid these problems were explored, including the addition of small amounts of tween-80 or BSA, however, these modifications to the assay did not improve the reproducibility. These irreproducible results, combined with the higher rate of haemolysis led us to the conclusion that shorter lipids were optimal. Since there was no clear difference between C10 and C12 in antimicrobial activity we decided to further optimize the C10 variant as it also exhibited a slightly lower rate of haemolysis.

3.5.4 UDP-MurNAc-pentapeptide accumulation assay

An established assay to evaluate the binding of antibiotics to lipid II (or precursors like C_{55}PP and C_{55}P) is to analyse the accumulation of the cytosolic lipid II precursor UDP-MurNAc-pentapeptide. Under normal conditions lipid II is processed by transglycosylases (PBPs) that incorporate the carbohydrate-pentapeptide component of lipid II into the peptidoglycan cell wall (see figure 10). During this reaction C_{55}PP is formed as a side-product, which is then dephosphorylated to C_{55}P. The C_{55}P is transferred back to the cytoplasmic side of the membrane and used for new lipid II synthesis. The initial step of this synthesis is coupling of UDP-MurNAc-pentapeptide to C_{55}P. When lipid II is bound by a peptide (e.g. vancomycin) on the outside of the membrane it is not available for incorporation into the peptidoglycan layer by the transglycosylases. Inhibition of this reaction prevents C_{55}P from being re-formed as well and it is therefore not recycled into the lipid II synthetic machinery leading to accumulation of UDP-MurNAc-pentapeptide in the cytoplasm.

In evaluating the activity of our lead compound, T2-1-C10 in the assay bacterial cells (*E. faecium* E980) were first treated with chloramphenicol, this prevents the hydrolysis of the accumulated UDP-MurNAc-pentapeptide) followed by addition of either T2-1-C10 or vancomycin which was used as a positive control. After harvesting the cells they were extracted with boiling water to isolate the intracellular water-soluble fraction which contains the UDP-MurNAc-pentapeptide. The extracts were analysed using an optimized HPLC method where an ion-pairing agent (NEt_3) is added to the running buffer and compared to untreated cells.[58] The results are shown in figure 11 and indicate that the accumulation of UDP-MurNAc-pentapeptide caused by treatment with T2-1-C10 is nearly as strong as for vancomycin. Pure UDP-MurNAc-pentapeptide was used as a reference and the mass of the corresponding peak was confirmed using negative mode LC-MS.

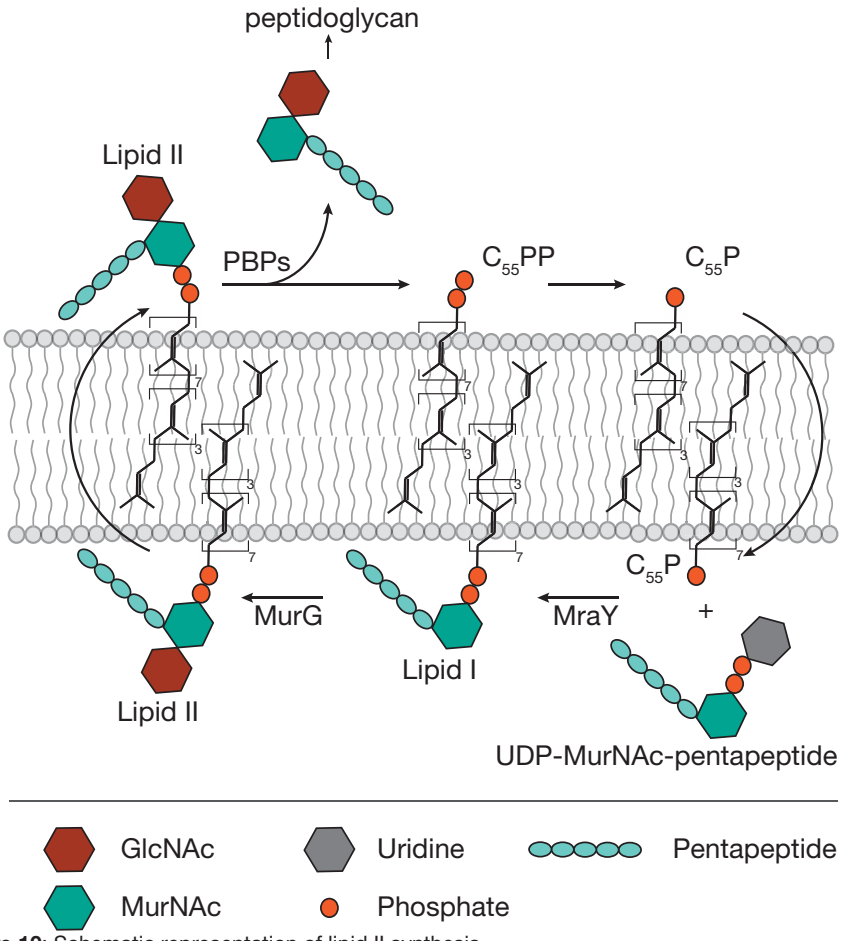

Figure 10: Schematic representation of lipid II synthesis.

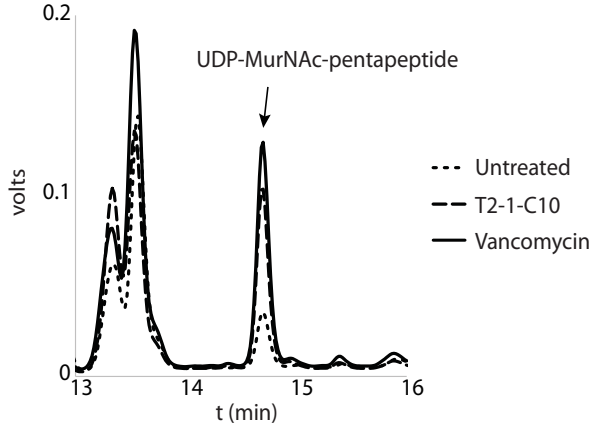

Figure 11: HPLC analysis of intracellular nucleotide pool of *E. faecium* E980 treated with either T2-1-C10, vancomycin, or untreated.

3.6 Conclusions

The data presented in this chapter shows that small molecular targets can be used in phage display experiments although the screening conditions require optimization. Whether our conditions are optimal to be used as a general method is unknown as we have only used a limited set of targets. However, the change in the order of events during biopanning by first incubating the phage with the target before immobilization on streptavidin beads seems to be a useful modification for small molecular targets. It efficiently avoided the enrichment of streptavidin binding sequences in all experiments performed in this manner. The extended incubation of our targets with the phage library also appears to be beneficial in allowing weaker binders to bind the target.

The optimized conditions were used in selections against four different targets designed to mimic lipid II. The results of the phage display experiments were analysed after two rounds of selection using high-throughput DNA sequencing methods. The sequence results obtained revealed unique peptide binders for each target with a remarkable degree of enrichment of one particular peptide identified as a binder for target **2** (lipid I-ent). For each target the peptides that were enriched by more than 1% of the entire population were synthesized using a combination of SPPS and the CLIPS cyclization reaction. All peptides were tested against *M. luteus*, an indicator organism known to be sensitive for lipid II binding antibiotics.[54] Several peptides were identified that were antimicrobially active with MIC values ranging from 32-512 µg/ml. Three of these peptides were chosen as lead compounds for further optimization. We chose the peptides that were identified by screening against the targets that represent lipid II the best, as these were most likely to actually bind to lipid II. Inspired by both nature and previous experience in our group, we next tried to optimize the activity of our lead compounds by modifying the peptide sequence with either an N- or C-terminally attached 10-carbon straight chain lipid. Especially C-terminal lipidation dramatically enhanced the activity of all three peptides against *M. luteus*. All peptides were tested against a broader panel of organisms which showed that peptides T1-4-C10 and T2-1-C10 were active against several other Gram-positive strains. Most notably was the activity of T2-1-C10 against *E. faecium* strains including a vancomycin resistant variant (VRE E155, MIC = 8µg/ml). The T2-1-C10 peptide does have some haemolytic properties but only at concentrations higher than 32 µg/ml (4x the MIC against VRE E155).

Encouraged by the activity of the novel peptides we also investigated their

interaction with lipid II by employing an antagonization assay similar to that described by Müller et al.[59] In this assay, the peptides are preincubated with varying concentrations of lipid II before they are added to culture of susceptible bacteria. This assay showed that all three peptides could be antagonized by lipid II. The best result was obtained for T2-1-C10 which was antagonized by a single molar equivalent of lipid II. Similar results were obtained with the known lipid II binder nisin.

Based on the broad spectrum of activity (including VRE), high enrichment in phage display, and the strong interaction with lipid II, we chose T2-1-C10 for further investigation. The peptide sequence was analysed by means of an alanine-scan which indicated several amino acids as being critical for antimicrobial activity. By comparison, residues Ser6 and His14 tolerated the mutation to alanine and the resulting peptides even showed a slight improvement in activity. Besides an alanine scan, we also varied the length of the lipid to investigate its influence on both the MIC and haemolysis. The data obtained showed that the C10 and C12 lipidated peptides had the same activity. While a C14 variant appeared to show a lower MIC, the results varied due to the poor solubility of this compound. The C14 variant also had a higher rate of haemolysis when compared to C10 and C12.

To further prove the mode of action of T2-1-C10 is via interaction with lipid II we employed an HPLC-based assay where accumulation of UDP-MurNAc-pentapeptide in bacterial cells treated with the antibiotic is measured. UDP-MurNAc-pentapeptide is an intermediate in the biosynthesis of lipid II and will accumulate if lipid II is sequestered by action of an antibiotic. The assay indicated that treatment of enterococci with T2-1-C10 does indeed result in the accumulation of this precursor, to nearly the same extent as treatment with vancomycin. Taken together these results further strengthen our hypothesis that the identified peptide is antimicrobially active through interaction with lipid II.

3.7 Future prospects

3.7.1 Optimization of T2-1

Based on the information from the alanine scan we propose that the T2-1 sequence could be optimized by synthesizing various analogues. Not only the antimicrobial activity could be optimized but also the haemolytic properties could potentially be reduced. The alanine-scan indicates that the arginine at position 15 is not critical as its mutation to alanine only reduces the activity minimally.

Since the arginine could be involved in the haemolysis caused by the T2-1-C10, an optimized peptide sequence could reduce this potentially. Optimization of the peptide sequence could also be done via a phage display affinity maturation approach. A new library could be constructed wherein the residues identified as critical for antimicrobial activity are fixed and with variation permitted at the other sites. Screening of this library could lead to sequences with improved affinity for lipid II.

Currently we have only investigated straight-chain saturated lipids as modifications of the identified peptide sequences. Although the lipids found on peptidic antibiotics produced by nature are often similar it might be beneficial to investigate other types as well. Furthermore the positions we explored for lipidation were limited to the N- or C-terminus. As we currently have no information about the orientation of the peptide while bound to lipid II, other positions for the lipid might be optimal. Such possibilities could be explored by replacing one of the amino acids in the sequence with a lipidated variant.

3.7.2 Phage display variation

Using our phage display method as a basis, various modifications on the screening strategy can be considered. Some peptide scaffolds could intrinsically be more effective at binding small molecular targets. Alternate peptide lengths, but also different cyclization strategies could also be introduced to find novel sequences. Besides variation of the peptide, changes in the target could also be an option. Although our synthetic analogues were shown to be useful, they take the target out of its membrane environment and the screening was done in aqueous conditions. Preparing model membranes with either native lipid II or a synthetic enantiomeric analogue could potentially be used as a means of presenting the target in a more biological relevant environment. Such systems have been used before to identify membrane protein binding peptides.[60]

3.8 Experimental

3.8.1 Phage display

3.8.1.1 Bicyclic phage production

Bicyclic phage production was initially performed as previously described.[8] The phage libraries were obtained from prof. Christian Heinis transformed into *E. coli* TG1. For each library a single flask with 0.5 L 2xYT (+30 µg/ml chloramphenicol) was inoculated with the library to an OD600 of 0.1. The culture was incubated at 30°C at 180 rpm. The cells were removed by centrifugation at 5000 rpm and 4°C for 30 min and the phage were precipitated by addition of 125 ml of PEG solution (20% PEG-6000, 2.5 M NaCl) to the supernatant. The mixed solution is kept on ice for 15 min and then centrifuged at 5000 rpm and 4°C for 30 min. The obtained pellet is resuspended in 20 ml buffer R (20 mM NH_4HCO_3, 5 mM EDTA, pH 8.0, degassed) and centrifuged at 4000 rpm for 15 min. After transferring the supernatant to a clean tube 1 ml of a fresh solution of 20 mM TCEP in dH_2O is added, mixed, and incubated at 42°C for 1 h. The tubes are cooled on ice before the supernatant is transferred to a 100 kDa MWCO spin filter (Vivapsin-20) and concentrated to 0.5 ml by centrifugation at 4000 rpm. Fresh buffer R is added (5 ml) before the solution is concentrated to 0.5 ml again, this step is repeated once more. The phage are recovered from the spin filter using 32 ml buffer R and 8 ml of TBMB solution (50µM in MeCN) is added. The tubes are inverted several times and then incubated at 30°C for 1 h. PEG-solution (10 ml) is added again and the after incubation on ice (15 min) the tubes are centrifuged at 4000 rpm for 30 min. After removal of the supernatant the phage are suspended in 3 ml buffer W (10 mM Tris-HCl, 150 mM NaCl, 10 mM $MgCl_2$, 1 mM $CaCl_2$, pH 7.4).

3.8.1.2 Phage selection

Phage display experiment 1 was performed as previously described.[8] For phage display experiment 2 and 3 the following procedure was used. Several cultures for phage production were started and each was treated as described above. To each phage suspension was added 1.5 ml of buffer W containing 3% BSA and 0.3% Tween-20 and the solutions were mixed for 30 min by rotation at 10 rpm. The blocked phage were mixed and separated in 5 equal portions. Each target was added to one of the portions at a final concentration of 1 µM and the last portion received no target to serve as a negative control. Each mixture was

incubated at room temperature by rotation at 10 rpm for 1 h while in the meantime 250 µl magnetic streptavidin beads were blocked using buffer W containing 1% BSA and 0.1% Tween-20 (for each second round of selection neutravidin beads are used instead). Every phage-target mixture and the negative control now receives 50 µl of the blocked streptavidin beads and is incubated for another 10 min. Using a magnetic Eppendorf holder the liquid is removed from the beads and the beads are washed 4x using buffer W containing 0.1% Tween-20 and 2x using buffer W. Each target was now treated with 100 µl buffer G (Glycine-HCl, pH 2.2) for 5 min with regular flicking. The supernatant is transferred to a tube containing 50 µl buffer F (1M Tris, pH 8.0) to neutralize and temporarily stored at 4°C. A culture of E. coli TG1 cells was incubated until it reached $OD_{600} \approx 0.5$ before it is split into 25 ml portions and the each eluted phage solution is added to one of the portions and incubated at 37°C for 1.5 h. A 100 µl portion is taken from each tube for phage titer determination before the tubes are centrifuged at 4000 rpm at 4°C for 5 min. The supernatant is removed until the last 1-2 ml in which the pellet is resuspended. The bacterial suspension is spread out on a large 2xYT agar plate (+30µg/ml chloramphenicol) and the plates are incubated for 16 h at 37°C. The cells are harvested and stored as 10% glycerol-stocks until the next round of selection.

Experiment 4 was performed as experiment 2 and 3 with the following modifications. After the phage are blocked they are cooled on ice before the targets are added. Incubation with the target, streptavidin capture, and elution are all done at 4°C. The rest of the protocol was performed as described above.

3.8.1.3 DNA analysis

For experiments 1-3 DNA was analyzed by picking single colonies and extracting the plasmid DNA using a Qiagen Miniprep kit. DNA analysis was performed by Macrogen using the primer: TAATTGCTCGACCTCCTCTC. Sequencing results were then aligned and analysed using Mega5 software. For experiment 4 the phage DNA pool using the IonTorrent method was as described by Rebollo et al.[8]

3.8.2 Peptide synthesis

3.8.2.1 Non-lipidated peptides

Peptides were synthesized on either 0.05 mmol scale using a Protein Technologies Symphony peptide synthesizer or on 0.1 and 0.25 mmol scale using a CS Bio 336X peptide synthesizer. Non-lipidated peptides were prepared

on Rink-amide resin using standard Fmoc/tBu solid phase peptide synthesis conditions. Each peptide was cleaved from the resin and deprotected by treating it with TFA/H_2O/EDT/TIPS (90:5:2.5:2.5, 5 ml per 0.05 mmol) for 1 h, followed by filtration and precipitation in MTBE/Hex (1:1, 50ml per 0.05 mmol). The peptide suspension was centrifuged at 3500 rpm for 5 min and the obtained pellets was suspended in MTBE/Hex again followed by centrifugation and this was repeated once more. The obtained pellet was dissolved in a mixture of 20 mM NH_4HCO_3 and MeCN (typically 3:1 but ratio can be varied depending on peptide solubility, total volume should be 90 ml per 0.05 mmol). TBMB (0.075 mmol; 26.8 mg) was then added as a solution in MeCN (5 ml). The reaction mixture was stirred for 1 h at room temperature followed by evaporation of MeCN and subsequent lyophilisation. Peptides were purified by preparative HPLC using a Dr. Maisch Reprosil-Pur 120 C18-AQ column (250 x 25 mm, 10 µm) using a gradient of 25% buffer B to 75% buffer B over 45 min (buffer A: 95% H_2O, 5% MeCN, 0.1% TFA; buffer B: 5% H_2O, 95% MeCN, 0.1% TFA).

Table 10: Analytical data of non-lipidated peptides.

Peptide	R_t (min)[a]	Exact mass (calculated) $[M+2H]^{2+}$	Exact mass (measured)
T1-1	24.0	1057.39	1058.40[b]
T1-2	16.6	958.44	959.50[b]
T1-3	27.4	1044.89	1045.25[b]
T1-4	18.5	997.49	997.40[b]
T1-5		Could not be synthesized	
T1-6	29.7	1048.44	1048.45[b]
T1-7	17.3	990.40	989.95[b]
T2-1	16.5	989.48	989.48[b]
T3-1	19.0	892.40	891.75[b]
T3-2	20.3	1006.46	1006.60[b]
T3-3	22.3	946.39	946.60[b]
T3-4	19.0	925.91	926.35[b]
T3-5	18.6	954.43	954.30[b]
T3-6	24.8	879.38	880.00[b]
T4-1	20.7	1009.00	1008.95[b]
T4-2	21.9	945.95	946.25[b]
T4-3	23.9	971.43	971.80[b]
T4-4	24.7	1011.98	1012.10[b]
T2-1_L3A	14.8	968.4555	968.4558[c]
T2-1_L4A	14.1	968.4555	968.4538[c]
T2-1_Q5A	17.1	960.9683	960.9668[c]
T2-1_S6A	17.8	981.4815	981.4824[c]

Peptide	R_t (min)[a]	Exact mass (calculated) $[M+2H]^{2+}$	Exact mass (measured)
T2-1_L7A	13.5	968.4555	968.4536 [c]
T2-1_L8A	22.6	1935.9032 [d]	1935.9052 [c]
T2-1_P10A	15.5	976.4712	976.4709 [c]
T2-1_Y11A	16	943.4659	943.4690 [c]
T2-1_S12A	16.8	981.4815	981.4824 [c]
T2-1_T13A	16.4	974.4737	974.4778 [c]
T2-1_H14A	17.3	956.4681	956.4691 [c]
T2-1_R15A	17.5	946.9470	946.9485 [c]

[a] Peptides were analysed using a Dr. Maisch Reprosil-Pur 120 C18-AQ column (250 x 4.6 mm, 5 µm) by applying a gradient of 0 - 100% buffer B over 48 minutes (buffer A: 95% H_2O, 5% MeCN, 0.1% TFA; buffer B: 5% H_2O, 95% MeCN, 0.1% TFA). [b] ESI-LRMS. [c] ESI-HRMS. [d] $[M+H]^+$

3.8.2.2 Lipidated peptides

Peptides were synthesized on either 0.05 mmol scale using a Protein Technologies Symphony peptide synthesizer or on 0.1 and 0.25 mmol scale using a CS Bio 336X peptide synthesizer. Lipidated peptides were prepared on Chlorotrityl chloride resin using standard Fmoc/tBu solid phase peptide synthesis conditions. Peptides were cleaved from the resin by treating it with HFIP/DCM (1:3, 4ml per 0.05 mmol) for 1 h at room temperature. The resin was removed by filtration and the filtrate was evaporated to dryness. The protected peptide was dissolved in DCM (3 ml) and the lipid-amine of interest (0.5 mmol per 0.05 mmol peptide) was added, followed by BOP (44.2 mg, 0.1 mmol) and DIPEA (35 µl, 0.2 mmol). The mixture was stirred for 1 h before it is evaporated to dryness. The peptide was deprotected by treating it with TFA/H_2O/EDT/TIPS (90:5:2.5:2.5, 5 ml per 0.05 mmol) for 1 h and precipitated in MTBE/Hex (1:1, 50ml per 0.05 mmol). The peptide was centrifuged at 3500 rpm for 5 min and the obtained pellets was suspended in MTBE/Hex again followed by centrifugation and this was repeated once more. The obtained pellet was dissolved in 1.5 ml DMF and then sonicated to ensure good dissolution followed by further addition of a mixture of 20 mM NH_4HCO_3 and MeCN (typically 2:1 but ratio can be varied depending on peptide solubility, total volume should be 90 ml per 0.05 mmol). TBMB (0.075 mmol; 26.8 mg) was then added as a solution in MeCN (5 ml). The reaction mixture was stirred for 1 h at room temperature followed by evaporation of MeCN and subsequent lyophilisation. Peptides were purified by preparative HPLC using a Dr. Maisch Reprosil-Pur 120 C18-AQ column (250 x 25 mm, 10 µm) using a gradient of 40-100% buffer B over 72 minutes (buffer A: 95% H_2O, 5% MeCN, 0.1% TFA; buffer B: 5% H_2O, 95% MeCN, 0.1% TFA).

Table 11: Analytical data of lipidated peptides.

Peptide	R_t (min)[a]	Exact mass (calculated) $[M+2H]^{2+}$	Exact mass (measured)
C10-T1-4	16.9	1074.56	1075.55 [c]
T1-4-C10	17.4	1067.57	1067.80 [c]
C10-T1-6	12.5[b]	1125.51	1124.75 [c]
T1-6-C10	12.8[b]	1118.52	1119.40 [c]
C10-T2-1	21.6	1066.5469	1066.5494 [d]
T2-1-C10	22.6	1059.5573	1059.5643 [d]
T2-1-C6	18.9	1031.526	1031.5253 [d]
T2-1-C8	20.7	1045.5416	1045.5472 [d]
T2-1-C12	25	1073.5651	1073.5777 [d]
T2-1-C14	27.9	1087.5886	1087.5922 [d]

[a] Peptides were analysed using a Dr. Maisch Reprosil-Pur 120 C18-AQ column (250 x 4.6 mm, 5 µm) by applying a gradient of 0 – 100 % buffer B over 24 minutes (buffer A: 95% H_2O, 5% MeCN, 0.1% TFA; buffer B: 5% H_2O, 95% MeCN, 0.1% TFA). [b] gradient used was 50-100 % over 24 minutes. [c] ESI-LRMS. [d] ESI-HRMS

3.8.3 Minimum inhibitory concentration assay

MIC values were determined by using the broth microdilution method. Peptides were dissolved first in DMSO and diluted with broth so that the final peptide concentration was 1024 µg/ml and the DMSO concentration was 4%. Peptide serial dilutions were made in TSB in a polypropylene 96-wells plate using 50 µl volumes. An overnight culture of the organism of interest was diluted to and OD600 of 0.01 and grown until they reach 0.5. The culture is then diluted to 1 x 10^6 CFU/ml and 50 µl of this suspension was added to each well. The highest concentrations were then 512 µg/ml peptide and 2% DMSO. The plates were incubated at the preferred growth temperature of the organism that was used. After 16 h the MIC was determined visually.

Lipidated peptides were dissolved first in DMSO and diluted with TSB so that the peptide concentration was 128 µg/ml and the DMSO concentration was 4%. After inoculation the highest peptide concentration is 64 µg/ml and the DMSO concentration was 2%.

3.8.4 Antagonization of antimicrobial activity by lipid II and its precursors

Stock solutions of each peptide were prepared so that their final concentration in the assay would be 4 times MIC. Peptides are transferred to a 96 wells plate and Lipid II (or other lipid) was added in 0.5 – 4 molar equivalents in a final volume of 50 µl. Each well received 50 µl of bacterial suspension (*M. luteus*) at 1 x 10^6 CFU/ml and the plates were incubated for 16 h at 250 rpm and 30°C. Growth was observed visually.

3.8.5 Haemolysis assay

Sheep blood in Alsever's solution (2 mL) was diluted with PBS (13 mL) and centrifuged (2,000 RPM, 5 min). The supernatant was discarded and the cells were washed with another 13 mL of PBS and centrifuged. Washing was continued until the supernatant was clear. After the final wash the supernatant was discarded and the packed cells were kept on ice. Serial dilutions of each peptide were made in 50 µl PBS with the highest tested concentration 64 µg/mL in PBS, 2% DMSO. The packed cells (150 µL) were suspended in PBS (10 mL) and 50 µL of this suspension was added to each well. A column with 0.1% triton in DI water was used as the 100% lysis control, and a column with PBS (with 2% DMSO) as the 0% lysis control. After incubation at 37°C the plates were centrifuged (2,000 RPM, 5 min) and 25 µL of the supernatant was added to 100 µL DI water in a flat-bottom 96-wells plate (polystyrene). Haemolysis was determined by measuring the absorption at 414 nm to measure the amount of free haemoglobin.

3.8.6 UDP-MurNAc-pentapeptide accumulation assay

An overnight culture of *E. faecium* E980 was diluted 1000x in TSB and grown until an OD_{600} of 0.5. Chloramphenicol (130 µg/ml) was added and the culture was further incubated for 15 min. The culture is split into 5 ml portions and peptides are added at a final concentration of 10x MIC and the negative control receives no peptide. After further incubation for 30 min the cells were harvested by centrifugation at 3900 rpm for 5 min. The cells were transferred to glass tubes using 1 ml MilliW water and kept in a boiling water bath for 15 min followed by rapid cooling on ice. The liquid was transferred to eppendorfs and cell debris was removed by centrifugation at 12000 rpm for 30 min. The supernatant was removed and lyophilized. The obtained powder was reconstituted in buffer A (50 mM NH_4HCO_3, 5 mM NEt_3, pH 8.3) and analysed by LCMS using a linear gradient of 0-25 % buffer B over 15 minutes (buffer B: MeOH). Pure UDP-MurNAc-pentapeptide was obtained as a gift from E. Breukink and used as a reference.

References

[1] G. D. Wright, *Nat. Rev. Microbiol.* **2007**, *5*, 175–186.

[2] J. Nesme, P. Simonet, *Environ. Microbiol.* **2015**, *17*, 913–930.

[3] P. J. Rutledge, G. L. Challis, *Nat. Rev. Microbiol.* **2015**, *13*, 509–523.

[4] R. H. Baltz, *J. Ind. Microbiol. Biotechnol.* **2006**, *33*, 507–513.

[5] M. Tulp, L. Bohlin, *Bioorganic Med. Chem.* **2005**, *13*, 5274–5282.

[6] G. D. Wright, *Chem. Biol.* **2012**, *19*, 3–10.

[7] C. Heinis, T. Rutherford, S. Freund, G. Winter, *Nat. Chem. Biol.* **2009**, *5*, 502–507.

[8] I. Rentero Rebollo, C. Heinis, *Methods* **2013**, *60*, 46–54.

[9] G. P. Smith, *Science* **1985**, *228*, 1315–1317.

[10] J. Molina-López, F. Sanschagrin, R. C. Levesque, *Peptides* **2006**, *27*, 3115–3121.

[11] A. El Zoeiby, F. Sanschagrin, R. C. Levesque, *Mol. Microbiol.* **2003**, *47*, 1–12.

[12] C. Paradis-Bleau, M. Beaumont, L. Boudreault, A. Lloyd, F. Sanschagrin, T. D. H. Bugg, R. C. Levesque, *Peptides* **2006**, *27*, 1693–1700.

[13] C. Paradis-Bleau, A. Lloyd, F. Sanschagrin, T. Clarke, A. Blewett, T. D. H. Bugg, R. C. Levesque, *BMC Biochem.* **2008**, *9*, 33–43.

[14] C. Paradis-Bleau, A. Lloyd, F. Sanschagrin, H. Maaroufi, T. Clarke, A. Blewett, C. Dowson, D. I. Roper, T. D. H. Bugg, R. C. Levesque, *Biochem. J.* **2009**, *421*, 263–272.

[15] C. Paradis-Bleau, F. Sanschagrin, R. C. Levesque, *Protein Eng. Des. Sel.* **2005**, *18*, 85–91.

[16] C. Paradis-Bleau, F. Sanschagrin, R. C. Levesque, *J. Antimicrob. Chemother.* **2004**, *54*, 278–280.

[17] B. Llano-Sotelo, D. Klepacki, A. S. Mankin, *J. Mol. Biol.* **2009**, *391*, 813–819.

[18] M. Li, A.-C. E. Duc, E. Klosi, S. Pattabiraman, M. R. Spaller, C. S. Chow, *Biochemistry* **2009**, *48*, 8299–8311.

[19] T. N. Lamichhane, N. D. Abeydeera, A.-C. E. Duc, P. R. Cunningham, C. S. Chow, *Molecules* **2011**, *16*, 1211–1239.

[20] S. Sainath Rao, K. V. K. Mohan, C. D. Atreya, *PLoS One* **2013**, *8*, e56081.

[21] S. L. Bishop-Hurley, P. J. Rea, C. S. McSweeney, *Protein Eng. Des. Sel.* **2010**, *23*, 751–757.

[22] SetLance, "http://www.setlance.com/products/," **2015**.
[23] K. Noda, R. Yamasaki, Y. Hironaka, A. Kitagawa, *FEMS Microbiol. Lett.* **2001**, *205*, 349–354.
[24] C. J. Thomas, S. Sharma, G. Kumar, S. S. Visweswariah, A. Surolia, *Biochem. Biophys. Res. Commun.* **2003**, *307*, 133–138.
[25] Y. G. Kim, C. S. Lee, W. J. Chung, E. M. Kim, D. S. Shin, J. H. Rhim, Y. S. Lee, B. G. Kim, J. Chung, *Biochem. Biophys. Res. Commun.* **2005**, *329*, 312–317.
[26] X. Guo, R. R. Chen, *Biotechnol. Prog.* **2006**, *22*, 601–604.
[27] Y.-G. Kim, C.-S. Lee, W.-J. Chung, E.-M. Kim, D.-S. Shin, J.-H. Kim, Y.-S. Lee, J. Chung, B.-G. Kim, *Biotechnol. Lett.* **2006**, *28*, 79–84.
[28] M. Matsumoto, Y. Horiuchi, A. Yamamoto, M. Ochiai, M. Niwa, T. Takagi, H. Omi, T. Kobayashi, M.-M. Suzuki, *J. Microbiol. Methods* **2010**, *82*, 54–8.
[29] N. I. Martin, E. Breukink, *Future Microbiol.* **2007**, *2*, 513–525.
[30] E. Breukink, B. de Kruijff, *Nat. Rev. Drug Discov.* **2006**, *5*, 321–332.
[31] L. V. J. Blair, J. M. A., Webber, M. A., Baylay, A. J., Ogbolu, D. O, Piddock, *Nat. Rev. Microbiol.* **2015**, *42*, 42–51.
[32] L. S. Redgrave, S. B. Sutton, M. a. Webber, L. J. V Piddock, *Trends Microbiol.* **2014**, *22*, 438–445.
[33] P. Timmerman, J. Beld, W. C. Puijk, R. H. Meloen, *ChemBioChem* **2005**, *6*, 821–824.
[34] J. S. Davies, *J. Pept. Sci.* **2003**, *9*, 471–501.
[35] S.-T. D. Hsu, E. Breukink, E. Tischenko, M. A. G. Lutters, B. de Kruijff, R. Kaptein, A. M. J. J. Bonvin, N. A. J. van Nuland, *Nat. Struct. Mol. Biol.* **2004**, *11*, 963–967.
[36] I. R. Rebollo, A. Angelini, C. Heinis, *MedChemComm* **2012**, 145–150.
[37] A. Angelini, L. Cendron, S. Chen, J. Touati, G. Winter, G. Zanotti, C. Heinis, *ACS Chem. Biol.* **2012**, *7*, 817–21.
[38] N. Sun, S. A. Funke, D. Willbold, *J. Biotechnol.* **2012**, *161*, 121–125.
[39] T. Schumacher, L. Mayr, D. Minor Jr., M. Milhollen, M. Burgess, P. Kim, *Science* **1996**, *271*, 1854–1857.
[40] L. E. Zawadzke, J. M. Berg, *J. Am. Chem. Soc.* **1992**, *114*, 4002–4003.
[41] M. T. Weinstock, J. N. Francis, J. S. Redman, M. S. Kay, *Biopolymers* **2012**, *98*, 431–442.
[42] H. M. Dintzis, D. E. Symer, R. Z. Dintzis, L. E. Zawadzke, J. M. Berg, *Proteins Struct. Funct. Genet.* **1993**, *16*, 306–8.

[43] M. H. Van Regenmortel, S. Muller, *Curr. Opin. Biotechnol.* **1998**, *9*, 377–382.

[44] M. S. VanNieuwenhze, S. C. Mauldin, M. Zia-Ebrahimi, J. A. Aikins, L. C. Blaszczak, *J. Am. Chem. Soc.* **2001**, *123*, 6983–6988.

[45] M. S. VanNieuwenhze, S. C. Mauldin, M. Zia-Ebrahimi, B. E. Winger, W. J. Hornback, S. L. Saha, J. A. Aikins, L. C. Blaszczak, *J. Am. Chem. Soc.* **2002**, *124*, 3656–3660.

[46] B. Schwartz, J. A. Markwalder, Y. Wang, *J. Am. Chem. Soc.* **2001**, *123*, 11638–11643.

[47] X. Ye, M. Lo, L. Brunner, D. Walker, D. Kahne, S. Walker, *J. Am. Chem. Soc.* **2001**, *123*, 3155–3156.

[48] L. L. Ling, T. Schneider, A. J. Peoples, A. L. Spoering, I. Engels, B. P. Conlon, A. Mueller, D. E. Hughes, S. Epstein, M. Jones, et al., *Nature* **2015**, *517*, 455–459.

[49] A. Müller, H. Ulm, K. Reder-Christ, H.-G. Sahl, T. Schneider, *Microb. Drug Resist.* **2012**, *18*, 261–270.

[50] K. Nishiyama, Y. Takakusagi, T. Kusayanagi, Y. Matsumoto, S. Habu, K. Kuramochi, F. Sugawara, K. Sakaguchi, H. Takahashi, H. Natsugari, et al., *Bioorganic Med. Chem.* **2009**, *17*, 195–202.

[51] M. W. Smith, J. W. Smith, C. Harris, A. Brancale, C. J. Allender, M. Gumbleton, *Biochem. Biophys. Res. Commun.* **2007**, *358*, 285–291.

[52] B. Van Dorst, J. Mehta, E. Rouah-Martin, R. Blust, J. Robbens, *Methods* **2012**, *58*, 56–61.

[53] K. A. Günay, H.-A. Klok, *Bioconjug. Chem.* **2015**, 150908093205004.

[54] W. C. Chan, M. Leyland, J. Clark, H. M. Dodd, L.-Y. Lian, M. J. Gasson, B. W. Bycroft, G. C. K. Roberts, *FEBS Lett.* **1996**, *390*, 129–132.

[55] T. Koopmans, T. M. Wood, P. 't Hart, L. H. J. Kleijn, A. P. A. Hendrickx, R. J. L. Willems, E. Breukink, N. I. Martin, *J. Am. Chem. Soc.* **2015**, *137*, 9382–9389.

[56] A. Hänchen, S. Rausch, B. Landmann, L. Toti, A. Nusser, R. D. Süssmuth, *ChemBioChem* **2013**, *14*, 625–632.

[57] C. Urech-Varenne, F. Radtke, C. Heinis, *ChemMedChem* **2015**, *10*, 1754–1761.

[58] S. Hyeon Lee, J. Lee, W. Y. Lee, B. C. Chung, M. H. Choi, *Mass Spectrom. Lett.* **2011**, *2*, 92–96.

[59] A. Müller, D. Münch, Y. Schmidt, K. Reder-Christ, G. Schiffer, G. Bendas, H. Gross, H.-G. Sahl, T. Schneider, H. Brötz-Oesterhelt, *J.*

Biol. Chem. **2012**, *287*, 20270–20280.

[60] M. Pavlidou, K. Hänel, L. Möckel, D. Willbold, *PLoS One* **2013**, *8*, 1–8.

Chapter 4

New insight into nisin's mode of action by biophysical studies using synthetic analogues of lipid II

Abstract: Nisin is the preeminent lantibiotic, and to date its antibacterial mechanism has been investigated using a variety of techniques. While nisin's lipid II-mediated mode of action is well-established, a detailed analysis of the thermodynamic parameters governing this interaction has not been previously reported. We here describe an approach employing isothermal titration calorimetry to directly measure the affinity of nisin for lipid II and a number of synthetic lipid II precursors and analogues. Our measurements confirm the pyrophosphate unit of lipid II as the primary site of nisin binding and also indicate that the complete MurNAc moiety is required for a high-affinity interaction. Additionally, we find that while the pentapeptide unit of the lipid II molecule is not required for strong binding by nisin, it does play an important role in stabilizing the subsequently formed nisin–lipid II pore complex, albeit at an entropic cost.

Parts of this chapter have been published in: P. 't Hart, S.F. Oppedijk, E. Breukink, N.I. Martin, *Biochemistry*, **2016**, *55* , 232 - 237

4.1 Interaction between nisin and lipid II

4.1.1 Background

In order to address the growing threat posed by antimicrobial resistance it is important that the mechanisms of action of new and existing antibiotics be clearly understood. The emergence of resistance against all major classes of clinically used antibiotics has led to an increased interest in less traditional antimicrobial agents, including antimicrobial peptides (AMPs) which often operate with unique modes of action. Among the best-studied of the AMPs is the bacteriocin nisin. Produced by strains of Lactococcus lactis, nisin is a member of the lanthipeptide family of AMPs owing to the presence of (methyl)lanthionine rings and dehydro residues (Figure 1A).[1]

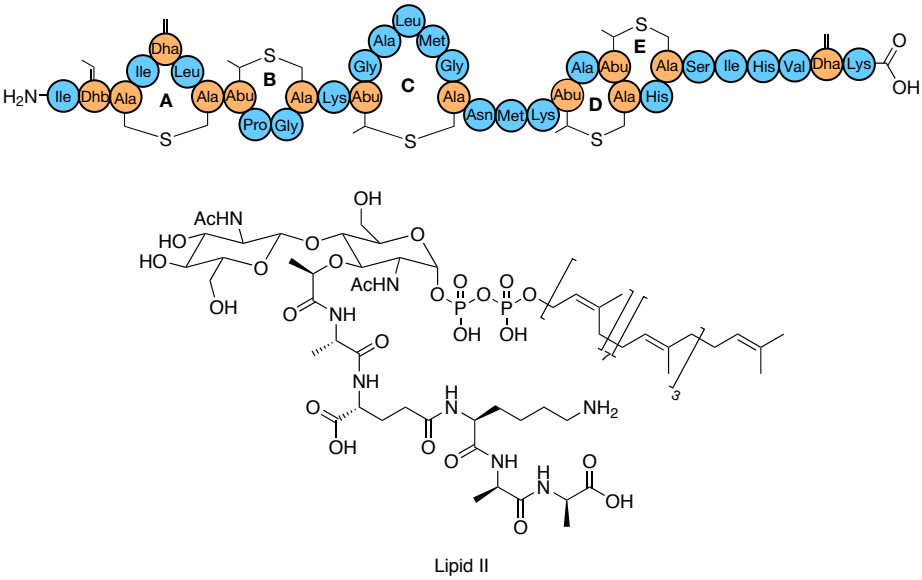

Figure 1: A) Structure of nisin. B) Structure of lipid II.

Nisin is widely active against Gram-positive bacteria including drug-resistant pathogens and, while not suitable for use as a therapeutic drug in humans, it is used widely in food preservation. As the preeminent lantibiotic (lanthipeptide antibiotic) nisin has received much attention and its mode of action has been thoroughly studied (see section 1.6.2).[1–4] A number of biochemical, biophysical, and NMR studies have shown that nisin interacts with the peptidoglycan precursor molecule lipid II. Upon binding to lipid II nisin then goes on to form stable pores in

the bacterial membrane leading to rapid membrane depolarization and bacterial cell death. The lipid II molecule (Figure 1B) consists of a disaccharide core built from *N*-acetyl glucosamine (GlcNAc) and *N*-acetylmuramic acid (MurNAc) wherein the MurNAc unit bears a pentapeptide at the 3 position. In addition, a C_{55} undecaprenol lipid is connected to the MurNAc anomeric centre via a pyrophosphate linkage. Further details about lipid II are described in section 1.5.

It is generally accepted that the pyrophosphate moiety of lipid II is recognized by the N-terminal part of nisin containing lanthionine ring A and B.[5] The remaining C-terminal region of the nisin peptide (ring C,D and E) is then thought to insert into the bacterial membrane leading to the formation of a pore complex with a nisin-lipid II stoichiometry of 8:4 (Figure 2).[6,7] In addition to nisin, a number of other lantibiotics have also been found to contain homologous A/B ring systems indicating that targeting the pyrophosphate unit of lipid II is an antibacterial strategy employed by many organisms.[1,8] Such a strategy may in fact be particularly advantageous with respect to avoiding or delaying the development of resistance as mutation of the pyrophosphate group does not appear to be readily feasible for the bacterium.[9]

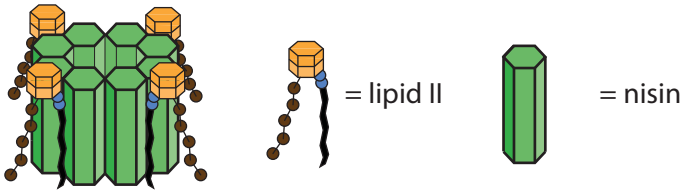

Figure 2: Schematic representation of the proposed nisin-lipid II pore complex with 8:4 stoichiometry.

4.1.2 Previous biophysical studies on nisin

The published solution-state NMR structure of the nisin-lipid II complex employed a soluble lipid II analogue bearing a shorter farnesyl lipid in place of the full C_{55} undecaprenol tail.[5] While the structure thus obtained reveals the details of the interaction of the nisin A/B ring system with the lipid II pyrophosphate moiety, the factors governing pore formation are not readily elucidated via such an approach. In this regard a more commonly used technique for studying nisin-induced pore formation makes use of 1,2-dioleoyl-sn-glycero-3-phosphocholine (DOPC) vesicles loaded with carboxyfluorescein. When such vesicles are treated with nisin, pore formation can occur resulting in dye leakage that can be detected as an increase in fluorescent signal. Using such an approach, Bonev and co-

workers previously showed that nisin causes pore formation in vesicles that are supplemented with 1% lipid I or lipid II.[10] Conversely, nisin was found to be unable to induce pore formation in vesicles supplemented with undecaprenol pyrophosphate (C_{55}-PP) or monophosphate (C_{55}-P). They further studied the interaction of nisin with these vesicles using ^{31}P solid state NMR and observed an interaction with lipid II, lipid I, and C_{55}-PP. In an alternative approach, the groups of Sahl and Bendas employed a quartz crystal microbalance approach to show that nisin has an enhanced affinity towards membranes containing lipid II.[11] In a more recent study, Schneider and coworkers used the same technique to measure the interaction of nisin with different undecaprenol-bound cell envelope precursors. They observed that the affinity of nisin was very similar for a variety of pyrophosphate containing undecaprenol lipids with K_d values in the 300-500 nM range.[12]

4.1.3 Isothermal titration calorimetry

Another technique with the power to complement the approaches described above is isothermal titration calorimetry (ITC). ITC is one of the few techniques where interactions between binding partners can be directly observed and quantified by measuring the change in heat that occurs upon binding. In a typical ITC experiment the ITC cell is filled with a receptor (e.g. a protein) and the syringe is filled with a ligand (e.g. small molecule). Besides the measuring cell there is also a reference cell which is filled with water. Both cells are kept equal in temperature by a constant power. When a binding event takes place in the measuring cell the temperature will change which is sensed by the change in the amount of power required to keep the temperature constant (Figure 3A).[13] Small injections from the syringe are made into the cell and binding between the receptor and the ligand will take place. The heat generated by the ligand-receptor interaction is measured as the change in power in µcal/s or µJ/s (µWatt). When the signal is plotted against time one can integrate the peak areas to convert the signal to a plot of kJ/mol versus the molar ratio of the 2 binding partners (Figure 3B). From the resulting plot various parameters can be extracted, including the K_a, ΔH, and the stoichiometry. Other parameter such as the K_d, ΔG and ΔS can then be calculated as well.

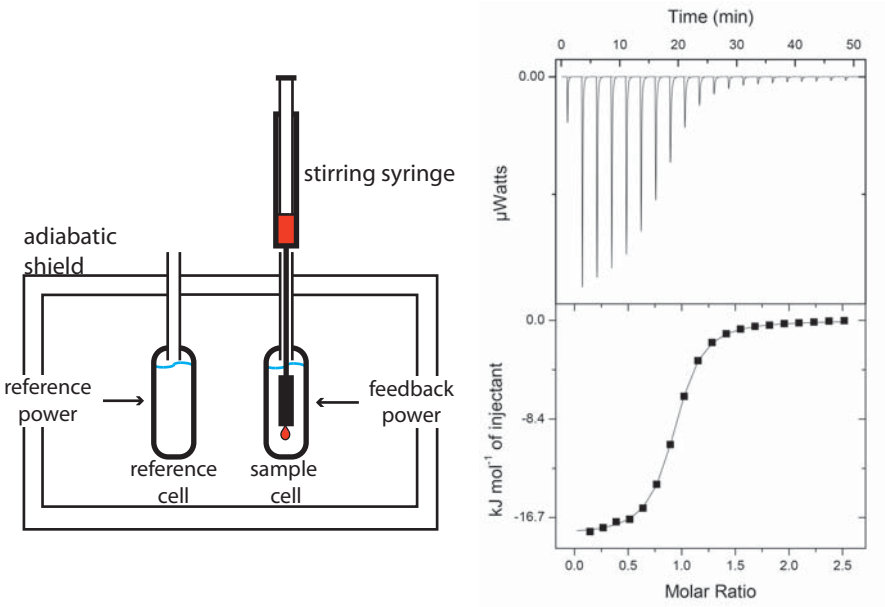

Figure 3: **A**) Schematic representation of an ITC set-up. **B**) A typical binding curve, top graph shows the power plotted versus time, the bottom graph shows the heat change per mol titrated versus the total molar ratio.

4

4.1.4 Lipid II and analogues for ITC studies

Despite nisin's prominence as the best-studied lantibiotic, no comprehensive ITC study has yet been reported with the aim of examining its interaction with lipid II and related cell wall precursors. While it is clear that the pyrophosphate unit of lipid II is essential for nisin binding, less is known about the roles played by the carbohydrate and peptidic components in both the initial recognition by nisin and the subsequent formation of the nisin-lipid II pore complex. In this chapter we describe the application of ITC to further study nisin's binding to lipid II as well as a variety of lipid II analogues. By doing so it is possible to identify the elements needed for high affinity binding by nisin and to more fully elucidate the specific parameters that govern pore formation and stabilization.

4.1.5 Preparation of lipid II and its precursors

A variety of lipid II precursors and derivatives were required for the ITC investigations here described. Lipid II itself was synthesized via a previously described *in vitro* approach[2] using membrane preparations of *Micrococcus flavus* supplemented with C_{55}-P, UDP-*N*-acetylmuramic acid pentapeptide, and UDP-GlcNAc (courtesy of the group of Eefjan Breukink). To assess the impact

of omitting the GlcNAc moiety on nisin binding, lipid I was synthesized following the route developed by VanNieuwenhze and coworkers.[14] In addition, a lipid I analogue lacking the pentapeptide moiety was prepared so as to examine its role in nisin binding and pore formation. In addition, we synthesized a lipid I analogue with a shorter lipid that renders it water soluble to assess the importance of the lipid environment. All studied components are shown in Figure 4 and the synthesis is described in chapter 2.

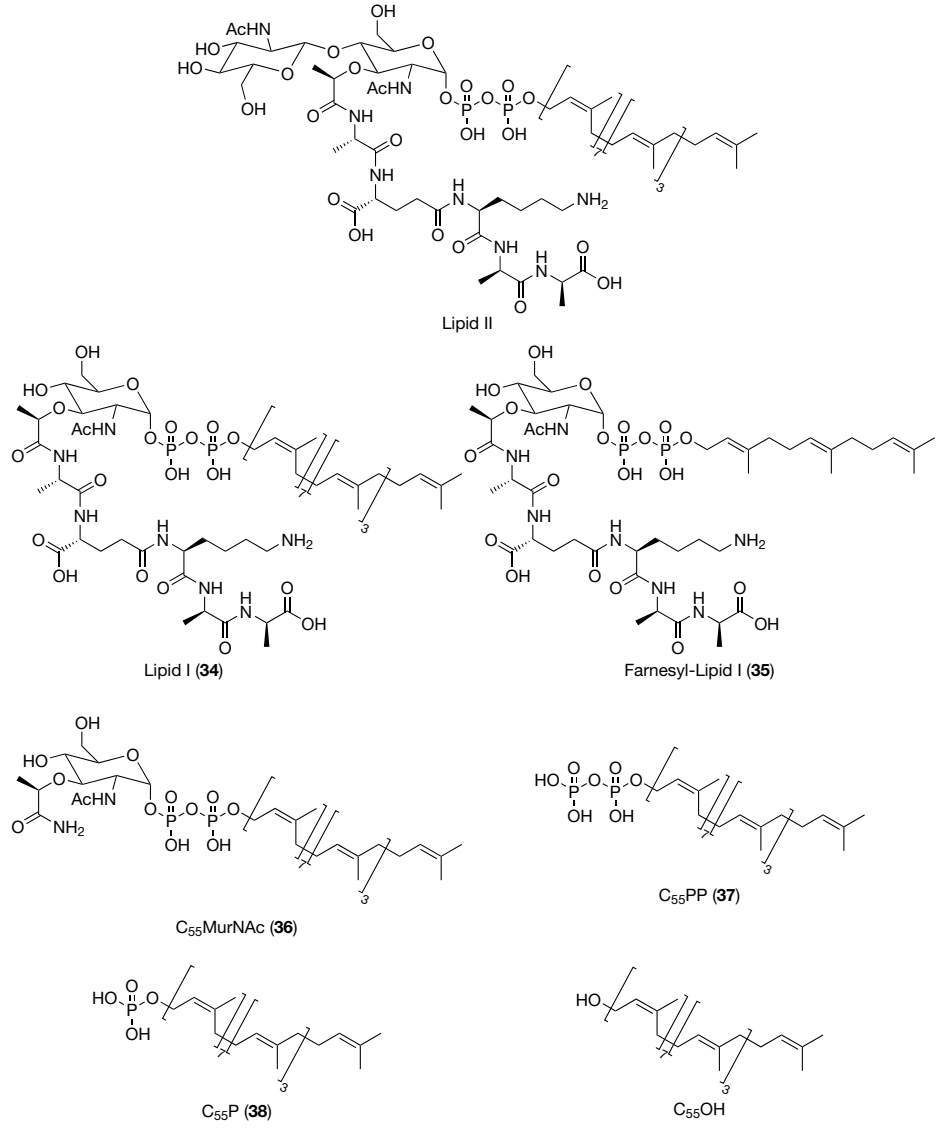

Figure 4: Different lipids used in the ITC experiments.

4.2 Biophysical experiments with nisin

4.2.1 ITC experiments with full length nisin

The ITC experiments were performed using the undecaprenol-type lipids incorporated into DOPC vesicles at a final concentration of 0.1 mM (DOPC concentration was 10 mM). When solutions of these vesicle preparations were titrated into the ITC sample cell containing nisin at a concentration of 20 μM it was possible to obtain high quality binding curves for all pyrophosphate containing lipid species (Figure 5A-E). Of particular note is the observation that the order of addition is of key importance; attempts at titrating nisin into solutions of the lipid containing vesicles failed to produce reliable ITC data. The results of the titrations performed are summarized in Table 1 and reveal low nanomolar dissociation constants for each carbohydrate-based species evaluated (lipid II, lipid I (**34**) and C_{55}MurNAc (**36**)).

Table 1: Thermodynamic parameters of nisin binding measured by ITC at 25oC

Compound	K_d (nM)	ΔH (kJ mol^{-1})	ΔS (J K^{-1} mol^{-1})	ΔG (kJ mol^{-1})
Lipid II[a]	14.6 ± 3.8	-51.2 ± 2.3	-21.9 ± 8.0	-44.7 ± 0.6
Lipid I (**34**)[a]	34.1 ± 8.2	-49.8 ± 0.8	-24.1 ± 3.3	-42.6 ± 0.6
C55MurNAc (**36**)[a]	25.7 ± 7.0	-35.1 ± 1.1	27.6 ± 4.4	-43.3 ± 0.7
C55PP (**37**)[b]	132.6 ± 29.7	-21.7 ± 0.3	59.0 ± 2.1	-39.2 ± 0.6
C55P (**38**)[a]	n.b.[d]			
C55OH[a]	n.b.[d]			
Farnesyl-Lipid I (**35**)[c]	(1.2 ± 0.3) x 10^3	16.8 ± 1.2	169.9 ± 4.7	-33.9 ± 0.6

Each datapoint is the average of three independent experiments (mean ± S.E.). Estimation of the errors in the thermodynamic parameters was performed by Monte Carlo simulations using the standard deviations of each individual measurement. [a] titration of vesicles containing 0.1 mM lipid, 10 mM DOPC into 0.02 mM nisin. [b] titration of vesicles containing 0.5 mM lipid, 10 mM DOPC into 0.05 mM nisin. [c] titration of 0.8 mM lipid into 0.08 mM nisin. [d] n.b. = no binding.

The K_d of 14.6 nM obtained for nisin's binding to lipid II is in reasonably good agreement with the previously reported value of 50 nM as determined based upon the binding behavior of radiolabeled nisin to DOPC vesicles containing 0.5 mol % lipid II.[15] In addition, that finding that nisin binds to both lipid II and lipid I with nearly the same affinity is in agreement with previously reported dye-leakage studies which indicate that the GlcNAc unit is not required for nisin binding.[10] The high affinity binding of nisin measured with compound **36** (wherein the pentapeptide has been completely eliminated) further implicates the pyrophosphate diester moiety as the primary target for nisin binding. The ITC measurements also revealed nisin to have a relatively strong interaction with C_{55}-PP (**37**) with only a 10-fold decrease in affinity compared to lipid II. The

observed difference in binding may be explained by the presence of the extra negative charge in the pyrophosphate monoester moiety. In addition, titration of nisin with vesicles containing C_{55}-P (**38**) and C_{55}-OH did not result in any observable binding. These results are also in line with previous dye-leakage studies which found that both C_{55}-P and C_{55}-OH are unable to support nisin-induced pore formation.[10] To probe the influence of the membrane environment in which the lipid II derivatives are anchored, we also examined nisin binding to a soluble lipid I analogue (**35**) in which the C_{55} lipid is replaced by a farnesyl tail. When a vesicle-free solution of compound **35** was titrated into nisin, binding was observed (Figure 5E) albeit with a significant loss of affinity relative to the membrane anchored lipid II and lipid I species.

As indicated in Table 1 the K_d for nisin's interaction with compound **35** is approximately 100 times higher than for lipid II. Also of note is the observation that nisin binding to compound **35** is an endothermic process and as such is completely entropy driven. The large gain in entropy upon binding to **35** is likely due to the displacement of organized water molecules that occurs upon formation of the nisin-compound **35** complex as is also evidenced by the visible aggregation and precipitation of the complex in aqueous solutions.[5] However, the precipitation event might lead to heat changes as well and obscure the actual binding event.

Interesting trends also emerge from the ITC data obtained for the various membrane-anchored C_{55} species. In moving from lipid II and lipid I (**34**) to compound **36** and C_{55}-PP (**37**), a gradual decrease in the enthalpy of the nisin-binding interaction is observed (Table 1) suggesting the loss of stabilizing interactions (i.e. hydrogen bonds) and a decreased pore stability. Another important finding is that for compound **7** and C_{55}-PP (**37**), both lacking the pentapeptide, nisin binding is accompanied by a favorable gain in entropy compared with binding to lipid II and lipid I (**34**) where binding comes at an entropic cost. This indicates that the pentapeptide experiences a restricted mobility within the nisin pore-complex, leading to a high entropic penalty when it transitions from a free form into a pore-complex. Removing the pentapeptide appears to relieve this penalty.

4.2.2 ITC experiments with nisin 1-12

As the NMR-structure shows that nisin binding is governed mostly by the A/B-ring part of nisin (nisin 1-12)[5] we attempted to measure the affinity of this

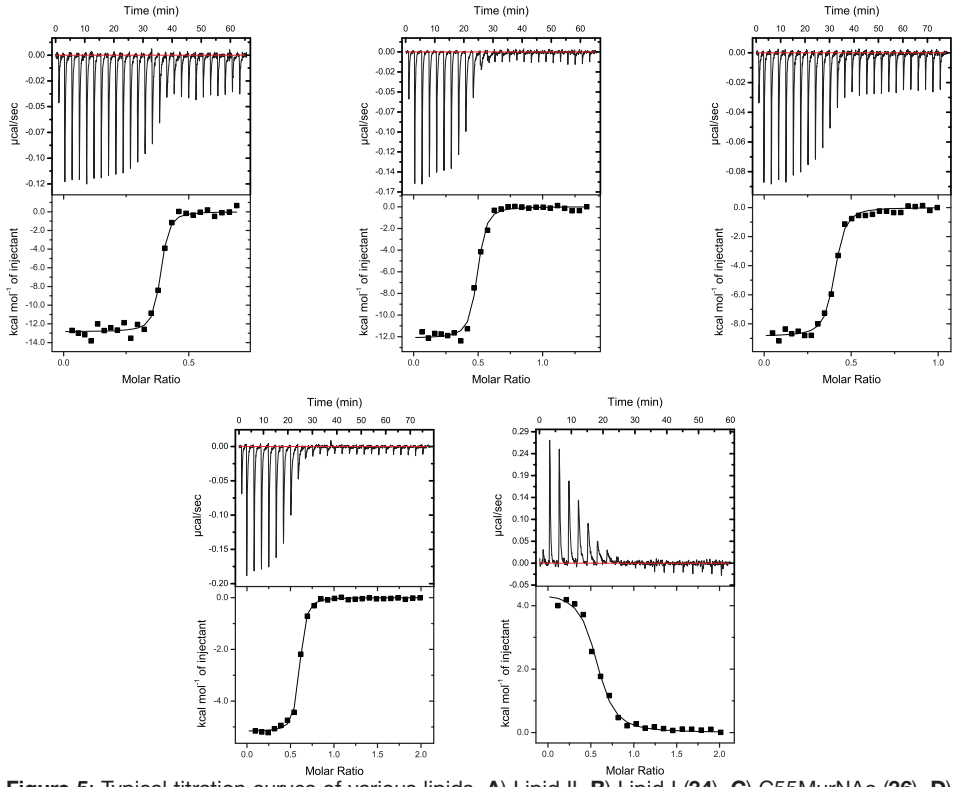

Figure 5: Typical titration curves of various lipids. **A**) Lipid II, **B**) Lipid I (**34**), **C**) C55MurNAc (**36**), **D**) C55PP (**37**), **E**) 3-lipid I (**35**).

fragment for lipid II in DOPC vesicles. The nisin 1-12 fragment can be easily obtained by using an optimized method recently described by our group where nisin is digested with trypsin.[16,17] Direct titrations of the nisin 1-12 peptide with lipid II vesicles as we had done for full length nisin showed no significant binding curve, indicating that the affinity is strongly reduced. Repeated attempts using increased concentrations of the peptide (200 µM) and lipid II (1 mM in 20 mM DOPC) also did not result in any observable binding. As higher concentrations of lipid II are not feasible, we next turned to a displacement method to determine the affinity of this nisin 1-12 fragment for lipid II. In a displacement titration the receptor is presaturated with a weak ligand and then titrated with a strong ligand of known affinity.[18] The affinity of the weak ligand is calculated from the apparent Ka using the formula:

$$K_2 = \left(\frac{K_1}{K_{\text{app}}} - 1\right) \cdot \frac{1}{L_{2\,t\,o\,t}}$$

Where K_1 is the affinity of the high affinity ligand, K_2 is the affinity of the low-affinity ligand, K_{app} is the measured affinity and L_{2tot} is the final concentration of the low-affinity ligand in the cell. The ΔH can be determined as well using the formula:

$$\Delta H_2 = (\Delta H_1 - \Delta H_{\text{app}}) \left(1 + \frac{1}{K_2 \cdot L_{2\,t\,o\,t}}\right)$$

Where ΔH1 is the enthalpy change for the high-affinity ligand, ΔH2 is the enthalpy change for the low-affinity ligand and ΔH_{app} is the measured enthalpy change. Thus, to successfully detect the interaction between nisin 1-12 and lipid II we used the same conditions as for the initial lipid II - nisin titration but the lipid II vesicles were first treated with 1 mM nisin 1-12. The obtained data is shown in Figure 6 and indicates a strongly reduced affinity. Although the nisin 1-12 fragment is the pyrophosphate recognition domain as shown in the NMR-structure[5], the other part of nisin is required for strong binding. Possibly due to an interaction with the membrane or by interaction with other nisin molecules during pore formation.

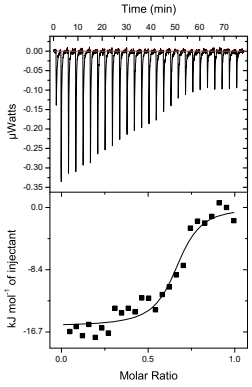

Thermodynamic parameters:
Kd = 20.8 µM
ΔH = -40.0 ± 2.7 kJ mol^{-1}
TΔS = -44.6 ± 9.4 kJ mol^{-1}
ΔG = -26.7 ± 0.9 kJ mol^{-1}

Figure 6: Typical titration curve obtained for the displacement experiment. Titration of lipid II (0.1 mM) vesicles saturated with nisin 1-12 (1 mM) into nisin (0.02 mM). Reported values are averages of three independent experiments.

4.3 Dye leakage experiments

4.3.1 Dye leakage experiments with truncated lipid II analogues

The ITC experiments here described provide new insights into the structural requirements for high affinity binding of lipid II by nisin. To correlate these findings with those elements of lipid II that are also required for nisin-induced pore-formation, we next performed a series of dye-leakage experiments with those lipid II derivatives that displayed the strongest nisin binding. To this end we prepared a series of carboxyfluorescein-loaded DOPC vesicles containing the different C_{55} species and evaluated nisin's ability to induce pore formation as evidenced by dye leakage.[2] As illustrated in Figure 7A and B, the addition of nisin to vesicles containing lipid II, lipid I, or compound **36** resulted in similar levels of dye leakage. By comparison, and in agreement with previous reports,[10] nisin does not cause pore formation in vesicles containing C_{55}-PP (**37**). The measured K_d of **37** of 133 nM for nisin binding to C_{55}-PP does, however, appear to support the hypothesis that aside from targeting lipid II, nisin also inhibits bacterial growth by the sequestration of C_{55}-PP. Sequestration of C_{55}-PP leads to the inhibition of the lipid II biosynthesis route.[10] Also of note is the observation that compound **36**, despite lacking the pentapeptide, is still able to support formation of a viable pore-complex with nisin. It was previously proposed that the MurNAc-pentapeptide motif was critical for pore formation[10] however our data indicate that the MurNAc unit itself is largely sufficient. Following up on this finding we next evaluated the stability of the pore-complexes formed between nisin and lipid II, lipid I, or compound **36**. The stability of the various pore-complexes was examined by pre-incubating nisin with "empty" (no carboxyfluorescein) DOPC vesicles containing the various C_{55} lipid species. The stability of the pore-complexes formed in the empty vesicles was then assessed by adding carboxyfluorescein-loaded, lipid II-containing vesicles. The ability of nisin to dissociate from the initially-formed pore-complex in the empty vesicles is readily observed as any free nisin will rapidly rebind to the carboxyfluorescein-loaded, lipid II-containing vesicles resulting in dye leakage.[2] The results of the pore stability study are illustrated in Figure 7C and show that the nisin-lipid II pore-complex is quite stable as reflected by the low level of leakage detected (<5%) while the pore-complex formed with lipid I is slightly less stable (9% leakage). By comparison, the complex formed between nisin and compound **36** is significantly destabilized as indicated by >25% leakage observed, in

line with our ITC results. Taken together these findings suggest that while the pentapeptide unit is not required for strong binding by nisin and pore formation, it does play a role in stabilizing the nisin-lipid II pore-complex.

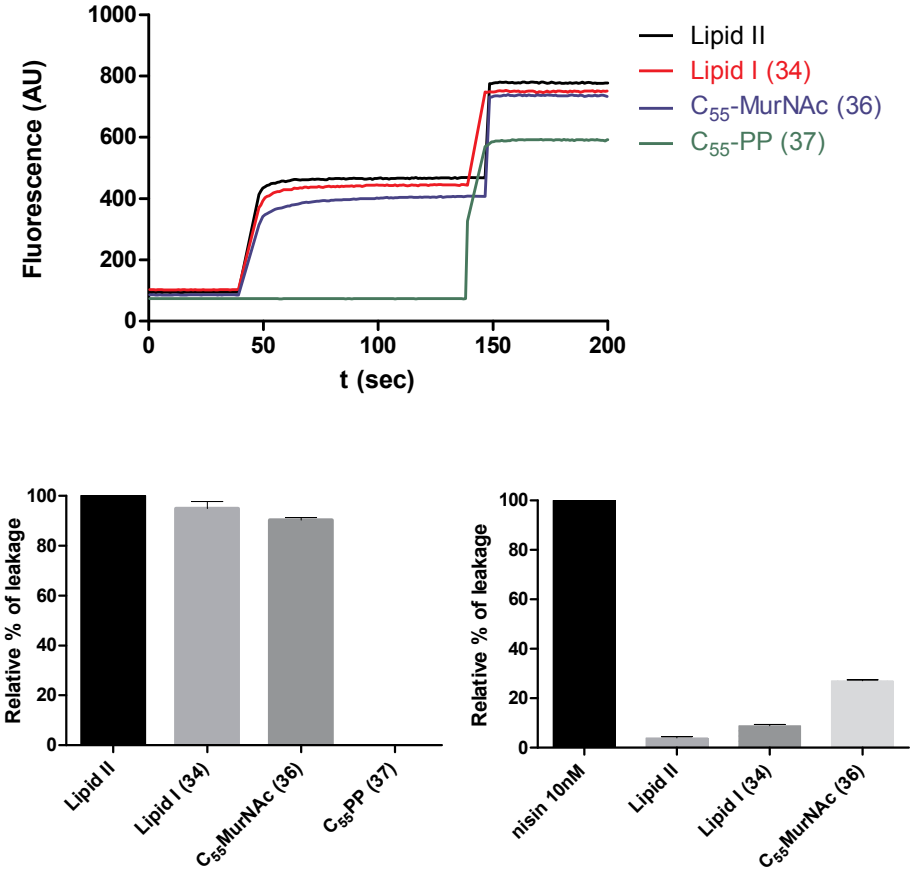

Figure 7: **A**) Fluorescence measurements of carboxyfluorescein loaded DOPC vesicles containing either lipid II, lipid I (**34**), compound **36** or compound **37**. After 40 sec nisin is added and the measurement is continued for another 100s before triton x-100 is added for full lysis of the vesicles and the 100% signal is recorded. Each graph represents the average of two independent measurements. **B**) Quantification of dye leakage from DOPC vesicles prepared with different lipids. Leakage in the presence of lipid II was set as 100%. **C**) Pore stability assay results. Dye leakage from treatment without "empty" vesicles (nisin 10 nM) was used as the 100% signal.

4.4 Conclusions

In summary, we have performed a comprehensive ITC-based investigation of the binding of nisin to its bacterial target molecule, lipid II. To date only a few

lipid II-binding studies with other lantibiotics have been reported[19–21] and the present study is the first of its kind involving nisin. The ITC approach reveals subtle differences in the affinity of nisin for lipid II and derivatives lacking various structural features. The pyrophosphate moiety of lipid II was confirmed as the primary site of nisin binding and new insights into the entropic features that accompany formation of the nisin pore-complex were also revealed. Importantly, the ITC approaches here described are also expected to be of value in characterizing the modes of action of other antibiotics which target lipid II and related bacterial cell-wall precursors.

4.5 Experimental

4.5.1 Isothermal Titration Calorimetry

Large unilamellar vesicles were prepared containing 10 mM DOPC and 0.1 mM of the lipid of interest by suspending the dried lipid films in 50 mM Tris and 100 mM NaCl (pH 7.0). The solution was then extruded through 0.2 µm pore carbonate filters ten times. For C_{55}-PP the vesicles were prepared using 10 mM DOPC and 0.5 mM C_{55}-PP. The nisin solution was freshly prepared before every experiment in the same buffer as used for the vesicles.

Every experiment consisted of 25 injections of 1.5 µl (with a starting injection of 0.5 µl) into the cell containing 20 µM nisin (200 µl) or 50 µM for measurement with C_{55}-PP (**37**). The spacing time between each injection was 180 seconds and all measurements were done at 25°C and with the reference power set at 2. Feedback mode/Gain was set at low to obtain a better signal to noise ratio.

For the titration with compound **35** a different program was used. Compound 35 was dissolved at 800 µM and nisin at 80 µM. The measurement was done using 19 injections of 2 µl (with a starting injection of 0.5 µl) and 180 sec spacing time.

Every measurement was done in triplicate and was corrected by subtraction of a "blank" titration of the corresponding syringe solution into buffer. Obtained data was analysed using the Origin 7.0 software that is supplied with the machine. All measurements were performed in triplicate and reported values are averages. Estimation of the errors in the thermodynamic parameters was done by Monte Carlo simulations using the standard deviations of each individual measurement.

4.5.2 Nisin 1-12 ITC competition experiments

For competitive binding experiments nisin 1-12 was dissolved at a

concentration of 1 mM in the lipid II vesicle solution. The titration was performed the same as for lipid II. The affinity and change in enthalpy was calculated using formulas 1 and 2 described by Zhang et al.[18] The reported errors are propagated using the same formulas.

4.5.3 Dye Leakage experiments

Dye leakage assays and pore stability assays were performed as described in Breukink et al.[2] In short, carboxyfluorescein loaded large unilamellar vesicles were prepared from 10 mM DOPC containing 0.2% of the lipid of interest. These vesicles were used at a concentration of 25 μM in the cuvette and fluorescence was measured for 200 s. At approximately 40 s nisin is added at a concentration of 10 nM and after 140 s triton-x 100 at a final concentration of 0.1%. The baseline signal was determined as the average of the first 40 sec (A_0) and the maximum signal as the average of the last 40 sec (A_{max}). The value at 120 sec ($A_{measured}$) was used to calculate the percentage of dye leakage using the formula:

$$\%\ \text{leakage} = \frac{A_{\text{measured}} - A_0}{A_{\max} - A_0} \times 100\%$$

Every measurement was done in duplicate.

4.5.4 Pore stability experiments

The experiments to assess pore stability were performed as described by Breukink et al.[2] For these experiments nisin was premixed with “empty” DOPC vesicles containing the lipid of interest. The cuvette was filled with CF loaded lipid II vesicles and after 40 s the premixed vesicles are added. At 140 s triton-x 100 is added to obtain the 100 % fluorescence signal. Every measurement was done in duplicate. For these experiments the signal obtained by using just nisin and no vesicles was considered to be 100%.

References

[1] E. Breukink, B. de Kruijff, *Nat. Rev. Drug Discov.* **2006**, *5*, 321–332.

[2] E. Breukink, H. E. van Heusden, P. J. Vollmerhaus, E. Swiezewska, L. Brunner, S. Walker, A. J. R. Heck, B. de Kruijff, *J. Biol. Chem.* **2003**, *278*, 19898–19903.

[3] E. Breukink, I. Wiedemann, C. Van Kraaij, O. P. Kuipers, H.-G. Sahl, B. de Kruijff, *Science* **1999**, *286*, 2361–2364.

[4] G. Bierbaum, H.-G. Sahl, *Curr. Pharm. Biotechnol.* **2009**, *10*, 2–18.

[5] S.-T. D. Hsu, E. Breukink, E. Tischenko, M. A. G. Lutters, B. de Kruijff, R. Kaptein, A. M. J. J. Bonvin, N. A. J. van Nuland, *Nat. Struct. Mol. Biol.* **2004**, *11*, 963–967.

[6] E. Breukink, C. Van Kraaij, R. A. Demel, R. J. Siezen, O. P. Kuipers, B. de Kruijff, *Biochemistry* **1997**, *36*, 6968–6976.

[7] H. Brötz, M. Josten, I. Wiedemann, U. Schneider, F. Götz, G. Bierbaum, H.-G. Sahl, *Mol. Microbiol.* **1998**, *30*, 317–327.

[8] J. M. Willey, W. A. van der Donk, *Annu. Rev. Microbiol.* **2007**, *61*, 477–501.

[9] H. Zhou, J. Fang, Y. Tian, X. Y. Lu, *Ann. Microbiol.* **2014**, *64*, 413–420.

[10] B. B. Bonev, E. Breukink, E. Swiezewska, B. De Kruijff, A. Watts, *FASEB J.* **2004**, *18*, 1862–1869.

[11] K. Christ, I. Wiedemann, U. Bakowsky, H.-G. Sahl, G. Bendas, *Biochim. Biophys. Acta - Biomembr.* **2007**, *1768*, 694–704.

[12] A. Müller, H. Ulm, K. Reder-Christ, H.-G. Sahl, T. Schneider, *Microb. Drug Resist.* **2012**, *18*, 261–270.

[13] M. W. Freyer, E. A. Lewis, *Methods Cell Biol.* **2008**, *84*, 79–113.

[14] M. S. VanNieuwenhze, S. C. Mauldin, M. Zia-Ebrahimi, J. A. Aikins, L. C. Blaszczak, *J. Am. Chem. Soc.* **2001**, *123*, 6983–6988.

[15] I. Wiedemann, E. Breukink, C. Van Kraaij, O. P. Kuipers, G. Bierbaum, B. de Kruijff, H.-G. Sahl, *J. Biol. Chem.* **2001**, *276*, 1772–1779.

[16] T. Koopmans, T. M. Wood, P. 't Hart, L. H. J. Kleijn, A. P. a. Hendrickx, R. J. L. Willems, E. Breukink, N. I. Martin, *J. Am. Chem. Soc.* **2015**, *137*, 9382–9389.

[17] W. C. Chan, M. Leyland, J. Clark, H. M. Dodd, L.-Y. Lian, M. J. Gasson, B. W. Bycroft, G. C. K. Roberts, *FEBS Lett.* **1996**, *390*, 129–132.

[18] Y.-L. Zhang, Z.-Y. Zhang, *Anal. Biochem.* **1998**, *261*, 139–148.

[19] M. R. Islam, M. Nishie, J. Nagao, T. Zendo, S. Keller, J. Nakayama, D.

Kohda, H.-G. Sahl, K. Sonomoto, *J. Am. Chem. Soc.* **2012**, *134*, 3687–90.

[20] A. D. Paiva, E. Breukink, H. C. Mantovani, *Antimicrob. Agents Chemother.* **2011**, *55*, 5284–5293.

[21] S. Al-Kaddah, K. Reder-Christ, G. Klocek, I. Wiedemann, M. Brunschweiger, G. Bendas, *Biophys. Chem.* **2010**, *152*, 145–152.

Chapter 5

Synthesis and evaluation of daptomycin analogues

Abstract: The calcium-dependent lipopeptide antibiotics represent a promising new class of antimicrobials for use in combating drug-resistant bacteria. At present, daptomycin is the only such lipopeptide used clinically and displays potent antimicrobial activity against a number of pathogenic Gram-positive bacteria. Given the increasing need for new antibiotics, practical synthetic access to unnatural analogues of daptomycin and related antimicrobial lipopeptides is of value. We here report an efficient synthetic route combining solid- and solution-phase techniques that allows for the rapid preparation of daptomycin analogues. Using this approach, four such analogues, including two enantiomeric variants, were synthesized and their antimicrobial activities and hydrolytic stabilities evaluated.

Parts of this chapter have been published in: P. 't Hart, L.H.J. Kleijn, G. de Bruin, S.F. Oppedijk, J. Kemmink N.I. Martin, *Org. Biomol. Chem*, **2014**, *12*, 913 - 918

5.1 Daptomycin

5.1.1 Daptomycin structure and properties

Despite a growing need for new antibiotics, only two mechanistically and structurally new classes of antibiotics have reached the clinic in the past 40 years: linezolid and daptomycin.[1,2] While linezolid is of synthetic origin, daptomycin (Figure 1) is a natural product isolated from fermentations of *Streptomyces roseosporus*. Daptomycin is rapidly bactericidal against *Staphylococcus aureus*, including methicillin-resistant *S. aureus* (MRSA), vancomycin-intermediate *S. aureus* (VISA) and vancomycin-resistant *S. aureus* (VRSA) strains.[3–5] Marketed under the trade name Cubicin, daptomycin is the first lipopeptide antibiotic of its kind to be approved for clinical use. Structurally unique, daptomycin is a cyclic depsipeptide composed of 13 amino acids (including nonproteinogenic and D-amino acids) and bears an N-terminal 10-carbon lipophilic tail (Figure 1).

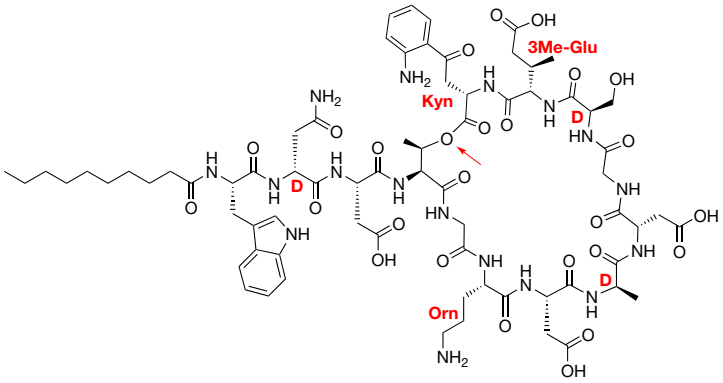

Figure 1: Structure of daptomycin. Indicated are the unnatural amino acids, D-amino acids and the ester bond (arrow).

5.1.2 Proposed mode of action of daptomycin

While the precise mechanistic details of daptomycin's antibacterial activity are unclear, it is known to disrupt aspects of bacterial cell membrane function.[6,7] In this regard, the current model for daptomycin's mode of action involves interaction with the bacterial membrane leading to rapid depolarization and a loss of membrane potential resulting in bacterial cell death without rupturing the cell.[7–10] Daptomycin's activity is calcium-dependent with serum levels of free calcium (45-55 µg/ml) sufficient to induce full antimicrobial activity.[11] Owing to the presence of four carboxylate side chains in the peptide, daptomycin is

negatively charged at physiological pH and as such interacts with Ca^{2+} ions.[12] Upon binding to Ca^{2+} daptomycin is believed to oligomerize after which it is able to effectively disrupt the cell membranes of sensitive bacteria leading to defective cell division and cell wall synthesis.[6,12–15] Such models do not include an explicit role for a specific biomolecular target(s) in daptomycin's antibacterial mechanism. Recent findings have shown that the cell membranes of daptomycin-resistant strains of enterococci and *S. aureus* exhibit significantly reduced levels of phosphatidylglycerol,[16,17] however this does not appear to be the case for all resistant strains.[18] Additionally, YycG, a membrane-spanning histidine kinase, has also been proposed to play a role in daptomycin's mode of action.[6] Genomic analyses of bacterial strains with reduced susceptibility to daptomycin have identified mutations in the gene encoding for YycG.[19,20] While it has been speculated that daptomycin binds to YycG and blocks signal transduction, there is no experimental evidence that specifically addresses this hypothesis.[6] Moreover, daptomycin resistance has also been observed for *S. aureus* strains lacking the YycG mutation further illustrating the complexity that underlies daptomycin's mode of action.[21]

5.2 Aim of the project

While it has also been postulated that daptomycin does not target a specific bacterial biomolecule, others point to daptomycin's antibacterial potency as evidence for a target.[22] Furthermore, when compared to the relatively simple structures of known non-targeted, membrane-disrupting antimicrobial peptides such as the magainins, daptomycin's structural complexity may also suggest a targeted mode of action. To address this issue from a new perspective we set out to develop a straightforward synthetic approach allowing for access to sets of daptomycin analogues in both enantiomeric forms. By employing such an approach it may be possible to gain insight into the stereochemical factors that are involved in daptomycin's mode of action. If, as some have proposed, daptomycin kills bacteria via membrane disruption without invoking a specific chiral bacterial target biomolecule, one would expect the "mirror-image" enantiomeric form of daptomycin to show an equal antibiotic activity. Conversely, should the enantiomeric form of daptomycin not show antibacterial activity, it can be taken as an indication that a chiral interaction with a specific biomolecular target is integral to daptomycin's mode of action. Similar reasoning has also been applied in previously described investigations into the modes of action of other biologically active peptides.[23–25]

5.3 Synthesis of daptomycin analogues

5.3.1 Previously reported syntheses of daptomycin and analogues

Previous approaches toward the synthesis of daptomycin have relied upon either chemo-enzymatic approaches or laborious total synthesis. The Marahiel group demonstrated that linear precursor peptide thioesters could be efficiently converted to their corresponding daptomycin macrocycles by action of the appropriate recombinant cyclase enzyme.[26] This approach however, is unlikely to be applicable in generating the enantiomeric daptomycin species given that the cyclase is expected to act only on precursor peptides containing natural stereochemistry. In addition, two total syntheses of daptomycin have also been reported to date.[27,28] In both cases the synthetic routes described are labour intensive and make use of multi-step synthetic strategies. For these reasons we were drawn towards developing a more convenient synthesis of daptomycin analogues that could also be readily applied to the preparation of the enantiomeric species and other derivatives.

5.3.2 Design of the initial daptomycin analogue

In designing the daptomycin analogues (Figure 2) we opted to replace the L-threonine residue at position 4 with L-diaminiopropionic acid. In doing so we were able to circumvent incorporation of the synthetically challenging[27,28] ester linkage between Thr4 and Kyn13 found in the daptomycin macrocycle by replacing it with the more accessible amide linkage. In this regard, we also speculated that the corresponding macrocyclic amide analogue of daptomycin might show improved hydrolytic stability (*vide infra*). Aside from the amide for ester modification, we also incorporated L-glutamic acid at position 12 in place of the (2*S*,3*R*)-3-methyl glutamate found in daptomycin. While published preparations of (2*S*,3*R*)-3-methyl glutamate are available,[27–29] they are lengthy (>10 steps) and for our purposes would need to be performed twice so to provide access to both enantiomers of 3-MeGlu. In addition, Marahiel and coworkers previously investigated the same Glu for 3-MeGlu substitution in their chemo-enzymatic approach to daptomycin analogues and found it to have a relatively small effect on antimicrobial activity (MIC values increased by ca. 7-fold).[26] Another analogue was designed based on the findings of Marahiel as well, where the kynurenine residue is exchanged for a tryptophan. Although they showed it had a significantly reduced activity (100 µg/ml against *B. subtilis*)[26] it is an easy to make peptide as it completely consists of commercially available amino acids.

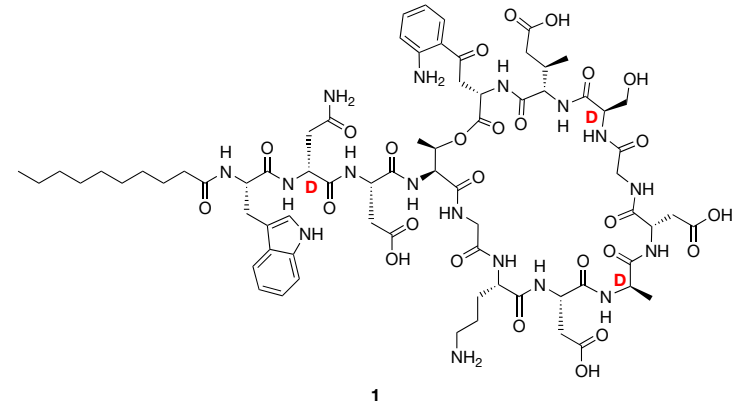

1

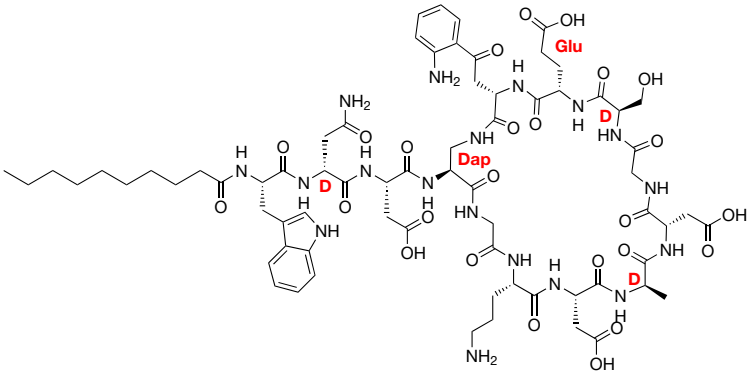

2

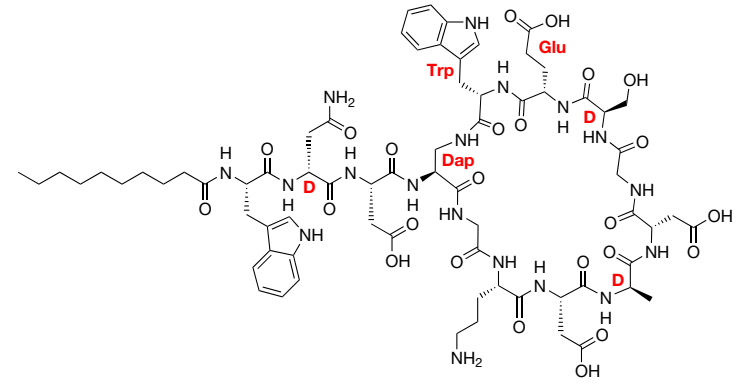

3

Figure 2: Design of daptomycin analogues **2** and **3**.

5.3.3 Synthesis of daptomycin analogues

A variety of synthetic approaches were considered and explored in developing the route towards the daptomycin analogue illustrated in Scheme 1. Initial attempts at performing the entire synthesis, including peptide cyclization, on the solid phase were unsuccessful leading us to explore the combined solid- and solution- phase approach indicated. To avoid any racemization in the later cyclization step, the peptide synthesis began at the glycine residue corresponding to position 5 in daptomycin. Employing an acid sensitive resin (2-chlorotrityl) and using standard SPPS techniques, the N-terminus of the peptide was first installed, including the C_{10} fatty acid tail. At this point, the diaminopropionic acid side chain was deprotected providing an attachment point for the kynurenine residue (position 13) after which the remainder of the peptide was assembled without incident. Of particular note was the need to incorporate a rare Fmoc-Kyn building block which was obtained via a recently described methodology for the gram-scale production of kynurenine in either L- or D- stereochemistry.[30] In addition, DMB-protected glycine was introduced at position 10 to avoid aspartamide formation with the neighboring Asp residue. Upon completion, the intermediate protected peptide was cleaved from the resin using mild acid conditions and dissolved in CH_2Cl_2 at high dilution (0.5 mM) followed by treatment with BOP/DIPEA leading to clean formation of the desired macrocycle (Scheme 1). Following deprotection and purification by RP-HPLC, daptomycin analogue **2** was obtained. Based upon the concise route developed for the preparation of daptomycin analogue **2**, a second analogue, compound **3**, was also prepared wherein L-kynurenine at position 13 was replaced by the structurally similar L-tryptophan. The synthesis of **3** proceeded without incident following the exact same route.

5.3.4 Evaluation of the biological activity and stability

Biological evaluation of the synthesized analogues was done in comparison with authentic daptomycin (Table 1). Using a standard broth dilution assay employing *S. aureus* (ATCC 29213) as an indicator strain, analogues **2** and **3** were both found to exhibit calcium-dependent antimicrobial activity albeit at a significantly reduced level relative to that of daptomycin. The approximate 100-fold decrease in activity was somewhat expected given the structural modifications introduced in analogues 2 and 3. Marahiel and coworkers reported similarly attenuated activities for daptomycin analogues obtained via their

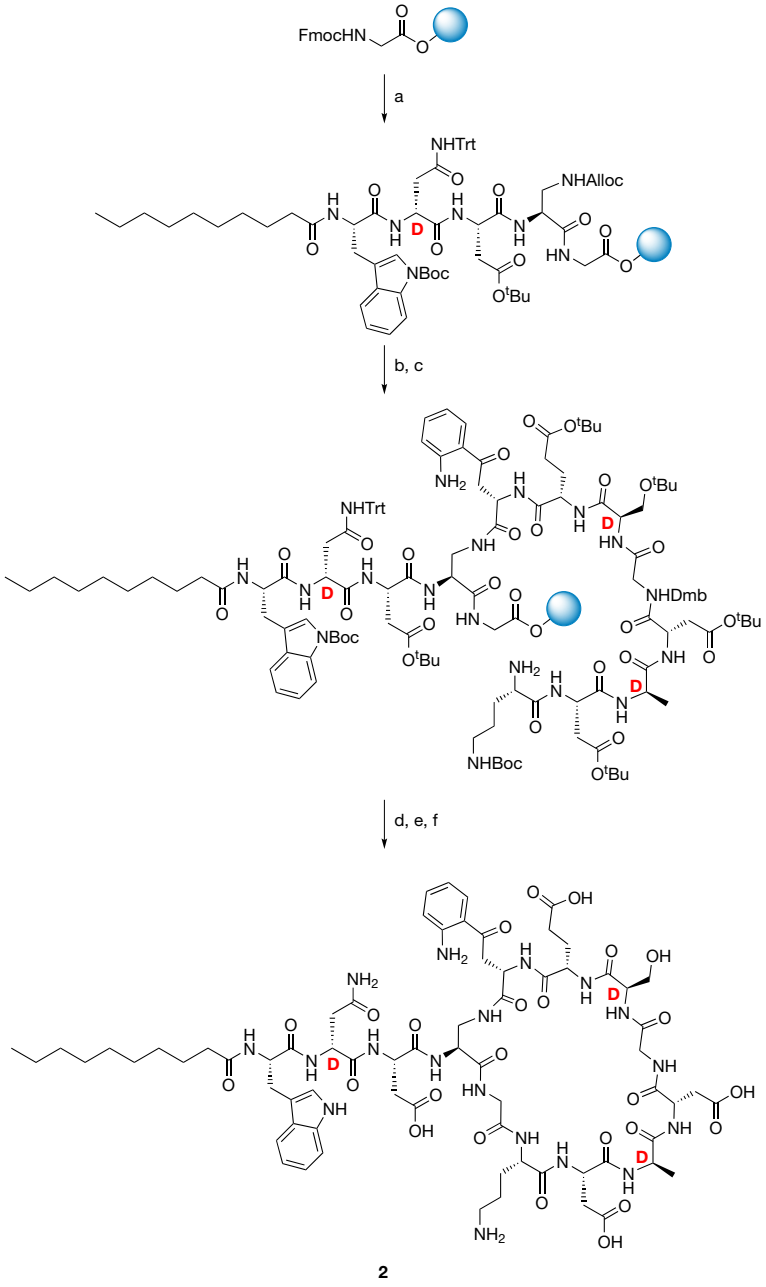

Scheme 1: Synthesis of analogue **2**.

chemo-enzymatic approach.[26] It is clear that replacement of the ester linkage in daptomycin with an amide dramatically alters antimicrobial activity. This effect may be due to conformational changes/restrictions in the macrocycle that result

from incorporation of the amide. The amide for ester substitution is also expected to impart greater hydrolytic stability. Thus, the serum stability of analogues **2** and **3** was also evaluated and compared with that of daptomycin. Each peptide was incubated with human plasma serum at 37 °C and sampled at specific time points. Under these conditions, daptomycin itself underwent significant degradation with an approximate 50% loss in the first 24 hours (Figure 3). This degradation is presumably due to hydrolytic opening of the macrocyclic lactone as evidenced by the appearance of a new M + H_2O species. By comparison, amide analogues **2** and **3** were much more stable under the same conditions with only minimal degradation detected over extended time periods of up to 48 hours.

Table 1: Antimicrobial activity of daptomycin analogues against *S. aureus* (ATCC 29213)

	MIC (μM)[a]	
Compound	$+Ca^{2+}$	$-Ca^{2+}$
1 (Daptomycin)	1.23	79.0
2	201.2	>400
3	100.8	>400
ent-2	>400	>400
ent-3	>400	>400

[a] Where indicated culture broth supplemented with Ca^{2+} (50 mg/L).

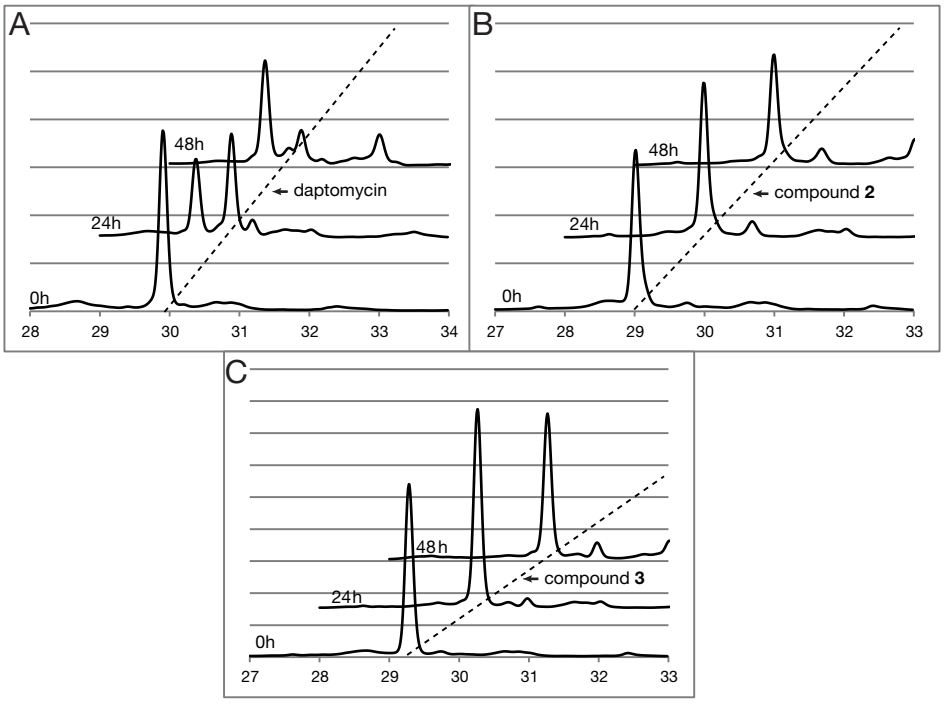

Figure 3: Degradation of A: daptomycin, B: compound **2** and C: compound **3** in serum.

5.4 Synthesis and evaluation of enantiomeric daptomycin analogues

The relative ease with which analogues **2** and **3** where assembled prompted us to also prepare the corresponding enantiomeric analogues **ent-2** and **ent-3**. The preparation of biologically active peptides in both enantiomeric forms is an established approach used in establishing the role of chiral biomolecular targets.[23–25,31] If, as some have proposed, daptomycin kills bacteria via membrane disruption without invoking a specific chiral bacterial target biomolecule, one would expect the "mirror-image" enantiomeric form of daptomycin to show an equal antibiotic activity. Conversely, should the enantiomeric form of daptomycin not show antibacterial activity, it can be taken as an indication that a chiral interaction with a specific biomolecular target is integral to daptomycin's mode of action. To this end the enantiomeric analogues **ent-2** and **ent-3** were assembled using the appropriate stereochemically inverted amino acid building blocks. As expected, the enantiomeric analogues were shown to have identical retention times by analytical RP-HPLC (Figure 4A) and exhibited optical rotations of equal magnitude but opposite sign (Table 2 section 5.6.5). In addition, the circular dichroism spectra obtained for the daptomycin analogues further supported their enantiomeric nature (Figure 4C). The antibacterial activities of **ent-2** and **ent-3** were next evaluated using the same assay as described above and revealed no detectable activity for both enantiomeric analogues (Table 1). These results indicate that a specific chiral interaction(s) is required for the activity of those analogues bearing the "native" daptomycin stereochemistry and may also support a similarly stereospecific mode of action for daptomycin itself. Plausible candidates for the requisite chiral target could include any number of membrane proteins or chiral phospholipids. In this regard, recent reports suggest that phosphatidylglycerol may play a role. Specifically, in daptomycin-resistant strains of enterococci and *S. aureus* levels of phosphatidylglycerol are significantly reduced.[17]

5.5 Conclusion

In summary, we have developed a convenient approach employing both solid- and solution phase techniques for the preparation of analogues of the calcium-dependent lipopeptide family of antibiotics. While the antibacterial activity of the synthetic analogues was significantly reduced relative to that of daptomycin,

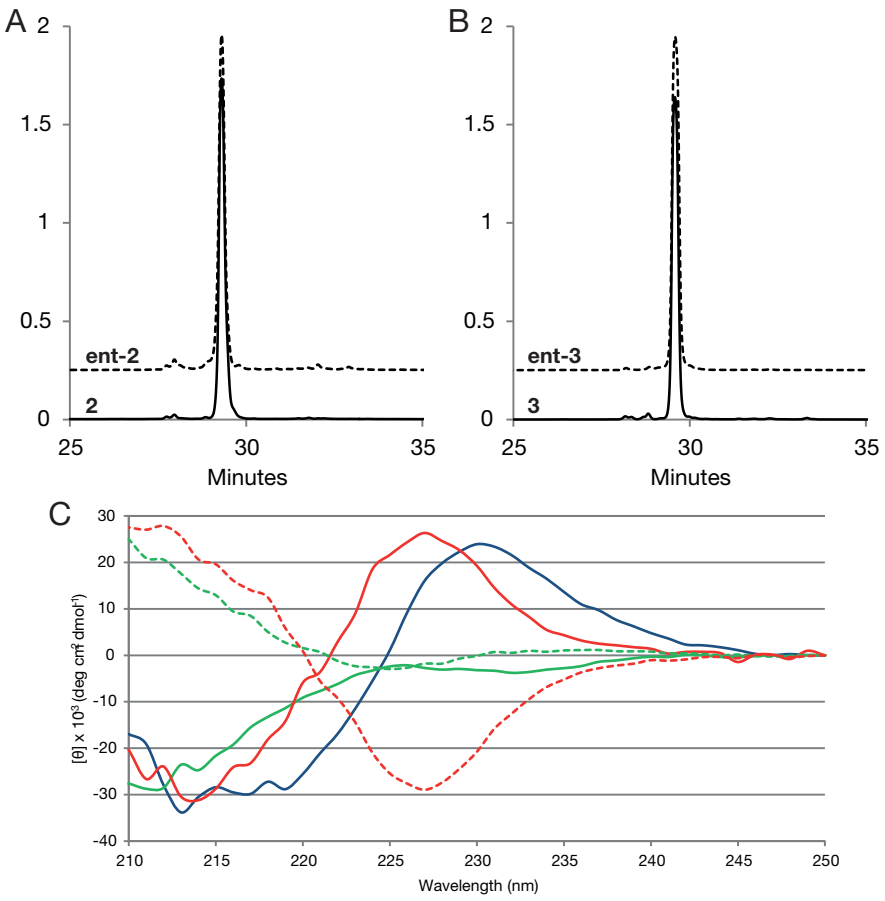

Figure 4: HPLC data of A) Compound **2** and **ent-2**, B) compound **3** and **ent-3**. C) CD spectra of daptomycin (blue), **2** (green), **ent-2** (dashed green), **3** (red) and **ent-3** (dashed red).

their hydrolytic stability was greatly increased. The synthetic route here described should also be readily amenable to the production of new lipopeptide analogues with enhanced properties. Future work will be aimed at evaluating the effect of incorporating different amino acids in an attempt to increase antibacterial activity while maintaining the hydrolytic stability of these analogues. Support for this approach is evidenced by the observation that a tryptophan-for-kynurenine substitution as in compound **3** results in a more active analogue. In addition, our findings with the enantiomeric analogues implicate the involvement of a specific chiral target biomolecule(s) in bacterial strains that are sensitive to daptomycin.

5.6 Experimental

5.6.1 Reagents and general methods

All reagents employed were of American Chemical Society (ACS) grade or finer and were used without further purification unless otherwise stated. Both L-and D-kynurenine were synthesized according to a previously described procedure[30] and converted into the requisite Fmoc-building blocks based on established protocols.[26] A large scale preparation of Fmoc-(Dmb)Gly-OH was also developed based on existing literature procedures.[32,33] All known compounds prepared had NMR spectra, mass spectra, and optical rotation values consistent with the assigned structures. Orthogonally protected Fmoc-L-Dap(Alloc)-OH and Fmoc-D-Dap(Alloc)-OH were obtained from Iris Biotech GmbH. All reagents employed were of American Chemical Society (ACS) grade or finer and were used without further purification unless otherwise stated. All reactions and fractions from column chromatography were monitored by thin layer chromatography (TLC) using plates with a UV fluorescent indicator (normal SiO_2, Merck 60 F254). One or more of the following methods were used for visualization: UV absorption by fluorescence quenching; iodine staining; phosphomolybdic acid : ceric sulfate : sulfuric acid : H_2O (10 g : 1.25 g : 12 mL : 238 mL) spray; and ninhydrin staining. Flash chromatography was performed using Merck type 60, 230–400 mesh silica gel.

5.6.2 Instrumentation for compound characterization

NMR spectra were recorded at 300 or 500 MHz with chemical shifts reported in parts per million (ppm) downfield relative to tetramethylsilane (TMS). ^{1}H NMR data are reported in the following order: multiplicity (s, singlet; d, doublet; t, triplet; q, quartet; qn, quintet and m, multiplet), number of protons and coupling constant (J) in hertz (Hz). When appropriate, the multiplicity is preceded by br, indicating that the signal was broad. ^{13}C NMR spectra were recorded at 75.5 MHz with chemical shifts reported relative to $CDCl_3$ δ 77.0. 2D NMR experiments (TOCSY and HSQC) were performed on a 500 MHz instrument. High-resolution mass spectrometry (HRMS) analysis was performed using an ESI instrument. Circular dichroism spectra were recorded on a Jasco J-810 CD-spectrometer using a 2 mm cuvet.

5.6.3 Synthesis of Fmoc,Dmb-Gly-OH

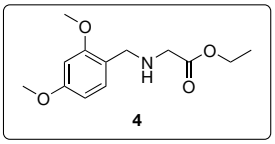

4

Synthesis of Ethyl 2-((2,4-dimethoxybenzyl)amino) acetate (4)

2,4-dimethoxybenzaldehyde (3.0 g, 18.0 mmol) was dissolved in dichloroethane (100 ml) and NEt_3 (7.5 ml, 54.0 mmol) was added, followed by glycine ethyl ester hydrochloride (3.77 g, 27.0 mmol). While stirring vigorously $NaB(OAc)_3H$ (7.66 g, 36.2 mmol) was added. After 17 h the reaction was quenched with saturated $NaHCO_3$ (100 ml) and the mixture was extracted with CH_2Cl_2 (3 x 40 ml). The combined organic layers were concentrated under vacuum and applied on a silica column (4:1 EtOAc/ CH_2Cl_2). The product was obtained as a white solid (4.57 g, quant.) with analytical data matching that previously reported for the same compound.[3] ^{1}H NMR (300 MHz, $CDCl_3$) δ 7.11 (d, J = 7.7 Hz, 1H), 6.44-6.40 (m, 2H), 4.215-4.11 (q, *J* = 7.2 Hz, 2H), 3.80 (s, 3H), 3.78 (s, 3H), 3.73 (s, 2H), 3.36 (s,2H), 1.30-1.22 (m, 3H).

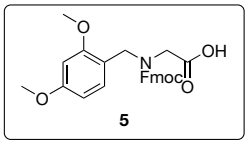

5

Synthesis of 2-((((9H-Fluoren-9-yl)methoxy)carbonyl) (2,4-dimethoxybenzyl)amino)acetic acid (5)

Ethyl 2-((2,4-dimethoxybenzyl)amino)acetate (4.57 g, 18.0 mmol) was dissolved in dioxane (20 ml) and 1M NaOH (20 ml) was added in 4 ml portions every 5 minutes. After one hour TLC indicated full hydrolysis of the ethyl ester. The mixture was then diluted with saturated $NaHCO_3$ (50 ml) followed by the dropwise addition of Fmoc-OSu (6.41 g, 19.0 mmol) as a solution in dioxane (25 ml) over 30 minutes. The reaction was stirred overnight after which dioxane was removed under vacuum and water was added to a total volume of 100 ml. Solid citric acid was then added to achieve neutral pH. The mixture was then extracted with EtOAc (3 x 100 ml) and the organic layer dried over Na_2SO_4 and concentrated under vacuum. The product was applied to a silica column initially eluting with CH_2Cl_2, moving up to CH_2Cl_2/methanol (9:1). Product containing fraction were combined and after solvent removal Fmoc-(Dmb)Gly-OH was obtained as a nanocrystalline foam (6.0 g, 74% over 2 steps) with analytical data matching that previously reported for the same compound.[4] ^{1}H NMR (300 MHz, $CDCl_3$) δ 9.95 (s, 1H), 7.78-7.72 (m, 2H), 7.60-7.54 (m, 2H), 7.43-7.20 (m, 4H), 6.82 (d, *J* = 8.3 Hz,1H), 6.45 (s, 1H), 6.37 (d, *J* = 8.3 Hz, 1H), 4.57-4.43 (m, 4H), 4.30-4.23 (m, 1H), 4.10 (s, 1H), 3.95 (s, 1H), 3.78 (s, 3H), 3.75 (s, 3H), ^{13}C NMR (75 MHz, $CDCl_3$) δ 175.6, 160.9, 158.8, 157.17, 156.4, 144.2, 141.6, 131.9, 130.9, 127.9, 127.4, 125.3, 120.2, 117.4, 104.5, 98.6, 68.1, 55.6, 48.6, 48.0, 47.5, 46.4.

5.6.4 Peptide synthesis

Lipopeptides were synthesized beginning with Fmoc-Gly loaded 2-chlorotrityl resin (410 mg, 0.25 mmol). Fmoc groups were removed with 20% piperidine in DMF (10 mL, 1x1 min., 1x30 min.). Coupling reactions were done in DMF (10 mL) with 4 equivalents of Fmoc-amino acid (or capric acid), 4 equivalents of BOP and 8 equivalents of DIPEA (1 hour). For removal of the Alloc protecting group, the resin was washed with CH_2Cl_2 (2x10 mL) under argon. $PhSiH_3$ (0.74 mL, 6.0 mmol) in CH_2Cl_2 (4 mL) and $Pd(PPh_3)_4$ (74 mg, 0.06 mmol) in CH_2Cl_2 (12 mL) were added under argon and swirled for 1 hour. The reaction mixture was drained and the procedure was repeated. The resin was washed with CH_2Cl_2 (5x10 mL), a 0.5% solution of diethyldithiocarbamic acid trihydrate sodium salt in DMF (5x10 mL) and DMF (5x10 mL). After Alloc removal, the remainder of the peptide was assembled on resin using standard SPPS approaches. The protected peptide was cleaved from the resin by addition of hexafluoroisopropanol (HFIP) in CH_2Cl_2 (1:4, 6 mL, 1 hour) and the filtrate collected. The resin was rinsed with additional HFIP/CH_2Cl_2 (2x3 mL) and the combined filtrates concentrated under vacuum. The crude linear peptide was dissolved in CH_2Cl_2 (500 ml, approximate peptide concentration of 0.5 mM) and BOP (0.22 g, 0.50 mmol) and DIPEA (0.17 mL, 1.0 mmol) were added. The cyclization reaction was monitored by TLC (5% MeOH in CH_2Cl_2) and was typically complete within 24 to 40 h. The reaction mixture was then concentrated, dissolved in EtOAc (250 mL) and washed (1M $KHSO_4$, 2x200 mL; saturated $NaHCO_3$, 2x200 mL). The organic layer was dried over Na_2SO_4, filtered and concentrated under vacuum. The protected cyclic peptide was then treated with a solution of TFA/TIS/CH_2Cl_2 (95:2.5:2.5, 10 ml) for 1.5 hours. The mixture was then added to cold ether and the precipitated peptide collected by centrifugation and further was washed with cold ether (2x). Crude peptides were purified by RP-HPLC using a Maisch ReproSil-Pur C18-AQ column (250 x 22 mm, 10µm) and employing a gradient of 30% to 70% Buffer B with a flow of 12 ml/min (Buffer A: 95% H_2O, 5% MeCN, 0.1% TFA; Buffer B: 5% H_2O, 95% MeCN, 0.1% TFA). Product containing fractions were pooled and lyophilized to yield between 5-10 mg of pure peptide (1.2-2.4% overall yield).

5.6.5 Analytical data of synthesized peptides

Table 2: Analytical data for daptomycin and compounds **2**, **ent-2**, **3** and **ent-3**.

Compound	Rt (min)	$[\alpha]_D$	Exact mass (calc.)	Exact mass (found)
Daptomycin (**1**)	30.2	N.D.	1620.7182 $[M+H]^+$	1620.7167 $[M+H]^+$
2	29.3	-7.98 (0.28, H_2O)	1591.7029 $[M+H]^+$	1591.6997 $[M+H]^+$
ent-2	29.3	+8.70 (0.28, H_2O)	1591.7029 $[M+H]^+$	1591.6995 $[M+H]^+$
3	29.6	-9.45 (0.65, H_2O)	1587.7080 $[M+H]^+$	1587.7069 $[M+H]^+$
ent-3	29.6	+9.24 (0.49, H_2O)	1587.7080 $[M+H]^+$	1587.7063 $[M+H]^+$

Table 3: Chemical shifts for compound **2**

Residue	$H^{\alpha}(C^{\alpha})$	H^{β} (C^{β})	Sidechain
Tail	---		CH_2 1.07-1.19 (28.5), CH_2 1.20 (31.0), CH_3 0.84 (13.7)
Trp-1	4.43 (53.8)	3.05/2.90 (26.9)	γ2 7.15 (123.4), δ4 7.56 (118.2), δ5 6.95 (117.9), δ6 7.03 (120.5), δ7 7.30 (111.0) H_N 10.77
Asn-2	4.59 (49.5)	2.69/2.53 (35.8)[a]	---
Asp-3	4.53 (49.5)[a]	2.69/2.53 (35.8)[a]	---
Dap-4	4.24-4.27 (51.9)[a]	NA	---
Gly-5	3.72/3.85 (42.0)	---	---
Orn-6	4.20 (52.3)	NA	γ 1.58 (22.9)
Asp-7	4.53 (49.5)[a]	2.69/2.53 (35.8)[a]	---
Ala-8	4.20 (48.2)	1.22 (17.2)	---
Asp-9	4.53 (49.5)[a]	2.69/2.53 (35.8)[a]	---
Gly-10	3.72/3.85 (42.0)	---	---
Ser-11	4.24-4.27 (51.9)[a]	3.60 (61.5)	---
Glu-12	4.45 (49.7)	NA	γ 2.26 (29.9)
Kyn-13	4.24-4.27 (51.9)[a]	3.05/2.90 (26.9)	γ3 6.74 (116.6), γ4 7.22 (133.9), γ5 6.53 (114.2) γ6 7.72 (131.0)

[a] Ambigous assignments due to overlap of the peaks, NA = not assigned

Table 4: Chemical shifts for compound **3**

Residue	**$H^{\alpha}(C^{\alpha})$**	**H^{β} (C^{β})**	**Sidechain**
Tail	---		CH_2 1.07-1.19 (28.5), CH_2 1.19 (31.0), CH_3 0.84 (13.7)
Trp-1	4.47 (53.8)	3.09/2.92 (26.9)	δ1 7.16 (123.4), ε3 7.58 (118.1), ζ3 6.96 (117.9), η2 7.04 (120.5), ζ2 7.31 (110.9) H_N 10.78
Asn-2	4.60 (49.4)	2.71/2.52 (35.9)[a]	---
Asp-3	4.53 (49.4)[a]	2.71/2.52 (35.9)[a]	---
Dap-4	4.16 (51.9)	3.64/3.03 (39.8)	---
Gly-5	3.87/3.67 (42.2)	---	---
Orn-6	4.33 (51.8)	2.75 (38.2)	γ 1.56 (23.1), δ 2.75 (38.3)
Asp-7	4.53 (49.4[a]	2.71/2.52 (35.9)[a]	---
Ala-8	4.22 (48.4)	1.18 (17.3)	---
Asp-9	4.53 (49.4)[a]	2.71/2.52 (35.9)[a]	---
Gly-10	3.87/3.67 (42.2)	---	---
Ser-11	4.40 (54.9)	3.60 (61.5)	---
Glu-12	4.35 (51.7)	1.90/1.71 (26.9)	γ 2.21 (29.7)
Trp-13	4.35 (54.0)	3.09/2.92 (26.9)	δ1 7.07 (123.4), ε3 7.47 (118.0), ζ3 6.96 (117.9), η2 7.04 (120.5), ζ2 7.31 (110.9) H_N 10.71

[a] Ambigous assignments due to overlap of the peaks

5.6.6 Antimicrobial activity assays

The daptomycin analogues were tested against *S. aureus* (ATCC 29213) as an indicator strain. Two-fold serial dilutions of each compound were made in microtiter plates using Mueller-Hinton broth. After incubation at 37°C for 16 h, MIC values were determined visually. In these assays calcium and magnesium free Mueller-Hinton broth (Fluka) was supplemented with $CaCl_2$ (final Ca^{2+} concentration 50 mg/L) and with $MgCl_2$ (final Mg^{2+} concentration 10 mg/L) or alternatively with $MgCl_2$ alone to assess the effect of calcium on antibacterial activity.

5.6.7 Serum stability assays

Daptomycin and analogues **2** and **3** were added to human plasma serum to a final concentration of 150 µg/ml, followed by incubation at 37°C. At 0, 24 and 48 hours a 100 µl aliquot was taken and 200 µl methanol (containing 0.075 mg/ml ethylparaben as an internal standard) was added to precipitate plasma proteins. The mixture was vortexed for 5 seconds and allowed to stand at room temperature for 15 minutes. After centrifugation at 13000 rpm for 5 minutes, the supernatant was removed and used for HPLC analysis. Analysis of the samples was performed by analytical RP-HPLC with an Maisch ReproSil-Pur 120 C18-AQ column (250 x 4.6 mm, 5µm) and a linear gradient of 0-100% buffer B over 48 minutes at a flow rate of 1ml/min (Buffer A: 95% H_2O, 5% MeCN, 0.1% TFA; Buffer B: 5% H_2O, 95% MeCN, 0.1% TFA). Both the internal standard and peptides were detected at 220 nm allowing for the amount of intact peptide to be calculated based upon the ratio of peak areas corresponding to the internal standard and the intact peptides.

5.6.8 Circular dichroism spectroscopy

A 60 µM solution of each peptide was prepared by dissolving them in a 20 mM HEPES buffer (pH 7.4). Samples were measured at room temperature from 210-250 nm at a scan rate of 20 nm min^{-1} and a bandwith of 0.1 nm. The spectra were converted to molar ellipticities in units of deg x cm^2 $dmol^{-1}$.

References

[1] T. Roemer, C. Boone, *Nat. Chem. Biol.* **2013**, *9*, 222–231.

[2] G. D. Wright, *Nat. Rev. Microbiol.* **2007**, *5*, 175–186.

[3] D. Patel, M. Husain, C. Vidaillac, M. E. Steed, M. J. Rybak, S. M. Seo, G. W. Kaatz, *Int. J. Antimicrob. Agents* **2011**, *38*, 442–446.

[4] H. S. Sader, R. N. Jones, *Diagn. Microbiol. Infect. Dis.* **2009**, *65*, 158–162.

[5] H. S. Sader, T. R. Fritsche, R. N. Jones, *Int. J. Infect. Dis.* **2009**, *13*, 291–295.

[6] R. H. Baltz, *Curr. Opin. Chem. Biol.* **2009**, *13*, 144–151.

[7] L. Robbel, M. A. Marahiel, *J. Biol. Chem.* **2010**, *285*, 27501–27508.

[8] D. Jung, J. P. Powers, S. K. Straus, R. E. W. Hancock, *Chem. Phys. Lipids* **2008**, *154*, 120–128.

[9] J. K. Hobbs, K. Miller, A. J. O'Neill, I. Chopra, *J. Antimicrob. Chemother.* **2008**, *62*, 1003–1008.

[10] J. A. Silverman, N. G. Perlmutter, H. M. Shapiro, *Antimicrob. Agents Chemother.* **2003**, *47*, 2538–2544.

[11] G. M. Eliopoulos, C. Thauvin, B. Gerson, R. C. Moellering, *Antimicrob. Agents Chemother.* **1985**, *27*, 357–362.

[12] R. H. Baltz, V. Miao, S. K. Wrigley, *Nat. Prod. Res.* **2005**, *22*, 717–741.

[13] S. K. Straus, R. E. W. Hancock, *Biochim. Biophys. Acta* **2006**, *1758*, 1215–1223.

[14] J. K. Muraih, A. Pearson, J. Silverman, M. Palmer, *Biochim. Biophys. Acta - Biomembr.* **2011**, *1808*, 1154–1160.

[15] J. Pogliano, N. Pogliano, J. A. Silverman, *J. Bacteriol.* **2012**, *194*, 4494–4504.

[16] N. N. Mishra, A. S. Bayer, T. T. Tran, Y. Shamoo, E. Mileykovskaya, W. Dowhan, Z. Guan, C. A. Arias, *PLoS One* **2012**, *7*, 1–10.

[17] N. N. Mishra, A. S. Bayer, *Antimicrob. Agents Chemother.* **2013**, *57*, 1082–5.

[18] Y. Song, A. Rubio, R. K. Jayaswal, J. A. Silverman, B. J. Wilkinson, *PLoS One* **2013**, *8*, DOI 10.1371/journal.pone.0058469.

[19] L. Friedman, J. D. Alder, J. A. Silverman, *Antimicrob. Agents Chemother.* **2006**, *50*, 2137–2145.

[20] T. T. Tran, D. Panesso, H. Gao, J. H. Roh, J. M. Munita, J. Reyes, L. Diaz, E. A. Lobos, Y. Shamoo, N. N. Mishra, et al., *Antimicrob.*

Agents Chemother. **2013**, *57*, 261–268.

[21] W. E. Rose, S. N. Leonard, G. Sakoulas, G. W. Kaatz, M. J. Zervos, A. Sheth, C. F. Carpenter, M. J. Rybak, *Antimicrob. Agents Chemother.* **2008**, *52*, 831–836.

[22] T. Schneider, K. Gries, M. Josten, I. Wiedemann, S. Pelzer, H. Labischinski, H.-G. Sahl, *Antimicrob. Agents Chemother.* **2009**, *53*, 1610–1618.

[23] D. Wade, A. Boman, B. Wåhlin, C. M. Drain, D. Andreu, H. G. Boman, R. B. Merrifield, *Proc. Natl. Acad. Sci. U. S. A.* **1990**, *87*, 4761–4765.

[24] L. Z. Yan, A. C. Gibbs, M. E. Stiles, D. S. Wishart, J. C. Vederas, *J. Med. Chem.* **2000**, *43*, 4579–4581.

[25] L. Sando, S. T. Henriques, F. Foley, S. M. Simonsen, N. L. Daly, K. N. Hall, K. R. Gustafson, M.-I. Aguilar, D. J. Craik, *ChemBioChem* **2011**, *12*, 2456–2462.

[26] J. Grünewald, S. A. Sieber, C. Mahlert, U. Linne, M. A. Marahiel, *J. Am. Chem. Soc.* **2004**, *126*, 17025–17031.

[27] *Antiinfective Lipopeptides*, **2007**, WO2006110185.

[28] H. Y. Lam, Y. Zhang, H. Liu, J. Xu, C. T. T. Wong, C. Xu, X. Li, *J. Am. Chem. Soc.* **2013**, *135*, 6272–6279.

[29] C. Milne, A. Powell, J. Jim, M. Al Nakeeb, C. P. Smith, J. Micklefield, *J. Am. Chem. Soc.* **2006**, *128*, 11250–11259.

[30] L. H. J. Kleijn, F. M. Müskens, S. F. Oppedijk, G. de Bruin, N. I. Martin, *Tetrahedron Lett.* **2012**, *53*, 6430–6432.

[31] F. Dettner, A. Hänchen, D. Schols, L. Toti, A. Nusser, R. D. Süssmuth, *Angew. Chem. Int. Ed.* **2009**, *48*, 1856–1861.

[32] J. S. Yadav, S. Dhara, S. S. Hossain, D. K. Mohapatra, *J. Org. Chem.* **2012**, *77*, 9628–9633.

[33] S. Zahariev, C. Guarnaccia, C. I. Pongor, L. Quaroni, M. Čemažar, S. Pongor, *Tetrahedron Lett.* **2006**, *47*, 4121–4124.

Chapter 6

Peptidic inhibitors of the protein arginine *N*-methyltransferases

Parts of this chapter have been published in: T.M. Lakowski*, P. 't Hart*, C.A. Ahern, N.I. Martin, A. Frankel, *ACS Chem. Biol.* **2010**, *5*, 1053–1063. P. 't Hart*, T.M. Lakowski*, D. Thomas, A. Frankel, N.I. Martin, *ChemBioChem* **2011**, *12*, 1427–1432 P. 't Hart*, D. Thomas*, R. van Ommeren, T.M. Lakowski, A. Frankel, N.I. Martin, *MedChemComm* **2012**, *3*, 1235–1244

6.1 Introduction

6.1.1 Arginine methylation by protein arginine N-methyltransferases

Protein arginine *N*-methyltransferases (PRMTs) are a family of conserved enzymes that catalyse the post-translational methylation of arginine residues within substrate proteins. PRMTs transfer methyl groups from the co-substrate *S*-adenosyl-L-methionine (AdoMet) to arginine residues within substrate proteins, forming the products *S*-adenosyl-L-homocysteine (AdoHcy) and *N*-methylated arginine residues (Figure 1). Two methyl groups can be transferred to each arginine residue, producing N^{η}-monomethyl-arginine (MMA) and asymmetric $N^{\eta 1},N^{\eta 1}$-dimethyl-arginine (aDMA) or symmetric $N^{\eta 1},N^{\eta 2}$-dimethyl-arginine (sDMA). (For the purpose of clarity the IUPAC convention of nomenclature for L-arginine and its derivatives is used.) PRMTs that produce aDMA or sDMA are called type I or type II enzymes, respectively.[1]

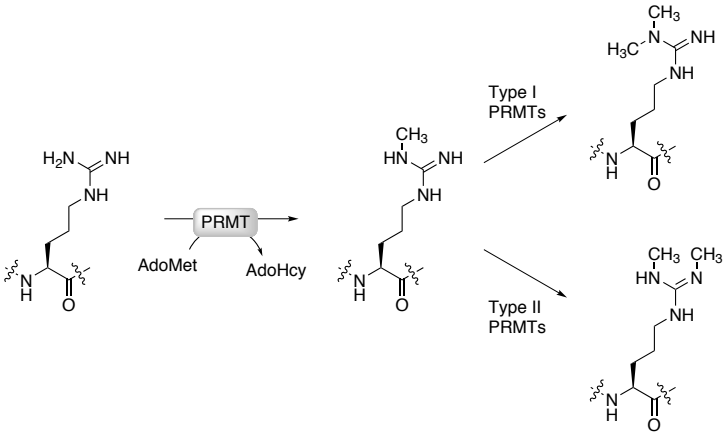

Figure 1: Methylation reaction as catalysed by the PRMTs.

6.1.2 Targets of PRMTs

PRMTs methylate RNA- and DNA-binding proteins such as small nuclear or heterogeneous nuclear ribonucleoproteins (snRNPs or hnRNPs) and histones. Through this activity, PRMTs influence RNA metabolism (*e.g.* transcription and splicing) and act as transcriptional corepressors or co-activators.[1] Along with lysine methylation, acetylation, and ubiquitination and serine phosphorylation, arginine methylation is an epigenetic histone modification that regulates gene expression as part of the histone code.[2] PRMTs appear to play roles in cancer

and viral replication[3–6] as well as cardiovascular disease.[7] In addition to the recent success of histone deacetylase inhibitors in treating cancer, the emerging role of PRMTs in disease suggests that these enzymes are viable targets for drug discovery.[8]

6.1.3 Mechanism of arginine methylation by PRMTs

PRMTs catalyze methylation(s) at the guanidino nitrogen N^{η} of specific arginine residues in target proteins. Mechanistically, PRMTs position the incoming nucleophilic N^{η} for attack at the AdoMet methyl group (Figure 2), leading to N^{η}-methylation and production of the byproduct AdoHcy.[9]

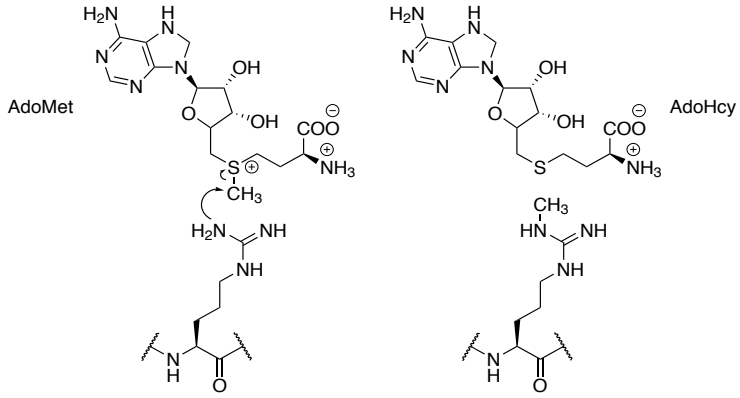

Figure 2: Mechanism of methylation by PRMTs.

6.1.4 Previously reported PRMT inhibitors

While transition state analogues are often pursued in the drug discovery process, the most potent PRMT inhibitors described to date tend to target the AdoMet binding site common to most methyltransferases and display little PRMT selectivity.[8] Recent screening efforts have, however, uncovered new classes of small molecules that display apparent selective inhibition of PRMTs while retaining potency (Figure 3).[10–12] The symmetric urea compound arginine methyltransferase inhibitor 1 (AMI-1) was the first PRMT inhibitor identified in this fashion.[10] By molecular docking AMI-1 was shown to span both the AdoMet and substrate arginine binding sites [13], whereas it did not inhibit UV crosslinking of AdoMet to PRMT1 (suggesting that it does not compete for the AdoMet binding site).[10] The related compound AMI-5 did reduce UV cross-linking and by molecular docking was found to bind exclusively to the AdoMet binding site.[10,13] The suramin-like sulfonated ureas, to which AMI-1 is related, bind to multiple proteins. To mitigate this issue, carboxy analogues of AMI-1 were designed that

are nearly as potent as the parent compound while retaining PRMT selectivity.[14] Identified in a virtual library screen, the thioglycolic amide RM65 has been shown to inhibit PRMT1 and cause histone hypomethylation in HepG2 cells.[12] Molecular docking suggests that this compound binds to the AdoMet binding site.

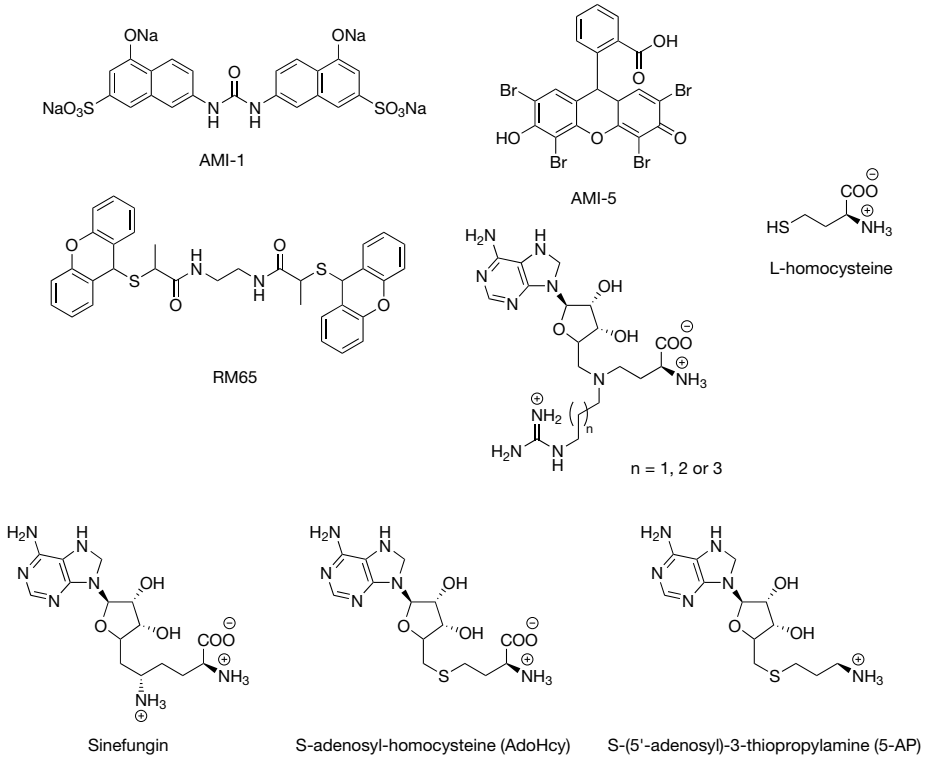

Figure 3: Previously reported PRMT inhibitors.

6

6.2 N$^{\eta}$-substituted arginyl peptide inhibitors of PRMTs

6.2.1 Design and synthesis of modified R1 peptides

6.2.1.1 Design of fluorinated R1 peptides

Rather than targeting the AdoMet binding site common to many methyltransferases, a more rational strategy for production of a PRMT-specific inhibitor is to target the substrate arginine-binding site. Potential inhibitors made this way could provide an intrinsic selectivity for PRMTs over other

methyltransferases. Using a recently developed methodology[15], a series of 12-mer peptides based on a consensus sequence for methylation in the PRMT substrate fibrillarin were prepared, each containing a single arginine residue substituted on the guanidino N^{η} with an ethyl group bearing an increasing number of fluorine atoms (Figure 4). These peptides are here designated **R1-1**, **-2**, **-3**, and **-4** and are based upon the previously described R1 series of substrate peptides (*i.e.*, R1, R1(MMA), R1(aDMA), and R1(sDMA)).[16]

R1: H–Trp–Gly-Gly-Tyr–Ser-Arg–Gly-Gly-Tyr–Gly-Gly-Trp–OH

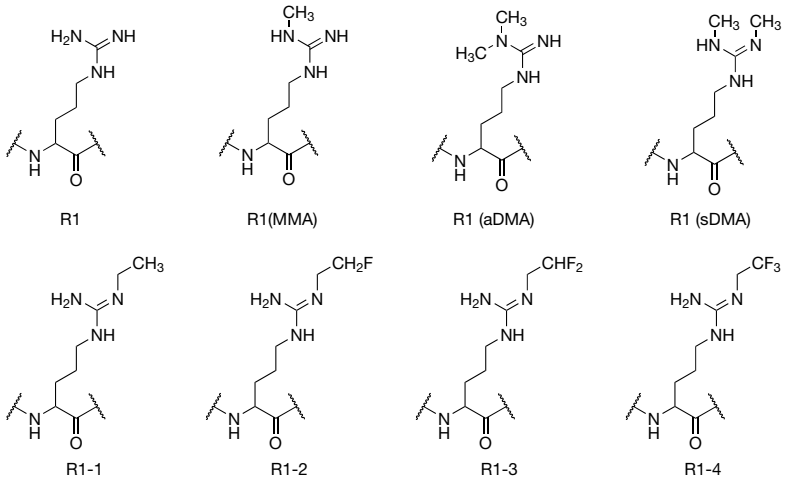

Figure 4: Structures of all used peptides.

6.2.1.2 Synthesis of required modified arginine building blocks

The required modified arginines, with suitable protection for SPPS, were prepared according to methodology developed in our lab and the synthesis is shown in Scheme 1. The synthesis starts from the commercially available Fmoc-L-Orn(Boc)-OH which is protected using allyl alcohol and DCC. The Boc group is removed by treatment with TFA and the free amine is reacted with Pbf-NCS. The obtained thiourea **1** can efficiently be converted to the substituted guanidines **2a**-**d** by treating it with the amine of interest after activation with EDC. After removal of the allyl group with $Pd(PPh_3)_4$ the obtained amino acids **3a**-**d** are ready to be incorporated into the peptide by standard SPPS protocols. The peptides were synthesized on the chlorotriyl chloride resin and purified using preparative HPLC.

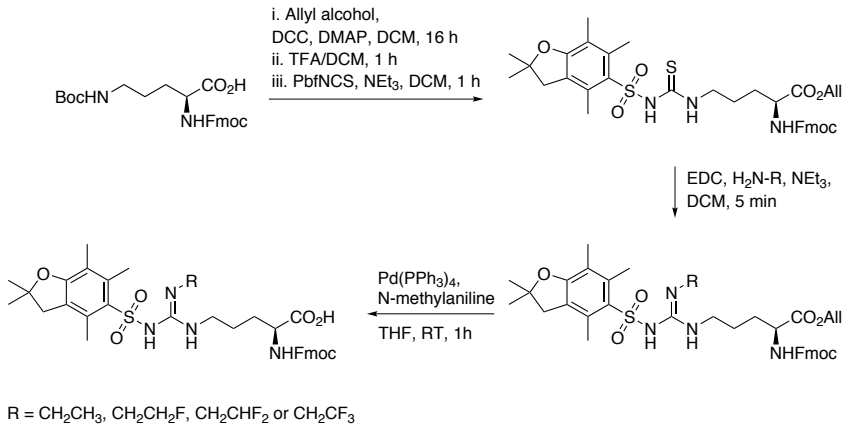

Scheme 1: Synthesis of the arginine building blocks for SPPS.

6.2.2 Biological evaluation of the modified R1 peptides

6.2.2.1 Methylation of N^{η}-Substituted Arginyl Peptides

The similarity of **R1-1**, **-2**, **-3**, and **-4** to R1 and R1(MMA) (Figure 4) suggested that they might be PRMT substrates as well as inhibitors. We tested the propensity of PRMT1, PRMT6, and PRMT4 to methylate **R1-1**, **-2**, **-3**, and **-4** by incubation with [methyl-^{14}C]AdoMet, followed by separation *via* tricine gel electrophoresis, and detection using storage phosphor screens (Figure 5A). In addition to the expected automethylation signal, we also observed a methylation signal only from the **R1-1** peptide when incubated with PRMT1 and not with PRMT4 (CARM1) or PRMT6. No other above-background methylation signals are observed for other combinations tested, including no-enzyme controls. These results indicate that the Et-Arg moiety fits into the active site of PRMT1 and is methylated. To confirm that methylation is enzyme-dependent, **R1-1** was incubated with [methyl-^{14}C]AdoMet along with increasing concentrations of PRMT1. Figure 5, panel B shows increasing methylation activity of **R1-1** with increasing PRMT concentrations.

The site of methylation was determined by incubating **R1-1** with and without PRMT1 in the presence of AdoMet or [methyl-^{14}C]AdoMet. The reactions were acid hydrolysed and analysed by UPLC-MS/MS. The results showed that **R1-1** is methylated on the same nitrogen as the ethyl-substituent. Methylation of other guanidino nitrogens was not detected. The same analysis was done for **R1-**

2, **-3** and **-4** but showed no methylation consistent with the storage phosphor screens. Furthermore, no methylation was observed with PRMT4 or PRMT6 for any of the peptides.

The rate of methylation was determined by measuring the accumulation of MMA and aDMA in hydrolysed reactions. The obtained data was fitted to the Michaelis-Menten-Henri equation and indicated that **R1-1** had a higher K_m value (263 ± 4.0 μM) compared to the parent R1 and R1(MMA) peptides (24.4 ± 2.6 and 24.8 ± 2.6 μM, respectively). The change in catalytic rate might indicate that the affinity of **R1-1** for PRMT 1 is different. However, it could also be that steric hindrance of the ethyl group influences the K_m and this might suggest that **R1-1** could be more accurately described as an inhibitor. The isosteric nature of the fluorine substituted ethyl groups on the other peptides suggest that they could well be able to bind as well and therefore be inhibitors as well.

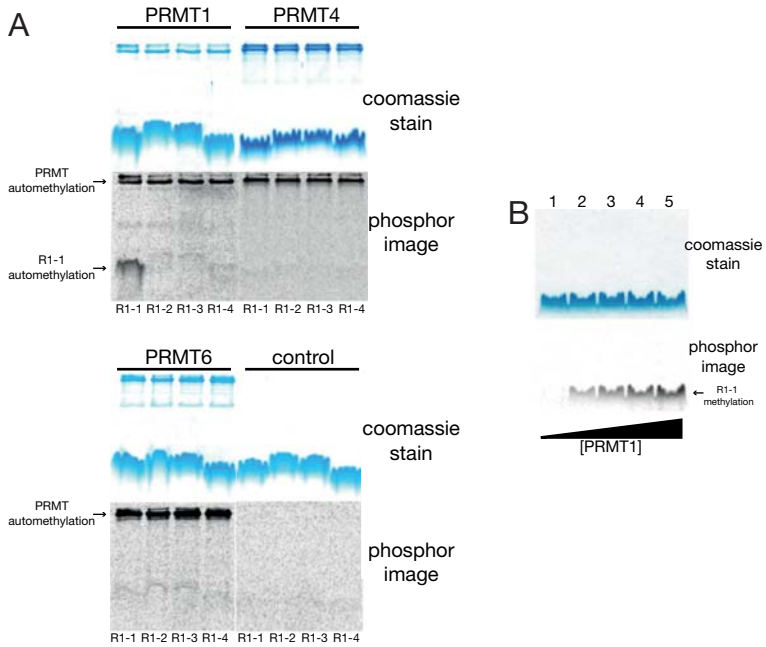

Figure 5: A: Coomassie stained gels and storage phosphorscreen of methylation reactions of PRTM1, PRMT4 (CARM1) and PRMT6 with **R1-1**, **-2**, **-3** and **-4**. B: Coomassie staind gel and storage phosphor screens of methylation of **R1-1** of with increasing concentrations of PRMT1.

6.2.2.2 Inhibition of PRMTs by the modified R1 peptides

To test the hypothesis that **R1-1**, **-2**, **-3**, and **-4** are PRMT inhibitors, their IC_{50} values were determined and compared to IC_{50} values for product inhibitors R1(aDMA) and R1(sDMA) (Figure 1) by measuring formation of the byproduct

AdoHcy. **R1-1**, **-2**, **-3**, and **-4** all appear to be inhibitors of PRMT1, and the resulting IC_{50} values are listed in Table 1. The proposed inhibitory mechanism of these peptides could be considered similar to the product inhibition that results from the formation of aDMA-containing products by PRMTs.[16] However, Figure 6, panel A and Table 1 show that **R1-1**, **-2**, **-3**, and **-4** are more potent inhibitors of PRMT1 than R1(aDMA) or R1(sDMA). The former peptides exhibit as much as a 5-fold greater inhibitory potency than R1(aDMA) and 24-fold greater inhibitory potency than R1(sDMA). Importantly, the assay to detect AdoHcy is used in this case because the addition of product inhibitors R1(aDMA) and R1(sDMA) would obscure *de novo* methylarginine formation in the reaction, rendering enzyme activity determination impossible using assays that detect N^{η}-methylarginines (MMA and aDMA). Although PRMT1 activity drops off precipitously, the maximal inhibition by **R1-2**, **-3**, and **-4** is 55-38% of enzyme activity. The remaining activity may be caused by PRMT automethylation, which could obscure the potency of candidate inhibitors. To remove the signal generated by automethylation in subsequent IC_{50} studies, the PRMT enzyme was removed by passage through centrifugal filters with molecular weight cut-offs sufficient to allow retention of the enzyme and complete passage of the substrate through the filter after the reaction was stopped. The filtrate, containing substrate and products free of enzyme, were hydrolyzed, and the activity was measured by detection of N^{η}-methylarginines using a mass-spectrometry based method. The results of these IC_{50} studies for PRMT1 are displayed in Figure 6, panel B and Table 1. Measuring N^{η}-methylarginine formation after removal of the automethylation products results in higher IC_{50} values. Although the maximal effect of inhibition improved for **R1-4** compared to the AdoHcy assay, (Figure 6, panels A and B), **R1-1**, **-2**,

Table 1: IC_{50} data for **R1-1** to **-4** versus PRMT1, 4, and 6

PRMT1			
Inhibitor	IC_{50} (μM)[a]	Inhibitor	IC_{50} (μM)[b]
R1-1	29.0 ± 25	**R1-1**	56.5 ± 22
R1-2	19.2 ± 6.1	**R1-2**	39.4 ± 7.8
R1-3	17.0 ± 4.5	**R1-3**	28.5 ± 10
R1-4	13.9 ± 1.8	**R1-4**	27.5 ± 1.2
R1(aDMA)	74.4 ± 10		
R1(sDMA)	350 ± 210		
PRMT4		PRMT6	
Inhibitor	IC_{50} (μM)[b]	Inhibitor	IC_{50} (μM)[b]
R1-1	179 ± 0.9	**R1-1**	4.82 ± 3.3
R1-2	260 ± 13	**R1-2**	14.2 ± 2.6
R1-3	254 ± 6.4	**R1-3**	13.9 ± 0.7
R1-4	168 ± 19	**R1-4**	9.43 ± 1.4

[a] AdoHcy production was measured, [b] MMA and aDMA production was measured

and **-3** still produced a maximal 40-50% reduction in enzyme activity. It is unclear why this may be the case, but it is interesting to note that the structure of PRMT1 has been shown to contain several accessory binding grooves distal to the active site[17], which may bind to peptide inhibitors and result in decreased inhibitory potency. However, we were unable to prepare reactions with very high inhibitor concentrations because of their low solubility beyond 500 μM.

The inhibition data for PRMT4 and PRMT6 by **R1-1**, **-2**, **-3**, and **-4** using the same assay to detect N^{η}-methylarginine formation are displayed in Figure 6, panels C and D, respectively, and the IC_{50} values are listed in Table 1. The IC_{50} values for these peptides against PRMT4 are 3- to 9-fold higher than the corresponding values for PRMT1 and 18- to 37-fold higher than for PRMT6. Significant inhibition of PRMT4 is not observed at concentrations below 250 μM, suggesting that relative to PRMT1 and PRMT6, **R1-1**, **-2**, **-3**, and **-4** are poor inhibitors of PRMT4. The IC_{50} values for these peptides against PRMT6 are 3- to 12-fold lower than for PRMT1, and concentrations from 250 to 500 μM result in as much as a 97% reduction in PRMT6 activity. Thus, **R1-1**, **-2**, **-3**, and **-4** are slightly more selective for PRMT6 than PRMT1. Structural studies have revealed the presence of acidic grooves for substrate binding on PRMT1[17], underscoring the importance of peptide sequence for targeting substrates or inhibitors to PRMT active sites. Accordingly, R1 and R1(MMA) are substrates for PRMT1 (Figure 4), PRMT6[16], and PRMT4 (data not shown). Therefore, the low inhibitory potency of **R1-1**, **-2**, **-3**, and **-4** for PRMT4 relative to PRMT1 and PRMT6 cannot be readily explained by the inability of the peptide portion of these inhibitors to bind to PRMT4. Moreover, the PRMT6 K_M values for R1 and R1(MMA) are 20- and 8-fold[16] higher than the corresponding K_M values for PRMT1, yet PRMT6 has lower IC_{50} values for **R1-1**, **-2**, **-3**, and **-4**. These results suggest that while important for targeting the N^{η}-substituted arginines to PRMT active sites, the peptide portion on its own is not predictive of inhibitory potency. For comparison, an IC_{50} study similar to that displayed in Figure 6B was performed with PRMT1 and the potent product inhibitor AdoHcy. The resulting IC_{50} of 6.94 ± 1.6 μM for AdoHcy is 4-fold more potent than the best PRMT1 inhibitors (**R1-3** and **R1-4**), but it is in the same range as **R1-1**, **-2**, **-3**, and **-4** against PRMT6.

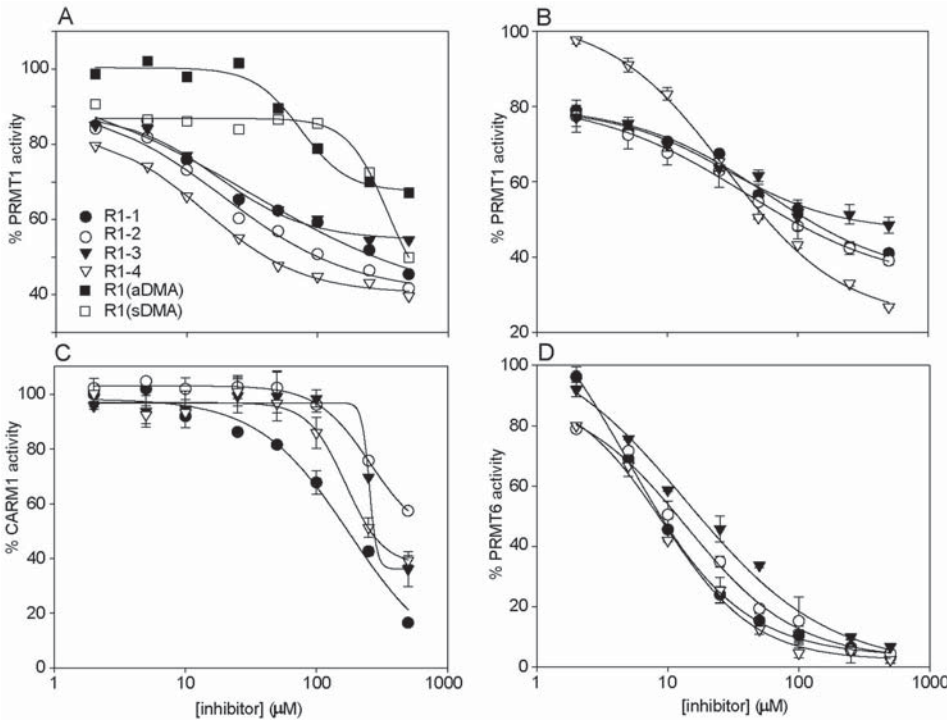

Figure 6: Inhibition of PRMT1, PRMT4, and PRMT6. A) The inhibition of PRMT1 by **R1-1** (●), **R1-2** (○), **R1-3** (▼), **R1-4** (▽), R1(aDMA) (■), and R1(sDMA) (□) as measured by the decrease in AdoHcy formation. The inhibition of PRMT1 B), PRMT4 C), or PRMT6 D) by **R1-1** (●), **R1-2** (○), **R1-3** (▼), and **R1-4** (▽) as measured by the decrease in methylarginine formation.

6.2.2.3 Fitting of N^{η}-substituted arginyl peptides into the PRMT1 active site

R1-1, **-2**, **-3**, and **-4** inhibit PRMT1 and PRMT6, and **R1-1** is a weak substrate for PRMT1. Given the nearly equivalent molecular volumes of Et-Arg and the product inhibitor aDMA (Figure 7B), it seems reasonable that both residues can fit into the active site of PRMT1. To examine the fit of substituted arginines within the active site of PRMT1, we used an existing crystal structure of PRMT1 with a peptide substrate and AdoHcy (occupying the AdoMet binding site).[17] Shown in Figure 7B is the enzyme-substrate complex in which an ethyl group has been added to the guanidino $N^{\eta 1}$ of the substrate arginine residue, chosen based upon the mechanism delineated in previous structural studies.[9] A methyl group is also added to the AdoHcy sulfur atom to mimic the structure of AdoMet. The structure shows that the PRMT1 active site can accommodate Et-Arg and suggests how a methyl group can be added to the ethylated $N^{\eta 1}$. In addition, when a structure of PRMT4 is superimposed onto the structure of PRMT1 described above (data not shown), there is a relatively good fit between the structures. However, no

obvious structural rationale can explain the poor inhibition of PRMT4 by **R1-1**, **-2**, **-3**, or **-4**.

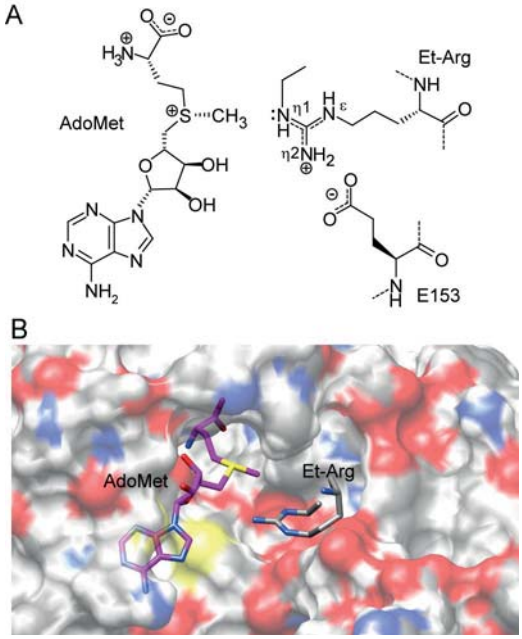

Figure 7: The proposed structure of Et-Arg in the active site of PRMT1. (A) Proposed schematic of the active site of PRMT1 showing the redistribution of the positive charge of the substrate Et-Arg guanidino group to the $N^{\eta 2}$, leaving the lone pair of electrons on $N^{\eta 1}$ free to attack the methyl group of AdoMet. (B) The active site transparent surface of PRMT1 with AdoHcy (*magenta*) and the target arginine residue (PDB 1OR8). An ethyl group is added to the arginine structure to mimic the potential binding of **R1-1**. A methyl group is added to the sulfur atom of AdoHcy to mimic the structure of AdoMet. The structure is rendered using Chimera.[18]

6.3 Design and synthesis of partial-bisubstrate peptide inhibitors

6.3.1 Design and synthesis of partial-bisubstrate peptide inhibitors

6.3.1.1 Designing partial-bisubstrate inhibitors

Mechanistically, the PRMTs facilitate substrate methylation by precisely orientating the electrophilic methylsulfonium group of AdoMet for an "S_N2-like" substitution reaction with the nucleophilic guanidino nitrogen of specific arginine side chain(s) contained within the bound substrate protein.[8,19,20] Structural evidence suggests that upon AdoMet binding, the PRMTs undergo a conformational change that provides access to a secondary binding groove for

the protein substrate.[8,21] With both substrates bound, a hydrophobic channel then provides a means through which the two partners interact and methyl group transfer can occur.[21] The bisubstrate mechanism employed by the PRMTs presents multiple options when considering design approaches towards new inhibitors. Most PRMT inhibitors described to date operate by interfering primarily with AdoMet binding. These compounds include natural products like sinefungin and AdoMet-derived AdoHcy along with its decarboxylation product *S*-(5′-adenosyl)-3-thiopropylamine (5-AP) (Figure 3).[8] While some of the compounds described above and in section 6.1.4 do exhibit selective inhibition among the PRMTs, it is unclear whether they do so by exploiting the peptide-binding groove unique to each PRMT. It stands to reason that inhibitors designed to mimic the specific peptide sequence(s) found in various PRMT substrate proteins may show enhanced selectivity among PRMTs. The modified R1 peptides described in section 6.2 already showed selectivity against the PRMTs tested. Building upon these results, we here describe the design, synthesis, and evaluation of new peptidic partial-bisubstrate analogues as PRMT inhibitors. In these hybrid compounds, a minimal AdoMet fragment is covalently tethered to the R1 peptide sequence at the guanidine moiety of the central arginine residue. This approach was taken with an aim to developing selective and tight-binding PRMT inhibitors capable of simultaneously binding to both substrate recognition sites.

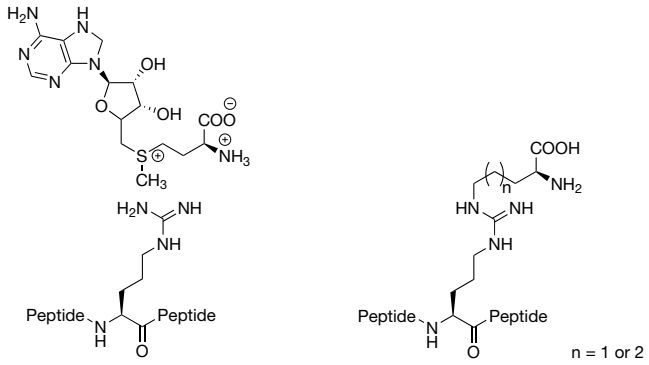

Figure 8: Design of partial-bisubstrate inhibitors. A) Position of AdoMet and arginine while bound to PRMT. B) partial bisubstrate

In considering possible AdoMet mimics to be covalently linked to the arginine guanidine group, the inclusion of a minimal amino acid motif presented the most direct way to access bisubstrate-like compounds (Figure 8A). The choice to use an amino acid fragment alone, without inclusion of the adenosine motif, was

based in part on previous reports describing L-homocysteine as a PRMT inhibitor (reported IC_{50} of 39.5 ± 11.1 μM).[22] Also, for reasons relating to synthetic ease, the inclusion of such an amino acid motif is desirable given the availability of suitably protected L-lysine and L-ornithine building blocks. Six bonds separate the guanidine moiety from the AdoMet carboxylate in the transition state model proposed for substrate methylation by PRMTs (Figure 8A). By this measure, partial-bisubstrate analogues incorporating an *N*-guanidino substituent derived from L-lysine or L-ornithine may accurately simulate this geometry (Figure 8B).

6.3.1.2 Synthesis of the partial-bisubstrate R1 peptides

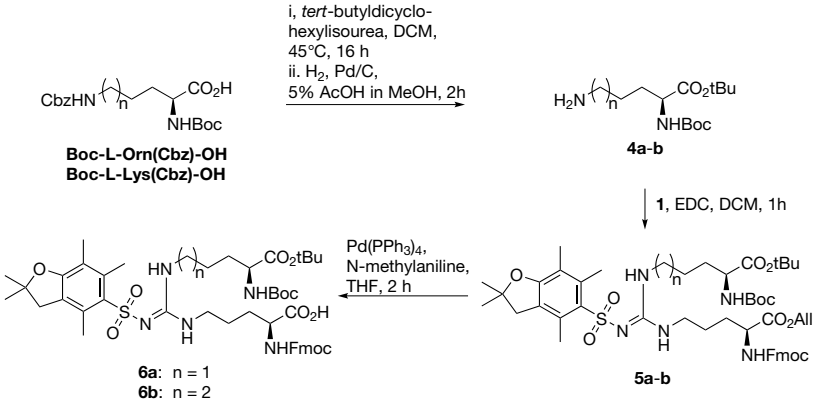

Scheme 2: Synthesis of the partial-bisubstrate building blocks **6a** and **6b**.

Assembly of the partial-bisubstrate inhibitors illustrated in Scheme 2 required initial preparation of two *N*-guanidino modified L-arginine building blocks suitable for use in SPPS. Boc-L-Orn(Cbz)-OH and Boc-L-Lys(Cbz)-OH were converted to their carboxylic acid protected species followed by removal of the side chain Cbz group. After activating thiourea precursor **1** described in section 6.2.1.2 with EDC it was reacted with the appropriately protected L-ornithine **4a** or L-lysine **4b** species to yield compounds **5a** and **5b**. Selective allyl ester deprotection then gave Fmoc amino acid building blocks **6a** and **6b**. Standard Fmoc SPPS conditions, with incorporation of building blocks **6a** and **6b**, provided the modified R1 peptide partial-bisubstrate inhibitors **R1-Orn** and **R1-Lys**, which were further purified to homogeneity.

6.3.2 Biological evaluation of the partial-bisubstrate R1 peptides

6.3.2.1 Inhibition of PRMTs by the partial-bisubstrate peptides

With partial-bisubstrate analogues **R1-Orn** and **R1-Lys** in hand, the inhibition

of PRMTs 1, 4, and 6 was investigated using a previously described LC/MS-MS method.[23,24] (Note: **R1-Orn** and **R1-Lys** were not methylated by the three PRMTs tested, data not shown.)

Figure 9 illustrates the results of the IC_{50} determination for PRMT1, 4 and 6 with **R1-Orn** and **R1-Lys** as well as with AdoMet-competitive compounds sinefungin, AdoHcy and 5-AP as reference inhibitors (Table 2).

Table 2: IC_{50} values for all **R1-Orn**, **R1-Lys** and controls

PRMT	Substrate	Inhibitor	IC_{50} (μM)
1	Histone H4 tail peptide	Sinefungin	3.70 ± 0.59
		AdoHcy	8.39 ± 0.40
		5-AP	4.42 ± 0.43
		R1-1	56.5 ± 22
		R1-Orn	>500
		R1-Lys	13.9 ± 1.1
4	Histone H3 tail peptide	Sinefungin	4.63 ± 0.53
		AdoHcy	1.31 ± 0.26
		5-AP	1.59 ± 0.17
		R1-1	179 ± 0.9
		R1-Orn	>500
		R1-Lys	35.7 ± 3.8
6	Histone H3 tail peptide	Sinefungin	4.35 ± 0.22
		AdoHcy	1.90 ± 0.08
		5-AP	>50
		R1-1	4.82 ± 3.3
		R1-Orn	36.7 ± 4.9
		R1-Lys	29.0 ± 7.2

As seen in Table 2, Sinefungin and AdoHcy are potent inhibitors of all PRMTs tested and generally more potent than the previously described **R1-1** peptide and the partial-bisubstrate inhibitors **R1-Orn** and **R1-Lys**. Although AdoHcy and 5-AP differ only by the presence of a carboxyl group, 5-AP displays some selectivity among PRMTs. AdoHcy and 5-AP are potent inhibitors of PRMTs 1 and 4, but only AdoHcy exhibited high potency against PRMT6 in contrast to 5-AP**.** This result implies that the carboxyl group present in AdoHcy is important for making an ionic interaction within the PRMT6 AdoMet binding site. Residues R54 and R168 in PRMTs 1 and 4, respectively, interact with this carboxyl group. By sequence alignment R66 in PRMT6 likely performs a similar function[25], yet the present data suggest that the carboxyl group on AdoHcy may be more important for PRMT6 binding than for other PRMTs and may be exploited to make PRMT6-selective inhibitors in future studies.

Also of note in Table 2 is the superior inhibition exhibited by peptide **R1-Lys,** bearing a lysine-derived substituent on the guanidine moiety, relative to peptide **R1-Orn** that contains the shorter ornithine-derived substituent. This observation

supports the binding mode envisioned for these partial-bisubstrate inhibitors considering the transition state model proposed for the PRMTs (Figure 8A). Six bonds separate the guanidine moiety of the substrate peptide and the carboxylate group of AdoMet. This bonding distance is best matched by peptide **R1-Lys** while **R1-Orn** is one bond short of being able to fully mimic this distance. In this light it is somewhat surprising that compound **R1-Orn** inhibits PRMT6 with a micromolar IC_{50} while only weak inhibition is seen against PRMTs 1 and 4. This may suggest that PRMT6 has a more promiscuous active site and is able to accommodate a variety of inhibitors. Alternatively, the importance of the interaction between R66 in PRMT6 and the carboxyl group may overcome the less favorable geometry of the shorter ornithine moiety in **R1-Orn**. It must also be noted that partial- bisubstrate inhibitors **R1-Orn** and **R1-Lys** showed a decrease in potency when compared to **R1-1** inhibition of PRMT6. However, **R1-Lys** displayed a 4-fold increase in potency relative to **R1-1** for PRMT1 and a 5-fold increase in potency relative to **R1-1** for PRMT4. These results suggest that N^{η} substitutions designed to mimic the bisubstrate transition state of PRMTs may improve binding in the active sites of PRMT 1 and 4 compared to a simple N^{η}-ethyl substituent.

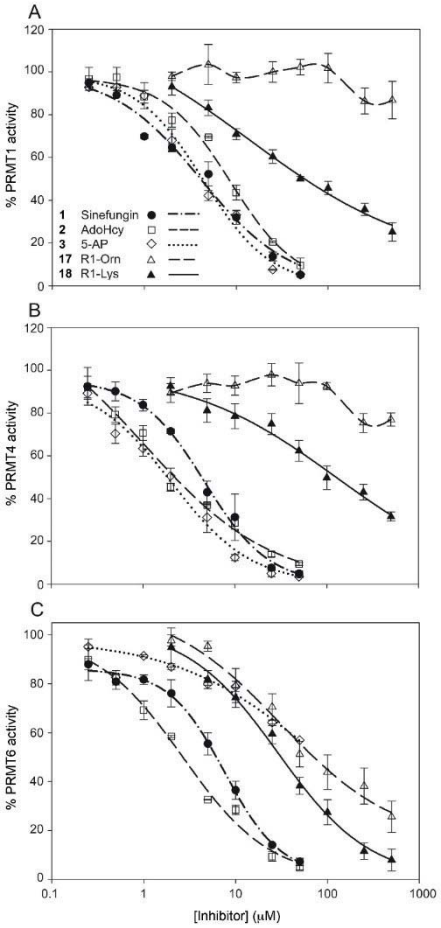

Figure 9: Inhibition curves for **R1-Orn** and **R1-Lys** and controls against PRMT1 (A), 4 (B) and 6 (C).

6.3.2.2 Photocrosslinking of radiolabeled AdoMet

The ability of **R1-Orn** and **R1-Lys** to directly interfere with AdoMet binding was next investigated using a photo-labeling assay. It is known that UV treatment of AdoMet-binding proteins in the presence of [^{14}C]AdoMet leads to incorporation of radioactivity. This photo-labeling assay can also be used

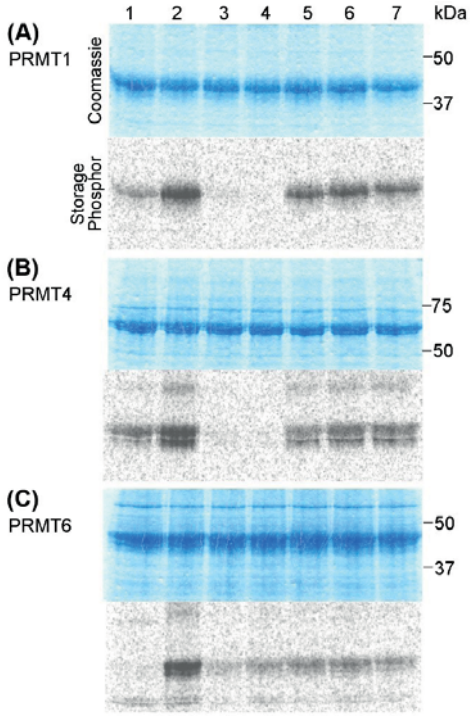

Figure 10: Photochemical cross-linking to probe inhibitor binding at the AdoMet site of PRMTs. **A)** PRMT1, **B)** PRMT4, and **C)** PRMT6 were incubated with [^{14}C]AdoMet (20 μM). As controls, enzyme samples were not (lane 1) or were (lane 2) exposed to UV in the absence of inhibitors. Inhibitor effects were assessed by performing UV exposure in the presence of 100 μM sinefungin (lane 3), 100 μM 5-AP (lane 4), 500 μM **R1-1** (lane 5), 500 μM **R1-Lys** (lane 6), or 500 μM **R1-Orn** (lane 7). In each group the Coomassie-stained gel is shown on the top panel and the scanned storage phosphor screen image is shown on the bottom panel.

to evaluate compounds that compete for the AdoMet binding pocket.[10] Using this approach, competition for AdoMet binding by PRMTs 1, 4, and 6 with **R1-Orn** and **R1-Lys** was characterized. As seen in Figure 10, sinefungin and 5-AP both effectively blocked AdoMet binding to PRMTs 1 and 4 (lanes 3 and 4 respectively). Similarly, AdoMet binding to PRMT6 was also inhibited by sinefungin, while compound 5-AP was less effective, an observation consistent with its poor inhibitory capacity for PRMT6 (Table 2). As an experimental control, enzymes and [^{14}C]AdoMet were incubated on ice without UV exposure (Figure 10, lane 1). Unexpectedly, both PRMTs 1 and 4 exhibited automethylation under these conditions, implying that some of the presumed cross-linking activity actually results from catalysis rather than photochemical cross-linking exclusively. This automethylation was therefore taken into account as background labeling. In this light, the inhibitor peptide **R1-1**, and partial-bisubstrate inhibitors **R1-Orn** and **R1-Lys** reduced the radioactive intensity approximately 3-fold by densitometry compared to corresponding samples without inhibitor for PRMTs 1, 4, and 6 (lane 2). We did not observe the PRMT selectivity for **R1-1**, **R1-Orn,** and **R1-Lys** reflected in enzyme inhibition studies due to the high peptide concentrations used in this experiment. Taken together, these data suggest that **R1-1**, **R1-Orn,** and **R1-Lys** can prevent [^{14}C]AdoMet cross-linking, albeit not to the level of AdoMet analogues sinefungin and 5-AP.

Given the results obtained for partial-bisubstrate inhibitors **R1-Orn** and **R1-Lys** in the AdoMet binding assay, we further investigated the inhibitory properties

of L-homocysteine. The amino acid moiety of L-homocysteine is the structural fragment common to compounds sinefungin and 5-AP and was incorporated as a minimal AdoMet mimic in **R1-Orn** and **R1-Lys**. Somewhat surprisingly, under the assay conditions employed, no inhibition of PRMTs 1, 4 or 6 was observed by L-homocysteine at concentrations ranging from 2 to 500 μM. In light of these findings, it is likely that a more representative AdoMet fragment, one able to occupy the nucleoside binding cleft within the active site, is required in order to achieve an optimal bisubstrate inhibitor.

6.4 N-modified arginine containing HIV-Tat peptides as PRMT inhibitors

6.4.1 Design and synthesis of modified HIV-Tat peptides as inhibitors of PRMT6

6.4.1.1 PRMT6 and its role in disease

In this section we describe the modification of the HIV-Tat peptide to produce inhibitors of PRMT6. PRMT6 is of particular interest as it is responsible for the majority of asymmetric *N*-methylation at arginine 2 in the histone H3 protein (H3R2). Recent evidence has shown that H3R2 methylation directly impacts other histone H3 modifications leading to the hypothesis that PRMT6 may serve as a master regulator of gene expression.[26–29] With respect to its role in cancer, it is now known that that PRMT6 is required for estrogen-stimulated proliferation of breast cancer cells.[29] In addition, a recent comprehensive study demonstrated that PRMT6 is significantly overexpressed in a number of human cancers.[6] Of particular note is the finding that knockdowns of PRMT6 by specific siRNAs led to suppressed growth of several cancer cells. Taken together, these observations point towards the possibility of targeting PRMT6 for inhibition as a means of developing of new anticancer therapies.

6.4.1.2 Design of modified HIV-Tat peptides

To generate peptidomimetic inhibitors capable of specifically targeting PRMT6 (relative to other PRMTs and lysine methyltransferases) we chose to modify a fragment of the HIV-Tat protein known to be a PRMT6-specific peptide substrate. Working together, the groups of Wainberg and Richard recently identified the HIV-1 transactivator protein (Tat) as a unique substrate for PRMT6.[30,31] In follow-up studies using smaller Tat-derived peptides, the same

authors further demonstrated that methylation occurs predominantly within the arginine rich motif (ARM) of Tat at R52 and to a lesser extent at R53. Single and double point mutations within the Tat-ARM sequence resulted in decreases in PRMT6-dependent HIV-1 repression, with R52K producing the largest impact.[31] Strikingly, a comparative analysis of the methylation of full-length Tat by PRMTs 1, 3, 4, 5, 6, and 7 revealed an exquisite specificity for methylation by PRMT6. This specificity, coupled with the Tat peptide's intrinsic cell penetrating ability,[32] suggests that the HIV-Tat peptide itself may serve as a template for the design of new cell permeable, PRMT6-selective peptidomimetic inhibitors. A range of modifications to the guanidine moiety of R52 was selected to include aromatic, aliphatic, electron withdrawing, cyclic and heteroatom substituents. In addition, peptides containing the native Tat sequence and an Arg52Ala analogue were also prepared.

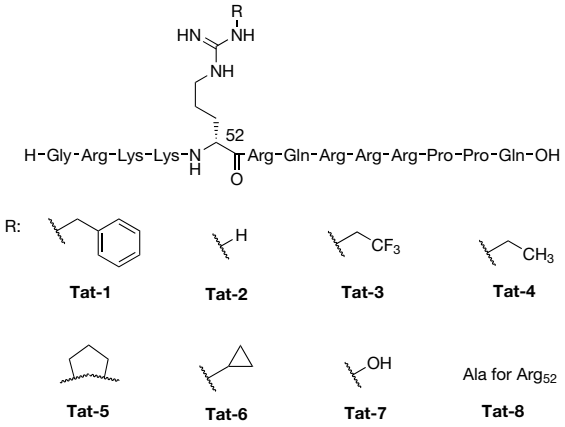

Figure 11: Design of the HIV-Tat peptide analogues bearing various susbtituents at Arg52.

6.4.1.3 Synthesis of modified HIV-Tat peptides

As for the other peptides described in section 6.2 and 6.3 the same strategy was used to prepare the modified arginine building blocks. Figure 11 shows the chosen substituents that were incorporated into the HIV-Tat peptide

6.4.2 Biological evaluation of the modified HIV-Tat peptides

6.4.2.1 Methylation of the modified HIV-Tat peptides

To initially determine if the modified Tat peptides were substrates for PRMT1, PRMT4 or PRMT6, these enzymes were used in radioactive methylation reactions with each peptide and ^{14}C-labeled AdoMet ([*methyl*-^{14}C]AdoMet) as a

source of methyl groups. The methylated peptides were separated using tricine gel electrophoresis and exposed to storage phosphor screens. The developed gels in Figure 12 demonstrate that all enzymes exhibit methylation above background for all peptides; however, PRMT1 and PRMT6 show much higher levels of methylation relative to PRMT4. These results were corroborated in reactions with unlabeled AdoMet analysed using mass spectrometry (MS) to measure enzymatically-produced aDMA and MMA. The no-enzyme control groups produced no quantifiable methylarginine species by MS (data not shown), consistent with gel-based results in Figure 12 (bottom gel). By MS we determined that PRMT1 and PRMT6 exhibited highest activity towards native Tat-peptide **2**, and analogues **4**, **7** and **8** in overnight methylation reactions, whereas PRMT4 was at least 10-fold less active than either PRMT1 or PRMT6. Generally, PRMT1 and PRMT6 produced more aDMA than MMA. In contrast, PRMT4 produced more MMA than aDMA for all peptides. The somewhat unexpected observation that the modified Tat peptides are robust substrates for PRMT1 and PRMT6 led us to examine if the *N*-modified R52 residues in analogues **1**, **3**, **4**, **5**, **6**, and **7** were methylated.

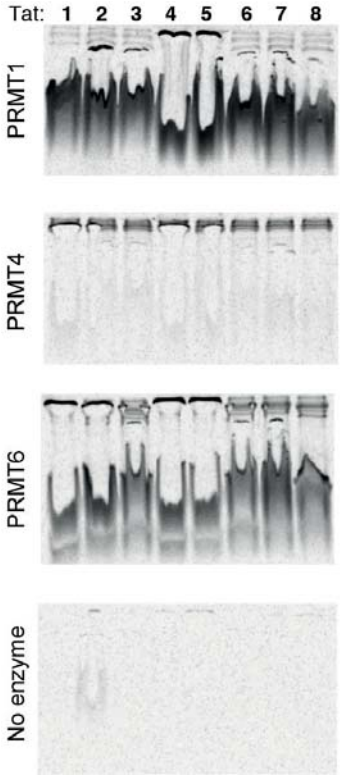

Figure 12: Methylation of modified Tat peptides. **Tat-1** to -**8** were methylated by PRMT1, PRMT4, and PRMT6 using [*methyl*-^{14}C] AdoMet and detected on a storage phosphor screen after separating peptides from proteins via 17% tricine gel electrophoresis. A no-enzyme control was included.

Using MS of hydrolysed methylation reactions of Tat peptides with and without PRMT1 or PRMT6, we could not detect any masses consistent with methylation of any of the substituted arginines. We could, however, detect the parent masses of the unmethylated, substituted arginines in all cases except for Tat-peptide analogues **6** and **7** (data not shown). These results are in contrast to our previous observation that PRMT1 can methylate an ethyl-substituted arginine residue within a peptide devoid of other arginine residues. The same substituted arginine residue in analogue **4** was not methylated by PRMTs in this study, suggesting that the presence of flanking, unmodified arginine residues presents more favourable targets for PRMTs.

6.4.3 Discussion

The observation that truncated Tat-ARM peptide analogues are readily methylated at arginine residues other than R52 by both PRMT1 and PRMT6 was somewhat unexpected considering the highly specific *N*-methylation of R52 by PRMT6.[31] These results suggest that in order to achieve PRMT6 selectivity, the full-length HIV-Tat peptide may be required. As can be seen in the solution structure of HIV-Tat (Figure 13),[34] the side chain of R52 is solvent exposed and likely resides in a unique steric and electronic environment, possibly contributing to PRMT6-selective methylation. By comparison, the arginine residue corresponding to R52 in the linear 13-mer Tat-ARM analogues used in the present study are not likely to possess the same unique properties relative to the other arginines present. To address this issue, one approach that may be of value in future investigations could involve examining the use of cyclized peptidomimetics of the Tat-ARM. Cyclization of the Tat-ARM is expected to restrict its conformation and may place the

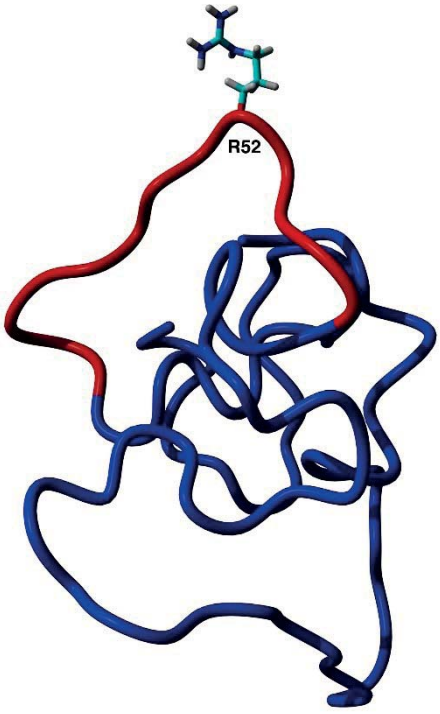

Figure 13: NMR solution structure of HIV-Tat.[34] Coloured in red is the Tat-ARM sequence used as a design template for the analogues prepared in the present study. As illustrated, the side chain of R52 is solvent exposed and may govern the specificity of *N*-methylation by PRMT6.

R52 residue in an environment that more accurately mimics that found in full-length Tat. Such cyclic Tat-ARM analogues have been previously described in the literature and are known to maintain the functional characteristics and cell permeability of full length HIV-Tat.[35] It may therefore be of value to evaluate the methylation behaviour of the various PRMTs towards cyclized mimetics of the Tat-ARM.

6.5 Conclusion

The fluorinated peptides described in section 6.2 were synthesized and analyzed as substrates and inhibitors of PRMT1, 4 and 6. The IC_{50} values derived under different conditions using different assays are not comparable.[36] However, the similarity between the IC_{50} values for R1-1, -2, -3, and -4 and the potent product inhibitor AdoHcy suggest that the substituted peptides are relatively potent against PRMT6 and to a lesser extent PRMT1. The recent development of irreversible chloroacetamidine inhibitors are additional illustrations of how peptides represent an excellent starting point for exploring PRMT-selective inhibition.[37] In the present study a 12-mer peptide scaffold is employed as a vehicle for the N^{η}-substituted arginine residue.

In section 6.3 the R1 peptide was further modified and investigated as partial-bisubstrate analogues to generate novel peptide-based PRMT inhibitors. In the analogue design employed, the R1 peptide, was modified to contain a minimal AdoMet fragment. Compound **R1-Lys**, bearing a six-carbon atom amino acid substituent, exhibits good inhibition of PRMT 1, 4 and 6. By comparison, analogue **R1-Orn** contains a shorter (five-carbon atom) amino acid substituent and only inhibits PRMT6. These results suggest that analogue **R1-Lys** may better mimic the transition state model proposed for the PRMT bisubstrate mechanism. Additionally, given the results of the AdoMet photo-labeling assay, it appears likely that the use of a more representative AdoMet-mimicking moiety will yield PRMT bisubstrate inhibitors with enhanced potency.

In section 6.4 we describe an approach inspired by published reports describing HIV-Tat as a selective substrate for PRMT6.[30,31] To this end we designed and synthesised a number of truncated Tat peptide analogues bearing *N*-substitutions at R52, the arginine residue known to be methylated. These analogues were generated with the aim of developing PRMT6-selective peptide inhibitors. The results obtained are intriguing as each of the peptides was found to be readily methylated by both PRMT1 and PRMT6 at other arginine residues

present in the peptide.

Future work may be aimed at minimizing or mimicking the peptidic motifs given the poor drug-like properties of peptides when compared to small molecules. The success of histone deacetylase inhibitors in the treatment of cancer suggests that targeting the epigenetic regulation of gene expression is a strategy for the treatment of cancer.[8,38] Arginine methylation is one of many forms of this regulation that has not been investigated thoroughly for its pharmaceutical potential. The evidence presented in our studies suggests that N^{η}-substituted arginyl peptides are promising leads to be further developed into future classes of PRMT-selective inhibitors.

6.6 Experimental

6.6.1 Synthesis of building blocks and peptides with fluorinated arginines

6.6.1.1 Synthesis of compounds 2a-d and 3a-d

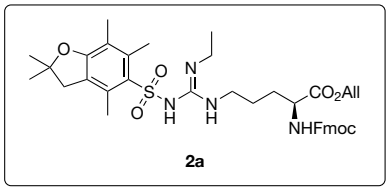

2a

Synthesis of: L-allyl 2-(((9*H*-fluoren-9-yl)methoxy)carbonylamino)-5-(3-ethyl-2-(2,2,4,6,7-pentamethyl-2,3-dihydrobenzofuran-5-ylsulfonyl)guanidino) pentanoate (2a)

The thiourea precursor[1] (1.35 g, 1.91 mmol) was dissolved in CH_2Cl_2 (25 mL) and treated with EDCI (733 mg, 3.82 mmol) followed by ethylamine HCl (310 mg, 3.8 mmol) and NEt_3 (530 µL, 3.8 mmol). After 5 minutes TLC showed full conversion and the mixture was concentrated under vacuum. The crude material was applied to a silica column eluting with a gradient of 1:1 to 2:1 EtOAc/hexane. After solvent removal compound **2a** was obtained as a white nanocrystalline foam (1.29 g, 94%). Compounds **2b**-**d** were prepared in analogous fashion. ^{1}H NMR (300 MHz, $CDCl_3$) δ 7.77-7.74 (m, 2H), 7.59-7.56 (m, 2H), 7.42-7.36 (m, 2H), 7.32-7.27 (m, 2H), 5.95-5.82 (m, 1H), 5.55 (br d, *J* = 8.0 Hz, 1H), 5.35-5.24 (m, 2H), 4.63 (br d, *J* = 5.8 Hz, 2H), 4.44-4.33 (m, 3H), 4.20 (t, *J* = 7.2 Hz, 1H), 3.58-3.16 (m, 3H), 2.93 (s, 2H), 2.61 (s, 3H), 2.53 (s, 3H), 2.09 (s, 3H), 1.90-1.53 (m, 4H), 1.44 (s, 6H), 1.12 (t, *J* = 7.2Hz, 3H); ^{13}C NMR (75 MHz, $CDCl_3$) δ 172.0, 158.7, 156.5, 154.9, 144.0, 143.8, 141.5, 138.5, 133.8, 132.4, 131.6, 128.0, 127.3, 125.3, 124.7, 120.3, 119.5, 117.6, 86.5, 67.4, 66.5, 53.4, 47.3, 43.5, 41.0, 36.6, 30.5, 28.8, 25.4, 19.5, 18.2, 14.8, 12.7; HRMS (MALDI) Calcd for $C_{39}H_{48}N_4O_7S$ $[M+H]^+$, 717.3322, found 717.3324.

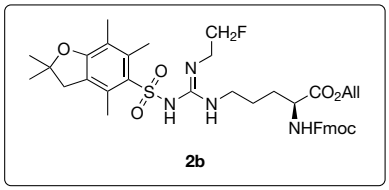

2b

Synthesis of: L-allyl 2-(((9*H*-fluoren-9-yl)methoxy)carbonylamino)-5-(3-(2-fluoroethyl)-2-(2,2,4,6,7-pentamethyl-2,3-dihydrobenzofuran-5-ylsulfonyl)guanidino) pentanoate (2b)

Yield 88%; ^{1}H NMR (300 MHz, $CDCl_3$) δ 7.77-7.75 (m, 2H), 7.59-7.57 (m, 2H), 7.42-7.37 (m, 2H), 7.33-7.26 (m, 2H), 5.96-5.83 (m, 1H), 5.54 (br d, *J* = 8.0 Hz, 1H), 5.36-5.25 (m, 2H), 4.64 (br d, *J* = 5.5 Hz, 2H), 4.52 (t, *J* = 4.7 Hz, 1H), 4.41-4.35 (m, 4H), 4.20 (t, *J* = 6.6 Hz, 1H), 3.57-3.40 (m, 2H), 3.36-3.06 (m, 2H), 2.94 (s, 2H), 2.59 (s, 3H), 2.52 (s, 3H), 2.09 (s, 3H), 1.96-1.54 (m, 4H), 1.45 (s, 6H); ^{13}C NMR (75 MHz, $CDCl_3$) δ 171.9, 158.8, 156.6, 155.0, 144.0, 143.8, 141.5, 138.5, 133.6, 132.4, 131.5, 128.0, 127.3, 125.2, 124.8, 120.3, 119.6, 117.7, 86.6, 83.0 (d, J_{CF} = 166.9 Hz), 67.4, 66.6, 53.2, 47.3, 43.4, 42.3 (d, J_{CF} = 20.1 Hz), 41.1, 30.7, 28.8, 25.2, 19.5, 18.2, 12.7; HRMS (MALDI) Calcd for $C_{39}H_{47}FN_4O_7S$ $[M+H]^+$, 735.3228, found 735.3225.

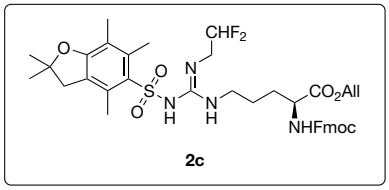

2c

Synthesis of: L-allyl 2-(((9*H*-fluoren-9-yl) methoxy)carbonylamino)-5-(3-(2,2-difluoroethyl)-2-(2,2,4,6,7-pentamethyl-2,3-dihydrobenzofuran-5-ylsulfonyl)guanidino) pentanoate (2c)

Yield 87%; ^{1}H NMR (300 MHz, $CDCl_3$) δ 7.77-7.75 (m, 2H), 7.58-7.56 (m, 2H), 7.42-7.36 (m, 2H), 7.33-7.27 (m, 2H), 5.94-5.85 (m, 1H), 5.83 (tt, J_{HH} = 4.4 Hz, J_{HF} = 56.4 Hz, 1H), 5.60 (br d, *J*=8.3 Hz, 1H), 5.36-5.26 (m, 2H), 4.65 (br d, *J*= 5.8 Hz, 2H), 4.40 (br d, *J* = 6.9 Hz, 2H), 4.36-4.34 (m, 1H), 4.20 (t, *J* = 6.9 Hz, 1H), 3.58-3.46 (m, 2H), 3.41-3.03 (m, 2H), 2.94 (s, 2H), 2.58 (s, 3H), 2.51 (s, 3H), 2.09 (s, 3H), 1.96-1.54 (m, 4H), 1.45 (s, 6H); ^{13}C NMR (75 MHz, $CDCl_3$) δ 171.8, 159.0, 156.9, 154.8, 143.8, 141.5, 138.5, 133.3, 132.4, 131.4, 128.1, 127.4, 125.2, 124.9, 120.3, 119.7, 117.8, 114.0 (t, J_{CF} = 241.7), 86.7, 67.5, 66.6, 52.9, 47.3, 43.9 (t, J_{CF} = 28.0 Hz), 43.4, 41.2, 30.9, 28.8, 25.3, 19.5, 18.1, 12.7; HRMS (MALDI) Calcd for $C_{39}H_{46}F_2N_4O_7S$ $[M+Na]^+$, 775.2953, found 775.2946.

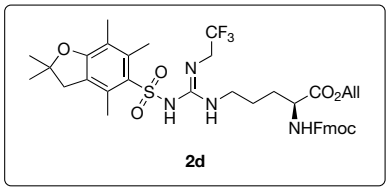

2d

Synthesis of: L-allyl 2-(((9*H*-fluoren-9-yl) methoxy)carbonyl-amino)-5-(2-(2,2,4,6,7-pentamethyl-2,3-dihydro-benzofuran-5-ylsulfonyl)-3-(2,2,2-trifluoroethyl)guanidino) pentanoate (2d)

Yield 89%; ^{1}H NMR (300 MHz, $CDCl_3$) δ 7.76-

7.74 (m, 2H), 7.57-7.55 (m, 2H), 7.41-7.39 (m, 2H), 7.32-7.29 (m, 2H), 5.95-5.82 (m, 1H), 5.67 (br d, 1H, *J* = 8.0 Hz), 5.40-5.21 (m, 2H), 4.63 (d, 2H, *J* = 5.5 Hz), 4.49-4.28 (m, 3H), 4.19 (t, 1H, *J* = 6.9 Hz), 4.06-3.67 (m, 2H), 3.45-3.06 (br m, 2H), 2.93 (s, 2H), 2.57 (s, 3H), 2.50 (s, 3H), 2.08 (s, 3H), 2.00-1.54 (m, 4H), 1.44 (s, 6H); ^{13}C NMR (75 MHz, $CDCl_3$) δ 171.9, 159.0, 156.9, 154.7, 143.9, 143.7, 141.5, 138.7, 133.0, 132.5, 131.5, 128.1, 127.4, 125.2, 124.8, 124.2 (q, J_{CF} = 279.2 Hz), 120.3, 119.6, 117.7, 86.7, 67.5, 66.6, 53.1, 47.3, 43.4, 42.5 (q, J_{CF} = 35.4 Hz), 41.2, 30.8, 28.8, 25.3, 19.4, 18.0, 12.6; HRMS (MALDI) Calcd for $C_{39}H_{46}F_3N_4O_7S$ $[M+H]^+$, 771.3039, found 771.3042.

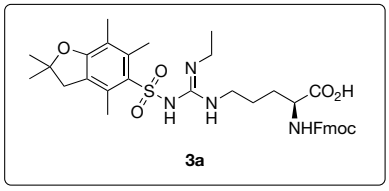

3a

Synthesis of: L-2-(((9*H*-fluoren-9-yl) methoxy)carbonylamino)-5-(3-ethyl-2-(2,2,4,6,7-pentamethyl-2,3-dihydrobenzofuran-5-ylsulfonyl)guanidino) pentanoic acid (3a)

Allyl ester **2a** (717 mg, 1 mmol) was dissolved in THF (25mL) and *N*-methylaniline (325 µL, 3mmol) was added, followed by $Pd(PPh_3)_4$ (5 mol%, 0.05mmol, 58 mg). The mixture was protected from light and stirred under N_2 (g) at room temperature for 1 hour. EtOAc (200ml) was added and washed with saturated NH_4Cl (100ml). The NH_4Cl layer was extracted with EtOAc (2 x 100 ml). After drying of the combined EtOAc layers over Na_2SO_4 the mixture was concentrated and applied to a silica column eluting with CH_2Cl_2/MeOH (50:1) followed by CH_2Cl_2/MeOH/AcOH (25:1:0.1). After solvent removal the product was obtained as a white nanocrystalline foam. (470 mg, 69%). Compounds **3b-d** were prepared in analogous fashion from allyl esters **4b-d**. ^{1}H NMR (300 MHz, $CDCl_3$) δ 8.70 (s, 1H), 7.72-7.70 (m, 2H), 7.58-7.53 (m, 2H), 7.37-7.32 (m, 2H), 7.27-7.22 (m, 2H), 6.05 (br d, 1H), 4.49-4.26 (m, 3H), 4.15 (t, *J* = 6.9 Hz, 1H), 3.28-3.04 (m, 4H), 2.90 (s, 2H), 2.59 (s, 3H), 2.51 (s, 3H), 2.07 (s, 3H), 1.98-1.52 (m, 4H), 1.42 (s, 6H), 1.06 (t, *J* = 7.2 Hz, 3H); ^{13}C NMR (75 MHz, $CDCl_3$) δ 175.1, 158.9, 156.7, 155.1, 144.0, 143.8, 141.5, 138.5, 133.3, 132.4, 128.0, 127.3, 125.4, 124.8, 120.2, 117.7, 86.6, 67.5, 53.5, 47.3, 43.4, 41.2, 36.7, 29.8, 28.8, 25.3, 19.5, 18.2, 14.7, 12.7; HRMS (MALDI) Calcd for $C_{36}H_{44}N_4O_7S$ $[M+Na]^+$, 699.2828, found 699.2846.

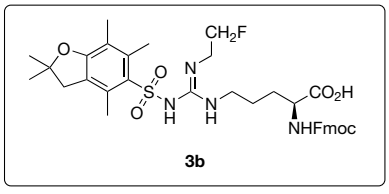

3b

Synthesis of: L-2-(((9*H*-fluoren-9-yl) methoxy)carbonylamino)-5-(3-(2-fluoroethyl)-2-(2,2-4,6,7-pentamethyl-2,3-dihydrobenzofuran-5-ylsulfonyl)guanidino) pentanoic acid (3b)

Yield 85%; ^{1}H NMR (300 MHz, $CDCl_3$) δ 8.82

(s, 1H) 7.73-7.71 (m, 2H), 7.57-7.53 (m, 2H), 7.37-7.32 (m, 2H), 7.27-7.22 (m, 2H), 6.02-5.99 (m, 1H), 4.50-4.27 (m, 5H) 4.15 (t, J = 6.9 Hz, 1H), 3.54-3.37 (m, 2H), 3.30-3.02 (m, 2H), 2.90 (s, 2H), 2.56 (s, 3H), 2.49 (s, 3H), 2.07 (s, 3H), 1.98-1.60 (m, 4H), 1.43 (s, 6H); ^{13}C NMR (75 MHz, $CDCl_3$) δ 175.1, 159.0, 156.8, 155.1, 144.0, 143.8, 141.5, 138.5, 133.1, 132.4, 128.0, 127.3, 125.4, 124.9, 120.2, 117.8, 86.7, 82.7 (d, J_{CF} = 167.5 Hz), 67.5, 53.3, 47.3, 43.4, 42.2 (d, J_{CF} = 20.4 Hz), 41.3, 29.8, 28.8, 25.1, 19.5, 18.2, 12.7; HRMS (MALDI) Calcd for $C_{36}H_{43}FN_4O_7S$ [M+Na]$^+$, 717.2734, found 717.2744.

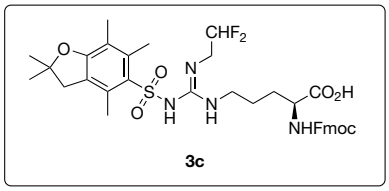

3c

Synthesis of: L-2-(((9*H*-fluoren-9-yl) methoxy)carbonylamino)-5-(3-(2,2-difluoroethyl)-2-(2,2,4,6,7-pentamethyl-2,3-dihydrobenzofuran-5-ylsulfonyl)guanidino) pentanoic acid (3c)

Yield 85%; ^{1}H NMR (300 MHz, $CDCl_3$) δ 9.36 (s, 1H), 7.71-7.69 (m, 2H), 7.54-7.50 (m, 2H), 7.35-7.30 (m, 2H), 7.26-7.20 (m, 2H), 6.01 (br d, 1H), 5.76 (tt, J_{HH} = 4.1 Hz, J_{HF} = 56.4 Hz, 1H), 4.50-4.25 (m, 3H), 4.12 (t, J = 7.2 Hz, 1H), 3.53-3.40 (m, 2H), 3.28-2.97 (m, 2H), 2.89 (s, 2H), 2.53 (s, 3H), 2.46 (s, 3H), 2.05 (s, 3H), 1.96-1.59 (m, 4H), 1.41 (s, 6H); ^{13}C NMR (75 MHz, $CDCl_3$) δ 175.1, 159.2, 156.9, 155.0, 143.9, 143.8, 141.5, 138.6, 132.7, 132.4, 128.0, 127.3, 125.3, 125.0, 120.2, 117.9, 113.9 (t, J_{CF} = 241.4 Hz), 86.8, 67.6, 53.2, 47.3, 43.8 (t, J_{CF} = 27.8), 43.3, 41.4, 29.9, 28.8, 25.1, 19.4, 18.1, 12.6; HRMS (MALDI) Calcd for $C_{36}H_{42}F_2N_4O_7S$ [M+H]$^+$, 713.2821, found 713.2822.

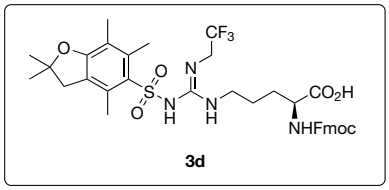

3d

Synthesis of: L-2-(((9*H*-fluoren-9-yl) methoxy)carbonylamino)-5-(2-(2,2,4,6,7-pentamethyl-2,3-dihydrobenzofuran-5-ylsulfonyl)-3-(2,2,2-trifluoroethyl)guanidino) pentanoic acid (3d)

Yield 88%; ^{1}H NMR (300 MHz, $CDCl_3$) δ 7.72-7.70 (m, 2H), 7.55-7.51 (m, 2H), 7.36-7.31 (m, 2H), 7.26-7.21 (m, 2H), 6.95-6.39 (br m, 2H), 6.06 (br d, 1H, J = 7.2 Hz), 4.49-4.28 (m, 3H), 4.21-4.01 (m, 1H), 4.00-3.68 (br m, 2H), 3.40-3.01 (br m, 2H), 2.89 (s, 2H), 2.53 (s, 3H), 2.47 (s, 3H), 2.06 (s, 3H), 2.00-1.52 (m, 4H), 1.42 (s, 6H); ^{13}C NMR (75 MHz, $CDCl_3$) δ 175.1, 159.2, 157.0, 154.9, 144.0, 143.7, 141.5, 138.7, 132.5, 128.0, 127.3, 125.3, 124.9, 124.2 (q, J_{CF} = 279.2 Hz), 120.2, 117.8, 86.8, 67.6, 53.3, 47.2, 43.3, 42.4 (q, J_{CF} = 33.6 Hz), 41.4, 29.8, 28.7, 25.1, 19.4, 18.0, 12.6; $[\alpha]_D$ = -6.1° (c 1.1, DMF); HRMS (MALDI) Calcd for $C_{36}H_{42}F_3N_4O_7S$ [M+H]$^+$, 731.2726, found 731.2739.

6.6.1.2 Synthesis of the fluorinated R1 peptides

The **R1-1**, **-2**, **-3**, and **-4** series of N^{η}-substituted peptides were prepared following standard Fmoc SPPS protocols. Peptides were assembled on the 2-chlorotrityl resin working at 0.25 mmol scale. With the exception of the N^{η}-modified L-arginine building blocks, peptide couplings were performed using 4.0 equivalents of protected Fmoc amino acid, 4.0 equivalents of BOP reagent, and 8.0 equivalents DIPEA in a total volume of 10 mL DMF at room temperature for 1 h. Alternatively, incorporation of the N^{η}-modified L-arginine building residues was performed using 2.0 equivalents of the N^{η}-modified L-arginine building blocks, 2.0 equivalents of BOP reagent, and 4.0 equivalents DIPEA in a total volume of 10 mL DMF at room temperature overnight. Peptide couplings were verified using the Kaiser and bromophenol blue tests. Upon completion of SPPS, peptides were cleaved from the resin and deprotected using a mixture of 95:2.5:2.5 TFA/TIS/H_2O followed by Et_2O precipitation to yield the crude peptides. Each peptide was purified to homogeneity using RP-HPLC, employing a Prosphere C18 column (250 x 22 mm, 300 Å, 10 µm) with a gradient of 5□95% acetonitrile (0.1 % TFA) in 90 minutes at a flow rate of 11.5 mL/minute. Peptide identity was confirmed by MALDI-MS analysis, in each case providing the expected mass.

Table 4: Analytical data of **R1-1**, **-2**, **-3**, and **-4**

Peptide	R_t (minutes)	Molecular Formula	Calculated MW $[M+H]^+$	Measured MW (MALDI-LRMS)
R1-1	26. 80	$C_{63}H_{79}N_{17}O_{16}$	1330.597	1330.457
R1-2	26.70	$C_{63}H_{78}N_{17}O_{16}F$	1348.587	1349.404
R1-3	27.19	$C_{63}H_{77}N_{17}O_{16}F_2$	1366.578	1366.471
R1-4	28.00	$C_{63}H_{76}N_{17}O_{16}F_3$	1384.569	1385.397

6.6.2 Biological experiments with fluorinated R1 peptides

The following experiments were performed by Ted Lakowski, Faculty of Pharmaceutical Sciences, The University of British Columbia, Vancouver, B.C., Canada

6.6.2.1 Methylation of N^{η}-ethylated R1 peptides

PRMT1, CARM1, or PRMT6 at 2.0 µM were incubated with 400 µM R1-1, -2, -3, or -4 and 190 µM [*methyl*-^{14}C]AdoMet (Amersham (2.06 GBq/mmol)) in methylation buffer (50 mM HEPES-KOH (pH 8.0), 10 mM NaCl, and 1.0 mM DTT) at 37 °C for 16 h. Samples were mixed with sample dilution buffer and separated using tricine gel electrophoresis.[39] Gels were fixed[40], stained with Coomassie

blue, dried, and exposed to storage phosphor screens (GE Healthcare). To show enzyme-dependent methylation, similar reactions were carried out on R1-1 with 0 to 11.7 μM PRMT1.

6.6.2.2 The position of methylation of R1-1

Two groups of reactions were prepared. The first group contained 100 μM AdoMet, and the second group contained 100 μM [methyl-^{14}C]AdoMet. Each group consisted of three 40-μL reactions: 1) 4.0 μM PRMT, 2) 400 μM R1-1, and 3) 4.0 μM PRMT with 400 μM R1-1. Reactions were incubated for 16 h, dried in a vacuum centrifuge, and hydrolysed in the vapour phase with 6 M HCl for 24 h at 110 °C. The dried hydrolysate was reconstituted in 100 mM HCl and basic amino acids purified using Oasis MCX SPE columns (Waters).[41] Extracted amino acids were reconstituted in 0.1% formic acid and 0.05% TFA, and analyzed via UPLC-MS/MS on a Quatro Premier XE electrospray mass spectrometer (Micromass MS Technologies). Fragment ions were recorded with a 30-V cone voltage and a 20-eV collision energy. For the AdoMet group the parent ions 203, 217, and 231 m/z were selected, corresponding respectively to Et-Arg, methyl-Et-Arg, and dimethyl-Et-Arg. The [methyl-^{14}C]AdoMet group was analyzed similarly except that the parent ions were 203, 219, and 235 m/z.

The apparent K_M of R1-1 for PRMT1 was measured using 0, to 500 μM R1-1 with 2.0 μM PRMT1 with a constant 250 μM AdoMet for 1 h. The reactions were processed as in the preceding paragraph and analyzed using UPLC-MS/MS multiple reaction monitoring for the parent ion 217 m/z (corresponding to methyl-Et-Arg) and the associated diagnostic fragment ions 60, 85, 102, and 172 m/z with a 30-V cone voltage and a 20-eV collision energy.

6.6.2.3 Determination of apparent K_M values

In order to compare IC_{50} values obtained from different bi-substrate enzyme reactions, inhibition experiments were performed at or near the K_M values for both substrates.[36] The AdoMet K_M values for PRMT1 and PRMT6 have been measured previously.[16,23] The apparent K_M values for PRMT1 with the histone H4 peptide and for PRMT6 with the histone H3 peptide were measured previously (unpublished results). The CARM1 apparent K_M for AdoMet and H3 tail were measured using a previously described MS assay.[23] Briefly, CARM1 at 800 nM was incubated with 100 μM H3 tail peptide and from 0.5 to 200 μM AdoMet, or with constant 200 μM AdoMet and from 1.0 to 200 μM H3 tail. The data for both sets of CARM1 reactions were fit to the Michaelis–Menten–Henri equation using SigmaPlot (SYSTAT), with resulting K_M values for AdoMet and H3 tail of 15.6 ±

1.8 and 13.2 ± 2.9 μM, respectively.

6.6.2.4 Inhibition studies

Inhibition studies were performed with 0 to 500 μM R1-1, -2, -3, or -4 and 200 nM PRMT1, PRMT6, or CARM1 in a 80-μL reaction volume. For PRMT1, the H4 tail and AdoMet concentrations were 15 and 10 μM, respectively. For CARM1, the H3 tail and AdoMet concentrations were both 20 μM. For PRMT6, the H3 tail and AdoMet concentrations were 5.0 and 20 μM, respectively. PRMT1 and PRMT6 were incubated for 1 h and CARM1 was incubated for 2 h. Reactions were stopped by flash freezing, thawed in ice, filtered through pre-chilled Microcon Ultracel YM-30 centrifugal filters in a pre-chilled centrifuge, and the filtrate dried in a vacuum centrifuge. Samples were hydrolysed and methylated arginines assayed.[23] Identical inhibition studies were performed as described above for PRMT1, but with the addition of the product inhibitors R1(aDMA) and R1(sDMA) for comparison. These reactions were assayed using a method that detects the co-product AdoHcy.[42]

6.6.3 Synthesis of building blocks and peptides as partial-bisubstrates

6.6.3.1 Synthesis of compounds 5a-b and 6a-b

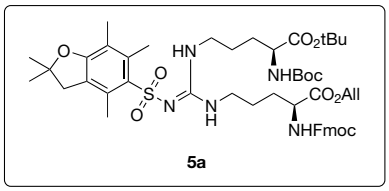

5a

Synthesis of (E)-prop-1-en-1-yl (6S,16S,Z)-16-((((9H-fluoren-9-yl)methoxy)carbonyl) amino)-6-(tert-butoxycarbonyl)-2,2-dimethyl-4-oxo-11-(((2,2,4,6,7-pentamethyl-2,3-dihydrobenzofuran-5-yl)sulfonyl)imino)-3-oxa-5,10,12-triazaheptadecan-17-oate (5a)

Boc-L-Orn(*Z*)-OH was converted to the corresponding *tert*-butyl ester according to established protocols.[43,44] Boc-L-Orn(Z)-OtBu (485 mg, 1.15 mmol) was dissolved in 10 mL EtOAc and treated with 10% Pd/C (150 mg) added as a suspension in EtOAc (6 mL). A hydrogen balloon was fixed to the reaction flask and the mixture stirred under hydrogen atmosphere for 2 hours at which point TLC indicated completed consumption of starting material. The catalyst was removed by filtration though celite and the solvent removed to yield the free amino intermediate **4a** as a colourless oil that was used directly in the next step. Intermediate compound **4a** was next dissolved in CH_2Cl_2 (20 mL) and treated with thiourea **1** (750 mg, 1.06 mmol) followed by addition of EDCI (382 mg, 2.0 mmol). After 5 minutes TLC showed full conversion and the mixture was concentrated

under vacuum. The crude material was applied to a silica column eluting with a gradient of 1:1 to 2:1 EtOAc/hexane. After solvent removal compound 13 was obtained as a white foam (562 mg, 55%). Yield 55%; ^{1}H NMR (300 MHz, $CDCl_3$) *mixture of rotamers* δ 7.77-7.74 (m, 2H), 7.59-7.56 (m, 2H), 7.42-7.36 (m, 2H), 7.32-7.27 (m, 2H), 5.95-5.80 (m, 1H), 5.55 (br m, 1H), 5.38-5.07 (m, 3H), 4.63 (br d, *J* = 5.8 Hz, 2H), 4.44-4.33 (m, 3H), 4.20 (t, *J* = 6.9 Hz, 1H), 4.11 (m, 1H), 3.35-3.08 (m, 4H), 2.93 (s, 2H), 2.60 (s, 3H), 2.53 (s, 3H), 2.09 (s, 3H), 1.90-1.50 (m, 8H), 1.45-1.38 (m, 24H); ^{13}C NMR (75 MHz, $CDCl_3$) *mixture of rotamers* δ 172.2, 172.0, 171.7, 160.5, 158.8, 156.4, 156.0, 155.0, 152.5, 144.0, 143.9, 141.5, 140.0, 138.4, 135.0, 133.8, 132.3, 131.8, 131.6, 128.4, 128.0, 127.9, 127.3, 125.3, 124.7, 120.22, 120.17, 119.4, 119.2, 118.2, 117.6, 87.2, 86.5, 82.6, 80.2, 67.4, 66.4, 66.2, 54.0, 53.6, 53.3, 47.3, 43.5, 43.3, 41.2, 39.7, 31.0, 30.4, 29.9, 28.8, 28.5, 28.2, 26.0, 25.5, 25.4, 19.6, 19.5, 18.2, 17.8, 12.7; HRMS (MALDI) Calcd for $C_{51}H_{69}N_5O_{11}S$ $[M+H]^+$ 960.4793, found 960.4792.

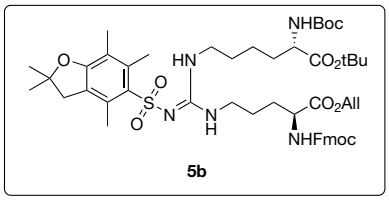

5b

Synthesis of (E)-prop-1-en-1-yl (6S,17S,E)-17-((((9H-fluoren-9-yl)methoxy)carbonyl) amino)-6-(tert-butoxycarbonyl)-2,2-dimethyl-4-oxo-12-(((2,2,4,6,7-pentamethyl-2,3-dihydrobenzofuran-5-yl)sulfonyl)imino)-3-oxa-5,11,13-triazaoctadecan-18-oate (5b)

Synthesis as for compound **5a** but starting from Boc-L-Lys(Cbz)-OH. Yield 65%; ^{1}H NMR (300 MHz, $CDCl_3$) *mixture of rotamers* δ 7.77-7.74 (m, 2H), 7.59-7.56 (m, 2H), 7.42-7.34 (m, 2H), 7.32-7.25 (m, 2H), 5.95-5.80 (m, 1H), 5.54 (br m, 1H), 5.38-5.18 (m, 2H), 5.07 (br d, *J* = 7.4 Hz, 1H), 4.63 (br m, 2H), 4.44-4.26 (m, 3H), 4.20 (m, 1H), 4.11 (m, 1H), 3.30-3.02 (m, 4H), 2.93 (s, 2H), 2.60 (s, 3H), 2.53 (s, 3H), 2.08 (s, 3H), 1.97-1.20 (m, 34H); ^{13}C NMR (75 MHz, $CDCl_3$) *mixture of rotamers* δ 172.0, 160.6, 158.7, 156.4, 156.3, 155.8, 155.0, 152.4, 144.0, 143.8, 141.5, 140.0, 138.5, 134.9, 133.8, 132.4, 131.7, 131.6, 128.3, 128.0, 127.3, 125.5, 125.3, 124.7, 120.25, 120.18, 119.5, 118.3, 117.6, 87.3, 86.5, 82.3, 80.0, 67.4, 66.5, 54.0, 53.7, 53.5, 47.3, 43.5, 43.3, 41.7, 41.1, 39.8, 32.9, 30.5, 29.9, 28.8, 28.6, 28.2, 25.5, 22.7, 19.6, 19.5, 18.2, 17.8, 12.7; HRMS (MALDI) Calcd for $C_{52}H_{71}N_5O_{11}S$ $[M+H]^+$ 974.4949, found 974.4976.

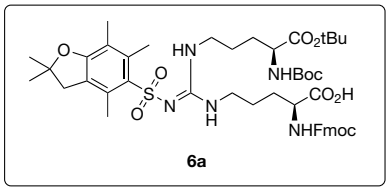

6a

Synthesis of (6S,16S,Z)-16-((((9H-fluoren-9-yl)methoxy)carbonyl)amino)-6-(tert-butoxycarbonyl)-2,2-dimethyl-4-oxo-11-(((2,2,4,6,7-pentamethyl-2,3-dihydrobenzofuran-5-yl)sulfonyl)imino)-3-oxa-5,10,12-triazaheptadecan-17-oic acid (6a)

Allyl ester **5a** (480 mg, 0.50 mmol) was dissolved in THF (15mL) and *N*-methylaniline (163 µL, 1.5 mmol) was added, followed by $Pd(PPh_3)_4$ (10 mol%, 0.05mmol, 50 mg). The mixture was protected from light and stirred under N_2 (g) at room temperature for 1 hour. EtOAc (100ml) was added and washed with saturated NH_4Cl (50ml). The NH_4Cl layer was extracted with EtOAc (2 x 50 ml). After drying of the combined EtOAc layers over Na_2SO_4 the mixture was concentrated and applied to a silica column eluting with CH_2Cl_2/MeOH (50:1) followed by CH_2Cl_2/MeOH/AcOH (25:1:0.1). After solvent removal the product was obtained as a white foam. (450 mg, quantitative). ^{1}H NMR (300 MHz, $CDCl_3$) *mixture of rotamers* δ 7.75-7.72 (m, 2H), 7.59-7.56 (m, 2H), 7.40-7.36 (m, 2H), 7.32-7.27 (m, 2H), 5.81 (br m, 1H), 5.25 (br m, 1H), 4.44-4.30 (m, 3H), 4.19 (t, *J* = 7.2 Hz, 1H), 4.10 (m, 1H), 3.34-3.06 (m, 4H), 2.93 (s, 2H), 2.59 (s, 3H), 2.52 (s, 3H), 2.08 (s, 3H), 1.90-1.45 (m, 8H), 1.45-1.30 (m, 24H); ^{13}C NMR (75 MHz, $CDCl_3$) *mixture of rotamers* δ 175.2, 174.6, 171.9, 171.5, 160.5, 158.8, 156.4, 156.1, 155.1, 153.3, 144.0, 143.9, 141.5, 140.1, 138.5, 135.1, 133.5, 132.4, 128.0, 127.3, 125.5, 125.4, 124.7, 120.2, 118.3, 117.6, 87.2, 86.6, 82.8, 82.5, 82.1, 80.6, 67.3, 55.1, 53.6, 53.4, 47.3, 43.4, 43.3, 41.2, 40.8, 39.5, 30.8, 30.4, 29.8, 29.4, 28.8, 28.5, 28.2, 25.5, 25.3, 19.5, 19.4, 18.2, 17.7, 12.7; HRMS (MALDI) Calcd for $C_{48}H_{65}N_5O_{11}S$ $[M+Na]^+$ 942.4299, found 942.4310.

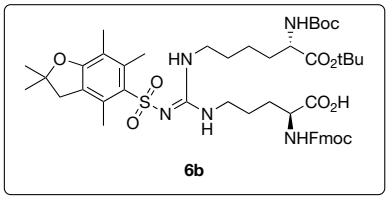

6b

Synthesis of (6S,17S,E)-17-((((9H-fluoren-9-yl)methoxy)carbonyl)amino)-6-(tert-butoxycarbonyl)-2,2-dimethyl-4-oxo-12-(((2,2,4,6,7-pentamethyl-2,3-dihydrobenzofuran-5-yl)sulfonyl)imino)-3-oxa-5,11,13-triazaoctadecan-18-oic acid (6b)

Synthesis as for compound **6a**. Yield 85%; ^{1}H NMR (300 MHz, $CDCl_3$) *mixture of rotamers* δ 7.75-7.72 (m, 2H), 7.59-7.56 (m, 2H), 7.40-7.35 (m, 2H), 7.32-7.26 (m, 2H), 5.81-5.54 (br m, 1H), 5.18 (br m, 1H), 4.46-4.28 (m, 3H), 4.19 (t, *J* = 6.9 Hz, 1H), 4.11 (m, 1H), 3.29-3.04 (m, 4H), 2.93 (s, 2H), 2.60 (s, 3H), 2.53 (s, 3H), 2.08 (s, 3H), 1.98-1.18 (m, 34H); ^{13}C NMR (75 MHz, $CDCl_3$) *mixture of*

rotamers δ 175.8, 174.6, 172.2, 171.5, 158.8, 158.2, 156.4, 156.0, 155.0, 144.0, 143.9, 141.5, 138.5, 133.6, 132.4, 128.0, 127.4, 125.3, 124.7, 120.2, 117.6, 86.5, 82.5, 82.0, 80.4, 67.3, 55.2, 53.9, 53.3, 47.4, 43.5, 41.6, 41.0, 32.9, 31.2, 29.8, 28.8, 28.5, 28.2, 25.3, 22.7, 20.9, 19.5, 18.2, 12.7; HRMS (MALDI) Calcd for $C_{49}H_{67}N_5O_{11}S$ $[M+Na]^+$ 956.4455, found 956.4449.

6.6.3.2 Synthesis of N^{η}-Substituted R1 Peptide Partial-Bisubstrate Inhibitors R1-Orn and R1-Lys.

N^{η}-Substituted peptides **R1-Orn** and **R1-Lys** were prepared following standard Fmoc SPPS protocols. Peptides were assembled on the 2-chlorotrityl resin working at 0.10 mmol scale. With the exception of the N^{η}-modified L-arginine building blocks, peptide couplings were performed using 4.0 equiv of protected Fmoc amino acid, 4.0 equiv of BOP reagent, and 8.0 equiv of DIPEA in a total volume of 5 mL of DMF at ambient temperature for 1 h. Incorporation of the N^{η}-modified L-arginine residues **6a** and **6b** was performed using 2.0 equiv of the N^{η}-modified L-arginine building block, 2.0 equiv of BOP reagent, and 4.0 equiv of DIPEA in a total volume of 5 mL of DMF at ambient temperature overnight. Peptide couplings were verified using the Kaiser and bromophenol blue tests. Upon completion of SPPS, peptides were cleaved from the resin and deprotected using a mixture of 95:2.5:2.5 TFA/TIS/H_2O followed by Et_2O precipitation to yield the crude peptides. Peptides **R1-Orn** and **R1-Lys** were purified to homogeneity using RP-HPLC, employing a Prosphere C18 column (250×22 mm, 300 Å, 10 µm) with a gradient of 5 to 95% acetonitrile (0.1% TFA) in 90 min at a flow rate of 11.5 mL min^{-1}. Peptide identity was confirmed by MALDI-MS analysis.

6.6.4 Biological evaluation of R1-Orn and R1-Lys

The following experiments were performed by Ted Lakowski and Dylan Thomas, Faculty of Pharmaceutical Sciences, The University of British Columbia, Vancouver, B.C., Canada

6.6.4.1 Inhibition Studies.

Inhibition studies were performed as described in section 6.5.2. Briefly, sinefungin **1,** AdoHyc **2**, and 5-AP **3** (at 0.25 to 50 µM), or partial-bisubstrate inhibitors **17** and **18** (at 2 to 500 µM), were incubated with 200 nM PRMT1, 400 nM PRMT4, or 200 nM PRMT6 in a total volume of 120 µL (reactions with PRMT1) or 160 µL (reactions with PRMTs 4 and 6). For PRMT1, the H4 tail and AdoMet concentrations were 15 and 10 µM, respectively. For PRMT4, the H3

tail and AdoMet concentrations were both 20 μM. For PRMT6, the H3 tail and AdoMet concentrations were 5.0 and 20 μM, respectively.

6.6.4.2 Photochemical cross-linking.

[^{14}C]AdoMet (Perkin Elmer) was vacuum centrifuged for 20 min at ambient temperature prior to use to remove the 10% ethanol in which it was supplied. The concentration was then calculated using ε_{256} = 14700 M^{-1} cm^{-1}.[45] PRMTs 1, 4, and 6 were photo-chemically cross-linked to [^{14}C]AdoMet using UV radiation according to previously described methods.[46] Briefly, 5.0 μM enzyme was UV-irradiated at 250 nm (at 0.16 Amps) with 20 μM [^{14}C]AdoMet (0.54 Bq) in a 15-μL volume for 20 min on ice in the presence or absence of inhibitors. One control sample was not exposed to UV or inhibitors. Samples were then mixed with dilution buffer and separated by gel electrophoresis on a 10% SDS-PAGE gel. The gel was stained, dried, and exposed to storage phosphor screens (GE Healthcare).

6.6.5 Synthesis of modified Tat peptides

The *N*-substituted Tat peptide analogues **1**-**8** were synthesized following standard Fmoc SPPS protocols. The required *N*-modified L-arginine building blocks were prepared from a common thiourea precursor as previously described.[15] Peptides were assembled on the 2-chlorotrityl resin working on a 0.25 mmol scale. With the exception of the *N*-modified L-arginine building blocks, peptide couplings were performed using 4.0 equiv of protected Fmoc amino acid, 4.0 equiv of BOP reagent, and 8.0 equiv of DIPEA in a total volume of 10 mL of DMF at RT for 1 h. Alternatively, incorporation of the *N*-modified L-arginine building residues was performed using 2.0 equiv of the *N*-modified L-arginine building blocks, 2.0 equiv of BOP reagent, and 4.0 equiv of DIPEA in a total volume of 10 mL of DMF at RT overnight. Peptide couplings were verified using the Kaiser and bromophenol blue tests. Upon completion of SPPS, peptides were cleaved from the resin and deprotected using a mixture of 95:2.5:2.5 TFA/TIS/H_2O followed by Et_2O precipitation to yield the crude peptides. Each peptide was purified to homogeneity using RP-HPLC, employing a semipreparative C18 column (250×10 mm, 90 Å, 10 μm) with a gradient of 5–35% acetonitrile (0.1% TFA) in 65 min at a flow rate of 4 mL/min. Peptide identity was confirmed by MALDI-MS analysis, in each case providing the expected mass.

Table 5: Analytical data of Tat peptide analogues **1-8**.

Peptide	R_t (min)	Molecular Formula	Calculated MW $[M+H]^+$	Measured MW (MALDI-LRMS)
1	14.35	$C_{77}H_{137}N_{35}O_{16}$	1809.106	1809.209
2	12.27	$C_{70}H_{131}N_{35}O_{16}$	1719.059	1719.663
3	13.06	$C_{72}H_{132}F_3N_{35}O_{16}$	1801.062	1801.706
4	13.56	$C_{72}H_{135}N_{35}O_{16}$	1747.091	1747.605
5	9.98	$C_{74}H_{137}N_{35}O_{16}$	1773.106	1773.631
6	14.19	$C_{73}H_{135}N_{35}O_{16}$	1759.091	1759.626
7	10.25	$C_{70}H_{131}N_{35}O_{17}$	1735.054	1735.227
8	12.79	$C_{67}H_{124}N_{32}O_{16}$	1633.995	1634.579

6.6.6 Biological evaluation of the modified Tat peptides

The following experiments were performed by Dylan Thomas, Faculty of Pharmaceutical Sciences, The University of British Columbia, Vancouver, B.C., Canada

6.6.6.1 Methylation of the Tat peptides

Each Tat peptide at 250 μM was incubated at 37 ˚C overnight (16 h) with 150 μM [*methyl*-^{14}C]AdoMet and 2.0 μM PRMT1, PRMT4 or PRMT6 in methylation buffer (50 mM HEPES 10 mM NaCl, 1.0 mM DTT, pH 8) in a 20-μL final volume. The reactions were terminated by addition of 5x tricine sample dilution buffer and the methylated peptides were separated by 17% tricine gel electrophoresis according to the method described in section 6.5.2. The gels were fixed with 5% glutaraldehyde and stained according to previous protocols. Similar to our experiences with other peptides we found that failure to fix the gels in this way resulted in leakage of peptides from the gel during staining, destaining, and drying. Dried gels were exposed to storage phosphor screens (GE Healthcare) for 16 h and scanned on a Typhoon 9400 imager (GE Healthcare). The above reactions were repeated except that the source of methyl groups was unlabelled AdoMet. These reactions were passed through a 30-kDa molecular weight cut-off filter (VWR 82031-354) to remove the enzyme from the peptides, dried, and hydrolysed (see above). The amounts of aDMA and MMA were measured according to methods described below.

6.6.6.2 Detection of methylation at substituted R52

We utilized MS to determine the potential for PRMT-mediated methylation at the modified R52 residue in the Tat peptide series with the same reaction

samples of PRMT1, PRMT4, or PRMT6 with the Tat peptides described above. Using a series of product ion scans we selected masses corresponding to [M+H], [M+CH_3+H] and [M+2CH_3+H] for Tat peptide analogues **1**, **3**, **4**, **5**, **6**, and **7** by scanning over a range of 30 to 350 m/z.

6.6.6.3 Enzyme assays

For substrate inhibition assays, mixes of enzyme (50-800 nM) and Tat peptide analogues **1**-**8** (0.25-200 μM) and 200 μM AdoMet (Sigma) were incubated at 37 ˚C in 1x reaction buffer.[23] To keep all reactions within the linear range 400- and 800-nM enzyme reactions were incubated for 60 min and 50- and 100-nM enzyme reactions were incubated for 120 min. Samples were flash frozen in liquid nitrogen to stop catalysis, thawed, and spin-filtered at 12,000 x *g* at 4 ˚C using 30-kDa molecular weight cut-off filters for 15 min to separate the enzyme from the peptide substrate. Sample eluates were transferred into 300-μL glass inserts and dried using a Thermo Savant SC110A speed vacuum. The dried reactions were hydrolysed with 200 μL 6N HCl at 110 ˚C for 24 h *in vacuo* and reconstituted in 0.5% acetic acid and 0.01% trifluoroacetic acid (TFA). Reactions containing Tat analogue **4** were reconstituted in 0.5% acetic acid and 0.05% TFA.

MMA and aDMA were separated and quantified using the same LC-MS/MS instrumentation described above. Liquid chromatography was performed for 5.5 min at 45 ˚C at 0.150 mL/min. For all Tat peptides except **4**, buffer A contained 0.5% acetic acid and 0.01% TFA, and buffer B contained 30% methanol, 0.5% acetic acid and 0.01% TFA. Buffer A and B for **4** were identical except 0.05% TFA was used to help chromatographically separate *N*-ethyl-L-arginine from aDMA. Ions were acquired using a 30-V cone voltage at 400°C. Fragments were generated using 20-meV collision energy. Precursor ions 203.1 and 189.2 m/z were selected corresponding to aDMA and MMA, respectively, and were quantified via multiple reaction monitoring using their generated 46.1 and 74.2 m/z product ions as previously described.

References

[1] M. T. Bedford, S. G. Clarke, *Mol. Cell* **2009**, *33*, 1–13.

[2] B. D. Strahl, C. D. Allis, *Nature* **2000**, *403*, 41–45.

[3] S. Frietze, M. Lupien, P. A. Silver, M. Brown, *Cancer Res.* **2008**, *68*, 301–306.

[4] J. Michaud-Levesque, S. Richard, *J. Biol. Chem.* **2009**, *284*, 21338–21346.

[5] B. Xie, C. F. Invernizzi, S. Richard, M. A. Wainberg, *J. Virol.* **2007**, *81*, 4226–4234.

[6] M. Yoshimatsu, G. Toyokawa, S. Hayami, M. Unoki, T. Tsunoda, H. I. Field, J. D. Kelly, D. E. Neal, Y. Maehara, B. A. J. Ponder, et al., *Int. J. Cancer* **2011**, *128*, 562–573.

[7] T. Teerlink, Z. Luo, F. Palm, C. S. Wilcox, *Pharmacol. Res.* **2009**, *60*, 448–460.

[8] R. A. Copeland, M. E. Solomon, V. M. Richon, *Nat. Rev. Drug Discov.* **2009**, *8*, 724–732.

[9] X. Zhang, L. Zhou, X. Cheng, *EMBO J.* **2000**, *19*, 3509–3519.

[10] D. Cheng, N. Yadav, R. W. King, M. S. Swanson, E. J. Weinstein, M. T. Bedford, *J. Biol. Chem.* **2004**, *279*, 23892–23899.

[11] A. Spannhoff, R. Heinke, I. Bauer, P. Trojer, E. Metzger, R. Gust, R. Schule, G. Brosch, W. Sippl, M. Jung, *J. Med. Chem.* **2007**, *50* , 2319–2325.

[12] A. Spannhoff, R. Machmur, R. Heinke, P. Trojer, I. Bauer, G. Brosch, R. Schüle, W. Hanefeld, W. Sippl, M. Jung, *Bioorganic Med. Chem. Lett.* **2007**, *17*, 4150–4153.

[13] R. Ragno, R. Ragno, S. Simeoni, S. Simeoni, S. Castellano, S. Castellano, C. Vicidomini, C. Vicidomini, A. Mai, A. Mai, et al., *J. Med. Chem.* **2007**, *50*, 1241–1253.

[14] S. Castellano, C. Milite, R. Ragno, S. Simeoni, A. Mai, V. Limongelli, E. Novellino, I. Bauer, G. Brosch, A. Spannhoff, et al., *ChemMedChem* **2010**, *5*, 398–414.

[15] N. I. Martin, R. M. J. Liskamp, *J. Org. Chem.* **2008**, *73*, 7849–7851.

[16] T. M. Lakowski, A. Frankel, *J. Biol. Chem.* **2008**, *283*, 10015–10025.

[17] X. Zhang, X. Cheng, *Structure* **2003**, *11*, 509–520.

[18] E. F. Pettersen, T. D. Goddard, C. C. Huang, G. S. Couch, D. M. Greenblatt, E. C. Meng, T. E. Ferrin, *J. Comput. Chem.* **2004**, *25*, 1605–

1612.
[19] B. C. Smith, J. M. Denu, *Biochim. Biophys. Acta - Gene Regul. Mech.* **2009**, *1789*, 45–57.
[20] X. Cheng, R. E. Collins, X. Zhang, *Annu. Rev. Biophys. Biomol. Struct.* **2005**, *34*, 267–294.
[21] W. W. Yue, M. Hassler, S. M. Roe, V. Thompson-Vale, L. H. Pearl, *EMBO J.* **2007**, *26*, 4402–4412.
[22] T. C. Osborne, O. Obianyo, X. Zhang, X. Cheng, P. R. Thompson, *Biochemistry* **2007**, *46*, 13370–13381.
[23] T. M. Lakowski, A. Frankel, *Biochem. J.* **2009**, *421*, 253–261.
[24] T. M. Lakowski, C. Zurita-lopez, S. G. Clarke, A. Frankel, *Anal. Biochem.* **2010**, *397*, 1–11.
[25] A. Frankel, N. Yadav, J. Lee, T. L. Branscombe, S. Clarke, M. T. Bedford, *J. Biol. Chem.* **2002**, *277*, 3537–3543.
[26] E. Guccione, C. Bassi, F. Casadio, F. Martinato, M. Cesaroni, H. Schuchlautz, B. Lüscher, B. Amati, *Nature* **2007**, *449*, 933–937.
[27] D. Hyllus, C. Stein, K. Schnabel, E. Schiltz, A. Imhof, Y. Dou, J. Hsieh, U. M. Bauer, *Genes Dev.* **2007**, *21*, 3369–3380.
[28] A. N. Iberg, A. Espejo, D. Cheng, D. Kim, J. Michaud-Levesque, S. Richard, M. T. Bedford, *J. Biol. Chem.* **2008**, *283*, 3006–3010.
[29] M. J. Harrison, Y. H. Tang, D. H. Dowhan, *Nucleic Acids Res.* **2010**, *38*, 2201–2216.
[30] M. Boulanger, C. Liang, R. S. Russell, R. Lin, M. T. Bedford, M. A. Wainberg, S. Richard, *J. Virol.* **2005**, *79*, 124–131.
[31] B. Xie, C. F. Invernizzi, S. Richard, M. A. Wainberg, *J. Virol.* **2007**, *81*, 4226–4234.
[32] A. Mishra, G. H. Lai, N. W. Schmidt, V. Z. Sun, A. R. Rodriguez, R. Tong, L. Tang, J. Cheng, T. J. Deming, D. T. Kamei, et al., *Proc. Natl. Acad. Sci.* **2011**, *108*, 16883–16888.
[33] I. H. Segel, Enzyme Kinetics: Behaviour and Analysis of Rapid Equilibrium and Steady-State Enzyme Systems, Wiley, New York, 1993.
[34] P. Bayer, M. Kraft, A. Ejchart, M. Westendorp, R. Frank, P. Rösch, J. Mol. Biol. 1995, 247, 529–535.
[35] A. Friedler, D. Friedler, N. W. Luedtke, Y. Tor, A. Loyter, C. Gilon, J. Biol. Chem. 2000, 275, 23783–23789.
[36] J. Yang, R. A. Copeland, Z. Lai, J. Biomol. Screen. Off. J. Soc.

Biomol. Screen. 2009, 14, 111–120.
[37] O. Obianyo, C. P. Causey, T. C. Osborne, J. E. Jones, Y.-H. Lee, M. R. Stallcup, P. R. Thompson, ChemBioChem 2010, 11, 1219–1223.
[38] J. E. Bolden, M. J. Peart, R. W. Johnstone, Nat. Rev. Drug Discov. 2006, 5, 769–784.
[39] H. Schägger, G. von Jagow, Anal. Biochem. 1987, 166, 368–379.
[40] J. Wiltfang, N. Arold, V. Neuhoff, Electrophoresis 1991, 12, 352 – 366.
[41] T. Teerlink, R. J. Nijveldt, S. de Jong, P. A. M. van Leeuwen, Anal. Biochem. 2002, 303, 131–137.
[42] T. M. Lakowski, A. Frankel, Anal. Biochem. 2010, 396, 158–160.
[43] L. J. Mathias, Synthesis (Stuttg). 1979, 8, 561–576.
[44] N. I. Martin, J. J. Woodward, M. B. Winter, M. A. Marletta, Bioorganic Med. Chem. Lett. 2009, 19, 1758–1762.
[45] V. G. Kossykh, S. L. Schlagman, S. Hattman, FEBS Lett. 1995, 370, 75–77.
[46] J. H. Hurst, M. L. Billingsley, W. Lovenberg, Biochem. Biophys. Res. Commun. 1984, 122, 499–508.

Chapter 7

Summary / samenvatting

7.1 Summary

The topics discussed in this thesis span the development of novel antibiotic peptides, studies on the mode of action of existing antimicrobial peptides and several series of peptides designed to inhibit epigenetic proteins (protein arginine methyl transferases).

Chapter 1 gives a background to this thesis and discusses the need for new antibiotics. Without any intervention to combat antimicrobial resistance the outlook for the next decades is grim. The human burden will be huge and this also causes a high economic burden. While regulation of the use of antibiotics will be an important factor to combat resistance, novel compounds will be required as well. Currently, there are several different classes of antibiotics used in the clinic with the most famous ones being the beta-lactam based penicillins and cephalosporins. The different classes are categorized by their mode of action with the most common strategy is inhibition of bacterial cell wall synthesis. Other modes of action are through inhibition of bacterial protein synthesis, inhibition of RNA synthesis, interference with DNA repair, inhibition of folic acid metabolism or disruption of the bacterial cell membrane. Although we have a good selection of different compounds, resistance will occur after long-term usage. Resistance is often acquired from other bacteria through a method referred to as horizontal gene transfer (HGT). This method allows small fragments of DNA to be exchanged between bacteria and can transfer the genomic information that encodes for resistance. Since many antibiotics are obtained from nature (e.g. soil bacteria) resistance mechanisms have coevolved in other strains and often already exist before the antibiotic is used clinically.

The antibacterial target we focus on in this thesis is a biomolecule called lipid II. Lipid II is a compound that contain two carbohydrate units modified with a pentapeptide. This glycopeptide is attached to a 55-carbon lipid by means of a pyrophosphate and is anchored into the bacterial cell membrane. The carbohydrates are cleaved of and polymerized into long chains followed by crosslinking of the pentapeptide to form peptidoglycan. It is this polymeric peptidoglycan layer around the bacterium that makes up the rigid cell wall and protects the bacterium from influences from outside. When this process is interfered, the cell wall can't be properly synthesized leading to bacterial cell death. There are several known naturally occurring lipid II binding peptides and one of the most famous ones is nisin. Nisin is a 34 amino acid peptide and

a so called lantibiotic as it contains 5 rings formed by lanthionine bridges. A lanthionine is a thio-ether formed from cysteine and dehydroalanine. Nisin is a potent antibiotic against a wide variety of gram-positive bacteria. The proposed mode of action of nisin is a two-step sequence starting with the N-terminal A and B ring binding to lipid II, followed by insertion of the C-terminus into the bacterial membrane leading to pore formation. Vancomycin is another potent lipid II binding antibiotic and is clinically used for several types of infections. It binds to the D-Ala-D-Ala motif of the lipid II pentapeptide. Although it is very potent resistance is now commonly observed in bacteria where D-Ala-D-Ala has mutated to D-Ala-D-Lac.

In the introductory chapter we also describe phage display as a technique to rapidly screen large peptide libraries. Phage are bacterioviruses that can be easily modified by mutating their DNA. In a phage display experiment M13 phage (which selectively infect E.coli) are modified so that one of their outer coat-proteins carries a random peptide. By using random fragments inserted into the phage DNA a large library of peptides can be produced in a single experiment. Such a library can be exposed to an immobilized target, followed by washing to remove all non-binding phage. The phage carrying a peptide that binds to the target will then be eluted and analyzed to identify the binding peptide. A modified phage display technique was described in 2009 where each peptide carries three cysteine residues at fixed positions. These peptides are treated with a tribromide reagent that selectively reacts with the cysteine thiols to form a bicyclic peptide. As this reduces the flexibility of the peptides they intrinsically have a smaller entropic penalty to pay upon binding. Another modification to the phage display technique is mirror-image phage display. Since the phages are produced ribosomally in *E. coli* they can only be made of L-amino acids. Peptides made from L-amino acids can suffer from proteolytical instability and therefore D-amino acids are preferred. In a mirror-image phage display experiment the target used is prepared in its entire enantiomeric form, then screened against the L-peptide library and binders are identified. These are then synthesized in there D-amino acid form which should bind to the natural target.

Chapter 2 describes the chemical synthesis of several lipid II analogues that were used for phage display experiments and mode of action studies. The first target for phage display was based on lipid I but lacks the large undecaprenol lipid. Instead, a hydrophobic spacer was installed with a biotin-tag on the other end. The second target is exactly the same but of the opposite stereochemistry

to be used in mirror-image phage display as described above. The synthesis of both targets was based on the total synthesis of lipid as described by the group of Blaszczak up until the point of installing the lipid. Two more targets were designed and synthesized which only contained the pentapeptide part of lipid II. This was done to direct the binding to this site to be able to find antibiotic peptides with a similar mode of action as vancomycin. These targets were made of the pentapeptide, a hydrophilic PEG-spacer, and a biotin tag. One of the targets again had the opposite stereochemistry.

Besides the compounds to be used in phage display this chapter also describes the synthesis of lipid I and truncated analogues to be used in ITC-studies with nisin. The truncated analogues included a lipid I analogue lacking the pentapeptide, a lipid I analogue carrying a farnesyl lipid instead of undecaprenyl, pyrophosphorylated undecaprenol and phosphorylated undecaprenol.

Chapter 3 described the use of synthetic lipid II analogues as targets in bicyclic phage display experiments. After optimization of the phage display screening technique we found conditions more optimal for small molecular targets. Important was to minimize the exposure of the phage library to streptavidin and cold conditions were preferred as well. We screened all our targets against a peptide library that contained 17-amino acid peptides with 3 fixed cysteine residues. Reaction of the library with 1,3,5-tris(bromomethyl) benzene affords bicyclic peptides with loops of 6 random amino acids. After exposing the libraries two our targets in 2 consecutive rounds we analysed the phage pool DNA with high-throughput DNA analysis. The information obtained shows enrichment of specific peptide sequences and each peptide abundant more than 1 % was synthesised and tested. To see if the compounds were active their minimum inhibitory concentration (MIC) was measured against an indicator strain (*M. luteus*) and activity ranging from 32-128 µg/ml were observed. Although target 4 gave a few active peptides as well we chose to continue the three peptides identified from target 1 and 2 (T1-4, T1-6 and T2-1) as they were more representative of the original lipid II. Especially the peptide identified as T2-1 (which was identified using target 2) was strongly enriched in phage display and therefore hypothesized to be a strong lipid II binder. To improve the activity of the lead peptides we chose to modify either the N- or C-terminus with a straight chain saturated 10 carbon lipid. This drastically improved the activity to a range of 2-8 µg/ml against *M. luteus* but more importantly T2-1-C10 was now also active against clinically relevant strains (*E. faecium* and vancomycin

resistant *E. faecium*). Haemolytic properties can often be a problem with membrane active compounds and was therefore tested using sheep red blood cells. The analysis indicated that both positively charged peptides T1-4-C10 and T2-1-C10 had some haemolytic properties but only at high concentrations (>32 µg/ml). The three best compounds were analysed by preincubating them with various amounts of lipid II and testing if they were still antimicrobially active. All compounds were inhibited but required various amounts of lipid II. T2-1-C10 was already inhibited by a single equivalent of lipid II indicating strong binding. This peptide sequence was further analysed by doing an alanine scan and varying the lipid length. The alanine scan identified several critical residues but also several residues that seemed to be mutatable without loss of activity. Lipid length seemed to be optimal at 10 carbons as longer lipids did not increase the activity significantly but decreased the solubility. Longer lipid lengths also had a negative impact on haemolysis. To further analyse the interaction of our compounds with lipid II we used an assay where the accumulation of UDP-MurNAc-pentapeptide in live cells is measured. When lipid II is sequestered, UDP-MurNAc-pentapeptide can't be used in the lipid II synthesis cycle and will accumulate in the cytoplasm. Our compounds were incubated with a sensitive *E. faecium* strain and showed accumulation to a similar level as the known lipid II binder vancomycin.

Chapter 4 describes the investigation of the binding affinity of nisin with lipid II and synthetic analogues. Nisin is shown to bind lipid II through interaction with the pyrophosphate by NMR. We attempted to gain further insights into this interaction by using Isothermal Titration Calorimetry (ITC). To this end we synthesised lipid I, a lipid I analogue lacking the pentapeptide (compound **36**), undecaprenylpyrophosphate (C_{55}PP), undecaprenylphosphate (C_{55}P) and a water-soluble lipid I analogue with a farnesyl lipid. All compounds (except for the farnesylated lipid I) were embedded into DOPC vesicles and titrated into nisin. The obtained thermograms indicated that binding affinity is similar for lipid II, lipid I and lipid I lacking the peptide, however subtle differences are observed in the thermodynamic parameters. Nisin can interact with C_{55}PP although the affinity is approximately 10x weaker and no affinity for C_{55}P or C_{55}OH was observed. The farnesylated lipid I analogue showed a binding affinity roughly 100 fold weaker than lipid II indicating a lipid environment is critical to good interaction. The compounds were further analysed using a dye leakage experiment where the same vesicles were prepared filled with carboxyfluorescein. When these vesicles

are treated with nisin a pore is formed and a fluorescent signal can be measured. These experiments showed that when the vesicles contained either lipid II, lipid I or compound **36** a strong signal was observed but vesicles with C_{55}PP showed no leakage at all. A similar experiment was used to measure the stability of the formed pores by first incubating vesicles containing no dye with nisin followed by addition of dye-loaded lipid II vesicles. This experiment showed that pores formed with lipid II or lipid I are very stable but with compound **36** a lower degree of stability is observed indicating the pentapeptide is involved in this aspect of the pore complex.

Chapter 5 describes the synthesis and evaluation of several analogues of the antibiotic peptide daptomycin. Daptomycin is calcium-dependent lipopeptide antibiotic and is used against several types of infections including MRSA. Although the compound has been studied thoroughly the mode of action remains under discussion. It has been proposed that upon binding calcium, daptomycin oligomerizes and interacts with the bacterial membrane to form pores. However, there are several other indications that daptomycin's mode of action relies on a specific biomolecule. To investigate this matter we set out to synthesise two analogues of daptomycin and their enantiomers. In these analogues we replaced several hard to obtain non-proteinogenic amino acids with commercially available amino acids. Although these types of mutations were previously shown to have a negative impact on activity they were much easier to synthesize than daptomycin itself. In the first analogue we replaced the methyl glutamic acid residue with normal glutamic acid and the original ester bond between threonine 4 and kynurenine 13 was replaced by an amide bond between diaminopropionic acid 4 and kynurenine 13. The other analogue was similar but with also kynurenine 13 replaced with tryptophan. For both analogues we also prepared the enantiomers by replacing each amino acid with its enantiomeric equivalent. When tested for activity against *S. aureus* the compounds of natural stereochemistry showed activity although strongly decreased. However in the absence of calcium they were inactive like daptomycin indicating a similar mode of action. The enantiomeric compounds were inactive also in the presence of calcium indicating a chiral biomolecule to be involved in the mode of action. Surprisingly, the tryptophan containing analogue was slightly more active than the analogue with the original kynurenine. When the compounds were analyzed by CD-spectroscopy the spectrum for the tryptophan corresponded more with authentic daptomycin than the other analogue. The secondary structure might

be an explanation for the improved activity.

Chapter 6 describes the research done on peptidic inhibitors for protein arginine methyl transferases (PRMTs) in collaboration with the group of Adam Frankel at the University of British Columbia. PRMTs catalyse the dimethylation of arginine residues and are implicated in several types of cancer. Three sets of peptides were synthesized and tested against PRMT1, -4 and -6 which are some of the clinically most relevant forms. The first set of peptides were based on a sequence of a known PRMT substrate (fibrillarin). The sequence contains one arginine residue which we modified on the guanidine with differently fluorinated ethyl substituents by chemistry developed in our group. The terminal CH_3-group of the ethyl substituent either had none, one, two, or three fluorine atoms. When incubated with PRMT1, -4, and -6 we observed that the non-fluorinated peptide was still methylated by PRMT1 indicating it was a substrate. The peptides were then further analyzed to see if they could inhibit these three enzymes. The lowest IC_{50} values were observed for observed for PRMT6 (4.8 – 14.2 μM) with PRMT1 being slightly above that. The IC_{50} values measured for PRMT4 were approximately 10-fold higher.

To further increase the binding affinity we designed two new peptides that were also modified on the guanidine. Instead of the ethyl-substituent we now chose to incorporate mimics of the amino acid part of the co-substrate AdoMet. In this way more binding interactions were possible and thereby a stronger interaction. The guanidine was this time modified with either ornithine or lysine and they were again tested for their inhibitory properties. The IC_{50} values for the lysine modified peptide were similar as what we had observed before and in the low μM range for all three tested PRMTs. Interestingly, the ornithine modified peptide only inhibited PRMT6 with no measureable inhibition of PRMT1 and -4.

Another attempt to gain selectivity was made in the last series of peptide that was this time based derived from the HIV-Tat protein. It had previously been shown that this peptide was selectively methylated by PRMT6 on only one specific arginine in the multi-arginine sequence. We modified this arginine with several substituents including our fluoroethyl substituents, heteroatoms, and aromatics. In contrast to the previously reported findings we observed that our peptides were methylated equally well by PRMT1 and -6 and that other arginine residues were methylated as well. We propose that the peptide could possibly be cyclized to mimic the loop structure the peptide has in the original protein and thereby inducing selectivity.

7.2 Samenvatting

Het onderzoek dat in dit proefschrift staat beschreven beslaat verschillende onderwerpen met als basis peptiden. Peptiden zijn ketens die worden opgebouwd uit aminozuren, welke ook gebruikt worden in ons lichaam om eiwitten mee op te bouwen. Deze aminozuren kunnen via scheikundige technieken aan elkaar gekoppeld worden tot het gewenste product (peptide) verkregen is. Ook kunnen deze aminozuren door middel van organische synthese, dan wel voor of na het inbouwen in het peptide, gemodificeerd worden om specifieke functionaliteit te verkrijgen. Op deze manier hebben wij peptiden ontwikkeld die verschillende biologische werkingen hebben, met een focus gericht op antibiotica.

In **hoofdstuk 1** staat de achtergrond van de verschillende projecten beschreven en begint met het belang van de ontwikkeling van nieuwe antibiotica. Ziekteverwekkende bacteriën bestrijden we momenteel met een arsenaal aan antibiotica; chemische stoffen die selectief bacteriële cellen kunnen doden en menselijke cellen onaangetast laten. Bacteriën zijn echter in staat zich aan te passen aan hun omgeving en zich uiteindelijk tegen zulke stoffen te beschermen. Deze resistentie vormt een steeds groter wordend probleem als er geen nieuwe antibiotica ontwikkeld worden.

De antibiotica die momenteel in gebruik zijn worden ingedeeld in verschillende klassen op basis van hun scheikundige structuur. Binnen deze klassen zijn de penicillines en de cefalosporines de meest beroemde. Naast deze indeling kan men de antibiotica ook categoriseren op basis van hun werkingsmechanisme. Een gebruikelijke manier waarop deze stoffen werken is door het blokkeren van de vorming van de bacteriële celwand. De celwand is een rigide kapsel om de bacteriële cel heen, die niet voor komt bij menselijke cellen. Deze celwand is vitaal voor een bacterie en als deze wordt aangetast door het antibioticum gaat de bacterie dood. Andere werkingsmechanismes zijn het blokkeren van bacteriële eiwit productie, het blokkeren van RNA synthese of verstoring van het cel membraan. Ondanks deze variatie aan werkingsmechanismen is het onvermijdelijk dat er resistentie ontstaat en voor bijna alle antibiotica is dit al ergens ontdekt. Deze resistentie kan worden uitgewisseld tussen verschillende soorten bacteriën door middel van horizontale genoverdracht. Hierbij worden stukjes DNA uitgewisseld tussen de bacterie-soorten en het kan zo zijn dat hierop de informatie voor resistentie gecodeerd staat. Antibiotica worden vaak gewonnen uit de natuur en deze resistentie genen zijn daardoor over lange tijd geëvolueerd.

In dit proefschrift ligt de focus op een biomolecuul genaamd lipid II. Dit molecuul bestaat uit twee koolhydraat fragmenten en een peptide van vijf aminozuren. Aan dit glycopeptide is een lange vetstaart van 55 koolstofatomen gekoppeld door middel van een pyrophosphaat. Het lipide bevindt zich in eerste instantie aan de binnenzijde van de membraan van een bacteriele cel. Hier wordt het geproduceerd en daarna na de buitenzijde getransporteerd. Aan de buitenzijde wordt het verder verwerkt om de bacteriele celwand op te bouwen. De koolhydraat fragmenten worden aan elkaar gekoppeld tot lange ketens en deze ketens worden onderling weer aan elkaar gekoppeld door middel van de peptides. Lipid II is de essentiele bouwsteen voor deze celwand synthese en als dit proces wordt geblokkeerd zorgt dit uiteindelijk voor doding van de cel. De natuur heeft verscheidene stoffen geproduceerd om een dergelijk effect te bewerkstelligen en een van de meest beroemde is nisine. Nisine is een peptide van 34 aminozuren gemodificeerd met zogenaamde lanthionine bruggen die 5 ringen (A-E) in het peptide vormen. Een lanthionine is een thio-ether gevormd uit cysteine en een dehydroalanine. Nisine is een zeer potent antibioticum en is werkzaam tegen veel verschillende Grampositieve bacteriën. De voorgestelde manier waarop nisine werkt bestaat uit twee stappen en begint door binding van ringen A en B aan de pyrophosphaat van lipid II. Daarna kan de rest van het peptide de celmembraan binnen dringen om zo een porie te vormen waardoor de inhoud van de cel naar buiten kan lekken en de bacterie sterft. Een ander zeer bekend en potent antibioticum wat bindt aan lipid II is vancomycine. Vancomycine wordt gebruikt als medicijn voor verscheidene infecties. Vancomycine bindt aan de twee aminozuren (D-Ala-D-Ala) aan het uiteinde van het peptide van lipid II.

In het eerste hoofdstuk wordt ook de techniek faagdisplay besproken. Een faag is een virus dat zich reproduceert in bacteriële cellen (en dus voor de mens ongevaarlijk) en bestaat uit een stuk circulair DNA dat ingekapseld is door een aantal verschillende eiwitten. Dit soort virussen kunnen eenvoudig worden gemodificeerd door het DNA van een van de kapsel eiwitten aan te passen. In een faagdisplay experiment maken we gebruik van zogenaamde M13 fagen die worden aangepast zodat ze aan de buitenkant een peptide bij zich dragen. Door willekeurig gegenereerd DNA te gebruiken kunnen zo grote bibliotheken van peptiden worden geproduceerd. Elk faagdeeltje draagt zo een uniek peptide bij zich met zijn sequentie gecodeerd in het DNA. Als de bibliotheek geproduceerd is kan deze blootgesteld worden aan een biomolecuul (in ons geval lipid II) dat vast gemaakt is aan een oppervlak. Vanwege de grote diversiteit in de bibliotheek (10^8 – 10^{10} verschillende peptiden) is de kans groot dat er een peptide is wat

bindt aan het biomolecuul. Alle niet bindende fagen worden weggewassen van het oppervlak, waarna de bindende fagen worden geïsoleerd. Het DNA van de geïsoleerde fagen wordt dan geanalyseerd zodat het peptide wat deze faag bij zich draagt kan worden bepaald. Zo'n peptide kan in het lab synthetisch worden gemaakt en getest op zijn activiteit. Fagen worden geproduceerd in bacterien en de peptiden die ze dragen kunnen zodoende alleen worden gemaakt van de natuurlijke L-aminozuren. Dit draagt echter enkele nadelen met zich mee, omdat peptiden van L-amino zuren vaak snel afgebroken worden en daardoor niet als medicijn gebruikt kunnen worden. Om dit probleem te voorkomen is spiegelbeeld faagdisplay bedacht. Hierbij wordt het biomolecuul in spiegelbeeld aan de peptide bibliotheek gepresenteerd. Als er een bindend peptide wordt geidentificeerd wordt deze in het lab van de spiegelbeeld D-aminozuren gesynthetiseerd. Het D-peptide moet volgens de regels van de symmetrie aan de natuurlijke vorm van het biomolecuul binden terwijl het een hogere stabiliteit heeft.

In **hoofdstuk 2** wordt de synthese van een aantal lipid II analogen beschreven. Deze analogen zijn door ons gebruikt als doelmoleculen voor zoals hierboven beschreven faagdisplay experimenten maar ook om natuurlijk voorkomende lipid II bindende stoffen te bestuderen. Het eerste beschreven molecuul is een analoog van lipid II waarbij het lange lipide is vervangen door een spacer en een biotine molecuul. Tevens mist het een van de twee suikermoleculen waardoor het eigenlijk beter beschreven wordt als analoog van lipid I. Het tweede molecuul is exact hetzelfde maar van tegenovergestelde stereochemie. Dit wil zeggen dat het in spiegelbeeld gemaakt is om hiermee de hierboven beschreven spiegelbeeld faagdisplay mee uit te voeren. De synthese van deze moleculen is gebaseerd op een route die eerder beschreven is door de groep van Blaszczak. Verder worden er nog twee doelmoleculen beschreven die bestaan uit het pentapeptide van lipid II met daaraan een spacer en een biotine, en een spiegelbeeld variant hiervan.

Naast de doelmoleculen voor faagdisplay worden er in hoofdstuk 2 ook een aantal moleculen beschreven die gebruikt zijn voor isotherme titratie calorimetrie (ITC). Deze moleculen zijn ook allemaal gebaseerd op lipid I en gesynthetiseerd volgens de methodes van Blaszczak. Ze bestaan uit lipid I analogen waarvan het peptide of het lipide is verkort. Daarnaast zijn er ook een aantal phospho- en pyrophospholipides gesynthetiseerd.

Hoofdstuk 3 beschrijft het gebruik van de vier lipid II analogen in faagdisplay experimenten. Hiervoor werd gebruik gemaakt van bicyclische faagdisplay waarbij de peptide bibliotheek eerst wordt gecycliseerd met behulp van een tribromide. Het tribromide reageert met drie cysteïne residuen die altijd in de peptidesequentie geprogrammeerd staan. Om de experimenten te laten slagen is de screening methode geoptimaliseerd waar bij bleek dat de bibliotheek niet te lang aan streptavidine blootgesteld mag worden. Daarnaast bleek het gunstig om het volledige experiment bij lage temperaturen uit te voeren. Na twee selectieronden werd de bibliotheek geanalyseerd met behulp van high-throughput DNA analyse. De analyse liet voor elk doelmolecuul een andere verrijking aan peptide sequenties welke werden gesynthetiseerd en getest. De antimicrobiële activiteit van deze peptiden werd bepaald door ze te testen tegen de bacterie *Micrococcus luteus*. Op deze manier werden er een aantal peptiden geïdentificeerd die de bacterien doodde bij een concentratie van 32-128 µg/ml. Voor verdere optimalisatie werden de actieve peptiden die werden geïdentificeerd met behulp van doelmolecuul 1 en 2 gekozen. De peptiden werden geoptimaliseerd door ze te modificeren met een lipide van 10 koolstofatomen welke N- of C-terminaal werd gekoppeld. Dit zorgde voor een vaak drastische verbetering van de activiteit tot een bereik van 2-8 µg/ml tegen *M. luteus*. Het peptide T2-1-C10 is door de modificatie ook actief tegen klinisch relevante stammen (*Enterococcus faecium* en vancomycine-resistente *E. faecium*). Na verdere analyse bleek dat de peptiden T1-4-C10 en T2-1-C10 wel wat hemolytische eigenschappen hebben maar alleen bij hoge concentraties (32 µg/ml). Om te bestuderen of de peptiden ook daadwerkelijk aan lipid II bindt zijn de peptiden eerst met lipid II geïncubeerd en het mengsel werd aan *M. luteus* toegevoegd. Hierbij bleek de activiteit te zijn verdwenen voor alle actieve peptiden waarbij er voor T2-1-C10 zelfs maar 1 equivalent lipid II nodig was, wat suggereert dat er een sterke interactie is. Om dit peptide verder te analyseren hebben we een alanine-scan uitgevoerd. Hierbij wordt elk aminozuur een keer vervangen door alanine en de activiteit van al deze peptiden gemeten. Op deze manier kan de invloed van elk aminozuur op de activiteit van het peptide worden bepaald. Daarnaast is ook het lipide in lengte gevarieerd waaruit bleek dat de initieel gekozen C10-lipide het beste werkt. Een experiment waarbij er gekeken wordt naar ophoping van UDP-MurNAc-pentapeptide werd succesvol uitgevoerd en toont aan dat de stof daadwerkelijk aan lipid II bindt in levende bacteriën.

In **hoofdstuk 4** hebben we het door de natuur geproduceerde lipid II

bindend peptide nisine in detail bestudeerd met behulp van synthetische lipid II analogen. Om de binding tussen lipid II en nisine te bestuderen hebben we gebruik gemaakt van isotherme titratie calorimetrie (ITC). Met deze techniek wordt direct het warmte verschil gemeten dat ontstaat als twee stoffen aan elkaar binden en kan de sterkte van deze interactie worden bepaald. Door lipid II analogen te gebruiken waar steeds een gedeelte weggelaten werd konden we inzicht krijgen in de stukken die belangrijk zijn voor goede binding. Omdat de stoffen een lang lipide dragen zijn ze niet wateroplosbaar en werden ze daarom in vesicles opgenomen. Deze vesicles zijn bootsen het bacteriële membraan na waarin lipid II zich in zijn natuurlijke omgeving ook bevind. De metingen lieten zien dat nisine voornamelijk aan de pyrophosphaat bindt en het peptide van lipid II weinig invloed heeft. Zelfs als alle onderdelen van lipid II verwijdert zijn op de pyrophosphaat na is er nog binding al is het wel 10 keer minder sterk. Als de meting zonder vesicles wordt vericht (hiervoor is een verkort lipide gebruikt) daalt de bindingssterkte 100 keer. Dezelfde lipid II analogen werden gebruikt voor een fluorescentie experiment. In dit experiment worden er vesicles gemaakt die gevuld zijn met een fluorescente kleurstof en de lipid II analogen worden in de membraan van deze vesicles opgenomen. Als nisine bindt aan de lipid II analogen vormt er een porie waardoor de fluorescente kleurstof naar buiten lekt en gemeten kan worden. Deze experimenten bevestigden de observaties van de ITC experimenten en lieten ook zien dat het peptide van lipid II niet heel belangrijk is voor het vormen van de porie maar wel een rol speelt bij het stabiliseren ervan.

Hoofdstuk 5 beschrijft de synthese en analyse van een aantal analogen van het antibiotische peptide daptomycine. Dit van calcium afhankelijke lipopeptide wordt gebruikt tegen verschillende MRSA infecties en ondanks dat het uitgebreid bestudeerd is, is het werkingsmechanisme nog steeds niet helemaal duidelijk. Om hier meer inzicht in te krijgen hebben we een aantal analogen van daptomycine gesynthetiseerd en ook de overeenkomstige spiegelbeeld enantiomeren. Er wordt gedacht dat daptomycine aspecifiek poriën vormt in de membraan van een bacterie en zo de cellen dood maakt. Indien dit het geval is zou een enantiomeer even actief moeten zijn. Als daptomycine echter werkt door te binden aan een chiraal biomolecuul dan is de verwachting dat de enantiomeren niet actief zijn. Daptomycine bevat een aantal non-proteïnogene aminozuren die niet eenvoudig te verkrijgen zijn. In onze analogen zijn deze vervangen door vergelijkbare commercieel beschikbare aminozuren. Ook is de esterbinding in het peptide

vervangen door een amidebinding. De stoffen zijn getest tegen *Staphylococcus aureus* en dit liet zien dat de analogen van de juiste stereochemie actief waren al was het significant minder dan daptomycine. De vermindering van de activiteit was wel verwacht door de gemaakte aanpassingen. De peptides waren echter wel nog steeds afhankelijk van calcium wat een indicatie is dat ze het zelfde werkingsmechanisme hebben als daptomycine. De spiegelbeeld isomeren van deze stoffen vertoonde echter helemaal geen activiteit wat de suggestie wekt dat daptomycine bind aan een chiraal biomolecuul.

Hoofdstuk 6 beschrijft het onderzoek naar op peptide gebaseerde inhibitoren voor protein arginine methyltransferases (PRMTs) dat is uitgevoerd in samenwerking met de groep van Adam Frankel van de University of British Columbia. Deze eiwitten katalyseren de methylering van arginine residuen en zijn betrokken bij verschillende vormen van kanker. De eerste set peptiden die gemaakt zijn bevatten een arginine die een ethyl-groep droeg met 0, 1, 2 of 3 fluor atomen. Na incubatie met PRMT1, -4, en -6 bleek dat het niet gefluorineerde peptide gemethyleerd kon worden door PRMT1. Dit was een indicatie dat de arginine past in het actieve gedeelte van het eiwit. De peptiden werden daarom verder getest als inhibitoren van deze PRMTs en de IC_{50} waarden waren het best tegen PRMT6 (4.8 – 14.2 μM), iets hoger tegen PRMT1 en ongeveer 10 keer hoger tegen PRMT4. De volgende twee peptiden waren gebaseerd op dezelfde sequentie maar de arginine was deze keer gemodificeerd met een gedeelte van de cofactor AdoMet die ook aan de PRMTs bindt en gebruikt wordt voor de methylering. Op deze manier werd een partieel bisubstraat gecreëerd in de hoop dat de bindingsactiviteit hierdoor beter zou worden. De peptiden werden getest tegen dezelfde PRMTs en hadden IC50 waarden in het lage micromolair bereik. Interessant was dat een van de peptiden alleen PRMT6 blokkeerde. De laatste serie peptiden was gebaseerd op de HIV-Tat eiwit. Uit eerdere studies bleek dat dit eiwit selectief gemethyleerd wordt door PRMT6. Na het synthetiseren van een serie verschillend gemodificeerde arginines werden deze in het Tat-peptide ingebouwd. In tegenstelling tot de eerdere resultaten zagen we dat onze peptiden ook substraten waren voor PRMT1. Op basis van de kristalstructuur van HIV-Tat stellen we voor dat de lineaire vorm van de peptiden waarschijnlijk de selectiviteit teniet doet en dat een cyclische vorm van het peptide misschien beter werkt.

Appendices

Curriculum vitae

Peter 't Hart was born on the 29th of September 1986 in Krimpen aan den IJssel, the Netherlands. In 2004 he graduated from the Comenius College in Capelle aan den IJssel. He then started his bachelor studies in Chemistry at Rotterdam University of Applied Sciences and graduated in 2007 after an internship at DSM Pharmaceutical Products working on the synthesis of beta-lactam antibiotics. In the next year he worked as a senior analyst at the Heineken brewery in Zoeterwoude. In 2008 he started at Utrecht University with a premaster Drug Innovation and in 2009 with the master's program Drug Innovation. During the master's program he first joined the Medicinal Chemistry and Chemical Biology group in Utrecht to work with Dr. Nathaniel I. Martin on analogues of daptomycin and peptidic inhibitors of protein arginine *N*-methyltransferases. For a second research project he joined the lab of prof. Michael Marletta at the University of California Berkeley working studying bacterial nitric oxide synthases and unnatural amino acid mutagenesis. After obtaining his MSc-degree in 2011 he again joined dr. Nathaniel I. Martin and prof. dr. Roland Pieters for his doctoral studies at the Medicinal Chemistry and Chemical Biology group at Utrecht University. During this time he worked mainly on lipid II binding peptides both novel and obtained from nature. In Januari 2016 he joined the Waldmann group at the Max Planck Institute for Molecular Physiology in Dortmund, Germany for a post-doctoral position focusing on macrocyclic inhibitors of protein-protein interactions.

List of publications

Publications from this thesis

- **'t Hart, P.**, Oppedijk, S.F., Breukink, E., Martin, N.I., New insights into nisin's antibacterial mechanism revealed by binding studies with synthetic lipid II analogues. *Biochemistry*, **2016**, *55* , 232-237
- **'t Hart, P.***, Kleijn, L.H.J.*, de Bruin, G., Oppedijk, S.F., Kemmink, J., Martin, N.I., A combined solid- and solution-phase approach provides convenient access to analogues of the calcium-dependent lipopeptide antibiotics. *Org. Biomol. Chem.,* **2014**, *12*, 913-918.
- **'t Hart, P.***, Thomas, D.*, van Ommeren, R., Lakowski, T.M., Frankel, A., Martin, N.I. Analogues of the HIV-Tat peptide containing N^{η}-modified arginines as potent inhibitors of protein arginine N-methyltransferases. *Med. Chem. Commun.,* **2012**, *3*, 1235-1244.
- **'t Hart, P.***, Lakowski, T.*, Thomas, D., Frankel, A., Martin, N.I. Peptidic partial bisubstrates as inhibitors of the protein arginine N-methyltransferases. *ChemBioChem,* **2011**, *12*, 1427-1432.
- Lakowski, T.*, **'t Hart, P.***, Ahern, C.A., Martin, N.I. & Frankel, A. N^{η}-substituted arginyl peptide inhibitors of protein arginine N-methyltransferases. *ACS Chem. Biol.,* **2010**, *5*, 1053-1063.
  (**co-first author, equal contribution*)

Other publications

- Koopmans, T., Wood, T.M., **'t Hart, P**., Kleijn, L.H.J., Hendrickx, A.P.A., Willems, R.J.L., Breukink, E., Martin, N.I. Semisynthetic lipopeptides derived from nisin display antibacterial activity and lipid-II binding on par with that of the parent compound. *J. Am. Chem. Soc.,* **2015**, 137, 9382-9389
- Mooney, C.A., Johnson, S.A., **'t Hart, P.**, Quarles van Ufford, L., de Haan, C.A.M., Moret, E. E., Martin, N.I. Oseltamivir analogues bearing N-substituted guanidines as potent neuraminidase inhibitors. *J. Med. Chem.,* **2014**, *57*, 3154-3160.

Manuscripts in preparation

- Working title: Bicyclic phage display to identify novel lipid II binding antibiotic peptides.

Dankwoord

Dear **Nathaniel**, first of all a big thanks to you of course. In the recent years you have written several very flattering recommendation letters for me and now it is my chance to do the same for you. If anyone would ask me whether they should join you for an internship or PhD I wouldn't hesitate to tell them: Absolutely! Since we met in 2009 you have been a great supervisor who has not only taught me a lot of practical skills but also trained me to become an independent critical scientist. I'm very proud of what we have achieved together and I'm looking forward to possible collaborations someday. Besides the professional relationship we've had a good social relationship as well. I'll remember all the pubquizes, queensnights, MedChemborrels and other beerdrinking events. I don't think many people ever crashed on the couch of their supervisor!

Timo, net zolang als ik Nathaniel ken, ken ik jou. We hebben samen een hoop gedaan: festivals, skivakanties, proton-feesten, etc. Ik ben je erg dankbaar voor de introductie bij proton waardoor ik veel mensen heb leren kennen en mijn tijd in Utrecht onvergetelijk is geworden. Het was altijd gezellig om naast jouw te zitten en leuk dat je mijn paranimf wil zijn. Ik hoop dat jullie veel succes hebben met de nisin-derivaten! Ik mis onze dagelijkse cola pauze nu al en dat brengt me ook bij **Paul**. We zijn bijna tegelijk gepromoveerd en hebben in die tijd veel samen gedaan. Als borrel commissie van MedChem hebben we het menig vrijdagavond laat gemaakt en later ook in de Primus natuurlijk. Qua projecten hebben we niet veel samen gewerkt maar we konden wel altijd samen lekker zeuren over onze collega's, zeker onder het genot van de zoveelste kop koffie. Ik vind het leuk dat ik ook jouw paranimf mag zijn en succes met de laatste loodjes! **Laurens**, als zuurkastburen hebben we veel tijd samen in het lab doorgebracht. Je bent altijd in voor een goed gesprek maar ook een flauwe grap. Bedankt voor een leuke samenwerking en heel veel succes in je laatste jaar en met SynAmp!

Niek, ik weet dat je het niet gelooft maar mijn "studententijd" is nu toch echt voorbij! En als paranimf kan je het ook nog eens van dichtbij meemaken. Ik hoop dat we elkaar nog vaak zullen zien in Duitsland of Nederland om een biertje te drinken. Misschien kan je zorgen voor een directe ICE van Dortmund naar Rotterdam! Bedankt voor de hulp met de kaft van dit boekje.

Roland, als promotor wil ik ook jou bedankten voor je hulp en je geduld

als ik weer in je kantoor stond om ergens geld voor te vragen. Ook stond je altijd open voor mijn suggesties en opmerkingen over het lab. **Johan**, bedankt voor alle hulp met de ITC en NMR-metingen. Deze hebben mijn proefschrift compleet gemaakt. **Linda**, ook jou wil ik bedanken voor al het advies en hulp met de biologische experimenten. **Eefjan** en **Sabine**, als co-auteurs wil ik ook jullie bedanken voor de prettige samenwerking en de gastvrijheid en hulp in jullie lab. De oneindige hoeveelheid lipid II die ik van jullie heb gekregen is van onschatbare waarde geweest voor dit proefschrift. **Christian** and **Inmaculada**, thanks for having me in your lab and your patience with teaching me phage display. I had a great time in Lausanne!

Tom, a great thanks to you in helping me synthesize, purify and test so many peptides! Your help and dedication have generated a very nice set of data that will definitely lead to another nice publication with your name on it. I hope you are having a good time at Stanford and good luck with the grant-application! **Roel** jij ook bedankt voor je inzet tijdens de afronding van mijn promotie! Jouw assays hebben het verhaal compleet gemaakt. **Ihaab**, **Kelvin**, en **Randy**, a thanks to you as well for your hard work.

Hilde, als grote zus kon ik voor goed advies altijd bij jou zijn. Bedankt voor alle info over Duitsland! **Steffen**, je was een waardige squash-tegenstander. Ook voor scheikundig advies kon ik je regelmatig vinden. Ik kan nog steeds met plezier terugdenken aan de discussies achter onze bureaus. **Alen**, thanks for all the great food and fun. I still haven't cooked for you so maybe that's worth a visit to Germany! **Gosia**, I would like to thank you as well for helping me to run the Symphony and prepare so many peptides. **Loek**, **Gwenn**, **Jack**, **Helmus**, **Raymond**, **Matthijs**, **Hao**, **Kamal**, and all other MedChem colleagues, thank you for a great time!

Joost, allereerst vind ik het heel leuk dat ik jouw paranimf mag zijn. Ik hoop dat we binnenkort weer eens bier kunnen brouwen. Het Duitse bier begin ik toch al wel een beetje eentonig te vinden. Ook hoop ik dat we hier en daar nog is een mooi feestje mee kunnen pakken en dat we jou en Els hier en daar nog eens in Duitsland zien. **Tim**, je stond altijd klaar voor een biertje en wat gamen. Zeker toen we ook nog huisgenoten waren hebben we een goeie tijd samen gehad. Veel succes met jouw promotie! **Frank**, **Anne-Marie**, **Els**, **Bieneke**, **Christine**, **Jeroen**, **Marjon**, **Janne-Mieke**, **Tiemen**, **Winnie**, **Kristel**, **Lilian**,

Joost W., **Arjan**, **Anoeska**, **Robin**, **Remy**, en iedereen die ik misschien vergeet. Ik hoop nog af en toe in de Primus aan te schuiven bij jullie als ik weer eens in Nederland ben. Bedankt voor alle barbecues, feestjes, festivals, vakanties en andere gezelligheid!

Jilles, **Arthur**, **Jaco**, **Irene**, **Lianne**, ik vind het heel leuk dat we elkaar nog met regelmatig zien. Tot in Spanje!

Sanne, **Sharon**, **Peter**, **Lotte**, **Martijn**, **Tim**, **Margot**, **Leon**, **Michelle**, **Erik**, **Laura**, **Tom**, **Marlot**, als 2e doctor in dit rijtje wil ik ook jullie bedanken voor veel alle gezelligheid!

Martin, **Ingrid**, **Judith**, ik hoop jullie nog vaak te zien in Dortmund/Wuppertal. Er is altijd een gastenkamer voor jullie vrij! En dat geldt natuurlijk ook voor **Pa** en **ma**, ik ben jullie allemaal ontzettend dankbaar voor al jullie steun en hulp. Niet alleen tijdens mijn promotie maar ook de weg er naar toe. Ik hoop dat het verhuizen naar Duitsland voor jullie een kans creëert om hier veel leuke weekendjes weg te beleven.

Lieve **Nikki**, ook al is mijn titel prachtig jij bent natuurlijk het mooiste wat ik aan mijn tijd bij MedChem heb over gehouden. Ik vind het nog steeds ontzettend fijn dat we het avontuur in Duitsland samen aan kunnen gaan. Je bent mijn rots in de branding en krijgt me altijd aan het lachen. De laatste loodjes had ik niet zonder jou gekund!

Peter